EPISTATIC INTERACTIONS IN THE SUPPRESSION OF AUTOIMMUNITY

APPROVED BY SUPERVISORY COMMITTEE

Edward K. Wakeland, Ph.D.

_____

J. David Farrar, Ph.D.

_____

James M. Forman, D.M.D., Ph.D.

_____

Chandra Mohan, M.D., Ph.D.

_____

Joseph Craft, M.D.

_____

EPISTATIC INTERACTIONS IN THE SUPPRESSION OF AUTOIMMUNITY

by

SRIVIDYA SUBRAMANIAN

DISSERTATION

Presented to the Faculty of the Graduate School of Biomedical Sciences

The University of Texas Southwestern Medical Center at Dallas

In Partial Fulfillment of the Requirements

For the Degree of

DOCTOR OF PHILOSOPHY

The University of Texas Southwestern Medical Center at Dallas

Dallas, Texas

August, 2005

Acknowledgements

"There is a theory which states that if ever anybody discovers exactly what the Universe is for and why it is here, it will instantly disappear and be replaced by something even more bizarre and inexplicable. There is another theory which states that this has already happened."- Douglas Adams (1952-2001)

During my years in graduate school at UT Southwestern, quite a number of people have supported and encouraged me, and helped maintain my sanity, in both my professional and personal life.

I am extremely grateful to my mentor, Dr. Edward K. Wakeland, for his support, patience, and sense of humor during my years in his lab, which was an environment where I developed both as an independent scientist and as an individual. I will always appreciate Ward's unwavering belief in me, even at my most despondent and pessimistic times, and his constant efforts to convince me of my scientific potential. I will really miss our discussions on everything from my projects in lab, to science policy, national politics, running, and our mutual favorite fantasy series, Lord of the Rings.

There are a number of people who have helped immensely in the successful completion of my dissertation work. The excellent maintainance and management of our mouse colony by José, Sergio, Leonel and Phillipe has greatly facilitated my mouse intensive projects. It has been a privledge to work with Kati, Charles, Kui, Quan, Ferdicia, Nisha, Katie and Lisa on a variety of projects, and I will always appreciate their help and expertise. I am extremely grateful for the scientific help, technical advice and constructive imput I received from different faculty members, especially Drs. Farrar, Forman, Miyazaki, Mohan and van Oers. I'd also like to acknowledge the Center for Immunology (Bettye, Karen and

Marie) and the Graduate Program in Immunology (Karen K.) for all their 'administrative' help over the years.

I relied heavily on my friends during graduate school, and will always treasure my memories with them. I was lucky enough to have friends who are not only a whole bunch of fun, but who also helped me get past the vagaries and frustrations of research, as well as difficult times in my personal life. Alice, Charles, Kati and Nisha saw me through some very 'dark' periods, and there are no words to express my gratitude for the love and support they gave when I was fighting my 'innermost demons'. I will always treasure the friendships of Ferdicia, Katie, Hillery, Karen, Marie, José, Bettye, Kui, and David, who have all listened to and encouraged me in many different ways over the years. Lisa, Jen, Jill and Ivan have not only 'been there' for me, but their individual crazy senses of humor have helped create some really great memories! Some of my friends date back to my college days- PV, Mali, Deepak and Garima- thanks for listening and being there all these (many) years. Ben was there for me during a period of graduate school and my life that perhaps I needed him the most, and I thank him for the memories and the love.

To finish, I'd like to thank my family. My parents at all times found the means to support my education, be that academics, music or sports, and always encouraged my dreams and aspirations, no matter how far away they took me. My dad taught me early lessons on aiming for perfection and not doing a 'half-ass' job, and instilled in me the value of never judging someone by your own standards and beliefs. My mom's courage in the face of great physical and emotional pain is both inspring and humbling, and her support of my educational aspirations over the years has been constant. I'm pretty sure I get my love of

fantasy and science fiction from her. My brother constantly amazes me with his attitude and his desire to achieve the most that he can with his education. His perseverance, despite all the difficulties he faces and has faced, makes him in my eyes the true achiever of the family. Finally, my extended family has encouraged and supported not only my efforts, but those of my mother and brother, for which I am forever grateful.

EPISTATIC INTERACTIONS IN THE SUPPRESSION OF AUTOIMMUNITY

Publication No. _____

Srividya Subramanian, Ph.D.

The University of Texas Southwestern Medical Center at Dallas, 2005

Supervising Professor: Edward K. Wakeland, Ph.D.

Sle1 is a susceptibility locus for autoimmunity derived from the lupus-prone NZM2410 mouse. The NZW-derived suppressive modifier *Sles1* was identified as a specific modifier of *Sle1* and prevents the development of anti-chromatin autoantibodies mediated by *Sle1* on the B6 background. Fine-mapping of *Sles1* with truncated congenic intervals localized it to a ~956 KB segment on mouse chromosome 17. *Sles1* completely abrogated the development of activated lymphocyte populations in B6.*Sle1*, but splenic B cells from B6.*Sle1*|*Sles1* still exhibited intrinsic ERK phosphorylation. Classic genetic complementation tests using the non-autoimmmune 129/SvJ mouse, suggests that this strain possesses a *Sles1* allele complementary to NZW, as evidenced by the lack of autoimmunity in [129 X

B6.*Sle1*|*Sles1*]F_1s. These findings localized and characterized the suppressive properties of *Sles1* and implicated 129 as a useful strain for aiding in the identification of this elusive epistatic modifier gene. In contrast, introduction of the suppressive modifiers *Sles2* and *Sles3* onto B6.*Sle1* led to a decrease in the penetrance and mean titres of autoantibody production, but not complete suppression.

These results suggested that genes, such as *Sles1*, which can specifically modify the effects of susceptibility alleles causing a breach in tolerance, could prevent systemic autoimmunity, even in the presence of additional susceptibility genes. To test this hypothesis we introduced the *Sle1*-specific suppressive locus *Sles1* onto two different lupus-prone models: B6.*Sle1*|*yaa* and B6.*Sle1*|*Sle2*|*Sle3/5*, to determine whether and how *Sles1* mediated suppression of *Sle1* impacts the highly penetrant systemic autoimmunity characteristic of these two mouse strains.

Comparing the development of a variety of pathological, immunological, functional and molecular phenotypes between the B6.*Sle1*|*yaa* and B6.*Sle1*|*Sles1*|*yaa* strains at different ages, revealed that *Sles1* mediated a profound and complete suppression of systemic autoimmunity in this model. In contrast, the introduction of *Sles1* onto the *B6.Sle1*|*Sle2*|*Sle3/5* strain improved survival, and altered the kinetics of disease, but did not completely suppress disease in this model. These data suggest that the nature of the additional susceptibility loci interacting with *Sle1* influences the degree of *Sles1*-mediated epistatic suppression of *Sle1*. Further characterization of these different models will help identify specific pathways *Sles1* impacts, and provide insight into potential therapeutic strategies.

TABLE OF CONTENTS

Publications

1. A.E. Wandstrat, Nguyen C., Limaye N., Chan A.Y., **Subramanian S.**, Tian X-H., Yim Y-S., Pertsemlidis A., Garner H.R., Morel L. and Wakeland E.K. 2004. Association of extensive polymorphisms in the SLAM/CD2 gene cluster with murine lupus. *Immunity*, **21** (6): 769-780

2. **S. Subramanian**, Wakeland E.K. 2005. The importance of epistatic interactions in the development of autoimmunity. In: The genetics of autoimmunity (Novartis Found Symp 267). Wiley, Chichester, p 76-93.

3. L.A. Pitcher, Mathis M.A., **Subramanian S.**, Young J.A., Wakeland E.K., Love P.E. and van Oers N.S.C. 2005. Selective Expression of the 21-kDa Tyrosine Phosphorylated Form of TCR zeta Promotes the Emergence of T cells with Autoreactive Potential. *J.Immunol*. **174** (10): 6071-6079

4. **S. Subramanian**, Yim Y-S., Liu K., Tus K., Zhou X.J. and Wakeland E.K. 2005. Epistatic Suppression of SLE: Fine-mapping of *Sles1* to Less Than 1 Mb. *J.Immunol.* **175** (2): 1062-1072

5. **S. Subramanian,** Tus K., Nguyen C., Zhou X.J., van Oers N.S.C. and Wakeland E.K. 2005. Epistatic Suppression of SLE: *Sles1* Abrogates Fatal Autoimmunity in the B6.*Sle1*|*yaa* Murine Lupus Model. *In preparation.*

List of Figures

List of Tables

Abbreviations

129: 129/SvJ

ADCC: antigen dependent cell cytotoxicity

AICD: activation induced cell death

ANA: anti-nuclear autoantibody

ANOVA: analysis of variance

ANU: arbritrary normalized units

APC: antigen presenting cell

autoAb: autoantibody

B6: C57Bl/6J

BAC: bacterial artificial chromosome

BCR: B cell receptor

BM: bone marrow

CFSE: carboxy fluorescein diacetate succinimydl ester

DC: dendritic cell

dsDNA: double-stranded DNA

EBV: Epstein Barr virus

ELISA: enzyme linked immunosorbent assay

ES: embryonic stem

FcγR: Fc gamma receptor

GBM: glomerular basement membrane

GC: germinal center

GN: glomerulonephritis

HEL: hen egg lysosome

HLA: Human leukocyte antigen

HSP: heat shock protein

IC: immune complex

IDDM: Insulin-dependent type I diabetes mellitus

IFN: interferon

Ig: immunoglobulin

IL: interleukin

ITAM: immunoreceptor based tyrosine activation motif

ITIM: immunoreceptor based tyrosine inhibitory motif

LD: linkage disequilibrium

LOD: logartithm of the odds

LN: lymph node

Mb: megabases

MFI: median fluorescent intensity

MHC: Major Histocomptability Complex

MS: Multiple Sclerosis

MZ: marginal zone

NK: natural killer

NZB: New Zealand Black

NZW: New Zealand White

PBMC: peripheral blood mononuclear cells

PC: plasma cell

PD-1: programmed cell death 1

PDT: pedigree disequilibrium test

perC: peritoneal cavity

PI3K: phosphatidylinositol 3-kinase

P/I: phorbol myristic acid/ ionomycin

PKB/C: protein kinase B/C

PTK: protein tyrosine kinase

PTP: protein tyrosine phosphatase

RA: rheumatoid arthritis

SAP: serum amyloid P

SEM: standard error of the mean

SLE: Systemic Lupus Erythematosus

SLEDAI: SLE disease activity index

Sles: SLE suppressor

SNP: single nucleotide polymorphism

SPF: specific pathogen free

T1: transitional 1

T2: transitional 2

TCR: T cell receptor

Tg: transgene

TLR: Toll-like receptor

TNF: tumor necrosis factor

T_{FH}: follicular T helper cells

T_{reg}: regulatory T cell

yaa: y-chromosome autoimmune accelerator

Chapter I. Introduction

The immune system has evolved a series of strategic checkpoints in order to ensure that the random generation of lymphocyte receptors, necessary for creating repertoires of immense diversity against pathogens, does not result in the generation of autoreactive T and B cells (reviewed in (1)). The most stringent of these checkpoints occur in the primary lymphoid organs, the bone marrow (BM) and thymus, and the identification of cells bearing self-reactive receptors in these organs can result in arrest of maturation, editing of the BCR (B cell receptor) light or TCR (T cell receptor) α chains and clonal deletion (reviewed in (2)).

While these events in the BM and thymus purge many of the cells with autoreactive specificities, there are a variety of mechanisms operating in the periphery that contribute to the maintenance of peripheral tolerance, including BCR/TCR tuning and anergy, control of co-stimulatory molecule expression, follicular exclusion, competition for survival and growth factors and regulation by T_{reg} cells (reviewed in (1)). Breakdown in both central and peripheral tolerogenic mechanisms can lead to the emergence of autoreactive cells and the development of either systemic or organ-specific autoimmunity.

Introduction to SLE: A Complex Immunological and Genetic Disease

Systemic lupus erythematosus (SLE) is considered the prototypic systemic autoimmune disorder, and is characterized by a loss in tolerance to a variety of ubiquitous self-antigens, such as chromatin, dsDNA, ribonucleoproteins and complement, and culminates in a variety of end-organ pathologies. There is wide heterogeneity in the clinical

symptoms of lupus patients, which can include glomerulonephritis (GN), non-deforming arthritis, pericarditis, vasculitis, pleuritis and the development of the characteristic malar rash. This diversity in symptoms significantly complicates the diagnosis of SLE, and current American College of Rheumatology guidelines require that four of eleven criteria be fulfilled to classify a patient as having lupus (reviewed in (3, 4)).

The global incidence of SLE is difficult to estimate due to the lack of definitive epidemiological information on the disease. It is believed that at least five million people worldwide have lupus and more than 100,000 new cases develop every year, based on the limited existing data. SLE shows a strong female:male gender bias of 9:1, and there is increased incidence of lupus in both African-American and Hispanic populations. The incidence of mortality due to SLE, particularly in certain ethnic groups, is believed to be on the rise, though this may be due to increased diagnosis, differential treatment access and/or compliance, and race-based variations in end-organ susceptibility ((3) and http://www.cdc.gov).

The Complex Genetic Basis of SLE

While the factors involved in the initiation of SLE are poorly understood, a wide body of work has clearly demonstrated that genetic predisposition is the major element determining lupus susceptibility. Classic twin concordance studies, which compare the incidence of disease in monozygotic *vs.* dizygotic twin pairs, have found that the concordance rate for SLE is approximately ten-fold higher in monozygotic (34%) *vs.* dizygotic (3%) twins (5, 6). Another epidemiologic approach to studying genetic

contributions is through the enumeration of the degree of familial aggregation. This value, known as the λ_s, is quantified as the ratio of the prevalence of disease in families with an affected member to the prevalence of disease in the populations as a whole. If this value is close to 1.0, it indicates there is no evidence for genetic factors, while for fully penetrant, single gene Mendelian diseases, such as Cystic Fibrosis, the value can be as high as 500. In the case of SLE and other complex autoimmune diseases, like Insulin-dependent type I diabetes mellitus (IDDM) and Mutiple Sclerosis (MS), the values range from 10-40, indicating that genetic susceptibility is not completely penetrant, and that more than one gene is involved (7).

Understanding the genetic etiology of complex traits, such as SLE, is a challenge for a variety of reasons, though recent advances in genetic and genomic technologies have greatly facilitated the ability to tackle these difficulties (8, 9). The genetic complexity inherent in diseases like SLE is related to the fact that each contributing allelic variant only partially increases the probability of disease expression and hence, no single gene is either necessary or sufficient, except in rare genetic abnormalities. Therefore, even if multiple susceptibility genes are present, overt disease may not develop, and this is known as incomplete penetrance (7, 10).

Genetic heterogeneity is another feature of SLE, whereby different combinations of susceptibility genes result in the same phenotypes in different ethnic groups, families and even murine model systems. Attempts to minimize this factor in human genetic studies have involved strictly stratifying patients according to various clinical phenotypes and ethnic groups (11-16).

The study of SLE genetics is further complicated by emerging evidence indicating that predisposing causal variants are common alleles that *per se* are non-deleterious, as most clearly exemplified by the HLA (Human Leukocyte Antigen) polymorphisms associated with autoimmunity. In contrast to the causal mutations in single-gene diseases, which are often associated with loss-of and/or significant alterations in function and hence, are selected against in natural populations, this is not the case for the alleles predisposing in autoimmunity (reviewed in (17)). This makes identification of the causal polymorphism difficult, as they are relatively common within the population, and as their phenotypic consequences are subtle and challenging to identify.

If the allelic variations predisposing to SLE are polymorphisms commonly found in the general populations as a whole, how then do they elicit systemic autoimmunity? The answer to this question, which has been most effectively demonstrated in murine models, lies in the fact that these loci can genetically interact with one another, classically known as epistasis. Hence, it is postulated that different combinations of polymorphic genes, due to their specific epistatic interactions, can lead to imbalances in immune regulation/function that potentiate the development and progression of autoimmunity (reviewed in (18)). The importance of epistasis is emerging as a paradigm in the study of genetic susceptibility to autoimmunity, and will be continually revisited in the following sections and chapters.

The Immunological Basis and Phenotypes of SLE

SLE is characterized by a variety of immunological aberrations that ultimately culminate in the pathogenic processes of lupus nephritis. These have been postulated to be a

consequence of changes in the activation thresholds and functions of immune cells, variations in the cytokine milieu produced, alterations in the clearance of apoptotic and necrotic debris by phagocytotic cells, as well as modulations in antigen-presentation capacities (reviewed in (19-22)).

The importance of the B cell in SLE is underscored by the fact that high titres of serum autoantibodies (autoAbs), particularly anti-dsDNA IgG, are a unique feature of SLE. These autoAbs are believed to result in the formation of immune-complexes (ICs), which then collect and deposit in kidney glomeruli, leading to IC-mediated GN. In addition to secreting pathogenic autoAbs, studies have shown that B cells from lupus patients have abnormal signaling properties and migration patterns, as well as enhanced co-stimulatory molecule expression and cytokine secretion. Besides modulating intrinsic B cell properties, such functional abnormalities can impact T cells, dendritic cells and NK cells (19, 23). Currently, anti-CD20 mediated B cell depletion therapies on SLE patients are being tested in clinical trials (24).

Various abnormalities in T cell signaling function have also been described in SLE patients including exaggerated calcium responses, increased intracellular phophorylation and decreased TCRζ chain, but upregulated FcRγ chain expression. In addition, SLE T cells have been found to show aberrant chemokine receptor expression, increased CD40L expression and a decreased propensity to undergo activation induced cell death (20). Abnormalities in different dendritic cell (DC) and antigen-presenting cell (APC) subsets have been reported in SLE patients, including the increased production of type I IFNα by plasmacytoid DCs,

resulting in the 'IFN signature' of peripheral blood lymphocytes ((25-29) and reviewed in (21)).

Genetic Studies in Human SLE

A number of strategies have been employed for the identification of lupus susceptibility genes in human populations, facilitated by the recent advances in genetics and genomic technologies that allow for large-scale genotyping efforts and the development of powerful software programs capable of analyzing these data. There are two main approaches used to identify SLE predisposing genes: hypothesis-driven candidate gene association studies and statistic-driven genome-wide linkage studies (30). Each method has its advantages and caveats, as detailed below.

Human SLE Association Studies and Candidate Genes Analyses

Candidate-gene-association studies are a classic genetic approach whereby the frequency of a particular allele in a gene-of-interest is compared between affected patients and the appropriate controls. Candidate genes may be chosen on the basis of their importance in the disease processes (e.g., cytokines), association in other autoimmune diseases (e.g., CTLA-4, PTPN22) and mechanistic insights gained from animal models. Also, candidate-gene-approaches are increasingly being applied to loci first identified via genome-wide linkage analyses. The main caveat associated with such studies is that they are subject to the problems of population admixture and drift, such that differences in allele frequencies may be more reflective of differences in population history, instead of true disease association (3,

30). In the following section, some of the most studied and well-accepted SLE candidate genes are discussed, along with any supporting evidence from murine studies. In addition, Table 1 lists these candidate genes and their human and mouse chromosomal locations.

The MHC and Lupus: Complement, Class II and TNF

The extended major histocompatibility complex (MHC) region on human 6p21 is the most gene-rich, transcriptionally active and polymorphic region of the genome and encodes numerous genes important to the immune system. These include the MHC Class I and II genes, the complement genes (C4, C2, C3 and Factor B), heat shock proteins and TNF family members (TNFα and Lymphotoxin). The major difficulty in the study of MHC associations is that the genes are in tight linkage disequilibrium (LD), forming stable haplotype blocks, thus making it difficult to discriminate between the effects of any single gene (31, 32).

In humans, the only known single-gene defects leading to the development of SLE are homozygous deficiencies in the early components of the complement pathway, C1Q, C4 and C2. In fact, in individuals with homozygous deficiency of C1Q, a rare defect so far only recorded and studied in 42 cases, the incidence of SLE is greater than 90% (reviewed in (33)). In humans, the C4 gene is tandemly duplicated, giving rise to the C4A and C4B isotypes. Like other MHC genes, C4 is very polymorphic and in fact, the null allele for either C4A or C4B is found in 6% of most populations (34). Some studies have documented an association between the null allele of C4A and SLE, but none so far have been reported for C4B. However, null alleles for both isotypes are rare and have only been recorded in 28 cases, and over 75% of these were reported to have SLE (35). Supporting evidence for the importance

of complement-mediated functions in lupus susceptibility comes from targeted deletion of these components in the mouse: both *c1q*$^{-/-}$ and *c4*$^{-/-}$ mice develop lupus-like phenotypes, the severity and manifestations of which are highly background genome dependent, as described later (36-39).

In contrast to C4 and C1q, while one null allele is relatively common for C2 (1:170 Western European Caucasians are hemizygous for C2), only one study has found significant association between C2 hemizygosity and SLE. In addition, the incidence of SLE is only 10% in individuals with homozygous C2 deficiency (reviewed in (40, 41)). This suggests that the association of SLE with complement is not specifically related with the ability to activate the classical complement pathway, since deficiency of the most downstream component (C2) is the least associated with susceptibility.

The association between specific Class II alleles and SLE has been the subject of investigation for a long time (42, 43). It is postulated that Class II polymorphisms may influence susceptibility due to their ability to influence thymic selection events and hence, the peripheral T cell repertoire. Furthermore, Class II polymorphisms have been shown to be associated with other autoimmune diseases, such as IDDM, MS and rheumatoid arthritis (RA) (reviewed in (44-46).

The DRB1*1501 (DR2) and DRB1*0301 (DR3) alleles have shown the most consistent associations in Caucasian SLE patients, though the effects seen are modest relative to other autoimmune diseases (47-49). The most extensive study to date was performed on 576 SLE patients from a predominantly European-American 334 family collection, both sib-pair and simplex, for which a dense panel of markers across the HLA region were genotyped.

The marker showing the greatest association by the pedigree disequilibium test (PDT), which is a family-based test examining the transmission of alleles from heterozygous parents, was D6S2446, which is within the Class II region. Further analysis within the region identified three haplotypes conferring increased risk in SLE patients: *DR2/DQ6*, *DR3/DQ2* and *DR8/DQ4*. Importantly, none of the families that did not show association with D6S2446 had any of these three haplotypes (50).

The effects for both the *DR2/DQ6* and *DR8/DQ4* haplotypes were further fine-mapped to a ~500 KB region, which includes the *DR* and *DQ* genes, as well as *ORF10* (*testis specific basic protein*), *BTNL2* (*butyrophilin-like family member II*), *DRA*, *DRB3*, *DRB5* and *DQA*. The *DR3/DQ2* haplotype was associated with the highest risk, but because of extensive LD, was not further narrowed (50). Interestingly, the *C4A*-null and *TNF-308A* alleles, also associated with SLE, are present in this extended haplotype, making it difficult to ascertain which gene(s) in this haplotype is/are responsible for the associations observed.

The MHC Class III region also contains the *TNF*α gene, which encodes for a cytokine important in both inflammatory and apoptotic responses. Some studies have shown that there is a correlation between higher levels of serum TNFα and disease activity in SLE patients, while others suggest a protective role for TNFα in SLE (51, 52). A variety of groups have analyzed promoter polymorphisms in the *TNF*α gene to look for association with SLE, the most commonly studied being -308G/A. Since the -308A allele forms part of the 'high TNF producing' *HLA-A1-B8-DR3* extended haplotype, some groups have reported that this SNP increases TNF transcriptional activity by modulating transcription factor binding, but others claim it has no functional consequences (53, 54). Association between this promoter

SNP and SLE has most often been seen in Caucasian populations, as well as in one African-American patient population, though again these findings are not consistent (55-62). The most confounding aspect of the association remains the strong LD between *TNFα* and *DR3*, which is also strongly associated with SLE in Caucasians, but two separate analyses have suggested that *HLA-DR3* and *TNF -308A* form independent risk factors for SLE (59, 60). Interestingly, a recent study indicated that the increased-308A association in Caucasians is dependent on fixing the IL-1α -889C/C genotype, suggestive of a genetic interaction between these two pro-inflammatory loci (62).

In the mouse, while transgenic overexpression of TNFα under the control of specific promoter elements has led to insulitis, arthritis and cachexia, no mechanistic insight has been provided specifically for SLE (63-65).

FcγR Complex and Lupus

The FcγR complex on human chromosome 1q21-23 encodes for a diverse group of eight receptors with varying specificities for the constant region of the different IgG isotypes. These receptors are considered the paradigm for receptor families having both inhibitory and activating members that can transduce opposing signals within the same cell upon ligation. Hence, any effector function mediated via these receptors represents the net consequence of the stimulatory *vs.* inhibitory signals in a particular cell, allowing for exquisite control of responsiveness (66-68).

The activating FcγRs include the high affinity FcγRI, intermediate affinity FcγRIIIA and FcγRIIIB and the low affinity FcγRIIA and FcγRIIC. Not all of these receptors are

present in the mouse. The biological functions initiated by the triggering of these receptors include phagocytosis, antibody-dependent cell cytoxixity (ADCC) and the release of inflammatory mediators. It is believed that the functional response triggered by a particular FcγR is more dependent upon the cell type it is being expressed upon than the receptor itself (66, 68).

The activating FcγRs have extracellular ligand binding domains and intracellular ITAMs (immunoreceptor based tyrosine activation motif; the exception is the GPI-linked FcγRIIIB). Clustering of FcγRs by multivalent antigen-antibody complexes results in ITAM phosphorylation by Src family kinases, recruitment of the tyrosine kinase Syk and activation of phosphatidylinositol-3-kinase (PI3K). These initial events culminate in Ca^{2+} influx, phosphorylation of MAPK and gene expression induction by activated transcription factors (69, 70).

The inhibitory receptors FcγRIIB1 and FcγRIIB2, generated by alternative splicing of the *FcγRIIB* gene, have similar extracellular domains as their activating counterparts, with an intracellular ITIM (immunoreceptor based tyrosine inhibitory motif) instead. These receptors act as negative regulators of signaling when co-aggregated with their activating counterpart, and FcγRIIB2 can also participate in endocytosis of multivalent ligands. Furthermore, inhibitory FcγRs can modulate activation by the BCR, TCR and FcRε. ITIM phosphorylation of these inhibitory receptors leads to phosphatase recruitment, inhibition of the influx of extracellular Ca^{2+}, and attenuation of effector function (66, 68).

The balance between activating and inhibitory signals mediated by Fcγ receptors suggests that polymorphisms in FcγRs that alter affinity and/or function can have profound

phenotypic consequences. In terms of inherited risk for SLE, this could be important, since these receptors, along with complement, are crucial for the removal of circulating ICs, tissue deposition of which leads to release of inflammatory mediators and influx of inflammatory cells.

Allelic variants have been identified for the activating receptors FcγRIIA and FcγRIIIA that have differential binding avidities for different IgG isotypes. The *FcγRIIA* 131H/R alleles can be co-dominantly expressed and differ significantly in their ability to bind IgG_2: the 131H allele is high-binding and essential for clearing IgG_2 ICs, which are poor at fixing complement. While the distribution of these alleles is similar in both Caucasians and African Americans, the low-affinity R allele is much less frequent in Asians. Studies have implicated the low-binding R allele as correlating with specific SLE symptoms/age of onset in Caucasian, Hispanic, German, Korean, Thai and Taiwanese patients, but it remains inconclusive as to whether it represents an independent risk factor for SLE development (49, 71-80).

Similarly, the activating receptor FcγRIIIA 176V/F alleles, present at similar frequencies in both Caucasians and African-Americans, differ in their ability to bind IgG_1 and IgG_3, with 176V homozygotes displaying increased binding. Association between the low-binding 176F allele and SLE has been found in different studies in Caucasian patients and African-Americans, but not Hispanics (73, 75, 81). In addition, no significant associations were seen for Korean and Taiwanese patients in other studies (49, 78, 82).

Some analyses have also indicated that the association between the low-binding alleles of *FcγRIIA* and *FcγRIIIA* and SLE could be due to a haplotype effect, whereby

homozygosity for the 131R and 176F alleles confers increased risk, due to an additive impairment in the ability to clear IgG_1, IgG_2 and IgG_3 ICs (74, 80).

The inhibitory *FcγRIIB* gene is also considered a key SLE candidate gene, based on its unique ability to transmit inhibitory signals in both B cells (FcγRIIB1) and myeloid lineage cells (FcγRIIB2) (68). In addition, genetic ablation studies in the mouse support a role for FcγRIIb, as detailed later (67, 83). Indeed, association studies have suggested that the 232T (*vs.* 232I) genotype is significantly enriched in Japanese, Thai and Chinese SLE patients (84-86). The functional significance of this polymorphism remains undetermined. No association for the *FcγRIIB* 232T allele was seen in a study involving Swedish and Mexican patients (80).

It is also important to note that cytokines can differentially modulate the function and expression of the FcγRs: increased levels of IFNγ augment and decrease activating and inhibitory receptor expression respectively, while IL-4 has the opposite effect (68). Most of the studies described above detailed associations of the FcγR polymorphisms with particular lupus phenotypes, rather than susceptibility *per se*. Given this, one could speculate that polymorphisms in the true causal genes cause a cumulative alteration in the cytokine milieu and initiation of inflammatory events, which in turn alter the regulation of the FcγRs. These modulations in expression in turn may then be augmented by the intrinsic polymorphisms in the FcγRs, leading to earlier age of onset and increased severity of SLE phenotypes, and differential end-organ targeting.

CTLA-4 and PD-1

Consistent with the idea that polymorphisms in molecules key to balancing inhibitory *vs.* activating signals in the immune system may confer increased risk to SLE susceptibility, are studies implicating associations of polymorphisms in *CTLA-4* and *PD-1* with SLE. Supporting their candidacy as SLE susceptibility genes, both of these molecules function to negatively regulate T-cell receptor mediated signaling and are present in regions associated with SLE (2q33 and 2q37, respectively) (87).

The best studied negative regulator of T cell signaling is CTLA-4, and its association with various autoimmune conditions, including SLE, has been the subject of investigation by various groups, leading to the idea that it may be a 'general' autoimmune susceptibility gene (88). CTLA-4 is induced in T cells upon TCR-mediated activation and, along with CD28, can bind to CD80 and CD86 on APCs. While CD28 functions as a co-stimulatory molecule and provides 'signal 2' for naïve T cell activation, CTLA-4 acts as a negative regulator following primary T cell activation and helps in maintaining peripheral tolerance (89).

Some of the more studied SNPs for *CTLA-4* include four in the promoter (-1722T/C, 1661A/G, -658 and -318C/T), two in the transcript (+49A/G and +6230 G/A) and an $(AT)_n$ repeat in the 3' untranslated region (88). Like many association studies, the results are inconsistent between ethnic groups. Studies of only the *CTLA4* exon 1 SNP, +49A/G, saw no association in British-Caucasian, Japanese, and Italian patients, while in a cohort of Slovakian lupus patients, there was enrichment for the +49G allele (90-93). In another study of Japanese patients, the frequency of both the 49G SNP and the106 bp $(AT)_n$ repeat were found to be enriched, while no difference was seen in the frequency of the -318

polymorphism (94). However, similar studies in two other Asian populations, Korean and Taiwanese, saw no association with either the +49 or -318 polymorphisms (95).

In contrast, another study found that +49A and +6320G corresponded to a susceptibility haplotype in Spanish patients (96). The latter +6320G SNP is believed to be associated with an alteration in the ratio of CTLA4 alternative splice forms. The -1722T/T genotype was found to significantly enriched in an analysis of Korean patients, while the opposite association (-1722C) was found to be true in one study of Spanish patients (95). Analyses of recently diagnosed African-American and Caucasian lupus patients demonstrated no association with SLE for four SNPs (-1722, -1661, -318 and +49) by themselves. However, in the African-American cohort, the -1661G allele was found to be associated with an increased risk in younger patients and demonstrated a possible interaction with HLA-DR2 (97).

In terms of functional changes in CTLA-4, the percentage of $CTLA4^{+}$ T cells and serum levels of the soluble form of CTLA-4 (sCTLA4) have been reported to be increased in SLE patients (98, 99). Another study reported similar surface CTLA4 expression in patients and controls, but found an impaired inhibitory effect of CTLA4 in lupus T cells (100). These data cumulatively indicate that CTLA-4 is a legitimate candidate gene, but suggest that the true causal polymorphisms might not yet be identified and also may be highly population specific. Furthermore, finding true association of CTLA-4 polymorphisms with SLE may be facilitated by first identifying stable haplotypes within the different ethnic groups.

Programmed cell death-1 (*PD-1*) is a key candidate gene within a locus originally identified via whole-genome linkage analyses (101). PD-1 is a cell-surface receptor with

sequence homology to the CD28/CTLA4/ICOS molecules, all of which are involved in regulation of T cell signaling. It is believed that like the activating/inhibitory co-receptor pair CD28/CTLA4, which regulate the activation phase of naïve T cells, ICOS/PD-1 act to modulate responses in the activation and effector phases of activated T and B cells. It has been shown that engagement of PD-1 leads to inhibition of B cell activation, and inhibits both proliferation and cytokine production by CD4 and CD8 T cells *in vitro* (87). Further evidence for its involvement in negative regulation of signaling comes from studies of the PD-1 knockout (102, 103).

In humans, *PD-1* is found on 2q37, within a locus initially found linked to SLE in individuals of Nordic descent (101). Based on its location within the susceptibility locus, its known functional roles and the fact that PD-1 deficient C57Bl/6J (B6) mice develop a late-onset lupus phenotype, the gene was sequenced to identify SNPs and corresponding haplotypes. Significant association of a promoter SNP, termed the PD-1.3A allele, was found in European patients, most strongly in those of Nordic descent. This promoter polymorphism was further shown to prevent the transcription factor RUNX1 from binding, which could lead to aberrant regulation of PD-1 and hence affect negative regulation of signaling (104).

In a follow-up study from the same group, association with the PD-1.3A allele was again seen in another large cohort of Swedish and European-American patients (105). However, a study conducted in a sizeable Spanish population failed to find this association, and instead found the PD-1.3A allele increased in control samples. This discrepancy may be due to the genetic heterogeneity in the two sample populations, such that actual causal polymorphism and the PD-1.3 alleles form two different haplotypes within each population

(106). Finally, a study of a Danish cohort also revealed an association with PD-1. Instead of the PD-1.3 allele (termed 7146A in this study), which showed some signs of elevation in patients, correlation was seen with a new SNP (6867G). Interestingly enough, this SNP is found within a putative transcriptional repressor-binding site (107). Clearly, the association between PD-1 and SLE warrants further investigation.

PTPN22

Protein tyrosine phosphatases (PTPs) function to regulate the reversible tyrosine phosphorylation of signaling molecules following activation of various cellular pathways. *PTPN22* encodes the lymphoid-specific phosphatase LyP. LyP function has been primarily investigated in T cells, and it is known that it can inhibit TCR mediated signaling pathways via dephosphorylation of ZAP-70 and Src family protein tyrosine kinases. LyP has also been shown to interact with the kinase Csk and the ubiquitin ligase c-Cbl to mediate its inhibitory effects on T cells. Furthermore, it has been demonstrated that LyP has functions in attenuating both B cell and myeloid cell responses and signaling (108, 109).

Recent studies have demonstrated that a 1858C/T polymorphism in the *PTPN22* gene results in a non-synonymous R620W substitution, which disrupts the interaction between Lyp and Csk that normally leads to synergistic inhibition of T cell responses (110). Evidence that this gene may be involved in lupus susceptibility comes from the fact that the 1858T allele has been shown to be associated with two other autoimmune diseases, IDDM and RA, and because of its location within the 1p13, a region with weak linkage to SLE (110-120).

An analysis of one multiplex and two case-control SLE cohorts of Caucasian origin demonstrated an association between the *PTPN22* 1858T allele and SLE. Interestingly, this study also revealed a dose effect, with the risk conferred by the homozygous 1858T genotype being twice that seen for heterozygosity (121). A similar association of the 1858T allele and SLE was seen in a study of Spanish-Caucasian SLE patients. The lack of an allele-dose effect in this latter study may be due to the reduced number of individuals overall with the homozygous 1858T genotype (114).

The existing data does suggest that *PTPN22* polymorphisms could impact SLE susceptibility. It would be informative to extend these association studies to non-Caucasian groups, particularly Hispanic and African-American lupus patients, in which the 1858T allele frequency is known to be lower than in individuals of Caucasian origin (122).

IL-10

Cytokines serve as soluble modulators of immune function and the balance between different cytokines can influence the outcome of an immune response. It is well established that genetic variations causing differences in cytokine production can have significant effects on the ability to clear pathogens, due to induction of 'inappropriate' or 'ineffective' immune responses, and it is postulated that predisposition to autoimmunity may also be influenced by such genetically encoded differences (reviewed in (123)).

IL-10, encoded within 1q32.1, is a cytokine involved in limiting and terminating inflammatory immune responses and regulating the growth and differentiation of a wide variety of immune lineages, including CD4 T cells, B cells, NK cells and different myeloid

populations. Interestingly, several viral genomes encode for IL-10 homologs, including Epstein-Barr virus (EBV), a viral agent long associated with SLE (124).

IL-10 levels have been shown in different studies to be increased in SLE patients, as well as in family members of lupus patients and furthermore, *in vitro* IL-10 production by PBMCs from SLE patients is significantly elevated relative to normal controls (125-127). IL-10 antagonists have been shown to prevent spontaneous *in vitro* Ig secretion by PBMCs from lupus patients and increase *in vitro* PBMC proliferative responses (128). In a small study of six lupus patients, *in vivo* administration of an IL-10 antagonist for 3 weeks significantly decreased SLEDAI (SLE Disease Activity Index) scores up to 6 months following cessation of treatment (129).

The *IL10* gene promoter is highly polymorphic and includes both microsattelite repeats and SNPs. The association of these different polymorphisms and SLE has been somewhat inconsistent. Most studies have not seen an association between specific *IL10* promoter polymorphisms and SLE *per se*, but have instead reported association with specific clinical features of SLE in a diverse array of ethnicities including Southern Chinese, Caucasian, Taiwanese and Dutch (130-133). Two investigations have seen an association of a promoter microsatellite repeat in Italian patients, while a study of a relatively large cohort of Mexicans revealed no association (92, 134, 135). Furthermore, in the latter study, two-point linkage analysis of duplex-families revealed no linkage with the *IL10* gene (134).

The lack of clear and consistent associations makes it difficult to draw any definitive conclusions regarding the association of IL-10 and SLE. Similar to other genes, there is a compelling need to examine the prevalence of the various IL-10 promoter polymorphisms in

different ethnic groups in order to define extended haplotypes. These haplotypes can then be investigated in non-lupus patients for association with variations in IL-10 production. The cumulative data can then be used to more effectively look at association between IL-10 promoter polymorphisms and SLE in various ethnic groups.

Such an approach has been recently utilized in a study of Dutch-Caucasian and African-American lupus patients. SNP discovery was performed to identify extended haplotypes and their association with quantitative variations in IL-10 production. Interestingly, a promoter polymorphism associated with high IL-10 production was enriched in both normal and patient African-American patients. Given the higher susceptibility of African-Americans to lupus, it is worth speculating whether such a difference could in part underlie this increased risk. Another promoter polymorphism was specifically enriched in African-American patients *vs.* controls (136). A similar study of an extended promoter haplotype in a large cohort of Chinese lupus patients revealed significant association with a 'high IL-10 production' haplotype (137).

Linkage Analyses in the Study of SLE

Whole-genome linkage analyses are typically performed on families with at least two affected siblings and oftentimes include a pedigree of affected and unaffected extended family members. In such studies, which make no *a priori* assumptions regarding the locations or functions of susceptibility genes, the enrichment of specific alleles in lupus patients is compared to unaffected relatives and controls. The ability to perform whole genome-wide linkage studies in human lupus patients has been greatly facilitated in recent

years by the availability of dense maps of polymorphic microsatellite markers and more recently, single-nucleotide polymorphisms (SNPs) (3, 10, 138). Furthermore, the technology to easily, rapidly and reliably test for whole-genome linkages has markedly improved.

To date, a large number of independent, genome-wide linkage scans have been performed in multiplex lupus families and have identified at least 50 loci that show linkage to disease or specific clinical phenotypes (3, 139). There are four main groups collecting patient populations and conducting these linkage studies: the Oklahoma Medical Research Foundation (OMRF), University of Minnesota (MN), UCLA/USC and the University of Uppsala (UU). The pedigrees being analyzed by these groups differ in their ethnic compositions such that the OMRF and UCLA/USC studies have a large number of African-American (AA) and Hispanic Americans (HA) patients respectively, while the MN panel is mostly Caucasian/European American (EA). The first genome-wide linkage study conducted by UU comprised mainly of Icelandic (Ic) and Swedish (Sw) families, two populations considered relatively genetically homogenous, due to geographical location and population history (101). Their most recent study included Italian (It) and Argentinian (Ar) pedigrees as well (140).

The OMRF group has also recently conducted numerous genome-wide linkage analyses in subsets of their pedigrees stratified by particular clinical phenotypes, such as dsDNA, renal disease and thrombocytopenia. This is based on the idea that if the phenotypic disparity seen in lupus is a consequence of genotypic heterogeneity, then such stratification may increase the power to detect linkage. However, it must be kept in mind that repeatedly testing such sub-groups can lead to increased false-positive results (139).

A compilation of the various loci identified in the different genome-wide linkage studies conducted to date are presented in Tables 2 and 3. Only those loci that have met the guidelines set by Lander and Kruglyak in at least one study, (significance: LOD ≥ 3.3 and strongly suggestive of significance: LOD ≥ 2.2), are included (141). If supporting linkage from other independent, genome-wide studies is available, these are indicated as well. Studies that specifically verified previously identified linkages, in the absence of a complete genome-wide scan, are not included in this table (50, 142-145).

Of the loci that meet the criteria outlined above, eleven chromosomal regions (bold and underlined in Table 2) meet criteria for significant linkage in at least one study, with strongly suggestive supporting evidence from at least one other study. In addition, two loci (11p11-15 and 11q14) have been repeatedly linked in 2 or more OMRF stratified analyses. Eight loci have shown strongly suggestive linkage in at least one study, with supporting evidence from at least one other analysis (underlined in Table 3).

There are a few major points to be made regarding the results of the various human linkage studies conducted in SLE patients to date. The repeated and strong linkage to 1q22-24, which contains the *FcγR* complex, *Serum Amyloid P component* (*SAP*) and acute-phase reactant *C-reactive protein* (*CRP*), as well as the *SLAM/CD2* family of receptors, is especially intriguing, since the syntenic region in mouse has also been repeatedly implicated in murine linkage analyses. Also, this region appears to be linked to specific clinical phenotypes, such as renal disease and anti-dsDNA autoAbs, also observed in the syntenic mouse interval (146-150). Somewhat surprisingly however, despite repeated linkage to this region in the EA pedigrees from the OMRF group, the predominantly EA MN pedigrees

have not been even suggestively linked to this region (151, 152). Interestingly, the linkage to the 1q41-44 region, which has been seen by all three American groups, corresponds to the NZM2410-derived interval *Sle1d* ((153) and K. Tus *et al.*, *unpublished observations*).

Similar to the results of the association studies, linkage to the human HLA region in SLE has not been as overwhelming as that observed in other autoimmune disorders. However, strong linkage was seen for the 6p11-22 region, most strikingly in the combined MN cohort (151). Additional regions with strong linkage in multiple studies and ethnic groups include 2q32-37, 4p16-13 and 16q12-21 (12, 14, 16, 101, 140, 145, 151, 154-159).

Spontaneous Models of Murine Lupus

The overall complexity of the genetics of human SLE susceptibility has led many investigators to turn to murine lupus models, in order to better study genetic predisposition to the disease. These studies are greatly facilitated by the availability of both spontaneous and engineered mouse models in which lupus develops. The spontaneous models are particularly useful as they represent genomes, which through different breeding schemes, contain enough susceptibility genes so that their 'autoimmune potential' is maximized and the animals develop overt disease.

Linkage analysis has been a powerful tool in the identification of predisposing loci in these spontaneous lupus models. Since the 95% confidence intervals obtained for these loci contain hundreds of potential candidate genes, making functional identification of the causal gene challenging and providing little insight into the specific contributions of individual loci to the disease process, congenic dissection of these strains has proven invaluable. This

involves introgressing the susceptibility locus of interest onto a non-autoimmune prone background, such as B6, and assessing for clinical and immunological phenotypes mediated by this locus in isolation. Importantly, these congenic lines can then be used to generate recombinants for fine-mapping of the susceptibility locus.

In addition, lupus-like phenotypes have been observed in mice in which genetic ablation and transgenic over-expression of genes has been performed. Both the spontaneous and engineered models provide tools with which to better identify genes contributing to underlying genetic susceptibility (3, 10, 30).

In the next few sections, the classic spontaneous models of murine lupus, MRL.*lpr*, BXSB.*yaa*, [NZB X NZW]F_1 (BWF_1) and NZM2410 will be discussed.

MRL.lpr

The *lpr* mutation was originally discovered during the derivation of the MRL/MpJ strain, and on this background resulted in hypergammaglobulinemia, anti-dsDNA autoAbs, profound lymphadenopathy and splenomegaly, and immune complex (IC) mediated GN. MRL.*lpr* mice are also characterized by the emergence of an unusual $CD4^-CD8^-CD3^+B220^+$ T cell population. It was later discovered that *lpr* encodes for the apoptosis-signaling receptor Fas antigen, and that the mutation results in premature termination of *Fas* transcription (160).

The mechanism by which lack of Fas mediated signaling results in autoimmunity is postulated to be due to the emergence of self-reactive T and B cells that would normally undergo apoptosis during thymic, BM and peripheral selection events. However, the effect of the *lpr* mutation is highly background genome dependent, as evidenced by the varying

degrees of autoimmunity seen when it is introduced onto the non-autoimmune strains B6, C3H and AKR, illustrating the importance of contributions from the rest of the genome for full expression of disease. Furthermore, Fas-intact MRL mice develop a late-onset autoimmunity culminating in 50% mortality by 18 months, suggesting that *lpr* is an accelerating factor, as opposed to a causal mutation (161). Consistent with this, it has been demonstrated that $CD4^+$ T cells from Fas-intact MRL mice have an intrinsic hyperresponsive phenotype following engagement with high and low affinity peptide-MHC complexes and a lower threshold for CD3 mediated activation. This suggests that the varying effects of the Fas mutation on different backgrounds may be a consequence of strain-specific differences in the intrinsic responsiveness of the T cell compartment (162, 163).

Further insights into mechanisms leading to autoimmunity in the MRL.*lpr* strain come from studies investigating how genetic ablation of various molecules potentiate or ameliorate disease. It has been demonstrated that in the absence of such molecules like IFN-RI, the C3 inhibitory factor DAF (decay-accelerating factor), IL-10 and the co-stimulatory molecule CD80, various aspects of disease were exacerbated (164-167). In contrast, deficiency in a variety of molecules involved in immune functions, such as IFN-RII, CSF, LFA-1, Nrf2, Tdt, IL-2, IL-12p40, Factor B, CD28, CD86 and IFNγR, has been observed to confer a protective effect on particular disease phenotypes (164, 167-176).

It must be kept in mind that in many of these studies, the deficiencies were studied on mixed genetic backgrounds, which can significantly influence disease phenotypes. This was seen in the case of IL-18R, where, in contrast to a previous report on a less homogenous genetic background, deficiency of the IL-18R, and consequently IL-18 mediated signaling,

was found to have no effect on disease development (177). Deficiency of the common FcγR chain was also shown to have no impact on disease development (178).

Linkage analyses have been performed on the MRL.*lpr* strain in order to identify loci contributing to the strain-specific effects of the *lpr* mutation described above. Using [MRL.*lpr* X Cast/Ei]F_1 X MRL.*lpr* backcross animals, MRL-derived loci on chromosomes 7 and 12 (*Lrdm1-2*) were identified as contributing to renal disease (161). Another cross utilizing [MRL.*lpr* X B6.*lpr*]F_2 intercross progeny identified four loci with significant linkage to lymphadenopathy and/or splenomegaly on chromosomes 4, 5, 7, and 10, termed *Lmb1-4* respectively. *Lmb1-3* were also associated with anti-dsDNA autoAbs, while *Lmb4* was associated with GN (179).

An analysis of [MRL.*lpr* X Balb/C]F_2 mice revealed linkage for anti-dsDNA autoAbs with chromosomes 2 and 11(180). Other linkage studies have been performed to identify loci involved in the development of arthritis and collagen disease in the MRL.*lpr* strain, which has also been used as a model of polyarteritis, rheumatoid arthritis, Sjogren's syndrome and ALPS (Autoimmune Lymphoproliferative Syndrome) (181-184).

BXSB.yaa

The BXSB.*yaa* strain is a recombinant inbred strain derived from B6 and SB/Le. Due to the presence of the as yet unidentified *y-chromosome autoimmune accelerator* (*yaa*) locus, male mice from this strain spontaneously develop humoral autoimmunity to a plethora of self-antigens, and lupus nephritis, ultimately culminating in 100% mortality by 6 months of age. Analyses of different consomic strains, carrying the BXSB-derived y-

chromosome have revealed that the ability of *yaa* to mediate severe autoimmunity is, like *lpr*, highly dependent on interactions between it and other susceptibility loci from the autosomal genome (185). Moreover, the addition of *yaa* to a variety of F_1 crosses, in which the progeny are normally non-autoimmune, such as [NZW X B6]F_1s and [NZB X B6]F_1s, can lead to the development of significant systemic autoimmunity (185-187). Importantly, *yaa* on the B6 background does not lead to fulminant autoimmunity, and it has been postulated that the capacity of *yaa* to promote autoimmunity is dependent on the ability of the autosomal background to promote the spontaneous development of autoAbs (188).

The course of disease in BXSB.*yaa* males is highly similar to that seen in other murine lupus models. In addition to clinical signs of disease, such as GN and the emergence of IgG autoAbs specific for different self-antigens, the animals develop with age a profoundly activated immune system and hypercellularity of the spleen and lymph nodes (LNs). This is characterized by dramatic increases in the percentage of $CD4^+$ T cell having effector-memory ($CD62L^-CD45RB^{lo}CD44^{hi}$) and activated ($CD25^+$) phenotypes. The $CD4^+$ cells have been shown to be refractive to stimulation-induced proliferation *in vitro*, yet produced increased amounts of IFNγ and IL-4 and decreased IL-2 (189). Notably, decreased IL-2 production is also a feature of human lupus T cells (190-192). These changes in the functional responses of CD4 T cells are also characteristic of replicative senescence.

Treatment with CTLA-4 Ig prevented these different CD4 cell-surface and functional phenotypes, and reduced both GN and anti-chromatin ANAs, presumably via negative regulation of T cells, but cessation of treatment resulted in a return towards the effector-memory phenotype (193). BXSB.*yaa* mice lacking the cyclin-dependent kinase inhibitor

(CDKI) p21 showed increased survival and reduced GN and anti-chromatin IgG. CD4 T cells were the only lymphocyte population that showed phenotypic changes in both the spleen and LN, and were reduced in overall number and had a less activated phenotype. Importantly, these CD4s produced less IFNγ and more of the $CD4^{+}CD44^{hi}$ cells were undergoing apoptosis, incorporated BrDU and were in the G_1 *vs.* G_o phase of the cell cycle (194). Hence, it may be that preventing the accrual of these CD4 cells can ameliorate some of the more pathogenic and morbidity-associated phenotypes.

There are numerous B cell associated differences in BXSB.*yaa* mice as well, some of which appear to be specifically associated with the *yaa* locus, and are independent of the development of systemic autoimmunity. Resting splenic B cells from both BXSB.*yaa* and B6.*yaa* mice were shown to proliferate more in response to stimulation with PMA/Ionomycin (P/I), LPS, anti-IgM and anti-CD40 +/- anti-IgM. These data would suggest that *yaa* acts downstream of initial signaling events, and is not Ca^{2+} or PKC dependent. Since this difference in B cell responsiveness was seen in both BXSB.*yaa* and B6.*yaa*, it indicates that such a change is not sufficient for the development of autoimmunity. In contrast, similar experiments performed with purified T cells from young B6.*yaa* mice, found no differences in proliferative responses to various stimuli. This increased B cell responsiveness was not amplified with age, and by 5 months, similar to the CD4 T cells, the B cells showed reduced proliferative responses, which was also mitigated in BXSB.*yaa*|*p21*$^{-/-}$ mice (194, 195).

The ultimate goal of identifying the causal gene within a susceptibility locus is unusually confounded in the case of *yaa*. Most murine positional cloning efforts utilize naturally occurring meiotic recombination events and subsequent phenotypic

characterizations to narrow the locus to a susceptibility interval amenable for causal gene identification. This is not possible for y-chromosome located genes and investigators have utilized other approaches to help elucidate the nature of the *yaa* gene.

Mixed BM chimeric experiments have demonstrated that only *yaa* bearing B cells produce autoantibodies, and that the presence of *yaa* bearing T cells is not sufficient to make non-*yaa* bearing B cells make autoantibodies (196). Further studies using both mixed BM chimeric experiments and BXSB.*yaa*|$TCR\alpha^{-/-}$ mice implicated CD4 T cells as being necessary for severe disease, but demonstrated that these cells do not need to express *yaa* to mediate full-blown disease (197, 198). These data indicate that while CD4 T cells are necessary, only the B cells actually need to functionally express *yaa* for disease development to occur in this lupus model.

Despite the difficulties associated with identifying *yaa*, a variety of linkage studies have been conducted in order to determine what autosomal genes are interacting with it to mediate lupus. Analyses of [NZW X B6.*yaa*]F_1 X B6 males, so that NZW dominant genes impacting susceptibility could be identified, revealed a major dominant locus contributing to severe GN and anti-dsDNA IgG susceptibility on chromosome 7. Interestingly, while there was no significant linkage of either of these phenotypes to chromosome 17 by itself, there appeared to be interactions between the chromosome 7 locus and chromosome 17, such that heterozygotes at chromosome 7 and B6 homozygotes at chromosome 17 had the highest titres. Somewhat surprisingly, no significant linkage for these phenotypes was obtained with chromosome 1 (187).

A similar study of [NZB X B6.*yaa*]F_1 X B6 males mapped NZB-contributed GN susceptibility to chromosomes 1 and 13, but not to chromosomes 7 and 17. Interestingly, anti-DNA and anti-chromatin IgG mapped to an NZB contribution on chromosome 1, but B6 homozygosity at chromosome 17 (186).

Congenic analyses of various autosomal *yaa*-interacting loci, identified via such linkage studies, revealed some interesting findings. The chromosome 1 *Bxs1-4* loci, originally identified in [BXSB.*yaa* X B10]F_1 reciprocal backcrosses, were moved in various combinations onto the B10.*yaa* background, similar to that done for the NZM2410 loci *Sle1a-c* (see later sections).

Bxs1 appeared to impact kidney pathology in the absence of significant ANA production, similar to what is observed for the NZM2410 *Sle1d* locus (K. Tus *et al., unpublished obseravtions*). *Bxs2* specifically contributed to anti-dsDNA IgG, while the most centromeric locus, *Bxs4*, appeared to interact with *Bxs1*, to mediate moderate GN. It is evident, however, that the major BXSB derived locus on chromosome 1 is *Bxs3*, which can interact with *yaa* on the B10 background to recapitulate most, if not all, of the phenotypes observed in BXSB.*yaa* (199). Interestingly, *Bxs3* corresponds to the same genomic interval as the NZB- and NZM2410-derived loci *Nba2* and *Sle1* respectively, both of which can also interact with *yaa* on the non-autoimmune B6 background to generate systemic autoimmunity (186, 200, 201). A limitation in the interpretation of the above-described studies is that none of the *Bxs* chromosome 1 loci have been studied in the absence of *yaa* on the B10 background. Given the importance of epistatic interactions in the development of various

lupus phenotypes, it would be informative to assess the component phenotypes of individual loci.

Similar studies with the NZB-derived chromosome 1 and 7 loci, *Nba2* and *Nba5*, respectively, demonstrated that both these loci can interact with *yaa* on the B6 background as well, in both cases resulting in increased 15 month mortality and severe GN. Only B6.*Nba2*|*yaa* mice showed increased anti-DNA and anti-chromatin IgG relative to both female controls and B6.*yaa* (186). A detailed description of the effects of the interactions between *Sle1* and *yaa* on the B6 background will be presented in later sections, as well as in Chapter IV.

[NZW X NZB]F$_1$: Insights into MHC and non-MHC Susceptibility Loci

One of the most well characterized models of murine lupus is the F_1 progeny of the New Zealand Black (NZB) and New Zealand White (NZW) inbred mouse strains (BWF_1). These mice develop progressive severe GN and high levels of anti-nuclear antigen specific IgG autoAbs, similar to both BXSB.*yaa* and MRL.*lpr*, but unlike those models, no single gene mutation is necessary for full disease expression. Interestingly, neither parental strain develops severe lupus phenotypes, though each is associated with a late-onset mild autoimmunity, illustrating the importance of genetic interactions in the F_1 genome for full expression of lupus phenotypes (202).

As observed in the other spontaneous lupus models, a variety of immunological abnormalities are observed in BWF_1 mice. B cells from young BWF_1 mice demonstrate elevated expression of co-stimulatory molecules *ex vivo* and show increased IgM secretion,

proliferation and expression of co-stimulatory molecules following stimulation *in vitro* in response to both cytokines and CD40 cross-linking (203). Furthermore, using different IgM Tg systems, it was found that while BWF_1 mice had intact central B cell tolerance, the frequency of anti-dsDNA IgG producing follicular B cells was increased, even in the setting of a very restricted B cell repertoire, suggesting significant alterations in the peripheral selection mechanisms in these mice (204, 205). Ectopic expression of CXCL13, a B lymphocyte chemoattractant, has been observed in myeloid dendritic cells in the thymus, kidney and lungs of BWF_1 mice, as well as impaired and aberrant B1 trafficking (206-208). Treatment of BWF_1 mice with CTLA4 Ig was shown to decrease the expansion of autoreactive B cells, inhibit Ig class switch and decrease numbers of activated $CD4^+$ T cells, though this effect was not permanent (209).

Numerous linkage studies, utilizing a variety of different crosses, have been undertaken in order to identify susceptibility loci in the BWF_1 murine lupus model. Most of these studies have concentrated on assessing NZB contributions to disease. As recently reviewed, loci associated with suggestive or significant linkage were implicated on over 14 of the autosomal chromosomes (30). Consistent linkages have been observed with distal chromosome 1, mid-distal chromosome 4, chromosome 7 and the MHC region of chromosome 17, as described below.

Backcross analyses of $[BWF_1 \text{ X NZW}]F_1$ progeny revealed a strong linkage on chromosome 4, termed *Nba1* (*New Zealand black autoimmunity*) (210, 211). This interval was also implicated in an independent backcross study of similar design, and in an analysis of $[\text{SWR X NZB}]F_1$ X NZB backcross progeny (212, 213). Linkage studies of BWF_2

intercross progeny also identified a chromosome 4 locus, designated *Lbw2* (*Lupus-NZB X NZW)*, as being involved in mortality, GN and splenomegaly but not anti-chromatin autoAbs. Interestingly, genome wide linkage utilizing two different non-autoimmune, $H2^z$ congenic strains revealed that while chromosome 4 is linked to nephritis in [BALB.$H2^z$ X NZB]F_1 X NZB backcross progeny, it is not when B6.$H2^z$ is used instead of BALB.$H2^z$ (148). This latter study illustrates the impact genetic interactions with loci from the non-autoimmune strain can have in such crosses. Linkage to anti-chromatin autoAbs and nephritis was also seen on chromosome 4 in a study of [B6 X NZB]F_2 mice (214).

Like chromosome 4, chromosome 1 has been implicated in a number of different experimental crosses. An NZB derived locus, designated *Nba2*, has been mapped in [NZB X SM/J]F_1 X NZW, [B6.$H2^z$ X NZB]F_1 X NZB and [BALB.$H2^z$ X NZB]F_1 X NZB backcross and [B6 X NZB]F_2 progeny as contributing to nephritis, hypergammaglobulinemia, autoAbs and polyclonal B cell activation phenotypes (147-150). *Lbw7*, an NZB derived locus on chromosome 1 contributing to anti-chromatin autoAbs, was mapped in BWF_2 intercross progeny in the same region as *Nba2* (215). Evidence for NZW contributions to IgG autoAb production on chromosome 1 have also been revealed using [BALB/c X NZW]F_1 X NZW backcross progeny (216).

Mice made congenic for the NZB-derived *Nba2* interval on the B6 background, (B6.*Nba2*), break tolerance to chromatin, had increased percentages of $CD69^+$ B cells and increased *in vitro* IgM secretion (217, 218). The causal gene has been postulated to be *Ifi202*, an interferon-inducible gene showing differential expression, identified via microarray analyses. Sequencing of the promoter region of *Ifi202* revealed eight different promoter

polymorphisms between B6 and NZB, and the one at position 95 correlates with known expression differences between mouse strains. However, the congenic interval introgressed in the study was over 30 cM in length, and contains hundred of genes, making it impossible to definitively conclude that *Ifi202* is the causal gene within *Nba2* (218).

The third non-MHC region consistently implicated in multiple studies is chromosome 7. In BWF_2 intercross progeny, the chromosome 7 locus *Lbw7*, was linked more strongly with heterozygosity than with NZB or NZW homozygosity, and similar results were observed in BWF_1 X NZB backcross progeny as well (215, 219). A dominant NZB chromosome 7 contribution, *Nba3*, was identified as contributing to nephritis and autoAbs in [NZB X SM/J] F_1 X NZW and [BWF_1 X NZW] backcross progeny respectively (147, 211).

Linkage of the murine MHC on chromosome 17 with lupus susceptibility, similar to the obervation in human studies, has proven to be very complicated and background specific. Studies of the BWF_1 model, which has a heterozygous MHC genotype, have implicated separate strong contributions from both $H2^d$ (NZB) and $H2^z$ (NZW). Analysis of BWF_2 intercross progeny identified *Lbw1* on chromosome 17, where $H2^{d/z}$ heterozygosity conferred increased risk for mortality, GN and anti-chromatin Abs (215). Linkage of various lupus phenotypes to MHC heterozygosity has also been observed in BWF_1 X NZW, BWF_1 X NZB and [BALB/c X NZW]F_1 X NZW backcross progeny (211, 212, 216, 219). In contrast to chromosome 4, [B6.$H2^z$ X NZB]F_1 X NZB backcross progeny showed linkage to the MHC, but when BALB.$H2^z$ was used this association was not observed, again illustrating the importance of non-MHC background loci in these two crosses (148). In addition, B6 MHC contributions were observed in linkage studies of [B6 X NZB]F_2 progeny, where maximum

susceptibility was observed for $H2^{b/b}$ (214). No MHC effect was observed in [NZB X SM/J] F_1 X NZW backcross progeny, indicating that $H2^{z/d}$ and $H2^{z./v}$ confer equal risk (220).

In order to evaluate the risk conferred by the Class II IE^z in the development of lupus, linkage analysis comparing [B6.$H2^z$ X NZB]F_1 X NZB and [B6.IE^z X NZB]F_1 X NZB backcross progeny was undertaken. In the latter cross, B6 mice express transgenic Class II IE^z, but have no other $H2^z$ contributions. No linkage was observed with transgenic Class II IE^z expression and lupus nephritis development, though the previously observed MHC association was again seen in the control [B6.$H2^z$ X NZB]F_1 X NZB backcross progeny (221). A similar lack of association was observed when C57BL/10 (B10) mice expressed a transgene for class II IA^z (222). This suggests that Class II IA^z and IE^z are not the culprit genes within the MHC and that mixed haplotye effects cannot explain the increased susceptibility observed in BWF_1 mice, as has been long postulated.

NZM2410 and the Congenic Derivatives

The major difficulty associated with studying the BWF_1 model of lupus, the spontaneous model most reminiscent of human lupus in terms of both disease phenotypes and underlying genetic complexity, is the fact that the hybrid genome is required for disease expression. This prevents the full utilization of the major advantage in using the mouse for the study of complex traits: the genetic uniformity of inbred mouse strains. Fortuitously, a series of 27 inbred strains, termed the New Zealand Mixed (NZM) strains, were derived from [NZB X NZW]F_1 X NZW backcross progeny, and show varying degrees of susceptibility to SLE (223).

The NZM2410 (NZM) strain is one of the most severely affected BWF_1 derivatives and spontaneously develops autoAbs by 4-6 months and lupus nephritis with 80% penetrance by six months. Linkage analyses of [NZM X B6]F_1 X NZM (BC_1) progeny were performed to map recessive NZM loci linked to GN and anti-dsDNA IgG production. Three NZM loci were found to be linked to GN susceptibility: *Sle1*, *Sle2* and *Sle3* on chromosomes 1, 4 and 7 respectively. Heterozygosity at a locus on chromosome 17, initially termed *Sle4*, was found to be associated with GN. This study also demonstrated that the incidence of disease correlated with the number of susceptibility loci that had segregated in the BC_1 progeny according to a threshold liability model, the first such demonstration in an animal model of autoimmunity (146).

Subsequently, a [NZM X B6]F_1 intercross was performed to identify dominant NZM genes contributing to GN and humoral autoimmunity, the effects of which would have been masked in the original BC_1 study. The age of GN onset in these F_2 animals was more delayed than in the BC_1 progeny, consistent with the recessive inheritance of loci contributing to this phenotype. This study again identified linkage for *Sle1* and *Sle3*, as well as a new locus on chromosome 7 termed *Sle5*, but not for *Sle2* and *Sle4* (224). In order to study component phenotype of these loci, each was introgressed onto the B6 background and studied as a B6.*Sle* strain.

Congenic Dissection of NZM2410

B6.*Sle1* mice were found to develop a progressive loss in tolerance, such that by 9-12 months, they made high titres of anti-chromatin IgG, as well as some degree of anti-dsDNA

IgG autoAbs, but did not develop GN (225-227). In addition, the mice developed mild splenomegaly and an age-associated increase in activated splenic B and T cells. Despite this intrinsic activation phenotype, B and T cells were shown to have normal *in vitro* proliferative responses to different stimuli and *in vivo* IgM and IgG responses to T dependent antigens. Furthermore, lymphocytes from B6.*Sle1* mice had comparable rates of spontaneous and receptor-engagement induced apoptosis (225, 226).

Mixed BM chimera experiments have revealed that *Sle1* is expressed in a BM-derived population and that the ability of a B cell to produce anti-chromatin autoantibodies and express an increased activation status is contingent on the B cell expressing *Sle1* (228). Subsequent experiments, using B6.*Sle1*|*TCR*$\alpha^{-/-}$ and B6.*Sle1*|μMT mice, revealed that conventional T cells were not required for the increased levels of total, anti-chromatin and anti-ssDNA IgM, or for the manifestation of cell-surface B cell activation phenotypes, but were required for the generation of high-titred IgG autoantibodies. In the absence of B cells, there were still increased percentages of activated CD4 T cells, which produced increased IFNγ in response to P/I stimulation (229). These data suggested that *Sle1* is expressed functionally at the level of both the B and T cell.

Fine-mapping of the *Sle1* locus revealed that this locus is actually a cluster of functionally related sub-loci termed *Sle1a-1d*. All of these loci, with the exception of *Sle1d*, are associated with varying degrees of humoral autoimmunity, with B6.*Sle1b* mice recapitulating most of the phenotypes observed for the entire locus, making it the most potent of the sub-loci (153). It has been proposed that the causal gene for the *Sle1c* locus is the

complement receptor *Cr2/Cr1*, as the allele from *Sle1c* has a novel glycosylation site that results in lowered functional responses to low and intermediate stimuli (230).

Fine-mapping and subsequent sequencing of the *Sle1b* interval linked extensive functional polymorphisms in the SLAM/CD2 family of genes with the autoimmune phenotypes of B6.*Sle1b* (231). Each family member is expressed in a specific set of immune cell lineages, and their expression can be altered by different stimuli, including antigen and Toll-like receptor (TLR) triggering, and cytokines. Studies have demonstrated that this family can impact numerous immune functions, including macrophage, NK and T cell activation, cell-cell interactions, cytokine secretion, and cytotoxicity (232, 233). Altogether, these data strongly indicate that the SLAM/CD2 family has the ability to modulate immune responses in a highly flexible fashion and hence may function as 'fine-tuners' of the immune response (reviewed in (234)).

It was also shown that the *Sle1b* SLAM/CD2 family haplotype is the more prevalent version in both non-autoimmune and autoimmune-prone laboratory mouse strains, and that only in the context of the B6 genome does this haplotype elicit autoimmunity, indicative of epistatic interactions (231). Further work has revealed that both haplotypes are being maintained in natural, outbred mouse populations and appear to be under balancing selection, supporting the idea that common variants can mediate autoimmunity in appropriate genomic contexts (N. Limaye *et al*., *unpublished observations*).

Characterization of the NZW-derived *Sle3/5* locus initially revealed primarily T cell phenotypes, including elevated CD4:CD8 ratios and increased CD4 T cell activation and proliferative responses, but reduced activation-induced cell death (AICD). With age, splenic

B cells showed increased expression of Class II, CD86 and CD44, and produced anti-chromatin autoAbs. Unlike B6.*Sle1*, there was no evidence for splenomegaly in aged mice, but the spleens did show an age-dependent change in splenic architecture. Despite the low-grade IgG humoral autoimmune response, these mice had a GN penetrance of ~20% (235).

Mixed BM chimera experiments revealed that, like *Sle1*, *Sle3/5* needs to be expressed in a BM-derived, radiation-sensitive population. Interestingly however, non-*Sle3/5* bearing T and B cells can express the phenotypes associated with this locus, such as elevated CD4:CD8 ratios and the production of anti-chromatin autoAbs, provided they develop in the presence of *Sle3/5* bearing BM. This suggested that *Sle3/5* is expressed in a non-B cell APC population or that *Sle3/5* T cells have both autocrine and paracrine effects (236). This has been subsequently shown to be a consequence of hyperstimulatory DCs and macrophages, that had more activated phenotypes, were less apoptotic, more pro-inflammatory and were more effective co-stimulators (237).

In contrast to *Sle1* and *Sle3/5*, the phenotypes associated with the chromosome 4 locus *Sle2* were very B cell specific. There was no evidence of splenomegaly, lympdenopathy, or changes in T cell percentages, activation status or functional response. The B cells however, were larger, had elevated activation marker expression, secreted increased levels of IgM and were more responsive to different stimuli *in vitro*. Both T-independent and T-dependent IgM *in vivo* responses were heightened, while there was no change in the secondary IgG response, consistent with *Sle2* not affecting the T cell compartment (238).

Starting at an early age, there was an increase in the peritoneal cavity (perC) B1a population in B6.*Sle2* mice, with a concomitant decrease in the conventional B2 population, which was also seen in the spleen at an older age. This B1a expansion was independent of the housing conditions of the mice and was recently shown to be CD5 independent (238, 239). Mixed fetal liver chimeras, the early source of the B1a population, further revealed that *Sle2* must be expressed in the B cell for this B1a expansion to occur (239).

Congenic dissection hence allowed the complex, polygenic lupus phenotypes characteristic of the NZM2410 strain to be broken down and 'assigned' to a specific chromosome interval. Careful characterizations of the various B6 congenic lines have revealed a variety of phenotypes, many of which are indicative of an overall heightened responsiveness to stimuli. This suggests that a more self-reactive immune system may be a consequence of the fact that the different immune cell populations bearing these susceptibility alleles are more prone to respond.

The above studies also clearly demonstrate that by themselves on the B6 background, none of these susceptibility loci are sufficient to mediate systemic autoimmunity. Based on the original modeling analysis, which demonstrated that disease liability increased as a function of the number susceptibility alleles present (146), it was predicted that combining these loci would reconstitute the severe lupus phenotypes associated with NZM2410. To test this hypothesis, a series of bi- and tri-congenic lines were created in order to assess the role of their different genetic interactions in the development of disease, as detailed below.

Epistatic Interactions in the Development of Pathogenic Autoimmunity

The combination of *Sle1* and *Sle3/5* on the B6 background resulted in significant humoral and pathogenic autoimmunity, much greater than what would be predicted by the phenotypes of these loci in isolation. By 9-12 months of age, these mice had significant mortality, 75% penetrance of GN, severe splenomegaly and increased reactivity to a spectrum of chromatin components, as well as increased glomerular basement membrane (GBM)-binding autoAbs. There were also increased percentages of both B and T cells expressing activation and effector-phenotype markers in the spleen (240). In contrast, B6.*Sle1*|*Sle2* mice had a slight increase in mortality (18%) with a low penetrance of proliferative GN, but like B6.*Sle1*|*Sle3/5* mice had spleen weights comparable to NZM2410. In addition, the level of humoral autoimmunity was not very high in this bi-congenic line and was similar to that seen in B6.*Sle1* (201).

These data indicate that the degree of epistatic interaction between *Sle1* and *Sle3/5* is higher than that seen between *Sle1* and *Sle2*. It is tempting to speculate that this may be due to the fact that in the former combination both loci have effects on both T and B cells, while this is not true for *Sle2* in the latter combination. Interestingly, the combination of *Sle2* and *Sle3* on the B6 background does not result in phenotypes significantly different from the parental congenics, suggesting that these loci do not epistatically interact in a multiplicative fashion. The kidneys from this particular bi-congenic combination, however, display numerous hyaline deposits and mesangial lesions. These types of kidney pathology are not observed in the parental congenic strains and are almost indistinguishable from that seen in NZW (201).

While *Sle1* and *Sle3/5* are sufficient to mediate a high degree of fatal lupus nephritis on the B6 background, the combined effects of these loci does not fully recapitulate the severity and kinetics of disease observed in NZM2410. The combination of *Sle1*, *Sle2* and *Sle3/5* on the B6 background, however, results in fully penetrant lupus nephritis. The degree of proliferative lesions, splenomegaly and 5-month anti-dsDNA IgG autoantibodies was in fact higher than that seen in NZM2410 (201). In addition, B6.*Sle1*|*Sle2*|*Sle3/5*, like NZM2410, accumulate long-lived splenic plasma cells that do not migrate normally in response to CXCL12, with a corresponding absence of BM plasma cells (241). These data demonstrate that this combination of NZM2410 loci, originally identified via linkage analyses, fulfill the genetic equivalent of Koch's postulates, as they are sufficient to reconstitute the development of fatal lupus nephritis on the non-autoimmune B6 background.

Sle1, *Sle2* and *Sle3/5* were also individually combined on the B6 background with the BXSB-derived y-chromosome locus, *yaa*, to test the degree of epistatic interactions between this amplifying locus and the NZM2410-derived lupus susceptibility loci. Interestingly, only *Sle1* interacts epistatically with *yaa*, culminating in fatal lupus nephritis and immunological characteristics similar to BXSB.*yaa*, while *yaa* combined with either *Sle2* or *Sle3/5* does not result in significantly different phenotypes from those observed by these loci in isolation (200, 201).

What stands out from these different studies is the necessity for the break in tolerance to chromatin, mediated by *Sle1*, for the development of pathogenic and systemic autoimmunity. Only the bi-congenic combinations in which *Sle1* is present (*Sle1*|*Sle2*, *Sle1*|*Sle3/5* and *Sle1*|*yaa*) resulted in significant potentiation of autoimmunity. This suggests

a multi-step pathway for the development of autoimmunity as illustrated in Fig. 1. This model postulates that a key step for the initiation and development of pathogenic autoimmunity is mediated by loci like the *Sle1a-c* sub-loci, all of which mediate a loss in tolerance to chromatin and are associated with minimal pathogenicity. It is believed that these loci modulate immune cell interactions, antigen clearance and response to antigen. This can be considered similar to the phenotype of seropositivity seen in first-degree relatives of SLE probands.

Genes such as *Sle2*, *Sle3/5*, *lpr* and *yaa* amplify and interact with the pathways modulated by the 'first-step' genes, via unknown mechanisms, resulting in the development of pathogenic autoimmunity. It may be postulated that the genes encoded by these loci might contribute to overall immune responsiveness and these particular allelic variants result in slightly dysregulated immune function on a non-autoimmune prone background.

The final class of susceptibility genes, such as *Sle1d*, *Sle6* and *FcγrIIb*, are believed to potentiate end-organ damage, via a variety of mechanisms such as modification of effector functions, increase in inflammatory processes or an alteration of end-organ susceptibility. This last class of genes may be responsible for the wide diversity in clinical end-organ pathogenesis seen in human lupus patients.

Epistatic Interactions in the Suppression of Pathogenic Autoimmunity

The importance of epistatic interactions in the development of autoimmunity is clearly exemplified by the amplified phenotypes elicited when different susceptibility loci are combined. The demonstration that *Sle1*, *Sle2* and *Sle3|5* are necessary and sufficient on the

B6 background to reconstitute the fatal autoimmunity seen in NZM2410, while validating the results of the original linkage analysis, also begets an important question. Since *Sle1*, *Sle3/5* and part of *Sle2* are derived from the non-autoimmune NZW parent of NZM2410, why does the NZW strain not develop penetrant and fatal lupus nephritis?

A genome wide analysis of [B6.*Sle1* X NZW]F_1 X NZW backcross progeny was conducted in order to identify putative, recessive epistatic suppressive modifiers. These analyses revealed four recessive *Sles* (*SLE suppressor*) loci: *Sles1*, *Sles2*, *Sles3* and *Sles4* on chromosomes 17, 4, 3 and 9 respectively, where B6/NZW heterozygosity was associated with increased susceptibility. Multivariate analysis of disease penetrance as a function of suppressive alleles supported the hypothesis that the cumulative effects of these four loci accounted for the lack of autoimmunity in NZW (242).

The described linkage analyses identified the chromosome 17 locus *Sles1* as strongest of the four suppressive modifier loci. Introgression of *Sles1* onto B6.*Sle1*, B6.*Sle2* and B6.*Sle3/5* was performed, via marker-assissted selection, to test its ability to modulate the various phenotypes associated with each of the single congenics. Interestingly, *Sles1* was able to completely suppress the anti-chromatin IgG autoAbs and increased B cell CD86 expression of *Sle1*, yet had no effect on the increased perC B1a/B2 ratio and anti-dsDNA IgG phenotypes of *Sle2* and *Sle3/5* respectively (242). This is consistent with the nature of the original linkage analysis, which was designed to identify suppressive modifiers in the context of *Sle1* homozygosity.

Impressively, when B6.*Sle1*|*Sles1* is crossed to NZW, instead of the severe GN, high autoAb titres and splenomegaly seen in [B6.*Sle1* X NZW]F_1 progeny, the mice have no

autoimmune phenotypes (242). These data indicate that homozygosity at *Sles1* is sufficient to suppress the autoimmunity elicited by homozygosity at *Sle1* in this particular lupus model, and that *Sles1* interacts specifically with *Sle1*. It is important to note, however, that in the BC_1 progeny, a percentage of the mice that are NZW homozygous at *Sles1* still develop fatal GN, again illustrating the importance of additional epistatic interactions in the modulation of these phenotypes. Furthermore, the lack of anti-dsDNA IgG suppression, in the B6.*Sle3/5*|*Sles1* bicongenic, would indicate that *Sles1* is not a global suppressor of humoral autoimmunity.

Insights into Lupus, Pathways and Epistasis from Genetically Manipulated Models

The ability to manipulate the mouse genome provides powerful tools with which to understand the functions of genes, classically either via transgenic over-expression or genetic ablation. Such systems have provided tremendous insight into the requirements for the expression of different molecules in the development and functional responses of the various lineages and subsets of the immune system. The utility of such models in the analysis of SLE susceptibility would be expected to be more limited, as the causal mutations for such a complex genetic trait are predicted to be minor polymorphisms resulting in slightly altered function, rather than complete ablation or aberrantly high over-expression (18). However, such knockouts and transgenics can provide insight into the requirement for certain molecules, for example cytokines, in the development of various phenotypes when introgressed onto spontaneously autoimmune strains, as has been detailed in the previous sections.

Interestingly, and somewhat surprisingly, a number of strains with targeted deletions of different molecules, involved in a variety of cellular functions, upon aging develop lupus-like phenotypes, such as GN and autoAb production (243). While many reflect a legitimate alteration of the pathways leading to autoimmunity, recent work has demonstrated that in many cases these late-onset autoimmune phenotypes may be a consequence of epistatic interactions between the 129 genome, derived from the ES cell in which the targeted deletion was made, and that of B6, the strain that many of knockouts are bred onto. Further proof of this comes from the fact that the SLE phenotypes oftentimes disappear when moved onto pure backgrounds.

In the next section, the various genes implicated by either knockout or transgenic technologies as influencing the development of systemic autoimmunity are organized according to pathways relevant to their function. Any evidence for the background genome impacting the autoimmune effects is discussed as well. In addition, Table 4 provides information regarding their murine and human chromosomal locations, the strain of origin of the ES cell used (for knockouts), the background genome used, and any modulations in phenotypes observed when studied on different backgrounds.

Antigen and Immune Complex Clearance

The components of the complement pathway play important roles in both the clearance of immune complexes and the determination of activation thresholds in lymphocytes. Hence, it has been postulated that complement deficiencies lead to an autoreactive B cell repertoire, perhaps due to altered peripheral tolerance (22). While

deficiencies in the early components of complement, C1q and C4, act in an almost monogenic fashion to mediate SLE in humans, the data from murine studies is less definitive and much more dependent on background genome effects (41).

The effects of c1q deficiency have been investigated on the B6/129 F_2, and the pure 129, B6 and MRL (Fas intact) backgrounds and provide clear examples of background genome effects. On both the pure B6 and 129 backgrounds, c1q deficiency did not lead to either autoAb production or GN (38, 244). However, *c1q*$^{-/-}$ B6/129 F_2 mice developed both autoAbs (54%) and severe GN (25%), significantly higher than that seen in B6, 129 and WT B6/129 F_2 controls. However, of the WT B6/129 F_2 controls, 33% developed IgG autoAbs and 4% GN, both of which were not observed in the parental B6 and 129 strains, clearly demonstrating the epistatic interactions occurring between these two genomes (244). On the autoimmune prone MRL background, c1q deficiency led to increased mortality, GN, autoAb production, larger spleen weights, monocytosis and increased B and T cell activation phenotypes, with a concomitant increase in plasma cells (36, 38). These data illustrate that the lack of c1q serves to amplify an existing predisposition to autoimmunity.

In the case of C4 deficiency, while the severity of the phenotypes varied, on all backgrounds some autoimmune phenotypes were present relative to appropriate controls. When compared with WT B6/129 F_2 controls, *C4*$^{-/-}$ mice had IC mediated GN, elevated autoAb titres, splenomegaly, increased activated B and T cells and CD11b^{+} percentages (39). When a separate study examined the effects of C4 deficiency on the B6, B6/129 F_2 and [B6X129] F_1 X BALB/c backgrounds, in all cases, relative to WT controls, the C4 deficient mice had increased anti-dsDNA autoAbs (37).

Serum amyloid P component (SAP) has been shown to bind, in a Ca^{2+} dependent manner, chromatin on the surface blebs of apoptotic cells and in nuclear debris (245-249). This functional data suggests that Sap could play an important role in efficient removal of key SLE self-antigens. The results of the targeted disruption of the *Apcs* gene, which encodes for SAP, are very similar to that seen for C1q: highly background specific effects on lupus phenotypes. The first study examining *Apcs*$^{-/-}$ mice on the B6/129 F_2 background, showed an increase in anti-chromatin and anti-dsDNA autoAbs and GN relative to WT F_2 controls (250). A follow-up study examining the lack of SAP on the pure B6 and 129 backgrounds demonstrated that while on the B6 background *Apcs*$^{-/-}$ mice had increased autoAbs and increased incidence of GN (75%), there was no 'lupus' phenotype on the 129 background. Furthermore, transgenic expression of human SAP did not prevent the development of the SLE phenotypes on the B6 background, suggesting that the mutation *per se* may not be causal (251).

A second study examining the lack of Sap on B6/129 F2 progeny demonstrated that in WT F_2 mice, if the chromosome 1 interval was fixed as 129 and compared to *Apcs*$^{-/-}$ mice of the same background, there were no differences in the anti-chromatin autoAbs between the two groups (252). These data clearly indicate that the chromosome 1 segment derived from 129 has the potential to mediate loss in tolerance to chromatin on the appropriate background, independent of the effects of targeted deletion of Sap. This was further supported by the break in tolerance to chromatin seen two independently derived 129 chromosome 1 congenic lines on the B6 background (231, 252). As previously mentioned, this 129 interval includes the same SLAM/CD2 family halpotype as that seen in *Sle1b*,

demonstrating the functional equivalency of this region from both strains in mediating a humoral autoimmune phenotype.

Intriguingly, the second F_2 study demonstrated that the in both WT and knock-out F_2 mice, a B6 interval on chromosome 17, encompassing the *Sles1* region, had suggestive association with increased GN susceptibility (252). Since 129 and B6 share the same MHC halpotype, (in particular Class II alleles) and the fact that 129 mice are non-autoimmune despite an autoimmune promoting SLAM/CD2 family halpotype, this suggests that like NZW, a suppressive modifier allele may be harbored within the 129 MHC region. Data supporting this hypothesis will be presented in Chapter III.

Two other molecules for which roles in 'antigen clearance' has been postulated to explain the lupus phenotypes seen in their absence are the nuclease DnaseI and the membrane tyrosine kinase c-mer. DnaseI is a nuclease expressed at sites of high cell turn-over such as the gastrointestinal tract, skin and haematopoietic system, and *DnaseI* deficient B6/129 F_2 mice developed higher autoAbs than that observed in WT controls, while the incidence of GN was not significantly increased (253). The effects of this mutation on a pure background have not been reported. The membrane tyrosine kinase c-mer regulates macrophage cytokine profiles and indirectly binds phosphatidyl serine. On the B6 background, *c-mer*$^{-/-}$ mice had decreased *in vitro* and *in vivo* phagocytosis of apoptotic cells, increased titres of autoAbs of various specificities and increased TNF-α production (254). This increase in pro-inflammatory cytokine production, coupled with impaired apoptotic clearance, may be responsible for the increased humoral autoimmune phenotype.

Regulation of Proliferation and Apoptosis

The canonical examples of defects in the regulation of apoptosis leading to the development of lymphoproliferation and lupus-like autoimmunity are the spontaneous *lpr* and *gld* mutations, which encode for Fas and FasL respectively, as previously described.

Gadd45α (growth arrest and DNA damage-inducible) has roles in various cellular processes including cell growth and apoptosis, is regulated by the tumor suppressor gene p53 and is expressed in many tissues, including resting T cells. It also interacts with the cyclin-dependent kinase, p21, which is involved in the inhibition of cell cycle progression (255, 256). Targeted deletion of *Gadd45α* and *p21*, both on the B6/129 F_2 background, revealed similar phenotypes, including increased mortality, GN and autoAb production, and these effects were exacerbated in the absence of both genes. Both knock-outs had increased T cell numbers, but their responses to various T cell stimuli differed. While *Gadd45α*$^{-/-}$ mice had increased proliferative responses to TCR stimulation in terms of both kinetics and magnitude, *p21*$^{-/-}$ mice had increased responses only to IL-2, while both phenotypes were seen in the double knock-out. These data indicate that p21 and Gadd45α act to negatively regulate cytokine-induced and TCR-mediated T cell proliferation respectively. Notably, they both normally act via inhibiting cell-cycle progression but not via increasing apoptosis. Neither targeted-deletion impacts the B cell compartment (255, 257).

The protein tyrosine phosphatase Pten has been shown to play a role in proliferation, differentiation and apoptosis. In the absence of Pten activity, there was increased activation of the survival-promoting factor protein kinase B (PKB/Akt) due to increased phosphatidylinositol 3-kinase (PI3K) activity. While *Pten*$^{-/-}$ mice are embryonic lethal, it has

been demonstrated that Pten haploinsufficiency on the B6/129 F_2 background background led to a severe lymphoproliferative disorder with increased mortality, IC mediated GN and increased autoAbs. These mice also showed an expansion of splenic CD4 T cells, increased peripheral B and T cell activation and Fas expression, with impaired AICD and responsiveness to Fas stimulation (258). Furthermore, Pten deletion specifically in either B or T cells, resulted in autoAb production, hypergammaglobulinemia, hyperproliferation and resistance to apoptosis. Interestingly, lymphocyte specific Pten deletion was not reported to result in increased GN (259, 260).

Consistent with the idea that increased cell-survival mediated by the PI3K/Akt axis can increase susceptibility to autoimmunity was the demonstration that T cell specific expression of a constitutively active form of PI3K led to IC mediated GN, autoAbs and an expansion of the CD4 compartment. These T cells developed an effector-memory phenotype and *in vitro* display increased survival and decreased cell death (261).

Protein kinase C δ (PKCδ) has been shown to be involved in apoptosis and the inhibition of cell differentiation and growth, and PKCδ deficiency on the B6/129 F_2 background led to GN and autoAb production. *Pkcδ*$^{-/-}$ mice had an expansion in their peripheral B cell population, and B cells *in vitro* displayed increased proliferative potential and IL-6 production (262). Similarly, genetic ablation of a member of the E2F family, E2F2, involved in regulation of cell-cycle, differentiation and apoptosis, resulted in GN, splenomegaly and serum autoAbs on the B6/129 F_2 background. T cells from *E2f*$^{-/-}$ mice showed increased proliferation *in vivo* and *in vitro*, with no change in responses to apoptotic stimuli. A matter of some concern regarding the studies on the *E2f*$^{-/-}$ mice is that the authors

report WT F_2 spleen weights in excess of 650 mg by 8-12 weeks of age, making interpretation of 'splenomegaly' a difficult issue (263).

Members of the Bcl2 family of molecules have also implicated dysregulation of apoptotic processes in lupus. Transgenic overexpression of the cell-survival promoting Bcl2 in B cells led to IC mediated GN and serum autoAbs, with B cell accumulation in the BM and periphery. Interestingly, these B cells had a quiescent phenotype indicative of increased survival but not proliferation (264). Similarly, the absence of Bim, a pro-apoptotic member of the Bcl2 family, on the B6/129 F_2 background, resulted in GN, splenomegaly and autoAbs, with elevated numbers of both B and T cells (265).

Lymphocyte Signaling

Early indications that aberrations in proximal signaling molecules can influence the development of autoimmunity came from studies of mice deficient in the Src family protein tyrosine kinase (PTK) Lyn. Despite a significant reduction in peripheral B cells and impairment in BCR mediated signaling, *Lyn*$^{-/-}$ mice developed GN, splenomegaly, IgG autoAbs and increased total IgM and plasma cells (266, 267). Additional deletion of another Src family PTK, Fyn, resulted in decreased survival, presumably due to the increased kidney disease seen in the double knock-out (268).

In the case of the receptor protein tyrosine phosphatase CD45, targeted knock-in of a mutation that prevents negative regulation of CD45 signaling, led to IC mediated GN, splenomegaly and serum autoAbs in an allele dose-dependent fashion, with concomitant activation of both B and T cells (269). These data suggest that the lack of the inhibitory

functions normally mediated by these molecules can result in the development of systemic autoimmunity on the appropriate genetic background.

The impact of deficiency in the inhibitory FcγR, FcγRIIb, on the development of autoimmunity, has a highly background dependent effect. On the mixed B6/129 F_2 and on the pure BALB/c backgrounds, *Fcγr*$IIb^{-/-}$ mice did not develop autoimmunity. However, on a pure B6 background FcγRIIb deficiency led to mortality, GN, splenomegaly, and autoAb production, as well as an activated lymphocyte population. In fact, with the exception of mortality and GN, B6.*Fcgr*$IIb^{-/-}$ mice had phenotypes almost identical to that seen for B6.*Sle1b* (67). The *Fcγr* gene cluster is just proximal to the *Slam/Cd2* family on chromosome 1, and 129 shares the same haplotype as that seen in *Sle1b* (231). It is hence tempting to speculate that the increased mortality and GN seen in B6.*Fcgr*$IIb^{-/-}$ mice is a consequence of the lack of the inhibitory FcγRIIb in the context of the predisposition to humoral autoimmunity conferred by the 129-derived *Slam/Cd2* haplotype on the B6 background.

Deficiencies in molecules that function downstream of initial signal transduction events have also been implicated in predisposition to lupus-like autoimmunity. Mice which lack the T cell adaptor molecule (TSAd), which is expressed in thymocytes and activated T cells, and mice deficient in the transcriptional repressor Stra13, normally induced upon naïve T cell activation, both developed with age IC-mediated GN, splenomegaly and autoAb production. In addition, both knockouts showed increased T and B cell activation phenotypes and impaired AICD, IL-2 and IFNγ induction in activated T cells (270, 271). T cells from

young *Stra13*$^{-/-}$ mice were also shown to have impaired proliferative and cytokine responses *in vitro* and *in vivo* (270).

Mice with a spontaneous deficiency in the Ras guanidine nucleotide exchange factor, Rasgrp1, which normally serves to activate Ras following TCR stimulation, also developed the characteristic lupus phenotypes of GN, splenomegaly and autoAbs. Interestingly, *Rasgrp*$^{-/-}$ mice were shown to have impaired thymic development that prevented selection of low affinity TCRs, yet showed an accumulation of splenic effector-memory CD4 T cells with reduced numbers of CD8 T cells. This is in accordance with data that has shown that low-affinity TCRs are highly dependent on Rasgrp1 signals for positive selection, and suggests that in its absence only high-affinity TCRs undergo positive selection (272). The phenotypes of *Rasgrp*$^{-/-}$ mice are, in fact, very similar to those seen for knock-in mice with a point mutation in LAT (Y136F) that disrupts PLCγ activation upon TCR signaling (273, 274).

Recently, members of the TNF superfamily of ligands and receptors have also emerged as modulators of systemic autoimmunity. Transgenic overexpression of BlyS, a potent B cell activating cytokine, both in a ubiquitous and in a B cell specific manner, resulted in the characteristic murine lupus phenotypes of GN, splenomegaly and autoAb production. While there were no gross changes in B cell development, there was increased *in vivo* B cell numbers and *in vitro* B cell viability in BLyS Tg mice (275, 276).

Consistent with the idea that overexpression of Blys and consequent B cell activation can result in murine lupus phenotypes, deficiency in the inhibitory receptor for BLyS mediated signaling, TACI, expressed on B cells and CD4 T cells, resulted in murine lupus. In addition to decreased survival, GN, splenomegaly and autoAbs, *TACI*$^{-/-}$ mice had increased B

cell percentages and *in vitro* proliferative responses and Ig secretion (277). These studies again emphasize the importance of appropriate inhibition of signaling in the prevention of autoimmunity.

Recent studies provide evidence for the idea that subtle modulations in the expression of key signaling molecules can facilitate the development of systemic autoimmunity. CD19 is the BCR co-receptor and undergoes rapid tyrosine phosphorylation upon BCR engagement, allowing it to interact with a variety of downstream signaling molecules. A transgenic line that overexpressed human CD19 by just 20% was shown to develop humoral autoimmunity in the absence of GN, with titres of IgG autoAbs comparable to that seen in a line that overexpressed two times the normal levels of CD19. Significantly, this small increase in CD19 expression did not result in detectable alterations in phosphorylation patterns of downstream signaling molecules or any changes in B cell numbers or percentages (278).

Future Directions and Objectives

The work presented herein discusses our findings on the importance of epistatic interactions in the suppression of humoral and systemic autoimmunity. These studies involved the generation and careful characterization of various multi-congenic strains containing both the *Sle* susceptibility and the *Sles* suppressive modifier loci. We find that suppression, like susceptibility, is highly dependent on the contributions of, and interactions between different loci.

Gene	Protein	Human Chromosome (cytoband)	Mouse Chromosome (Mb)
C1Q	C1Q	1p36.12	4 (135.4)
C4	C4	6p21.32	17 (33.2)
C2	C2	6p21.32	17 (33.4)
DR/DQ	DR/DQ	6p21.32	17 (32.8)***
TNFα	TNFα	6p21.33	17 (33.7)
FcGRIIA	FcγRIIA	1q23.3	absent
FcGRIIIA	FcγRIIIA	1q23.3	1 (171.1)
FcGRIIB	FcγRIIB	1q23.3	1 (171.0)
CTLA4	CTLA-4	2q33.2	1 (61.3)
PDCD1	PD-1	2q37	1 (93.8)
PTPN22	LyP	1p13.1	3 (103.8)
IL10	IL-10	1q32.1	1 (130.9)

Table 1. Candidate Genes in Human SLE Association Studies. Mouse chromosomal positions are indicated in Mb, while human chromosomal positions are listed by cytoband for easier comparison to the results of linkage studies presented in Table 2. Positions are based on NCBI build 35 and m33 for human and mouse respectively.
*** Since mouse and human MHC genes have different nomenclatures, the *DR/DQ* equivalent gene in mouse is listed for *H2-Eα*.

Locus	Study Center[a]	Marker[b]	Ethnicity[c]	LOD[d]	References	Numbers[e]
1q22-24	OMRF	FcgrIIA	All; AA	**3.45; 3.37**	(Moser, Neas et al. 1998)	220 A, 533 T
	USC, UCLA	D1s484	All	2.64 (Z)	(Shai, Quismorio et al. 1999)	188 A, 434 T
	OMRF expanded	D1S1679	All; AA	2.47; 2.75	(Gray-McGuire, Moser et al. 2000)	295 A, 744 T
	UCLA	D1S1653	All	0.004	(Cantor, Yuan et al. 2004)	132 A, 238 T
	OMRF- HA	FcgrIIA	All; EA	2.8; 3.0	(Kelly, Thompson et al. 2002)	91 A, 195 T
	OMRF- ANA	FcgrIIIA	All; EA	2.89; 1.99	(Sawalha, Namjou et al. 2002)	67 A, 155 T
	OMRF- dsDNA	FcgrIIA	All	3.01	(Namjou, Nath et al. 2002)	
	OMRF- thrombocytopenia	FcgrIIA	All; EA	**3.65**; 2.22	(Scofield, Bruner et al. 2003)	387 A,
	OMRF- RA	FcgrIIA	All	2.58	(Namjou, Nath et al. 2002)	147 A,
	OMRF- renal disease	FcgrIIA	All; AA	2.76; 1.99	(Quintero-Del-Rio, Kelly et al. 2002)	75 A
1q41-44	OMRF	D1S3462	AA	**3.50**	(Moser, Neas et al. 1998)	220 A, 533 T
	USC, UCLA	D1S2785	HA	3.33 (Z)	(Shai, Quismorio et al. 1999)	188 A, 434 T
	MN I + II	D1S235	All	1.92	(Gaffney, Ortmann et al. 2000)	399 A, 655 T
2q32-37	UU I	D2S125	All	**4.24**	(Lindqvist, Steinsson et al. 2000)	44 A, 150 T
	UU II	D2S427	E	2.44	(Johansson, Zunec et al. 2004)	113 A, 308 T
	UCLA	D2S1384	EA	0.004	(Cantor, Yuan et al. 2004)	132 A, 238 T
	OMRF- thrombocytopenia	D2S1384	All	2.35	(Scofield, Bruner et al. 2003)	387 A
	OMRF- RA	D2S1391	AA	1.95	(Namjou, Nath et al. 2002)	78 A
4p16-13	OMRF	D4s403	EA	2.18	(Moser, Neas et al. 1998)	220 A, 533 T
	OMRF expanded	D4S2366	All; EA	**3.44; 3.84**	(Gray-McGuire, Moser et al. 2000)	295 A, 744 T
	UU I	D4S1627	I	3.2	(Lindqvist, Steinsson et al. 2000)	16 A, 96 T
	UU II	D4S1627	All; E	2.65; 2.60	(Johansson, Zunec et al. 2004)	
	OMRF-NP	D4S3007	EA	**5.19**	(Nath, Kelly et al. 2002)	56 A, 92 T
	OMRF-renal	D4S3243	All	2.32	(Quintero-Del-Rio, Kelly et al. 2002)	75 A
5p15	OMRF- HA	D5S817	AA	2.1	(Kelly, Thompson et al. 2002)	41 A, 89 T
	OMRF- RA	D5S2502	EA	**5.49**	(Namjou, Nath et al. 2002)	55 A
	UU II	D5S1492	It	2.04	(Johansson, Zunec et al. 2004)	25 A, 67 T
6p11-22	MN I + II	D6S246	All	**4.19**	(Gaffney, Ortmann et al. 2000)	399 A, 655 T
	USC, UCLA	D6S276	All	1.60 (Z)	(Shai, Quismorio et al. 1999)	188 A, 434 T
	OMRF expanded	D6S1053	AA	2.36	(Gray-McGuire, Moser et al. 2000)	295 A, 744 T
	OMRF- HA	D6S2410	EA	2.3	(Kelly, Thompson et al. 2002)	45 A, 96 T
12q24	OMRF expanded	D12S395	EA	2.04	(Gray-McGuire, Moser et al. 2000)	295A, 744T
	OMRF II	D12S395	HA + EA-1	**4.19**	(Nath, Quintero-Del-Rio et al. 2004)	305A
16q12-21	MN I + II	D16S415	All	**3.85**	(Gaffney, Ortmann et al. 2000)	399 A, 655 T
	USC, UCLA	D16S3136	All	2.14 (Z)	(Shai, Quismorio et al. 1999)	188 A, 434 T
	UCLA	D16S3396	All	0.02	(Cantor, Yuan et al. 2004)	132 A, 238 T
	OMRF II	D16S3253-	HA	3.06 (Z)	(Nath, Quintero-Del-Rio et al. 2004)	91 A
17p12-13	UU II	D17S921	A	2.64	(Johansson, Zunec et al. 2004)	41 A, 89 T
	OMRF- Vitilgo	D17S974-	EA	**3.64**	(Nath, Kelly et al. 2001)	55 A, 95 T
	OMRF- HA	1298	All	2.3	(Kelly, Thompson et al. 2002)	91 A, 195 T
	OMRF- thrombocytopenia	D17S1298 D17S1308	EA	2.29	(Scofield, Bruner et al. 2003)	387 A,
17q11	UU II	D17S1294	A	**3.49**	(Johansson, Zunec et al. 2004)	41 A, 89 T
	UCLA	D17S1294	All	0.002	(Cantor, Yuan et al. 2004)	132 A, 238 T
18q21-23	USC, UCLA	D1S64	All	2.54 (Z)	(Shai, Quismorio et al. 1999)	188 A, 434 T
	UCLA	D18S1390	All	0.01	(Cantor, Yuan et al. 2004)	132 A, 238 T
	OMRF- dsDNA	D18S858	AA	**3.4**	(Namjou, Nath et al. 2002)	
	OMRF- thrombocytopenia	D18S878	AA	1.98	(Scofield, Bruner et al. 2003)	387 A
	OMRF- renal	D18S878	AA	1.99	(Quintero-Del-Rio, Kelly et al. 2002)	
19p13	UU I	D19S247	I	2.58	(Lindqvist, Steinsson et al. 2000)	16 A, 96 T
	OMRF- dsDNA	D19S714	EA	**4.93**	(Namjou, Nath et al. 2002)	
11p11-15	OMRF- ANA	D11S1985	All; AA	2.86; 2.47	(Sawalha, Namjou et al. 2002)	67 A, 155 T
	OMRF- dsDNA	ATA34e08	AA	2.55	(Namjou, Nath et al. 2002)	
	OMRF- thrombocytopenia	D11S1392	All; AA	2.99; **3.8**	(Scofield, Bruner et al. 2003)	387 A,
	OMRF- discoid rash	D11S1984	AA	**4.6**	(Nath, Namjou et al. 2004)	
	OMRF- renal	D11S1984	AA	**3.34**	(Quintero-Del-Rio, Kelly et al. 2002)	20 A, 35 T
11q14	OMRF- HA	D11S2002	AA	**4.5**	(Kelly, Thompson et al. 2002)	41 A, 89 T
	OMRF- ANA	D11S2002	All; AA	**3.46; 5.62**	(Sawalha, Namjou et al. 2002)	67 A, 155 T
	OMRF- dsDNA	D11S2002	AA	2.46	(Namjou, Nath et al. 2002)	
	OMRF- thrombocytopenia	D11S1392	All	2.09	(Scofield, Bruner et al. 2003)	387 A,

Table 2. Significant Results of Whole-genome Linkage Studies in Human SLE. Loci listed met criteria for significance (LOD ≥3.3) in at least one study, according to the guidelines of Lander and Kruglyak (141). Abbreviations and symbols are listed in the legend for Table 3.

Locus	Study Center[a]	Marker[b]	Ethnicity[c]	LOD[d]	References	Numbers[e]
1q31	UU II	D1S518	I	2.41	(Johansson, Zunec et al. 2004)	267 A, 705 T
	UU I	D1S1660	S	1.61	(Lindqvist, Steinsson et al. 2000)	28 A, 54 T
9p24-21	OMRF expanded	D9S925	AA	2.08	(Gray-McGuire, Moser et al. 2000)	295 A, 744 T
	UU I	gata62f03	I	2.27	(Lindqvist, Steinsson et al. 2000)	16 A, 96 T
11q23-24	UU II	D11S1998	E; It	2.69; 1.94	(Johansson, Zunec et al. 2004)	113 A, 308 T
	OMRF- ANA	D11S912	EA	1.99	(Sawalha, Namjou et al. 2002)	33 A, 88T
13q32	OMRF	D13s779	All	2.5	(Moser, Neas et al. 1998)	220 A, 533 T
	UCLA	D13S793	All	0.005	(Cantor, Yuan et al. 2004)	132 A, 238 T
14q21-23	MN I	D14S276	All	2.81	(Gaffney, Kearns et al. 1998)	220 A, 355 T
	USC, UCLA	D14S258	All	2.02 (Z)	(Shai, Quismorio et al. 1999)	188 A, 434 T
19q12-13	UU II	D19S246	A	3.16	(Johansson, Zunec et al. 2004)	41 A, 89 T
	UU I	D19S246	I	2.06	(Lindqvist, Steinsson et al. 2000)	16 A, 96 T
20p12-13	MN I	D20A186	All	2.62	(Gaffney, Kearns et al. 1998)	220 A, 355 T
	USC, UCLA	D20S115	All	2.28 (Z)	(Shai, Quismorio et al. 1999)	188 A, 434 T
20q12-13	OMRF	D20s481	All	2.49	(Moser, Neas et al. 1998)	220A, 533 T
	USC, UCLA	D20S195	All	1.57 (Z)	(Shai, Quismorio et al. 1999)	188A, 434 T
	OMRF- RA	D20S478	AA	2.89	(Namjou, Nath et al. 2002)	78A,
10q22-23	OMRF- ANA	D10S1239	AA	1.95	(Sawalha, Namjou et al. 2002)	30 A, 58T
	OMRF- thrombocytopenia	D10S2470	EA	2.51	(Scofield, Bruner et al. 2003)	387 A,
	OMRF- renal	D10S2470	All, EA	2.68, 3.16	(Quintero-Del-Rio, Kelly et al. 2002)	75 A

Table 3. Strongly Suggestive Results of Whole-genome Linkage Studies in Human SLE. Loci listed met the criteria for strongly suggestive of significance (LOD $\geq$2.2) in at least one study, according to the guidelines of Lander and Kruglyak (141).

[a] Study centers and their abbreviations: Oklahoma Medical Research Foundation (OMRF), University of Minnesota (MN), University of Uppsala (UU). I and II after a study center name refers to first and second cohorts respectively. For OMRF stratified studies, the clinical feature used to stratify are listed: haemagglutin (HA), anti-nuclear antibodies (ANA), dsDNA autoAbs (dsDNA), thrombocytopenia, discoid rash, rheumatoid arthritis (RA), renal disease (renal), vitilgo and neuropsychiatric symptoms (NP).

[b] Marker showing peak linkage in the study.

[c] Ethnicity showing linkage: All (all ethnicities tested), AA (African-American), EA (European American), Hispanic American (HA), Icelandic (I), Argentinian (A), Italian (It) and E (European).

[d] LOD score value obtained in the study, if available. (Z) refers to the Z score where LOD=Z^2/2ln10. *p* values are listed for the UCLA studies.

[e] Number of individuals studied in the linkage analysis if available: affected (A) and total (T)

Fig. 1

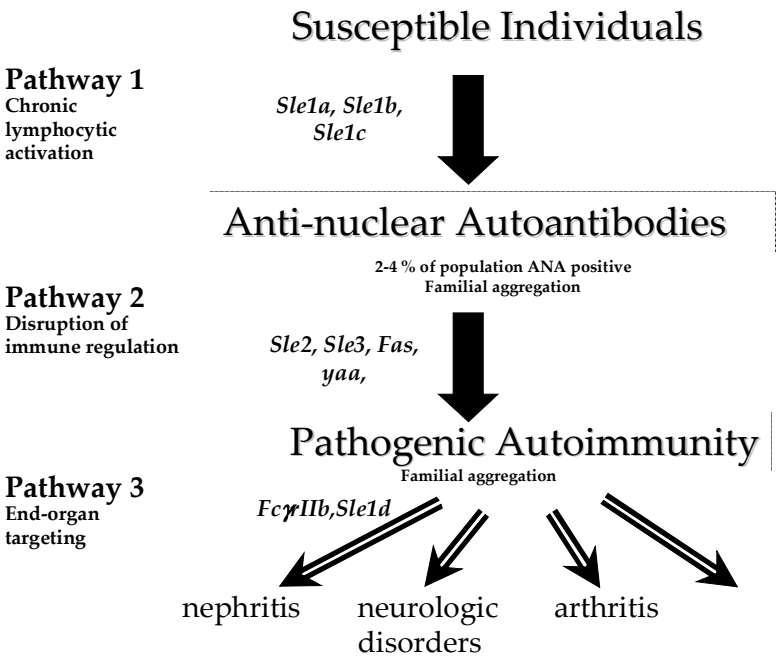

Figure 1. Model Pathway Demonstrating the Interactions of Genes Leading to Systemic Autoimmunity. We postulate that genes involved in mediating susceptibility to SLE belong to one of the three pathways shown above. The epistatic interactions between these loci culminate in the development of systemic autoimmunity. *Adapted from* (3).

Gene[a]	Protein	Mouse Chromosome (Mb)[b]	Human Chromosome (cytoband)	ES cell[c]	Background Genome[d]	Autoimmune Phenotypes[e] (GN, autoAbs)
Ptprc	CD45	1 (138.0)	1q31.3	129	129/B6	GN, autoAbs
Tnfsf6	FasL	1 (161.8)	1q24.3	***	C3H/HeJ	autoAbs
Fcgr2b	FcRII	1 (171.0)	1q23.3	129	129/B6	None
					BALB/c (N12)	None
					B6 (N12)	GN, autoAbs
Apcs	SAP	1 (173.0)	1q23.2	129	129/B6	GN, autoAbs
					129 (N6)	None
					B6 (N6)	GN, autoAbs
Rasgrp1	RASgrp1	2 (117.1)	15q14	129	129/B6	GN, autoAbs
Bcl2l11	Bim	2 (127.9)	2q13	129	129/B6	GN, autoAbs
Mertk	C-mer	2 (128.4)	2q13	129	B6 (N10)	autoAbs
Sh2d2a	TSAd	3 (88.3)	1q23.1	129	B6 (N10)	GN, autoAbs
Lyn		4 (3.6)	8q12.1	129	129/B6	GN, autoAbs
E2f2	E2F2	4 (134.6)	1p36.12	129		GN, autoAbs
C1qa	C1q	4 (135.4)	1p36.12	129	129/B6	GN, autoAbs
					B6 (N12)	None
					129 (N12)	None
					MRL/+ (N12)	GN, autoAbs
Gadd45a	GADD45a	6 (67.1)	1p31.2	129	129/B6	GN, autoAbs
Bhlhb2	Stra13	6 (109.1)	3p26.1	129	129/B6	GN, autoAbs
Tnfrsf13b	TACI	11 (60.7)	17p11.2	129	129/B6	GN, autoAbs
Prkcd	PKC delta	14 (26.6)	3p21.1	129	129/B6	GN, autoAbs
Dnase1	DNaseI	16 (3.7)	16p13.3	129	129/B6	autoAbs
Cdkn1a	p21	17 (27.7)	6p21.31	129	129/B6	GN, autoAbs
C4	C4	17 (33.2)	6p21.32	129	129/B6	GN, autoAbs
					B6 (N5)	GN, autoAbs
					mixed Balb/C	GN, autoAbs
Pten	PTEN	19 (32.1)	10q23.31	129	129/B6	GN, autoAbs
Tnfrsf6	Fas	19 (33.5)	10q23.31	***	MRL	GN, autoAbs
					B6	autoAbs
Bcl2 Tg	Bcl2	IgH enhancer		NA	B6/SJL	GN, autoAbs
PI3K Tg	PI3K	lck promoter		NA	B6/CBA X B6	GN, autoAbs
BlyS Tg	BlyS	ubiquitous/IgH		NA	B6/C3 X B6	GN, autoAbs
hCD19^{lo} Tg	hCD19	IgH enhancer		NA	B6 (N=7-12)	autoAbs

Table 4. Subset of Genes Implicated in Lupus Susceptibility through Knockout and Transgenic Technologies. Listed by murine chromosomal locations are the various genes discussed in the text that have been implicated in lupus susceptibility through transgenic or knockout methods.

[a] Gentically ablated or over-expressed genes.

[b] Chromosomal positions of genes that were knocked out and enhancer/promoter-type used in Tgs.

[c] Strain of ES cell line. *** spontaneous mutation; not applicable (NA)

[d] Background genome. (strain A/strain B): [strain A X strain B]F_2; N(x): number of backcross generations if known [e] Autoimmune phenotypes. None, GN or autoAbs.

Chapter II. Materials and Methods

Mice

All mice were housed in the UT Southwestern Medical Center Animal Resources Center's specific pathogen free (SPF) facility under the supervision of Dr. Jose Casco and with the approval of the Institutional Animal Care and Use Committee (IACUC) of The University of Texas Southwestern Medical Center.

C57BL/6J (B6) mice were originally obtained from the The Jackson Laboratory (Bar Harbor, ME). The derivation of B6 congenic mice carrying the NZM2410 derived *Sle1* interval (B6.*Sle1*) as well as bicongenic mice carrying *Sle1* and *Sles1* has been previously described (242, 279). Recombinant *Sles1* mice were obtained by intercrossing [B6.*Sle1*|*Sles1* X B6.*Sle1*]F_1 progeny and PCR screening F_1 intercross progeny for informative meioses within the *Sles1* interval. Recombinant chromosomes were rescued by backcrossing to B6.*Sle1*, and intercrossing *Sles1* recombinant progeny to produce homozygous B6.*Sle1*|*Sles1* recombinant lines. For the F_1 studies involving 129, B6, B6.*Sle1* and B6.*Sle1*|*Rec.4*$^{z/z}$ were crossed to the 129/SvJ strain to generate [129 X B6], [129 X B6.*Sle1*] and [129 X B6.*Sle1*|*Sles1*] F_1 progeny respectively.

C57Bl/6J mice carrying the BXSB derived y-chromosome *yaa* were obtained from The Jackson Laboratory and are referred to as B6.*yaa*. The B6.*Sle1*|*yaa* line was derived by breeding female B6.*Sle1* mice to male B6.*yaa*. Male progeny from these crosses (B6.*Sle1*^{het}|*yaa*) were backcrossed to female B6.*Sle1* mice, and male mice homozygous for the NZM2410 derived *Sle1* locus selected. These male B6.*Sle1*|*yaa* mice were backcrossed

to female B6.*Sle1* mice and subsequent progeny intercrossed, thus ensuring that males always carried *yaa* in this line. The introgression of the NZW derived *Sles1* interval was performed in a similar manner, using female B6.*Sle1*|*Sles1* crossed to male B6.*Sle1*|*yaa* mice. The primers used to select for and identify the *Sle1* and *Sles1* intervals for generating the various *yaa* strains are described under *PCR Genotyping*.

The generation of the B6.*Sle1*|*Sle2*|*Sle3/5* (B6.*TC*) triple congenic mice containing the NZM2410 derived *Sle1*, *Sle2* and *Sle3/5* intervals on the B6 background has been previously described. To introduce *Sles1* onto the triple congenic lupus model, B6.*Sle1*|*Sles1* mice were crossed and then backcrossed to B6.*Sle1*|*Sle2*|*Sle3/5* (B6.*QC*). These first backcross progeny were selected for heterozygosity at *Sles1*, homozygosity at *Sle2*, with *Sle3/5* being either homozygous or heterozygous (ie., B6.$Sle1^{z/z}$|$Sle2^{z/z}$|$Sle3/5^{het}$|$Sles1^{het}$ or B6.$Sle1^{z/z}$|$Sle2^{z/z}$|$Sle3/5^{z/z}$|$Sles1^{het}$). These mice were backcrossed to B6.*Sle1*|*Sle2*|*Sle3/5* and these second backcross progeny were selected for heterozygosity at *Sles1* and homozygosity at *Sle3/5*. These B6.$Sle1^{z/z}$|$Sle2^{z/z}$|$Sle3/5^{z/z}$|$Sles1^{het}$ were intercrossed to obtain homozygosity at *Sles1*, thus generating the B6.*Sle1*|*Sle2*|*Sle3/5*|*Sles1* (B6.*QC*) strain. Females were used for all studies comparing the B6.*Sle1*|*Sle2*|*Sle3/5* and B6.*Sle1*|*Sle2*|*Sle3/5*|*Sles1* strains.

PCR Genotyping

Tail clips were obtained at weaning and used to prepare tail lysates. Briefly, 250 µl of Tail Lysis Buffer (50 mM Tris, pH 8.0/ 50 mM KCl/ 2.5 mM EDTA/ 0.45% NP-40/ 0.45% Tween-20) and 0.4 mg/ml Proteinase K solution (Roche, Indianapolis, IN) were added per tail clip and kept for at least 20 hours in a 55°C water bath. Tail lysates were vortexed and

spun down at 14000 rpm for 10 minutes. For a 20 µl PCR reaction, 0.5 µl of tail lysate supernatant was used. PCR products were subsequently run out on 5-6.25% agarose gels to resolve the polymorphic bands. The fine-mapping of the recombinant chromosomes spanning the *Sles1* interval was performed using a series of 20 microsatellite markers within the original 25cM *Sles1* confidence interval. Those relevant to these studies include D17MIT100, D17MIT60, D17MIT146, D17MIT175, D17MIT16, D17MIT62, D17MIT28, D17MIT34, D17MIT83, D17MIT13 and TNF. In order to map the ends of the minimal *Sles1* interval (*Rec.6)*, sequence between the proximal and distal NZW and B6 breakpoints (D17MIT62-D17MIT28 and D17MIT83-D17MIT13 respectively) was obtained from the Ensembl database (www.ensembl.org/Mus_musculus/). Using Sequencer software (Gene Codes Corporation, Ann Arbor, MI), these sequences were analyzed for the presence of new microsatellite repeats for which flanking primers were designed. These novel microsatellite markers were then tested for B6 and NZW size polymorphisms and those polymorphic between these two strains were used to map the breakpoints. Relevant polymorphic proximal and distal breakpoint primer sequences and PCR annealing temperatures are listed below:

Proximal Breakpoint Primers

	Forward	Reverse	Annealing	Polymorphism
ms1	CTGCATCTCCCGTTGTCTTT	TGACTTCCACATTCTTGCCATA	53°C	B6 > NZW
ms2	TTTTCGACTGCAGACCAACTT	TCCCTAACTAGCCTAAAAACAAAAA	53°C	NZW > B6
ms3	CCTCTGATCTCCACGGATGT	CAAAACTACAAAGCTCCCCAAA	56°C	NZW > B6
ms4	ATCCCCTGGTTTCACTCCTT	TCATGCTCAAAGAAGCAACAA	56°C	B6 > NZW
ms5	GCATGCAGAGTGAGTTTCCA	CAGCCAATGCTCATAACTGC	56°C	B6 > NZW
ms6	AAGACAGTTCGGACCCTACAGA	TTGCTGGCTTCCAGGTTAAT	54°C	NZW > B6

Distal Breakpoint Primers

Primer	Forward	Reverse	Annealing	Polymorphism
ms7	GCAACACATGTTCTTGATAATCACT	GTTACAACTTTTGCTGGTTAGATTT	58°C	NZW > B6
ms8	CCAGGGCTACACAGGAGACT	CAGGACCTTTGGATGGCTTA	58°C	B6 > NZW
ms9	TCAAGTGAAAAGGAGACAAAGTTC	CACAGGCTAGGGTTGTGGTT	54°C	NZW > B6

	Gender	*Sle1 (chr. 1)* **D1MIT202 D1MIT17**	*Sle2 (chr. 4)* **D4MIT151 D4MIT9**	*Sle3/5 (chr. 7)* **D7MIT178 D7MIT31**	*Sles1 (chr. 17)* **D17MIT61 ms7**	*Sles2 (chr. 4)* **D4MIT9 D4MIT339**	*Sles2 (chr. 3)* **D3MIT95 D3MIT137**	*yaa (y chr.)*
B6	F/M	B6	B6	B6	B6	B6	B6	B6
B6.*Sle1*	F/M	NZM	B6	B6	B6	B6	B6	B6
B6.*Sle1*|*Sles1*	F	NZM	B6	B6	NZW	B6	B6	B6
B6.*yaa*	M	B6	B6	B6	B6	B6	B6	BXSB.*yaa*
B6.*Sle1*| *yaa*	M	NZM	B6	B6	B6	B6	B6	BXSB.*yaa*
B6.*Sle1*|*Sles1*|*yaa*	M	NZM	B6	B6	NZW	B6	B6	BXSB.*yaa*
B6.*TC*	F	NZM	NZM	NZM	B6	B6	B6	B6
B6.*QC*	F	NZM	NZM	NZM	NZW	B6	B6	B6
B6.*Sle1*|*Sles2*	F	NZM	B6	B6	B6	NZW	B6	B6
B6.*Sle1*|*Sles3*	F	NZM	B6	B6	B6	B6	NZW	B6

Table 5. Strains Used in Different Studies. Table 5 summarizes the various strains used and described under *Mice*, gender used in different studies, the strain of origin and chromosome (chr.) of the different loci and the proximal (above) and distal (below) markers used to type these loci are listed underneath the locus names.

Renal Pathology

Mice were terminated at 4-6 and 9-12 months, depending on the studies in question, and a longitudinal section of each kidney fixed in 10% neutral buffered formalin (Sigma-Aldrich, St. Louis, MO), paraffin embedded, cut into 3 μm sections, and stained with hematoxylin and eosin with periodic acid-Schiff. The sections were examined in a blind manner for evidence of pathologic changes in the glomeruli, tubules or interstitial areas by Dr. Xin J. Zhou (Department of Pathology, The University of Texas Southwestern Meical

Center). The glomeruli were screened for evidence of hypertrophy, proliferative changes, crescent formation, hyaline deposits, fibrosis/sclerosis and basement membrane thickening. The GN severity was graded on a scale of 0 to 4 where 0 = normal, 1 = mild increase in mesangial cellularity and matrix, 2 = moderate increase in mesangial cellularity and matrix with thickening of glomerular basement membrane (GBM), 3 = focal endocapillary hypercellularity with obliteration of capillary lumina and a substantial increase in the thickness and irregularity of the GBM and 4 = diffuse endocapillary hypercellularity, segmental necrosis, crescents and hyalinized end-stage glomeruli. Similarly, the severity of tubulointerstitial nephritis was graded on a 0 - 4 scale, based on the extent of tubular atrophy, inflammatory infiltrates and interstitial fibrosis, as described previously (280). The number of infiltrating polymorphonuclear leukocytes was directly enumerated based on their typical polymorphonuclear morphology, by examining 50 glomeruli per kidney per section per mouse.

Serology

Mice were bled at various ages, either by retro-orbital bleeding (survival studies) or cardiac puncture (at terminal sacrifice), and sera stored at -20°C. ELISA detection of IgM and IgG autoantibodies (autoAbs) directed against chromatin, dsDNA and GBM (glomerular basement membrane) self-antigens were performed as follows. All coating steps were for 30 minutes at 37°C followed by two washes in PBS (Sigma-Aldrich). Briefly, for all ELISAs, Immunlux HB (Dynatech, Chantilly, CA) plates were precoated with 50 µl/well of methylated BSA (mBSA). For anti-chromatin and anti-dsDNA ELISAs plates were coated

with 50 µl/well of 50 µg/ml dsDNA (Sigma-Aldrich; dissolved in PBS and filtered). For the anti-chromatin ELISAs, an additional coating step with 50 µl/well of 10 µg/ml total histones (Roche) was employed. For anti-GBM ELISAs, after the mBSA step, the plates were coated with 50 µl/well sonicated rat glomerular extract at 10 µg/ml . Following the last respective coating step and wash, ELISA plates were incubated overnight at 4°C with 200 µl/well of ELISA Blocking Buffer (PBS/ 0.1% gelatin/ 3% BSA/ 3 mM EDTA). Test sera were added at a final dilution of 1:100, 1:200 and 1:800 (serial) for anti-GBM, anti-dsDNA and anti-chromatin ELISAs respectively, in Serum Diluent (PBS/ 0.1% gelatin/ 2% BSA/ 3mM EDTA/ 0.05% Tween-20) and incubated for 2 hrs at room temperature. Bound IgM or IgG was detected using alkaline phosphatase conjugated goat anti-mouse IgG or IgM (Roche) and p-nitrophenyl phosphate (Sigma-Aldrich) as the substrate. OD450 was measured by an Elx800 Automated Microplate Reader (Bio-Tek Instruments, Winooski, VT). Raw optical densities (ODs) for anti-chromatin IgG ELISAs were converted to arbitrary normalized units (ANU) using a six-point standard curve generated by a monoclonal antibody derived from an NZM2410 mouse (281). A 1:250 dilution of this supernatant was set at 1000 U/ml. For anti-dsDNA and anti-GBM IgG and IgM ELISAs, the standard curve was set using six serial dilutions of sera from a female [NZW X B6.*Sle1*]F_1, with a 1:250 dilution of this sera set at 1000 U/ml.

Cell Preparation and Culture

Following the measurement of spleen weight, single cell splenocyte suspensions were prepared, passed through nylon mesh and depleted of red blood cells (RBCs) using RBC

Lysis Buffer (0.1mM EDTA/ 0.83% NH_4Cl / 0.1% $KHCO_3$). Bone marrow (BM) cells were obtained by flushing out the marrow from femoral bones with complete DMEM, crushing to obtain single cell suspensions and lysing RBCs. Thymic suspensions were prepared by isolating thymi and preparing single-cell suspensions. These cells were then used for flow cytometric analyses (described below).

Flow Cytometric Analysis and Antibodies

In each FACs experiment, at least one mouse per genotype was included. For all FACs analyses, B6.*Sle1*|*Sles1* indicates that the B6.*Sle1*|*Rec.1*$^{z/z}$ line was used. Cells were blocked with 2.4G2 (American Type Culture Collection, Rockville, MD) on ice. Cells (1.5 X 10^6 per antibody cocktail) were then stained on ice using optimal amounts of FITC, phycoerythrin (PE), PE-Texas Red, Cychrome, PerCPCy5.5, allophycocyanin or biotin-conjugated antibodies (Abs) at predetermined dilutions. Four-color combinations of the following antibodies, obtained from BD Biosciences Pharmingen (San Diego, CA) were used for the various analyses: CD21/35 (7G6); CD23 (B3B4); IgM (R6-60.2); CD86 (GL1); CD45R (RA36B2); CD5 (53-7.3); CD11b (M1/70); NK1.1 (PK126); CD25 (PC61); CD69 (H1.2F3); CD4 (H129.19); CD8 (53-6.7); CD3 (145-2C11); CD19 (1D3); CD43 (S7); CD1d (1B1); CD62L (MEL-14); CD44 (1M7) and CD138 (281-2). After two washes, biotin conjugated Abs were revealed using BD Pharmingen Streptavidin-allophycocyanin. Appropriate isotype controls for all antibody combinations were included in all analyses for all samples. Stained cells were acquired on a FACsCalibur with CellQuest software (BD Biosciences). Dead cells were excluded on the basis of forward and side scatter properties and 40,000 events within

the lymphocyte gate were acquired for spleen and thymic samples, while 100,000 total live events were collected for BM samples. Flow cytometric data was analyzed using FlowJo (Tree Star, Ashland, OR).

RNA Isolation and cDNA Prepration

$B220^+$ splenocytes were purified via positive selection using Dynabeads mouse pan B ($B220^+$) according to manufacturer's instructions (Dynal; Brown Deer, WI) and DNA-free RNA was isolated using the Qiagen Rneasy Mini Kit and on-column DNase I treatment (Qiagen; Valencia, CA). cDNA was synthesized from 1.5-2.0 µg total RNA with the Taqman Reverse Transcriptase Kit, according to manufacturer's instructions (Applied Biosystems; Foster City, CA).

Quantitative Real-time RT-PCR

Quantitative real-time PCR was performed on 10 ng cDNA using the 2X SYBR Green PCR Master Mix (Applied Biosystems) in 20ul reactions using the GeneAmp 5700 Sequence Detection System (Applied Biosystems). The run condition was a 3-step cycle: 95^{o}C for 20 sec, 55^{o}C for 20 sec, and 72^{o}C for 30 sec and was repeated for 40 cycles. For each primer set, standard curves were generated using serial dilutions of cDNA. To control for loading, G*apdh* was used as the reference gene for normalization. Primer sequences are as follows:

Ly108-1: For- GACCACACTCATGCCCTGAC

Rev- GTATTCAGCCTAGGAGAAATGG

Ly108-2: For- CCGGCTATAACCAACCCATT Rev- AAGCCAGAGCTGTGGTGACA

Gapdh: For- TGCACCACCAACTGCTTAG Rev- GGATGCAGGGATGATGTTC

Values normalized to Gapdh are presented.

SDS-PAGE and Immunoblotting

Splenic B lymphocytes were isolated using Dynal anti-B220 magnetic beads according to manufacturer's protocol (Dynal, Lake Success, NY). Isolated cells were lysed in Lysis Buffer (300 mM NaCl, 50 mM Tris-Cl, pH 7.6, 0.5% Triton X-100, 10 □g/ml leupeptin, 10 □g/ml aprotinin, 1mM PMSF, 1mM sodium orthovanadate, 1 mM sodium molybdate, 1mM NaF), incubated on ice for 30 min and then cleared by centrifuging at 12,000 × g for 20 min. Equivalent amounts of total cellular protein extract (4 □g) were fractionated on 10% SDS-polyacrylamide gel electrophoresis (PAGE) and electrotransferred to PVDF membrane using a Bio-Rad transblot apparatus. The membrane was blocked overnight with TBST buffer (10mM Tris-Cl, pH 8.0, 0.9% NaCl, 0.1% Tween 20) plus 4% BSA (for phosphorylated proteins) or 5% nonfat dry milk, and incubated for 1 hour with primary monoclonal antibody in TBST buffer plus 4% BSA (for phosphorylated proteins) or 5% nonfat dry milk. Following three washes in TBST, membranes were incubated with a secondary antibody for 1 h. The membranes were again washed three times in TBST, and then developed using an ECL Plus kit (Amersham, Piscataway, NJ) according to the manufacturer's instructions. Protein bands were quantified by densitometric analysis using a computerized densitometer (Molecular Dynamics) and ImageQuant software (Molecular Dynamics). Rabbit polyclonal antibodies specific for P44/42 MAP kinase were purchased from Cell Signaling (Beverly,

MA). Rabbit anti-phospho-ERK1/2 MAP kinases polyclonal antibodies were purchased from Promega (Madison, WI). The secondary antibodies (goat anti-rabbit IgG) were purchased from Santa Cruz Biotechnology (Santa Cruz, CA).

CFSE Proliferation Assays

Splenocytes at 10^6/ml were labeled with 2.5 μM carboxy-fluorescein diacetate succinimydl ester (CFSE) (Molecular Probes; Eugene OR) in complete RPMI-10 for 15 min at 37^{o}C. Cells were washed twice with media, and 100 μl of labeled cell plated in triplicate wells at 2.5 x10^6 cells/ml in 96-well round bottom plates in the presence of either F(ab')$_2$ anti-IgM (Jackson ImmunoResearch; West Grove, PA) or anti-CD3e (145-2C11) (BD Pharmingen). Cells were harvested at 24hr, 48hr, and 72hr time points and Fc-blocked with 2.4G2 (American Type Culture Collection; Rockville, MD). Cells were then stained on ice with CD19-PE (1D3) to assess for B cell proliferation or CD4-PE (H129.19) and CD8-PerCPCy5.5 (53-6.7) (BD Pharmingen) for T cell proliferation. Flow cytometric data on the stained cells were acquired on the FACsCalibur (Becton Dickinson) and analyzed using FlowJo (Tree Star).

Intracellular Cytokine Responses

RBC-depleted splenocyte suspensions were prepared under sterile conditions and some samples pre-stained at an optimal dilution with BD Pharmingen anti-CD4 (H129.19) FITC for 15 minutes on ice. Pre-stained and unstained cells were then plated at 10^6/ml in complete RPMI-10 and stimulated for four hours with 100 ng/ml PMA and 1 μM Ionomycin in the

presence of Golgi Stop. Cells were then harvested, blocked with 2.4G2 and pre-stained samples stained with BD Pharmingen anti-CD8 (53-6.7) PE-Cy5 and unstained cells with CD19 (1D3) FITC. Cells were fixed and permeabilized using the BD Pharmingen Golgi Stop kit, according to manufacturer's instruction, and stained with eBioscience anti-IL4 PE and anti-IFNγ APC, with appropriate isotype controls. Cells were acquired on a FACsCalibur with CellQuest software (BD Biosciences). Dead cells were excluded on the basis of forward and side scatter properties and 100,000 events within the lymphocyte gate were acquired. Flow cytometric data was analyzed using FlowJo (Tree Star).

Statistical Analysis

Data was analyzed using parametric and non-parametric ANOVAs as determined by InStat3 (Graphpad Software, San Diego, CA), unless otherwise indicated. Error bars represent SEMs or interquartile ranges depending on the distribution of the data.

Chapter III. Epistatic Suppression of SLE:

Fine-Mapping of *Sles1* to < 1 Mb

Introduction

Genetic predisposition to the autoimmune disorder Systemic Lupus Erythematous (SLE) is mediated by complex interactions between multiple susceptibility loci and environmental factors (3). Numerous SLE susceptibility loci have been mapped in a variety of mouse strains that spontaneously develop lupus, and genetically engineered models have implicated several additional genes in lupus predisposition (reviewed in (155, 282)). In addition**,** recent work has demonstrated suppressive modifier alleles that can significantly influence both the likelihood of lupus development and disease, as well as its severity and pathogenicity (37, 83, 242, 283).

We have utilized congenic dissection of loci identified via linkage analyses of the NZM2410 murine lupus model to better understand the underlying genetic mechanisms responsible for disease susceptibility. Characterization of the genetic and immunological properties of the different loci, in isolation and when genetically reassembled on the C57Bl/6J (B6) background, have revealed that each locus contributes unique phenotypes, together recapitulating what is seen in the parental NZM2410 (201, 225, 226, 235, 237-240, 284, 285).

Of relevance to this study, B6.*Sle1* mice develop with age a relatively benign autoimmune phenotype characterized by a loss in tolerance to chromatin and IgG autoantibody (autoAb) production, an increase in the proportion of activated B and T

lymphocytes and mild splenomegaly (153, 226). Addition of other susceptibility loci to *Sle1* has shown that this locus interacts epistatically with various loci, such as *yaa*, *lpr* and *Sle3*, to mediate systemic autoimmunity and fatal lupus nephritis (201, 240, 286).

Sle1 and *Sle3* are both derived from the NZW parent of NZM2410, which is a non-autoimmune inbred strain, suggesting that the NZW genome contains modifier loci that could prevent the development of autoimmunity normally driven by these potent susceptibility alleles. Linkage analyses of the NZW strain confirmed the presence of such loci, termed the *Sles* (SLE suppressor) loci. The most potent of these, *Sles1* on mouse chromosome 17, specifically interacts with *Sle1* to prevent the loss of immune tolerance to chromatin, but has no effect on the component phenotypes of the other NZM2410 derived loci, *Sle2* and *Sle3/5*, on the B6 background (242). Since *Sle1* has been shown to be key for the initiation of systemic autoimmunity in different murine lupus models, identification of *Sles1* and the mechanism(s) by which it specifically suppresses *Sle1* could provide insights useful for the development of strategies towards therapeutic intervention.

In this report, we demonstrate that the suppression mediated by *Sles1* maps to a ~956 KB interval on chromosome 17, beginning at the proximal end of the murine MHC (Major Histocomptability Complex) and terminating just distal to the complement cluster. This analysis excludes *TNF-*α and genes telomeric to it as possible candidates for *Sles1*. The majority of the splenic cell-surface phenotypes observed in aged B6.*Sle1* mice were abrogated in the presence of *Sles1*. In addition, using a classic genetic complementation test, we present evidence indicating that the non-autoimmune 129/SvJ (129) strain also harbors a complementary *Sles1*-like suppressive allele.

Results

Sles1 Maps to a 956 kB Interval That Excludes TNF-α

Our previous work demonstrated the presence of a recessive NZW derived epistatic modifier on mouse chromosome 17, termed *Sles1*, which specifically suppressed the break in tolerance to chromatin mediated by *Sle1* on the B6 background (242). Consequently, congenic recombinant fine-mapping was performed by intercrossing B6.*Sle1*|*Sles1*^{het} mice and identifying recombinant chromosomes in the *Sles1* interval by PCR screening tail DNA from testcross progeny with polymorphic microsatellite markers flanking the original *Sles1* interval. Once recombinant chromosomes were identified, additional markers were used to localize the recombinant breakpoint. The recombinant mice were backcrossed to B6.*Sle1* to 'rescue' the recombinant *Sles1* chromosomes and new *Sles1* recombinant lines. The new recombinant lines found to retain the recessive suppression phenotype of *Sles1* were used to generate more recombinant strains. Fig.2 shows a schematic representation of this recombinant congenic fine-mapping strategy.

As shown in Fig.3, a series of six, truncated recombinant chromosome lines, spanning the *Sles1* interval and termed B6.*Sle1*|*Rec.1-6*, were identified via the analysis of 1329 test-cross progeny. Interestingly, there appeared to be a recombinational hotspot between the markers D17MIT146 and D17MIT175, as evidenced by the greater than expected number of recombinants obtained between those two markers (χ^2= 22.3; $p<0.005$).

Progeny from these lines, homozygous and heterozygous for the recombinant chromosomes, were aged and assayed for IgG anti-chromatin autoantibodies (autoAbs) production by ELISA at 5, 7, 9 and 12 months of age. At the 12-month terminal sacrifice,

spleens were weighed to assess splenomegaly, a phenotype observed in aged B6.*Sle1* mice (226, 242, 279).

As depicted in Fig. 4A, aged B6.*Sle1* female mice had a significant increase in their mean spleen weights when compared to age- and sex-matched B6 (233.3 mg, interquartile range 163.9-280.2 mg *vs.* 107.4 mg, interquartile range 99.7-127.1 mg); $p< 0.001$, non-parametric ANOVA). Comparison of spleen weights from the various homozygous recombinant lines with B6 and B6.*Sle1*, indicated that B6.*Sle1*|*Rec.2* $^{z/z}$ and B6.*Sle1*|*Rec.3* $^{z/z}$ mice differed significantly from B6 ($p< 0.001;$ non-parametric ANOVA), while B6.*Sle1*|*Rec.1* $^{z/z}$, B6.*Sle1*|*Rec.4* $^{z/z}$, B6.*Sle1*|*Rec.5* $^{z/z}$ and B6.*Sle1*|*Rec.6* $^{z/z}$ mice were indistinguishable from B6 ($p> 0.05$), and different from B6.*Sle1* ($p< 0.001$ for all strains; non-parametric ANOVA). Importantly, mice heterozygous for all six recombinant chromosomes reverted to the roughly two-fold increase in spleen weights seen in B6.*Sle1*, which is consistent with the recessive inheritance of *Sles1* observed in the original bi-congenic analyses (242). These results map the suppression of splenomegaly into the genomic interval contained within *Rec.1* and *Rec.4-6*.

Suppression of ANA production by *Sles1* was assayed by anti-chromatin ELISAs at various timepoints. As shown in Fig.4B, in which titres from 9-12 month old female mice of the various genotypes are presented, B6.*Sle1*|*Rec.1* $^{z/z}$, B6.*Sle1*|*Rec.4* $^{z/z}$, B6.*Sle1*|*Rec.5* $^{z/z}$ and B6.*Sle1*|*Rec.6* $^{z/z}$ all suppressed anti-chromatin ANA production ($p< 0.001$ for all strains compared to B6.*Sle1* females; non-parametric ANOVA), hence mapping *Sles1* to these genomic segments. In contrast, B6.*Sle1*|*Rec.2* $^{z/z}$ and B6.*Sle1*|*Rec.3* $^{z/z}$ failed to suppress anti-chromatin ANA production ($p< 0.001$ for all strains compared to B6; non-parametric ANOVA). These results correlate with the lack of splenomegaly in the different congenic lines, consistent with a single gene mediating both effects.

These data place *Sles1* in the ~956 KB genomic interval contained in *Rec.6* (Fig.3). This interval includes the microsatellite markers D17MIT28 and D17MIT83, but excludes D17MIT62 and D17MIT13 at the proximal and distal ends respectively, and contains 65 genes (Fig.3 and Fig.5). Using public sequence available from the Ensembl database (NCBI m33), we designed primers surrounding microsatellite repeats at the proximal (D17MIT62-D17MIT28) and distal breakpoints (D17MIT83-D17MIT13) to further map the ends of this interval. The ~64 KB proximal and ~27 KB distal breakpoints (between the primer pairs ms3-ms4 and ms7-ms8, respectively) harbor two additional genes each (www.ensembl.org/Mus_musculus/). As shown in Fig.5, this brings the maximum number of candidate genes in the minimal *Sles1* interval to 69. This result is consistent with the gene-rich nature of this region of the genome, as has been recently reviewed (31, 32). In addition, given the recognized immunological functions of many of these genes, determining candidacy for *Sles1* remains a challenge.

Sles1 Suppresses the Activation of T cells Mediated by Sle1

The breach in tolerance to chromatin mediated by the *Sle1* locus is accompanied by an increase in the activation phenotypes in splenic T and B lymphocytes (153, 226, 242). We performed a comprehensive analysis of the various splenic cell populations in aged 9-12 month old female B6, B6.*Sle1* and B6.*Sle1*|*Sles1*$^{z/z}$ (B6.*Sle1*|*Rec.1*$^{z/z}$) mice in order to better characterize these changes and determine their association with the suppression mediated by the *Sles1* interval.

As shown in Table 6, there were numerous quantitative differences in the percentages of various splenic sub-populations when B6.*Sle1* mice were compared to age and gender-matched B6 controls. A small but significant decrease ($p<0.05$; ANOVA) in the percentage of $CD3^+$ T

cells in B6.*Sle1* mice was restored to B6 levels in the presence of *Sles1* (Table 6). As has been previously shown, B6.*Sle1* mice had a highly significant increase in the percentage of $CD3^+$ T cells expressing the early activation marker CD69, when compared to B6 controls (226). This activation phenotype was suppressed by *Sles1* (Fig.6A), as shown by the decrease in the percentage of $CD69^+$ CD3 T cells in B6.*Sle1*|*Sles1* mice *vs.* B6.*Sle1* ($p<0.001$; ANOVA). In addition, the overall cell-surface levels of CD69 on the $CD3^+$ population, as determined by comparing Median Fluorescent Intensities (MFIs), was significantly higher in B6.*Sle1* mice ($p<0.001$; ANOVA), which also was restored to B6 levels by *Sles1* (Fig.6B, Table 6).

A more detailed look within the CD4 T cell population at the $CD69^+$ cells revealed that the increase in the $CD69^+$ CD4 T cell population in B6.*Sle1 vs.* B6 mice occurred in both the $CD25^+$ and $CD25^-$ fractions (21.3 ± 0.6% *vs.* 13.0 ± 1.1%; 19.7 ± 1.3% *vs.* 10.1 ± 0.8% respectively; $p<0.001$ for both; ANOVA) (Fig.6C and Table 6). As expected from the $CD3^+$ data, in the presence of *Sles1*, neither subset showed this increase, and moreover, the $CD69^+CD25^-$ population was significantly decreased compared to both B6 and B6.*Sle1* ($p<0.01$ and $p<0.001$ respectively; ANOVA) (Table 6, Fig.6C). Significantly, we observed no change in the percentage of phenotypic regulatory T cells, defined as being $CD4^+CD25^+CD69^-$, in any of the strains examined (Fig.6C), which is in contrast to recent work from Morel's group (287).

Consistent with the increases observed in T cell activation status, the CD4 T cells in aged B6.*Sle1* mice are highly skewed towards an effector-memory phenotype, with the percentage of $CD62L^-CD44^{hi}$ CD4 T cells increasing from 23.4 ± 2.5% in B6 controls to 40.3± 4.8% ($p<0.01$, ANOVA). There was a corresponding decrease in the percentage of naïve ($CD62L^+CD44^{lo}$) CD4 T cells (Table 6, Fig.6D). In contrast, this decrease in the percentage of T cells expressing a naïve phenotype was not observed in the presence of *Sles1*, as these mice had a significant

increase in the percentage of naïve CD4 T cells in comparison to B6 controls (58.1 ± 2.0% *vs.* 38.2 ± 3.1%; $p<0.001$; ANOVA). Such shifts to an effector-memory CD4 population have been observed in a variety of more severely pathogenic lupus models, albeit with differing kinetics, and they appear to correlate with the development, but not necessarily the severity, of autoimmunity (36, 189, 193, 194, 200, 286).

B cell Cell-Surface Activation Phenotypes Are Suppressed by Sles1 Despite Intrinsic ERK Phosphorylation

We have previously demonstrated that various activation-induced changes develop in the splenic B cell compartment as B6.*Sle1* mice age (153, 226, 242, 285). In order to determine whether this might be the consequence of perturbations in splenic B cell selection events, we characterized the transitional 1 (T1), transitional 2 (T2), follicular and marginal zone (MZ) B cell developmental subsets. As shown in Fig.7A and Table 6, no differences were detected in the percentages of T1, T2 and MZ B cells, though there was a small but significant decrease in the follicular B cell population ($CD23^+CD21^+IgM^{int}$) in B6.*Sle1* mice versus B6 controls (23.2 ± 1.1% *vs*. 29.6 ± 1.3%; $p<0.01$; ANOVA). This decrease was not observed in B6.*Sle1*|*Sles1* mice: their percentage of follicular B cells was intermediate to B6 and B6.*Sle1*, and was not significantly different from either group. The decrease in the percentage of follicular B cells in aged B6.*Sle1* was not due to a block at the T2 stage, as there was no corresponding increase in this population. It may instead partially reflect the further differentiation of these cells into the $CD138^+CD19^-$plasma cell lineage (Table 6).

We also investigated the splenic B1 and B2 B cell populations in these strains, to look for potential changes in the splenic B1 population, as observed in some lupus models (239, 288). As

shown in Table 6, there were no significant differences in the splenic B1 lineages in any of the groups examined, but there was a decrease in the B2 population ($CD5^{-}CD23^{+}B220^{+}$) in B6.*Sle1* mice compared to B6 controls (29.4 ± 1.7% *vs*. 38.3 ± 1.0%; $p<0.01$; ANOVA), similar to the decrease seen in the follicular B cell population discussed above. Again, there was no change in B6.*Sle1*|*Sles1* mice compared to both B6 and B6.*Sle1*.

Similar to what was observed in the T cell compartment, there was also an increase in the percentage of B cells in B6.*Sle1* mice expressing the activation marker CD69. In Fig.7B, the percentage of B220 B cells that expressed CD69 is shown for the various strains, which increased from 2.7 ± 0.3% in B6 to 6.8 ± 1.1% in B6.*Sle1* mice ($p<0.001$; ANOVA). This increase in the activation status of the B cell compartment was also reflected in the increased cell-surface levels of the co-stimulatory molecule CD86 (B7.2) on follicular B cells in B6.*Sle1* mice, as determined by comparisons of MFIs (Table 6; $p<0.05$; repeated measures ANOVA). Neither change was seen in B6.*Sle1*|*Sles1* mice, in which the percentage of B220 B cells expressing CD69 is only 1.5 ± 0.2% ($p<0.001$ *vs.* B6.*Sle1*; ANOVA) and the MFI of CD86 on follicular B cells was correspondingly decreased (Table 6). These results indicate that the suppression of the activation status of lymphocytes introduced by *Sles1* affects both the T and B cell lineages, such that their splenic cell-surface profiles are comparable to B6.

We recently demonstrated that *ex vivo* B cells from B6.*Sle1* mice displayed an intrinsic increase in phosphorylated ERK2 *ex vivo* by 4 months of age (285). Based on this result, we compared splenic B cells from B6.*Sle1*|*Sles1* mice to determine whether the intrinsic ERK2 phosphorylation observed in B6. *Sle1* was affected by the presence of *Sles1*. As shown in Fig.7C, *ex vivo* splenic B cells from 10 month old B6.*Sle1*|*Sles1* mice showed an increase in the levels of phosphorylated ERK2 comparable to that seen in age and gender-matched B6.*Sle1* B cells. The

persistence of this B cell activation phenotype could suggest that B cells in B6.*Sle1*|*Sles1* mice are not receiving adequate T cell help for driving class switch to IgG anti-chromatin autoAb production. However, ELISA analyses for both IgM and IgG anti-chromatin autoAb production by B6.*Sle1Sles1* mice at different ages indicate otherwise, as neither isotype anti-chromatin autoAbs are present in B6.*Sle1*|*Sles1* (Fig.7D). These findings suggest that the suppressive *Sles1* allele acts downstream of these activated molecular pathways, and that hyperphosphorylation of ERK2 can be uncoupled from the humoral autoimmunity elicited by *Sle1*.

Genetic Complementation Suggests a 129 Sles1 Allele

Recent work by our group demonstrated that the break in tolerance to chromatin mediated by the *Sle1* subcongenic locus, *Sle1b*, is associated with functional polymorphisms in the *Slam/Cd2* family of immune receptor genes and that these polymorphisms are found in the majority of inbred strains examined, including the non-autoimmune 129/SvJ (129) (231). Furthermore, introgressing this chromosome 1 interval from 129 onto the B6 background was sufficient to cause a loss in tolerance in chromatin, resulting in the production of serum ANAs (252) (231). This raised the question of why the 129 strain remains non-autoimmune, despite the presence of a potent *Sle1*-related *Slam/Cd2* haplotype on chromosome 1. We hypothesized that, similar to what we previously observed in the NZW strain, epistatic modifiers might play a role in the lack of autoimmunity seen in 129.

To test whether one of the modifiers in 129 was a *Sles1*-like allele, we performed a classic genetic complementation test, comparing the autoimmunity elicited in [129 X B6.*Sle1*]F_1s to that seen in [129 X B6.*Sle1*|*Sles1*]F_1s, by crossing 129 to B6.*Sle1* and B6.*Sle1*|*Rec.4*$^{z/z}$ (B6.*Sle1*|*Sles1*), as illustrated in Fig.8. These comparisons are similar to the

original studies performed with NZW, in which it was shown that NZW homozygosity at *Sles1* is sufficient to prevent systemic autoimmunity in the [NZW X B6.*Sle1*]F_1 hybrid system.

The progeny of the described crosses with 129 are both homozygous for the autoimmunity-promoting SLAM/CD2 Haplotype 2 on chromsome 1, while the remainder of the genome is heterozygous for 129 and B6 alleles (231). However, these two crosses differ at *Sles1*, in that the [129 X B6.*Sle1*|*Sles1*]F_1s carry one copy of the NZW-derived *Sles1* allele (289). Since heterozygosity of the *Sles1* allele does not lead to suppression (see Fig.4), we expect that if the 129 and B6 derived *Sles1* loci are equivalent in their ability to potentiate autoimmunity mediated by homozygsoity of the *Slam/Cd2* family Haplotype 2, both sets of F_1 intercross progeny would have comparable autoimmunity. If however, the 129 strain has a protective *Sles1* allele, complementary to that of NZW, then the latter F_1 intercross progeny would be expected to have abrogated autoimmunity.

As shown in Fig.9A, the degree of moderate to severe GN, defined as being a GN score of 3 or higher, in 9 month old female [129 X B6.*Sle1*]F_1s was significantly higher than that observed in both [129 X B6.*Sle1*|*Sles1*]F_1s and [129 X B6]F_1s ($p<0.01$ and $p<0.001$ respectively; ANOVA). In addition, the [129 X B6.*Sle1*|*Sles1*]F_1 group was the only group with no evidence of lymphocyte infiltration of the kidneys (Table 7). Similarly, when spleen weights from the different mice were compared (Fig.9B), the [129 X B6.*Sle1*]F_1s exhibited significant splenomegaly ($p<0.001$ vs. B6; non-parametric ANOVA), whereas [129 X B6.*Sle1*|*Sles1*]F_1s did not. In fact, as clearly shown in Fig.9B, the only congenic lines with significant differences in spleen weights from B6 were those that have one or more copies of the B6 allele at the *Sles1* locus, when *Sle1* is homozygous. These data strongly support the presence of a complementary *Sles1* modifier in the 129 genome.

The quantification of IgG autoAb levels in the different strains further support this conclusion. As shown in Fig.10A-B, only the [129 X B6.*Sle1*]F_1s had significant levels of serum anti-dsDNA IgG autoAbs by 9 months of age (vs. B6, $p<0.01$). In contrast, the penetrance of anti-dsDNA autoAbs in [129 X B6.*Sle1*|*Sles1*]F_1s did not differ significantly from age and gender-matched B6 and 129 controls.

We also assayed for the more non-specific anti-chromatin autoAbs in the various strains. As shown in Fig.10C-D, at 9 months of age both the titres and penetrance of serum IgG ANAs in the [129 X B6.*Sle1*]F_1s was highly increased, when compared to any of the control groups ($p<0.001$; ANOVA). Interestingly, unlike anti-dsDNA autoantibodies, the [129 X B6]F_1s themselves had an increased (50%) penetrance of anti-chromatin autoAbs. In contrast to either of the other F_1 groups, the [129 X B6.*Sle1*|*Sles1*]F_1s had minimal serum anti-chromatin autoAbs at 9 months of age (Fig.10C-D).Significantly, differences in the titres and penetrance of anti-chromatin autoAbs were discernible as early as 5 months of age in [129 X B6.*Sle1*]F_1s (Fig.10E).

These data indicate that the 129-derived *Sles1* allele specifically complements the NZW *Sles1* allele in preventing both the more pathogenic phenotypes, such as GN development and anti-dsDNA autoAbs, as well as the development of the more benign serum anti-chromatin autoAbs. Overall, these results are practically identical to those originally obtained in the analysis of the [NZW X B6.*Sle1*|*Sles1*]F_1 hybrid system (242). However, the presence of *Sles1* in 129 is especially intriguing since classic analyses of the H2 complex in 129 have defined it as an $H2^b$ haplotype very closely related, but not identical, to the $H2^b$ haplotype carried by B6.

Discussion

The present study extends our previous work characterizing the suppression of autoimmunity mediated by *Sles1* in the bicongenic B6.*Sle1*|*Sles1* system. Our congenic fine-mapping localizes *Sles1* into an interval on chromosome 17 that encompasses approximately 956 KB of the proximal portion of the murine MHC. The current minimal *Sles1* interval still contains 69 genes, consistent with the gene rich nature of this segment of the genome (31, 32). Many of these positional candidates are known to possess immunological functions and are also highly polymorphic between the B6 and NZW strains (289, 290). However, our genetic fine-mapping analysis definitively excludes *TNF-α*, a known lupus susceptibility candidate gene and one implicated in other murine lupus models, as well as the genes distal to it, as possible *Sles1* candidates (55, 291-293). As shown in the schematic in Fig.11, this leaves many other potentially interesting candidates, including the Class II genes *H2-Ab1*, *Aa*, *Eb* and *Ea*, the complement genes proximal to *TNF-α*, as well as other relevant genes such as *Daxx*, *Notch4* and *Hspa1a*. Interestingly, unlike many other loci implicated in lupus and other autoimmune disease susceptibility, fine-mapping of *Sles1* did not reveal the presence of multiple sub-loci contributing to suppression (153, 294, 295).

In contrast to other autoimmune disorders, such as Insulin Dependent Diabetes Mellitus (IDDM) and Multiple Sclerosis (MS), the association of the Class II MHC genes with susceptibility to SLE has proven to be very complicated and highly dependent on epistatic interactions with other susceptibility loci, as demonstrated in a variety of linkage studies in both human SLE patients and murine lupus models. Earlier studies using the classic [NZB X NZW]F_1 (BWF_1) model, from which NZM2410 is derived, in various backcross analyses have suggested that the NZW allele at the H2 ($H2^z$) confers a high risk of developing renal disease, and in

particular it is the NZW Class II alleles that are the dominant contributors to disease in these models (296). Many of these studies have documented that heterozygosity at the H2 gene complex is crucial for lupus susceptibility, and is associated with many of the phenotypic characteristics of lupus, such as GN development, autoantibody production and splenomegaly (215). However, many such backcross studies have also indicated that homozygosity of the NZW alleles at the H2 region is protective. These somewhat contradictory data have led to a variety of hypotheses such as an increased self-recognition in heterozygotes due to mixed haplotype or mixed isotype Class II molecules, suppressive effects caused by increased Class II I-E expression, and competition by peptides derived from I-Ea resulting in decreased self-peptide presentation by Class II I-A molecules during thymic development leading to increased autoimmune susceptibility (146, 148, 210, 211, 216). A major limitation in interpreting the role of H2 loci in these backcross studies is that the remainder of the genome also contains susceptibility alleles that are randomly segregating. Considering the importance of epistatic interactions in the development of SLE, this heterogeneous segregation complicates the unambiguous association of phenotypes with a specific locus.

The use of transgenics for the various NZW Class II alleles ($I\text{-}E^z$ and $I\text{-}A^z$) on non-autoimmune backgrounds have also been used in various backcross studies to determine the contributions of these alleles to lupus susceptibility, and have shown that transgenic expression of the Class II molecules does not recapitulate what is seen when congenics for the entire NZW MHC are used in similar crosses. This suggests that non-Class II molecules in the MHC, in tight linkage disequilibrium with Class II genes, may be the ultimate culprits in modulating disease susceptibility (221, 222). Recently, Zhang *et al.*, used intra-MHC recombinants to try and elucidate the contribution of variances in the level of I-E expression, when the I-A molecule

haplotype is held constant, in a series of F_1 crosses. They concluded that expression of the Class II I-E molecule offers protection in a dose-dependent manner, and postulate that this may be due to mechanisms including thymic deletion of a self-reactive TCR repertoire, determinant capture, differences in cytokine balances and competition for signal transduction moities. However, the recombinant breakpoint in their intra-MHC recombinant, H2-^{g2r}, is defined only as occurring somewhere between *H2-Ea* and *TNF-α*, a region containing over 60 genes (Fig.5 and www.ensembl.org/Mus_musculus/) (297). It could hence also be concluded that a gene within this undefined interval, which partially overlaps with our minimal *Sles1* interval, is responsible for the dose-dependent protection seen in their studies.

In addition to Class II genes, the complement genes within the MHC have long been implicated in lupus susceptibility. Deficiencies in the complement components C1 and C4 are in fact the only known single gene deficiencies that are so strongly associated with human SLE (3). Furthermore, during lupus disease progression, acquired deficiencies in complement components are common, and are presumed to result from the immune complex (IC) utilization of complement. There are two main, non-mutually exclusive theories that have been proposed to explain the link between complement deficiency and susceptibility to lupus. One involves the role of complement in the clearance of apoptotic cells and immune complexes and the other invokes the known ability of complement to determine activation thresholds in B and T lymphocytes (41). Interestingly, ablation of the C4 gene, located at the peak marker used in the original linkage studies describing *Sles1*, has been demonstrated to alter negative selection of immature self-reactive B cells in both the double-transgenic HEL (Hen Egg Lysosome) and the *lpr* null models (242, 298). Furthermore, unlike other complement deficiencies (*C1qa*, *C3*, *Cr1/2*), the lack of C4 appears less dependent on a mixed 129 X B6 background for the

manifestation of some degree of autoimmunity (37). Serum levels of this complement component however, were found to be equivalent in young, pre-autoimmune B6, B6.*Sle1* and B6.*Sle1*|*Sles1* mice (data not shown).

Other candidate genes in the *Sles1* interval includes the MHC proximal gene *Daxx*, known to play an important role in the IFN-α mediated inhibition of B lymphopoeisis, which is interesting considering the large number of recent studies implicating Type I interferons in lupus susceptibility (25-29, 164, 299). Heat shock proteins (HSPs) are known to have effects on the maturation of antigen-presenting cells (APCs), in a manner reminiscent of cytokines, and Hsp70, encoded by *Hspa1a* on the distal end of the minimal *Sles1* interval, has been shown to be capable of converting T-cell tolerance to autoimmunity *in vivo* (300, 301). *Notch4* is also contained within the *Sles1* interval, and given the recent wave of papers implicating members of the Notch family of receptors and ligands in regulating B and T lymphocyte development and function, it remains an attractive candidate for *Sles1* (302-311).

Our phenotypic analyses of the cell-surface characteristics of the splenic immune cells from B6, B6.*Sle1* and B6.*Sle1*|*Sles1* mice reveal that many, but not all, of the differences seen in 9-12 month old B6.*Sle1* splenocytes are suppressed in the presence of *Sles1*. Aged B6.*Sle1* mice, despite their relatively benign autoimmune phenotype of ANA production, have significantly increased populations of activated B ($B220^{+}CD69^{+}$) and T ($CD4^{+}CD62L^{-}CD44^{hi}$; $CD3^{+}CD69^{+}$) cells, similar to those observed in much more severe lupus models (36, 189, 193, 197, 200, 286). It has been postulated that the spontaneous lymphocyte activation seen in these different lupus models is due to differences in thresholds for activation and immune regulation caused by the underlying genetic polymorphisms in relevant susceptibility loci (162, 195, 231). Intriguingly, both T and B cells from B6.*Sle1*|*Sles1* mice have a significantly reduced activation phenotype,

indistinguishable from B6, suggesting that *Sles1* is impacting both lymphocyte compartments. This indicates that a lack of T cell help to B cells is not the sole mechanism of suppression**.** This is further supported by the observation that B6.*Sle1*|*Sles1* mice do not produce serum IgM autoantibodies either, indicating that lack of class-switching is not the reason these mice do not produce high titres of serum IgG autoAbs. *Ex vivo* B cells from B6.*Sle1*|*Sles1* mice, however, demonstrate a comparable increase in phosphorylated ERK2 to those from B6.*Sle1*, indicating that this activated molecular pathway can be uncoupled from the humoral autoimmunity elicited by *Sle1*.

Given the density and polymorphic nature of the genes within the *Sles1* interval, definitive identification of the *Sles1* gene has proven to be quite a challenge. Our F_1 analyses with the non-autoimmune 129 strain, however, provide an alternative approach that may significantly accelerate this analysis. Since B6 and 129 have very closely related H2 haplotypes, most notably identity for Class II *I-A* and *I-E* alleles, the degree of variability between the B6 and 129 alleles will be much reduced in comparison to B6 *vs.* NZW. Consequently, we will seek variations in structure/function of candidate genes between B6 and 129, which should enhance our ability to quickly focus on relevant polymorphisms. Furthermore, this result excludes the candidacy of MHC Class II molecules for *Sles1*.

The use of congenic recombinants has now been used to fine-map both susceptibility and suppressive loci in efforts to identify the underlying genes (153, 231). These congenic systems allow individual key susceptibility and modifier loci to be specifically combined, so that phenotypes resulting from their genetic interactions can be studied. Hence, the ability of *Sles1* to specifically target *Sle1* could help elucidate the key epistatic interactions involved in the generation of severe systemic autoimmunity in lupus models where *Sle1* has been shown to be

necessary for initiation and development (200, 201, 286). Identification of *Sles1*, using both recombinant fine-mapping strategies and comparisons of B6, 129 and NZW alleles, will have important implications for our understanding of and ability to therapeutically intervene in SLE pathogenesis.

Fig. 2

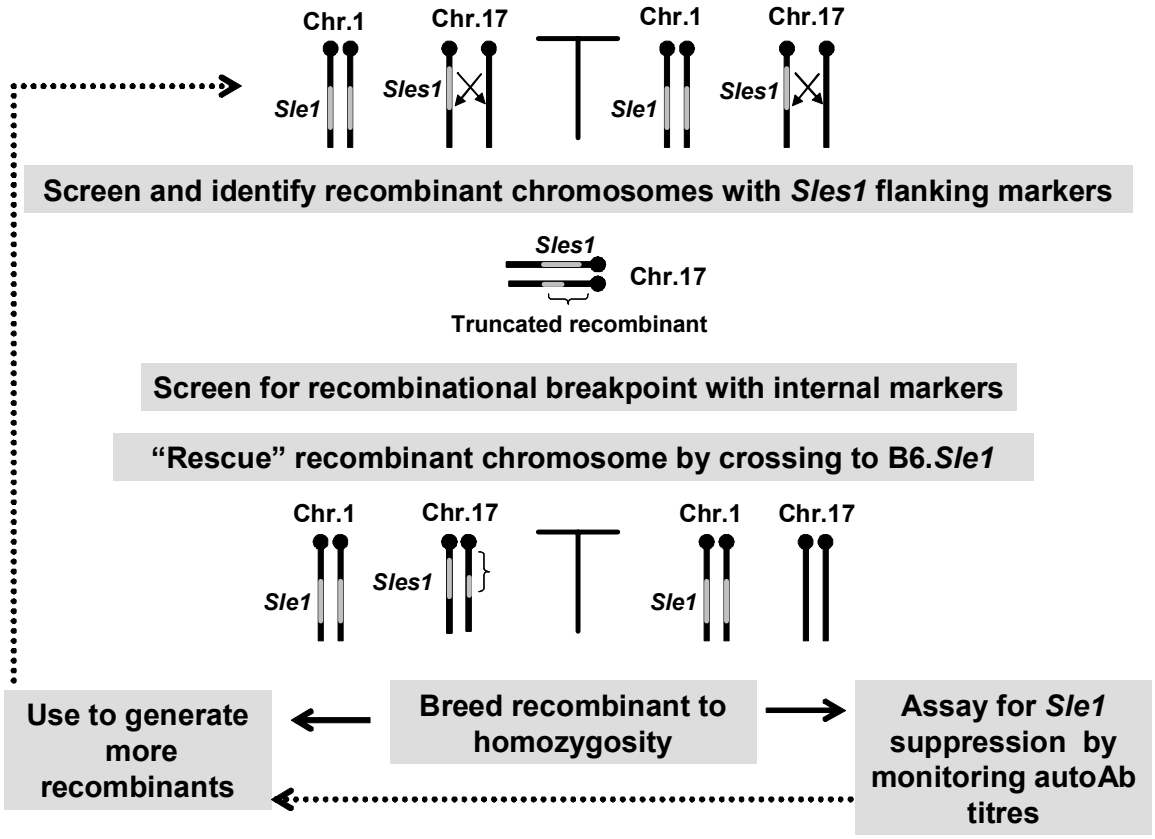

Figure 2. Recombinant congenic strategy used to fine-map *Sles1*. Mice heterozygous for *Sles1* were intercrossed and tail DNA from progeny screened for informative meioses using flanking markers. Once identified, recombinant chromosomes were screened with internal markers and the mice bred back to B6.*Sle1* to create a new recombinant line. Each line was aged to 12 months to assay for *Sle1* suppression, and recombinants were intercrossed to generate more smaller, truncated intervals in both directions across the *Sles1* interval.

Fig. 3

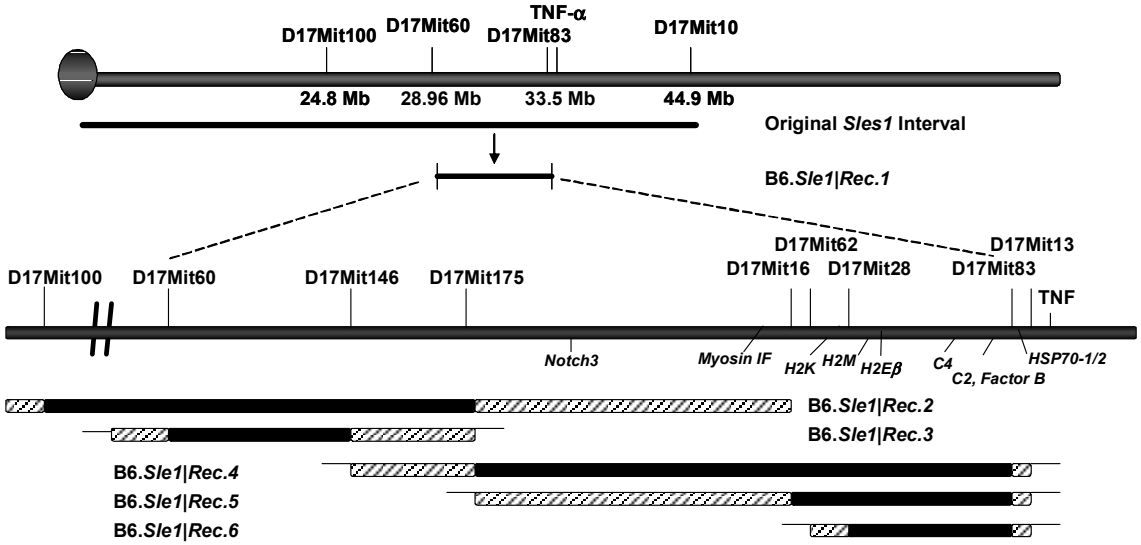

Figure 3. Six Recombinant Chromosomes Generated to Map *Sles1*. B6.*Sle1*|*Sles1*^{het} intercross progeny were screened for recombinant chromosomes using a panel of 20 polymorphic microsattelite markers, bred to homozygosity and assayed for suppression of *Sle1*. The interval spanned by B6.*Sle1*|*Rec.1* is expanded to better denote the placement of the remaining recombinant chromosomes.

Fig. 4A

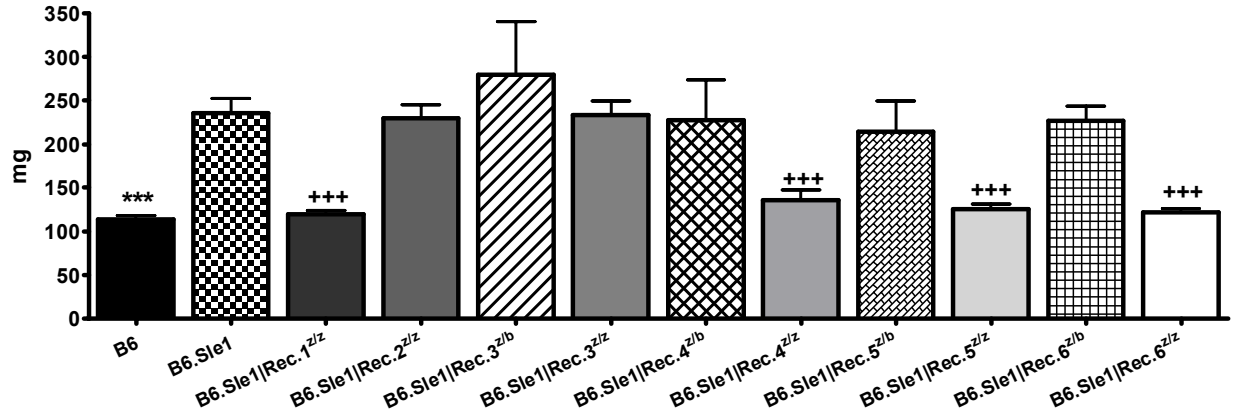

Fig. 4B

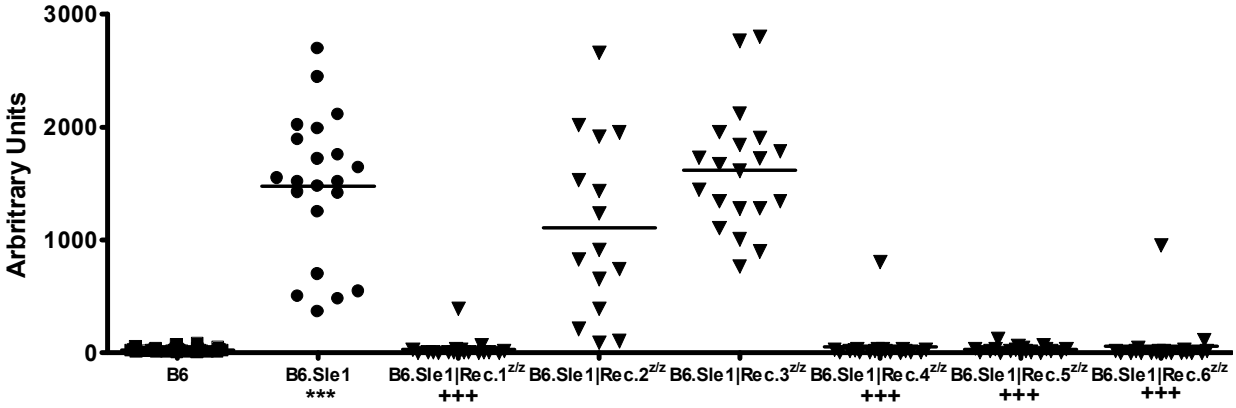

Figure 4. *Sles1* Maps to ~956 kB Interval That Excludes *TNF-α*. A. Spleens from female mice of the indicated genotypes at 9-12 months of age were weighed in order to assess for suppression of the mild splenomegaly seen in B6.*Sle1* mice in the presence of recombinant versions of *Sles1* (mean ± SEM). Serum levels of IgG ANAs in 9-12 month old female mice of the genotypes shown were ascertained by ELISA as described in *Materials and Methods*. To determine penetrance, samples were deemed positive if their value exceeded that of the mean ± 4SDs of the B6 controls. Each symbol represents an individual sample of the respective genotype. Horizontal lines show means.
n= 15-36/genotype; ** $p<0.01$, *** $p<0.001$ *vs.* B6; $^{+++}$ $p<0.001$ *vs.* B6.*Sle1*, as determined by non-parametric ANOVAs.

Fig. 5

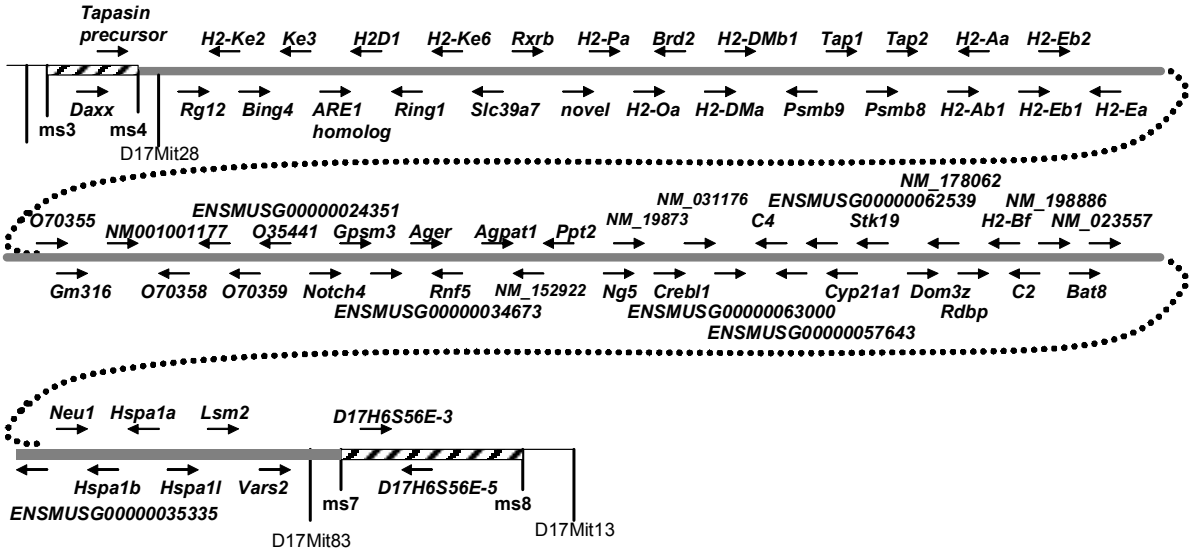

Figure 5. The Minimal *Sles1* Interval Contains 69 Genes. The region spanned by the *Rec.6* chromosome is expanded to present a physical map of the interval. Microsatellite primer sequences were used to delineate the boundaries of the *Sles1* minimal interval. Information regarding the gene content of the region and transcriptional directions was obtained by employing MartSearch to identify genes contained within the basepairs 32356249 and 33530533 on mouse chromosome 17, which represent the base pair positions of the forward ms3 and reverse ms8 primer pairs respectively on NCBI build m33 (www.ensembl.org/Mus_musculus/). Solid bars indicate NZW congenic intervals, hatched bars represent recombinational breakpoint regions and thin lines designate B6. Arrows indicate transcriptional direction.

Table 6

Splenic Cell Population[1]	B6 (n=14)	B6.*Sle1* (n=8)	B6.*Sle1*|*Sles1* (n=8)	B6 *vs.* B6.*Sle1*	B6.*Sle1 vs.* B6.*Sle1*|*Sles1*
$B220^+$	53.79 ± 1.23	46.88 ± 1.78	47.53 ± 2.38	***p<0.05***	ns
%$CD69^+$	2.71 ± 0.31	6.79 ± 1.06	1.49 ± 0.19	***p<0.001***	***p<0.001***
T1 ($CD23^-CD21^-IgM^+$)	4.58 ± 0.4	4.18 ± 0.68	3.94 ± 0.77	ns	ns
T2 ($CD23^+CD21^{hi}IgM^{hi}$)	1.87 ± 0.12	1.46 ± 0.16	1.76 ± 0.23	ns	ns
Follicular ($CD23^+CD21^+IgM^{lo}$)	29.59 ± 1.3	23.24 ± 1.14	28.46 ± 1.45	***p<0.01***	ns
CD86 MFI	69.1 ± 10.4	79.43 ± 8.53	62.51 ± 11.12	***p<0.05***	***p<0.001***
MZ ($CD23^-CD21^-IgM^+$)	4.89 ± 0.51	5.15 ± 0.53	4.62 ± 0.85	ns	ns
B1a ($CD5^+CD23^-B220^+$)	1.93 ± 0.25	1.56 ± 0.2	2.03 ± 0.43	ns	ns
B1b ($CD5^-CD23^-B220^{lo}$)	2.76 ± 0.18	4.15 ± 0.56	2.32 ± 0.07	ns	ns
B2 ($CD5^-CD23^+B220^+$)	38.32 ± 1.02	29.44 ± 1.69	34.06 ± 2.49	***p<0.01***	ns
Plasma ($CD19^-CD138^+$)	1.11 ± 0.11	2.63 ± 0.17	1.09 ± 0.07	***p<0.001***	***p<0.001***
$CD3^+$	31.65 ± 1.33	24.85 ± 1.82	31.79 ± 2.59	***p<0.05***	ns
%$CD69^+$	18.55 ± 1.27	36.85 ± 1.27	14.46 ± 1.71	***p<0.001***	***p<0.001***
CD69 MFI	35.74 ± 2.33	55.0 ± 3.53	29.84 ± 3.12	***p<0.001***	***p<0.001***
$CD4^+$	18.18 ± 0.54	17.46 ± 1.11	18.8 ± 1.35	ns	ns
%$CD25^+CD69^-$	10.46 ± 0.28	10.67 ± 0.59	11.84 ± 0.56	ns	ns
%$CD69^+CD25^+$	12.98 ± 1.09	21.32 ± 0.59	7.95 ± 0.63	***p<0.001***	***p<0.001***
%$CD69^+CD25^-$	10.14 ± 0.75	19.72 ± 1.33	4.16 ± 0.98	***p<0.001***	***p<0.001***
%$CD62L^+CD44^{lo}$	38.2 ± 3.06	11.56 ± 1.43	58.06 ± 2.04	***p<0.001***	***p<0.001***
%$CD62L^-CD44^{lo}$	25.67 ± 2.74	36.18 ± 6.55	12.12 ± 1.07	ns	***p<0.01***
%$CD62L^-CD44^{hi}$	23.44 ± 2.45	40.3 ± 4.82	17.94 ± 1.89	***p<0.01***	***p<0.01***
%$CD62L^+CD44^{hi}$	12.7 ± 1.46	11.92 ± 2.22	11.9 ± 1.54	ns	ns
$CD8^+$	11.84 ± 0.94	6.90 ± 0.44	14.9 ± 1.6	***p<0.01***	***p<0.001***
$CD11b^+$	4.63 ± 0.37	5.56 ± 0.45	5.78 ± 0.64	ns	ns
$NK1.1^+$	1.03 ± 0.12	0.76 ± 0.16	0.76 ± 0.13	ns	ns
$CD3^+NK1.1^+$	0.85 ± 0.19	0.70 ± 0.17	0.54 ± 0.19	ns	ns

Table 6. Cellular Compositions of B6, B6.*Sle1* and B6.*Sle1*|*Sles1* Spleens.
[1] Splenocytes from 9-12 month B6, B6.*Sle1* and B6.*Sle1*|*Sles1* were subjected to 4-color FACS analyses as detailed in Chapter II. Eight to fourteen mice of each strain were analyzed. Shown values represent mean ± SEM. Indented subsets indicate that the listed percentages are representative of the non-indented parent population listed above. All remaining values are percentages of live cells as determined by forward and side scatter profiles. All statistical analyses were conducted using parametric and non-parametric ANOVAs between all three groups as determined by InStat3, with the exception of the median fluorescence intensity (MFI) of CD86 on follicular B cells, for which repeated measures ANOVA was used. Comparisons listed are B6 *vs.* B6.*Sle1* and B6.*Sle1 vs.* B6.*Sle1*|*Sles1*. ns, not significant.

Fig. 6A

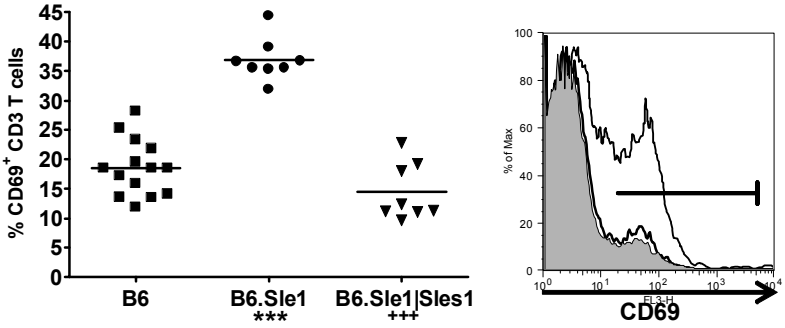

Fig. 6B

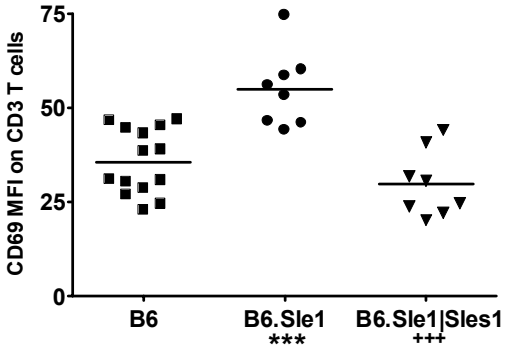

Fig. 6C

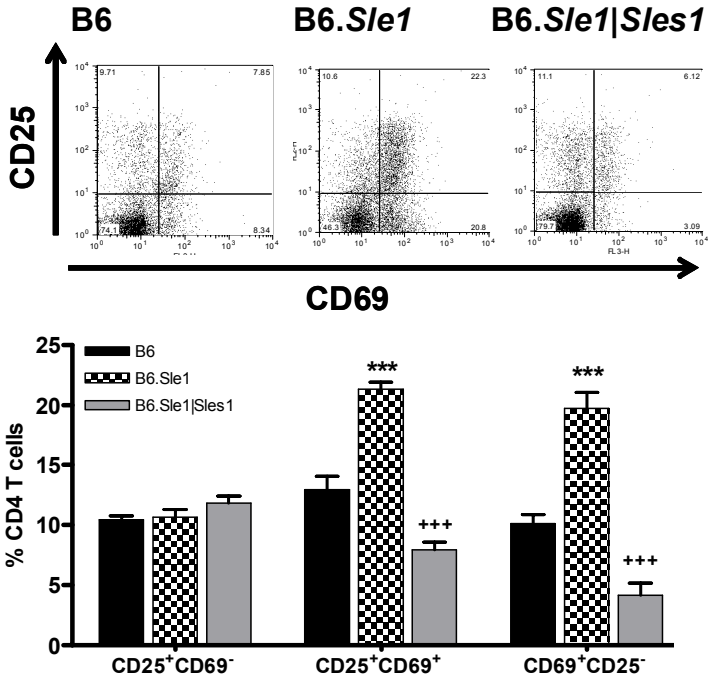

Fig. 6D

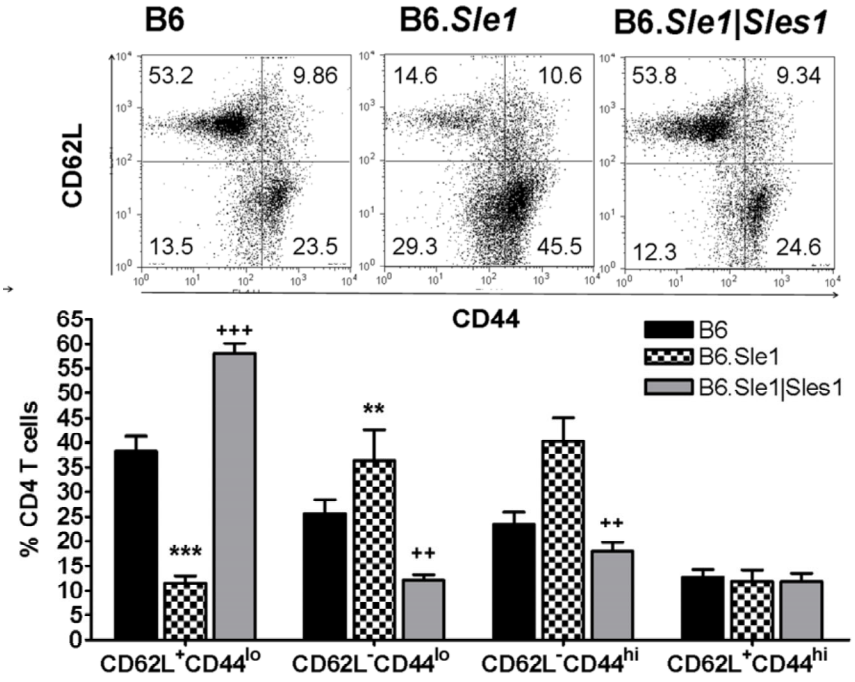

Figure 6. *Sle1* Mediated T cell Activation Phenotypes Suppressed in the Presence of *Sles1*. A. Increased $CD69^+$ CD3 T cell Percentages Absent in B6.*Sle1*|*Sles1* Mice. Percent of $CD69^+$ CD3 T cells are shown in individual mice as indicated by symbols and the horizontal lines designate averages (left). Representative histogram plots of CD69 expression gated on CD3 T cells (right). B6, shaded histogram; B6.*Sle1*, thin histogram; B6.*Sle1*|*Sles1*, bold histogram. B. B6.*Sle1*|*Sles1* Mice Do Not Have Increased CD69 MFI on CD3 T cells. MFIs of CD69 expression on cells gated on CD3 from individual mice are shown for the indicated genotypes. C. B6.*Sle1* Mice Have Increased $CD4^+CD69^+CD25^+$ and $CD4^+CD69^+CD25^-$ Percentages. Representative CD25 *vs.* CD69 dot plots, gated on CD4 T cells (top) are shown with the respective genotypes listed above. Percentages of $CD25^+CD69^-$, $CD69^+CD25^+$ and $CD69^+CD25^-$ within the gated CD4 T cell population at 9-12 months of age (mean ± SEM) (bottom). D. *Sle1* Mediated Decrease in Naïve CD4 T Cells Abrogated by *Sles1*. Representative CD62L *vs.* CD44 dot plots, gated on CD4 T cells from the indicated genotypes are shown (top). Cumulative percentages of $CD62L^+CD44^{lo}$, $CD62L^-CD44^{lo}$, $CD62L^-CD44^{hi}$ and $CD62L^+CD44^{hi}$ CD4 T cells from 9-12 month B6, B6.*Sle1* and B6.*Sle1*|*Sles1* mice are plotted (mean ± SEM) (bottom). ** $p<0.01$, *** $p<0.001$ *vs.* B6; $^{++}p<0.01$, $^{+++}p<0.001$ *vs.* B6.*Sle1*, as determined by parametric ANOVAs.

Fig. 7A

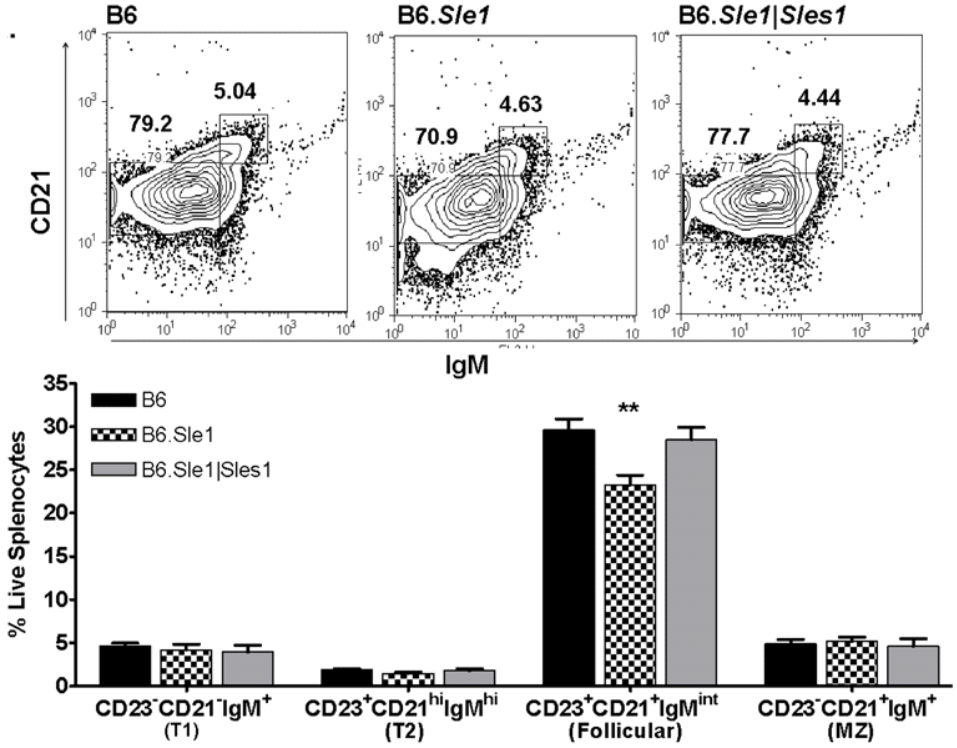

Fig. 7B

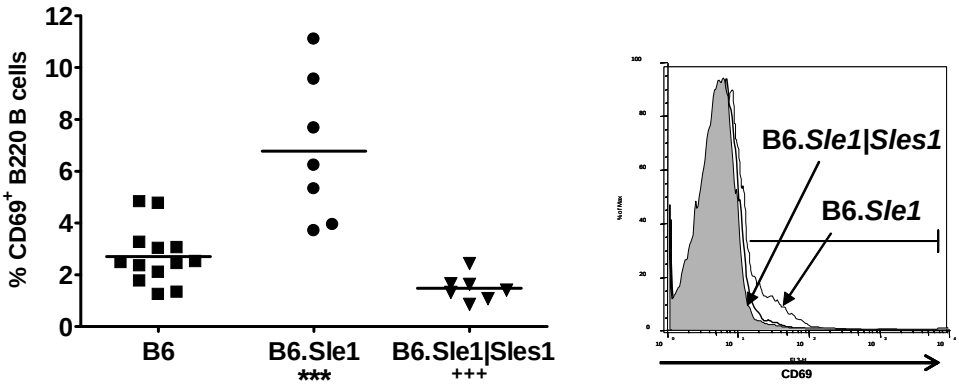

Fig. 7C

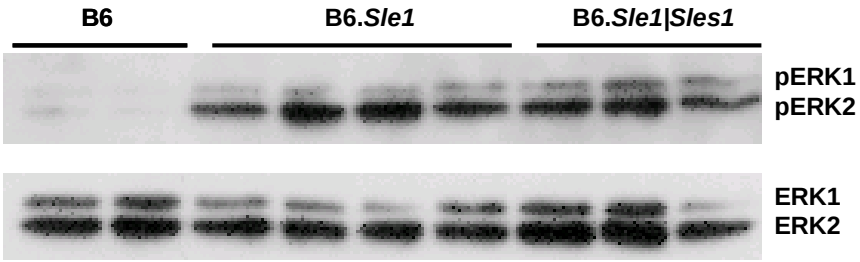

Fig. 7D

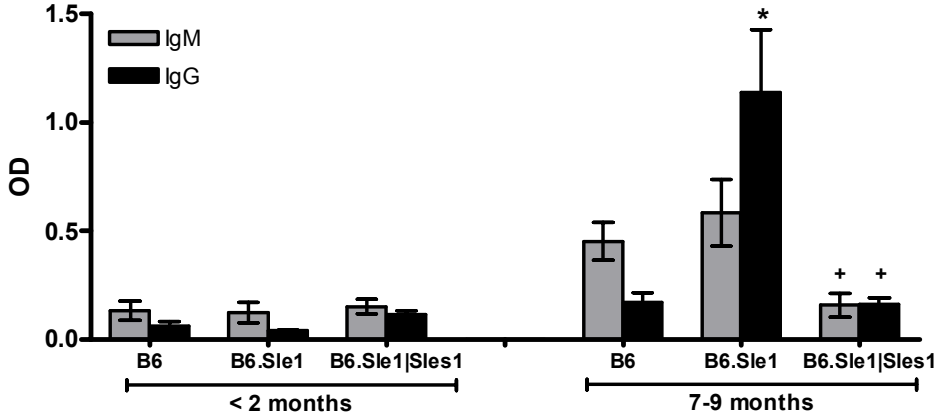

Figure 7. Cell-surface but Not Molecular B cell Activation Phenotypes Absent in B6.*Sle1*|*Sles1* Mice. A. Decreased Follicular B cells in B6.*Sle1* Mice. Representative contour plots of CD21 *vs.* IgM, pre-gated on $CD23^+$ cells, defining transitional 2 (T2) ($CD23^+CD21^{hi}IgM^{hi}$) and follicular ($CD23^+CD21^+IgM^{int/lo}$) B cells from the three different genotypes are shown (top). Percentages of $CD23^-CD21^-IgM^+$ (T1), $CD23^+CD21^{hi}IgM^{hi}$ (T2), $CD23^+CD21^+IgM^{int/lo}$ (follicular) and $CD23^-CD21^+IgM^+$ (MZ) B cells at 9-12 months of age (mean ± SEM) within the live, splenocyte population are displayed (bottom) (312). B. Lack of Increased $CD69^+$B cell Percentages in the Presence of *Sles1*. Percent of $CD69^+$ B220 B cells are shown in individual mice as denoted by symbols. Horizontal lines represent averages (left). Representative histogram plots of CD69 expression on B220 B cells. B6, shaded histogram; B6.*Sle1*, thin histogram; B6.*Sle1*|*Sles1*, bold histogram (right). C. Comparable Increases in Phosphorylated ERK2 Seen in B6.*Sle1* and B6.*Sle1*|*Sles1* B cells. Lysates from purified splenic B cells from the indicated genotypes were run out on SDS-PAGE gels and blotted for phosphorylated ERK1/2 kinases to look for changes in *ex vivo* phosphorylation patterns (top). Blots were stripped and reprobed with total ERK1/2 antibodies to compare overall ERK1/2 protein levels (bottom). D. Lack of Both Serum IgM and IgG ANAs in the Presence of *Sles1*. Sera from 1-2 month and 7-9 month mice of the indicated genotypes were assayed in parallel plates for the presence of ANAs of both IgM and IgG isotypes, to determine if *Sles1* was impacting B cell class switching. * $p<0.05$, ** $p<0.01$, *** $p<0.001$ *vs.* B6; $^+$ $p<0.05$, $^{+++}$ $p<0.001$ *vs.* B6.*Sle1*, as determined by ANOVAs.

Fig. 8

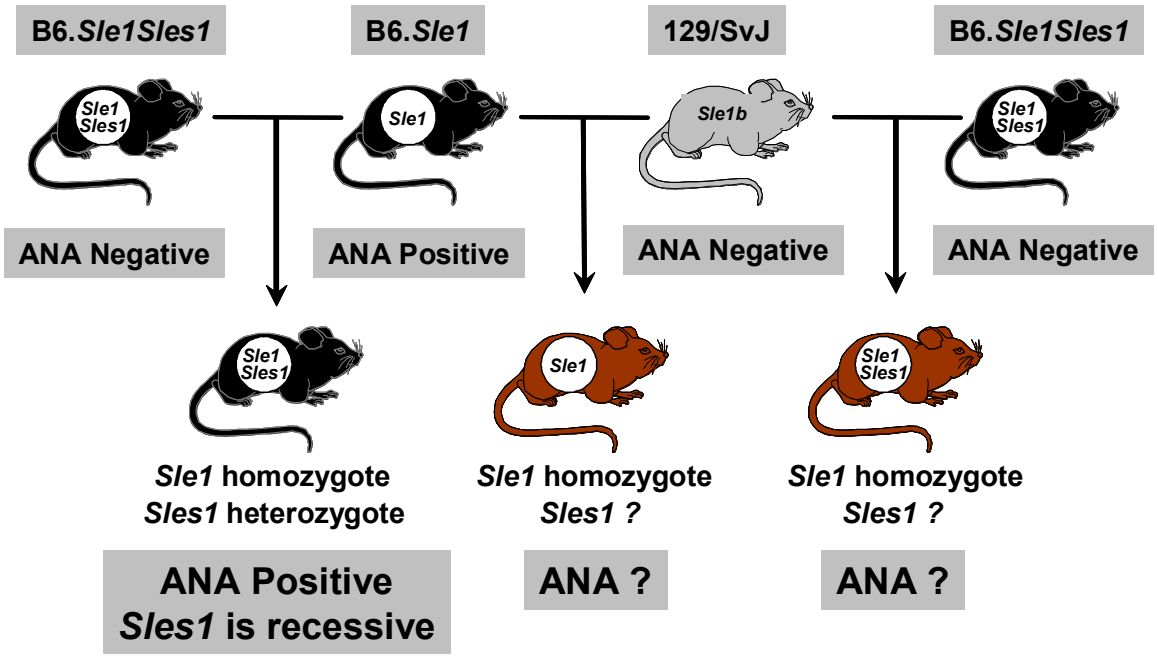

Figure 8. Strategy for Genetic Complementation Test. It is known that *Sles1* acts in a recessive fashion and that heterzoygosity at this locus in the context of *Sle1* homozygosity maintains an ANA positive phenotype (242). To test if 129 harbored a *Sles1* allele complementary to that of the NZW-derived *Sles1*, the mating strategy shown above was employed, where 129 was crossed to both B6.*Sle1* and B6.*Sle1*|*Sles1* and the resulting F_1 female progeny were aged and assayed for autoimmunity.

Fig. 9A

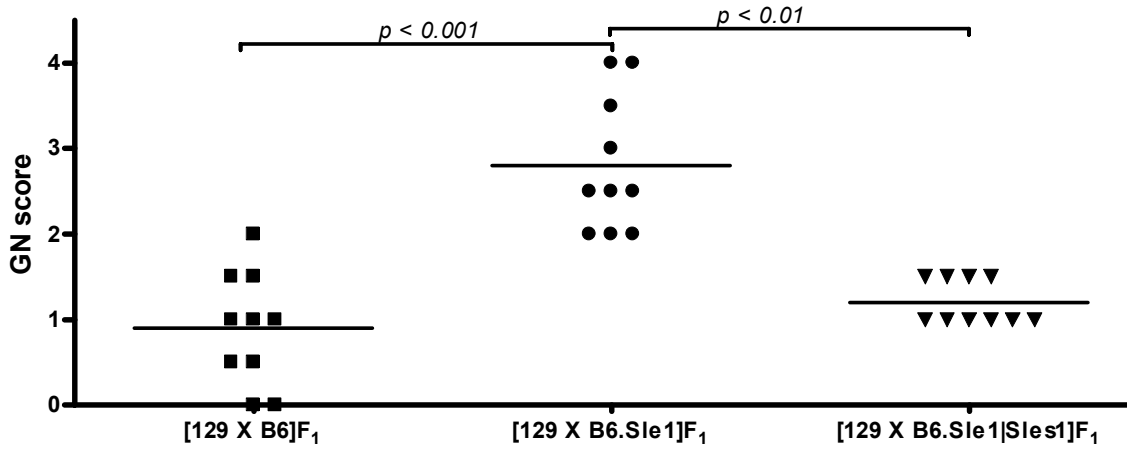

Fig. 9B

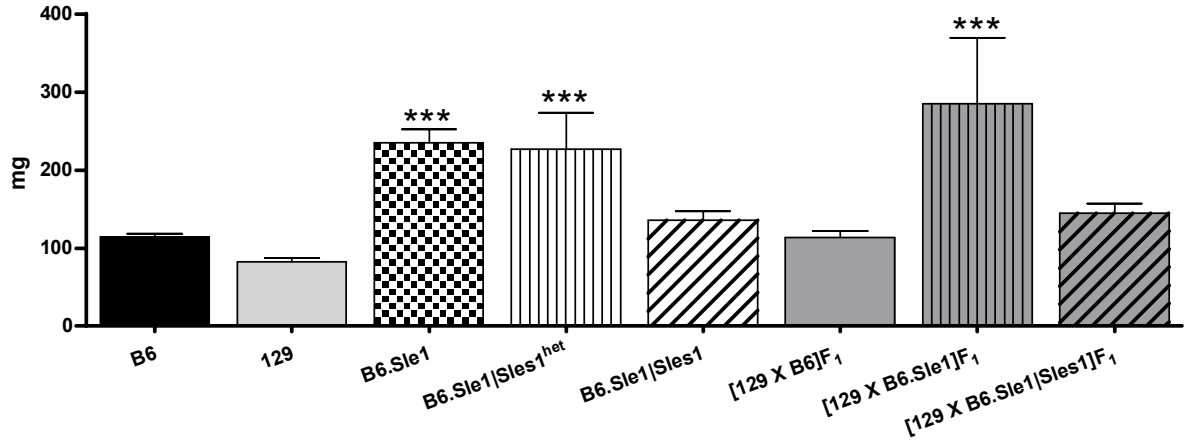

Figure 9. The NZW *Sles1* is Complemented by the 129 *Sles1* Interval to Prevent Severe Autoimmunity in [129 X B6.*Sle1*|*Sles1*]F_1s. A. Lack of Severe GN in [129 X B6.*Sle1*|*Sles1*]F_1s. B6, B6.*Sle1* and B6.*Sle1*|*Sles1* mice were crossed to 129, and resulting F_1 female progeny aged to 9 months and kidneys collected. Kidney sections were analyzed in a blind manner for evidence of pathologic changes in the glomeruli, tubules or interstitial areas. GN scores from 10 mice/genotype are shown. B. The Splenomegaly Seen in [129 X B6.*Sle1*]F_1s is Absent in [129 X B6.*Sle1*|*Sles1*]F_1s. Median and interquartile ranges from the indicated genotypes at 9-12 month are shown. *** $p<0.001$ *vs.* B6.

Table 7

No.	*Genotype*	*GN Score*	*Crescents*	*Tubules/ Interstitium*	*Lymphocyte Infiltration*
1	[129 X B6]F_1	0.5	0	0	mild
2	[129 X B6]F_1	0.5	0	0	mild
3	[129 X B6]F_1	0	0	0	negative
4	[129 X B6]F_1	2	0	0.5	mild
5	[129 X B6]F_1	1.5	0	0.5	negative
6	[129 X B6]F_1	1	0	0	negative
7	[129 X B6]F_1	0	0	0	mild
8	[129 X B6]F_1	1	0	0	negative
9	[129 X B6]F_1	1	0	0	mild
10	[129 X B6]F_1	1.5	0	0	negative
11	[129 X B6.*Sle1*]F_1	3	rare	1	mild
12	[129 X B6.*Sle1*]F_1	3.5	0	0.5	negative
13	[129 X B6.*Sle1*]F_1	4	10	1.5	mild
14	[129 X B6.*Sle1*]F_1	2.5	0	0.5	negative
15	[129 X B6.*Sle1*]F_1	2	0	0.5	mild
16	[129 X B6.*Sle1*]F_1	2	0	0.5	mild
17	[129 X B6.*Sle1*]F_1	4	20	1.5	negative
18	[129 X B6.*Sle1*]F_1	2.5	1	0.5	negative
19	[129 X B6.*Sle1*]F_1	2	0	0.5	mild
20	[129 X B6.*Sle1*]F_1	2.5	0	0.5	mild
21	[129 X B6.*Sle1Sles1*]F_1	1	0	0	negative
22	[129 X B6.*Sle1Sles1*]F_1	1	0	0	negative
23	[129 X B6.*Sle1Sles1*]F_1	1.5	0	0	negative
24	[129 X B6.*Sle1Sles1*]F_1	1	0	0	negative
25	[129 X B6.*Sle1Sles1*]F_1	1.5	0	0	negative
26	[129 X B6.*Sle1Sles1*]F_1	1	0	0	negative
27	[129 X B6.*Sle1Sles1*]F_1	1	0	0	negative
28	[129 X B6.*Sle1Sles1*]F_1	1	0	0	negative
29	[129 X B6.*Sle1Sles1*]F_1	1.5	0	0.5	negative
30	[129 X B6.*Sle1Sles1*]F_1	1.5	0	0	negative

Table 7. Histological Data from Kidneys of F_1 Animals. A more detailed representation of the pathological parameters examined in the kidneys from the various F_1 crosses is presented. Grading methodology is detailed in Chapter II. In terms of all parameters examined, [129 X B6.*Sle1*|*Sles1*]F_1 progeny have the least amount of disease.

Fig. 10A

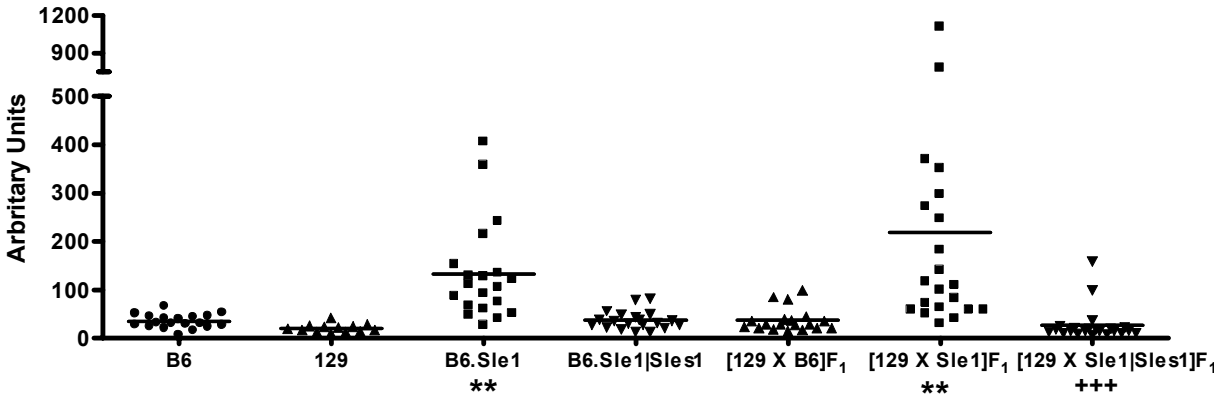

Fig. 10B

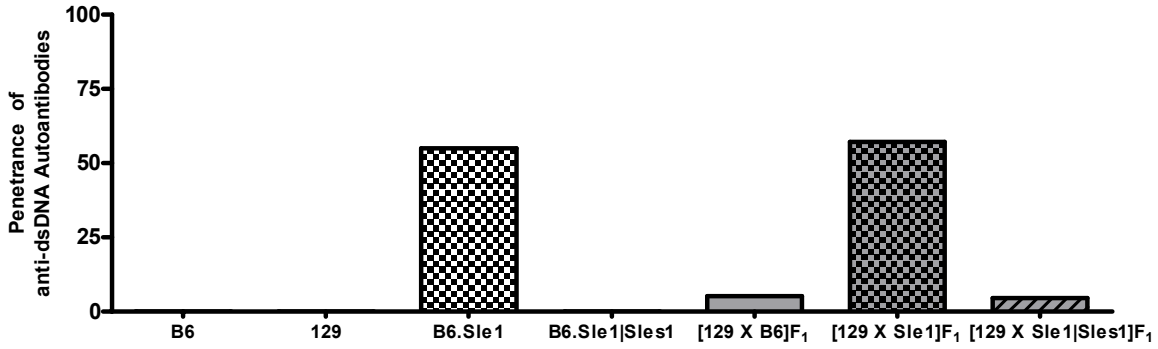

Fig. 10C

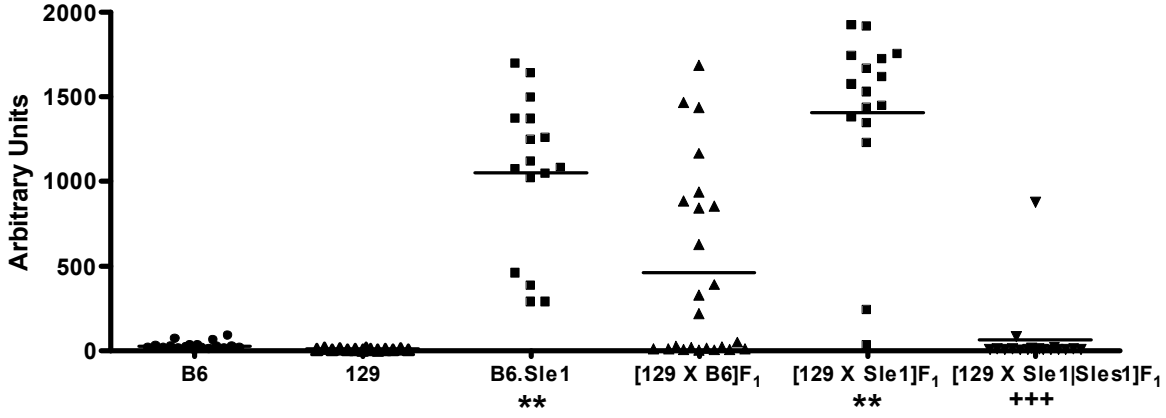

Fig. 10D

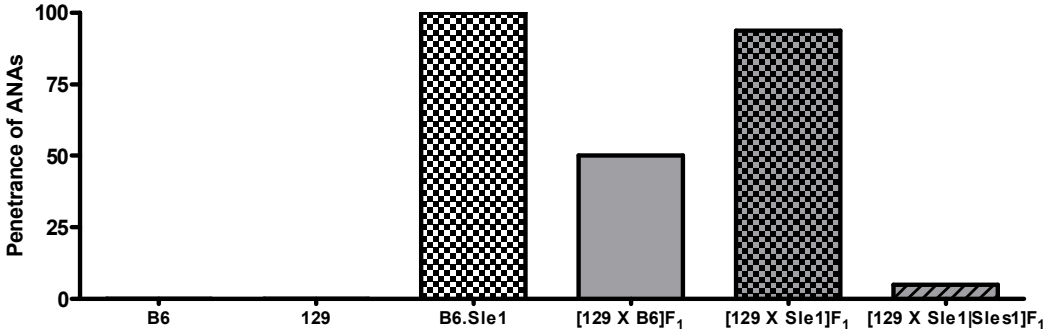

Fig. 10E

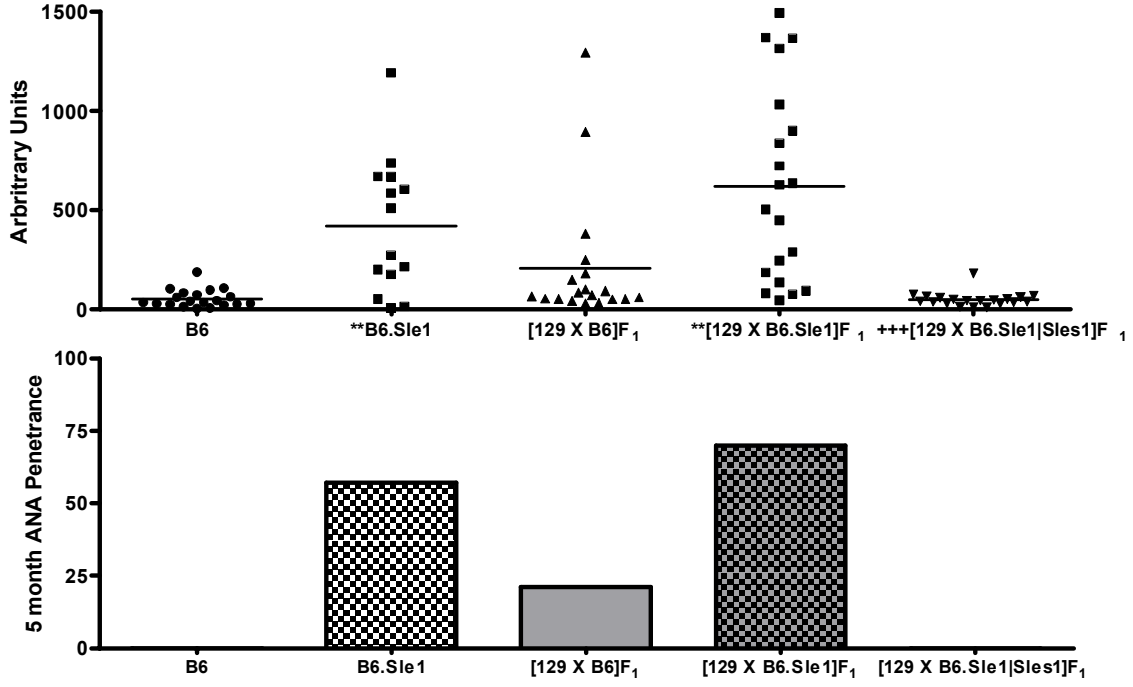

Figure 10. Humoral Autoimmunity Suppressed in [129 X B6.*Sle1*|*Sles1*]F_1s.
A. and B. Lack of anti-dsDNA IgGs in [129 X B6.*Sle1*|*Sles1*]F_1s at 9 months C. and D. [129 X B6.*Sle1*|*Sles1*]F_1s Do Not Produce ANAs at 9 months. E. Tires and Penetrance of anti-dsDNA Autoantibodies Significantly Increased in [129 X B6.*Sle1*]F_1s at 5 months. For all both ELISAs, age and gender-matched B6 and B6.*Sle1*sera were used as negative and positive controls respectively. To determine penetrance, samples were deemed positive if their value exceeded that of the mean ± 4SDs of the B6 controls at that age. Each symbol represents an individual sample of the respective genotype. Bars indicate averages. n= 16-23/genotype; ** $p<0.01$, ***$p<0.001$ *vs.* B6; $^{+++}$ $p<0.001$ *vs.* B6.*Sle1*, as determined by non-parametric ANOVAs.

Fig. 11

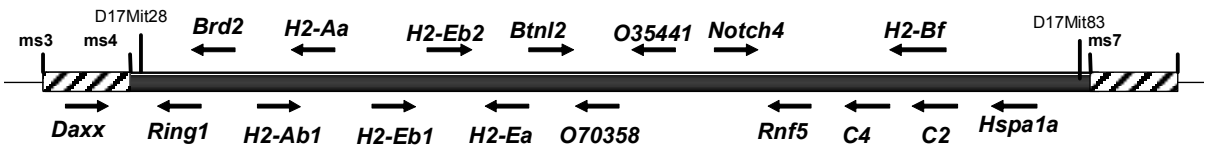

Figure 11. Candidate Genes in the *Sles1* Interval with Known Association with Autoimmunity. Schematic representation of discussed candidate genes with known association with SLE and/or autoimmunity, with arrows denoting transcriptional direction.

Chapter IV. Epistatic Suppression of SLE:

Sles1 Abrogates Fatal Autoimmunity in the B6.*Sle1*|*yaa* Murine Lupus Model

Introduction

The study of genetic susceptibility to the human autoimmune disorder Systemic Lupus Erythematosus (SLE) has been greatly facilitated by the availability of spontaneous inbred murine lupus models, which include the F_1 progeny of the NZB and NZW strains (BWF_1), the BWF_1 inbred derivative NZM2410, MRL.*lpr* and the BXSB.*yaa* strains. All these murine systems develop nuclear antigen specific IgG autoantibodies (autoAbs) and progressive, severe glomerulonephritis (GN), similar to what is observed in human SLE (reviewed in (3, 10)). Linkage analyses of these models have implicated a plethora of lupus susceptibility loci, and congenic dissection of some of the intervals has revealed their individual contributions to different component lupus phenotypes. Interestingly, comparison of the results of these linkage studies reveals that chromosome 1 is home to a number of overlapping susceptibility loci such as *Sle1*, *Bxs3*, *Lbw1* and *Nba2* (146, 153, 161, 179, 185, 186, 201, 215, 218, 225, 226, 235, 238, 240, 279, 285, 297, 313).

The BXSB.*yaa* lupus model is a recombinant inbred strain in which male mice develop a severe form of murine lupus and this male-specific disease development is associated with the as yet unidentified *y-linked autoimmune accelerator* (*yaa*) locus (reviewed in (314)). Using this model system, it has been demonstrated that only *yaa*-bearing B cells produce anti-DNA autoantibodies, and while CD4 T cells are necessary for severe disease development, they do not need to carry the *yaa* mutation (196-198). It has been postulated that this B cell intrinsic *yaa*

effect may promote a hyperresponsive B cell compartment by modulating signaling thresholds for B cell activation or by enhancing B and T cell interactions (195, 315).

Interestingly, the *yaa* locus cannot independently cause disease development on non-autoimmune supporting backgrounds such as C57Bl/6J (B6) or CBA/J, as evidenced by the lack of autoimmunity seen in B6.*yaa* mice (185, 316). However, when susceptibility loci from other lupus models are combined with the *yaa* locus on the B6 background, severe autoimmunity can be elicited, as has recently been demonstrated with the NZB derived susceptibility loci, *Nba2*, *Nba5* and *Spg3*, and with the NZM2410-derived locus *Sle1* (186, 200, 201). The severe pathogenic autoimmunity seen in these different congenic systems cannot be explained by the additive effects of the various loci, indicating that epistatic interactions play a key role in the development of lupus in these models. Of relevance to this study, the combination of the *Sle1* and the *yaa* loci on the B6 background (B6.*Sle1*|*yaa*) results in highly penetrant, early-onset, severe and fatal lupus nephritis in male mice. Interestingly, of the NZM2410-derived loci, *Sle1*, unlike *Sle2* and *Sle3*, is the only one that has this non-additive effect when combined with *yaa* on the B6 background, suggesting that these two loci impact a common pathway (200, 201).

We have recently demonstrated that the *Sle1*-specific suppressive modifier, *Sles1*, maps to a ~956 KB region at the proximal end of the murine MHC (Major Histocompatibility Complex). *Sles1* abrogates the activation phenotypes seen on splenic B and T lymphocytes from aged B6.*Sle1* mice, and our data suggests that the non-autoimmune 129/SvJ (129) strain harbors a complementary suppressive allele at this locus (227). These results and others indicate that SLE susceptibility is mediated via complex genetic interactions that include both susceptibility genes and suppressive modifiers (reviewed in (18)). Furthermore, it suggests that genes that can specifically modify the effects of susceptibility alleles that lead to breaches in self-tolerance may

prevent subsequent severe lupus pathogenesis, even in the presence of additional susceptibility genes. In this study, to test this latter hypothesis we introduced the *Sle1*-specific suppressive locus *Sles1* onto the B6.*Sle1*|*yaa* lupus prone mouse model, to determine whether and how *Sles1* mediated suppression of *Sle1* impacts phenotypes characteristic of male B6.*Sle1*|*yaa* mice.

Using a variety of parameters to investigate the different pathological, immunological, functional and molecular phenotypes of B6.*Sle1*|*yaa* mice, we demonstrate herein that the introduction of *Sles1* onto this genetically defined lupus model results in the profound suppression of pathogenic autoimmunity and associated phenotypes. This study provides strong support for the idea that targeting genes involved in breaking tolerance to chromatin can be a therapeutic means with which to prevent the development of pathogenic and systemic autoimmunity.

Results

In order to examine the effects of *Sles1* on the systemic autoimmunity resulting from the epistatic interactions of the *Sle1* and *yaa* loci on the B6 background, we generated B6.*Sle1*|*Sles1*|*yaa* mice to investigate and compare the different pathological, immunological, functional and molecular phenotypes that occur during disease progression. A schematic illustrating the various loci combinations used in this study is presented in Fig.12.

Normal Thymic And Slight Changes in Bone Marrow Development With Early Indications of Splenomegaly in B6.Sle1|yaa Males

Prior to their emergence in peripheral lymphoid organs, T and B cell lymphocytes undergo positive and negative selection events in the thymus and bone marrow (BM) respectively, resulting in peripheral repertoires with the ability to recognize foreign antigen but remain tolerant to self. Aberrations in these selection events can lead to T and B cells with the ability to recognize and respond to self-antigens (reviewed in (2, 301)).

Analyses of CD4, CD8 and CD3 expression on thymocytes isolated from the different strains at 6-8 weeks of age revealed no differences in the percentages of double-negative, double-positive, single-positive CD4 or single-positive CD8 thymocytes (Table 8). In addition, cell-surface levels of CD4, CD8 and CD3 were comparable between all groups, indicative that no gross changes in thymic development are occurring in B6.*Sle1*|*yaa*.

Characterization of the B cell developmental populations in the BM at 6-8 weeks of age revealed a decrease in the percentage of pre-B cells ($IgM^-CD43^-B220^+$) in B6.*Sle1*|*yaa* males *vs.* B6, but not compared to the other *yaa* containing strains (Table 8; $p < 0.01$; non-

parametric ANOVA). In contrast, the percentage of the next developmental stage, the immature B cell subset ($B220^{lo}IgM^{+}$), was comparable between all the groups (Table 8). A decrease in the percentage of mature, circulating B cells ($B220^{hi}IgM^{+}$) was also observed in B6.*Sle1*|*yaa* relative to B6 (Table 8; $p < 0.05$; non-parametric ANOVA). Both B6.*yaa* and B6.*Sle1*|*Sles1*|*yaa* males showed no significant changes relative to B6 or B6.*Sle1*|*yaa* in any of their BM B cell subsets (Table 8).

Despite the lack of major changes between the *yaa* containing groups in T and B cell populations in the thymus and BM, there was a significant increase in the spleen weights of male B6.*Sle1*|*yaa* mice by 6-8 weeks of age, as shown in Fig.13A and Table 8. While B6 and B6.*yaa* males had spleen weights of 76.7 ± 2.42 mg and 71.1 ± 3.36 mg respectively, those from B6.*Sle1*|*yaa* averaged 113.9 ± 6.11 mg ($p < 0.001$ *vs.* all groups; non-parametric ANOVA). This mild splenomegaly was not observed in mice containing *Sles1*, which had spleen weights comparable to both B6 and B6.*yaa* (74.4 ± 2.75 mg).

The early onset increase in spleen weights in B6.*Sle1*|*yaa* males occurred despite the apparently normal development and selection of T and B lymphocytes in the primary lymphoid compartments. This suggested that the underlying mechanisms might occur in the spleen itself, perhaps due to changes in peripheral selection and differentiation events. To assess this, we performed a detailed analysis of splenic populations in terms of different cell lineages and developmental subsets, as well as cell-surface activation and development markers.

As shown in Fig.13B and Table 8, no differences in the overall percentages of $CD4^{+}$ and $CD8^{+}$ T, $CD19^{+}$ B or $CD11b^{+}$ cells were found between any of the strains examined,

despite the increase in spleen size and cell numbers seen in B6.*Sle1*|*yaa* males. However, further investigation revealed significant changes in developmental and differentiation subsets of B and CD4 T cells in the spleen at this early age.

T2 and MZ Populations Restored in the Presence of Sles1

Subsequent to selection processes in the BM, immature B cells migrate to the spleen where they undergo further selection and differentiation events and are classified as transitional 1 (T1), transitional 2 (T2), follicular and marginal zone (MZ) B cells (reviewed in (317, 318)). As shown in Fig.14 and Table 8, all the strains had comparable percentages of T1 B cells at 6-8 weeks of age. There were however, significant decreases in the percentages of both T2 ($CD23^{+}CD21^{hi}IgM^{hi}$) and MZ ($CD23^{-}CD21^{+}IgM^{+}$) B cells in both B6.*yaa* and B6.*Sle1*|*yaa* mice compared to B6 ($p<0.01$ and $p<0.05$ for both populations in the respective strains; ANOVA). This is in agreement with a recent report demonstrating that the *yaa* locus impacts the development of both the T2 and MZ B cell subsets in the spleen in a B-cell intrinsic fashion, without appearing to influence the T1 B cell population (315). This did not result in the acceleration of follicular B cells maturation, as no differences were observed between any of the strains (Table 8). This decrease in MZ B cells is in contrast to studies in which this population has been shown to be expanded, wherein a role for these cells in autoAb production has been postulated due to their ability to produce natural, polyclonal self-reactive IgM antibodies (reviewed in (319)).

Intriguingly, as shown in Table 8 and Fig.14, B6.*Sle1*|*Sles1*|*yaa* mice had T2 and MZ percentages comparable to those of B6. The fact that *Sles1* was able to restore these

populations is probably not due to Class II MHC Eα expression, as both BXSB.*H2*^{d}|*yaa* and BXSB.*E*α^{Tg}|*yaa* mice were shown to have comparable decreases in their MZ populations (315).

Early Increases in Lymphocyte Activation in B6.Sle1|yaa Mice Suppressed by Sles1

A common observation in many different spontaneous murine lupus models is the emergence of highly activated B and T lymphocyte populations, believed to be indicative of the underlying chronic immune response to self-antigen (189, 195, 213, 226, 235, 236, 238). An examination of the early activation marker CD69 on B220^{+} B and CD3^{+} T cells revealed significant increases in the percentages of both B and T cells having an activated phenotype at 6-8 weeks of age in B6.*Sle1*|*yaa* males, compared to both B6 and B6.*yaa*, as shown in Table 8 and Fig.15A-15B ($p<0.001$; ANOVA). These increases were absent in B6.*Sle1*|*Sles1*|*yaa* males, and the percentages of activated CD69^{+} B and T cells were comparable to B6. No differences were found in the frequency of B cells expressing the co-stimulatory molecule CD86, and in the cell-surface density of either CD69 or CD86 on B cells between the strains (Table 8).

Further evaluation of activation markers on CD4^{+} T cells revealed that the increase in CD69^{+} T cells in B6.*Sle1*|*yaa* was within the CD69^{+}CD25^{-} population ($p<0.01$ *vs.* B6), as shown in Fig.15C. The CD69^{+}CD25^{+} CD4 T cells also showed a trend towards an increase as well, without actually reaching statistical significance. As expected from the CD3^{+} T cell data, there was no increase in the CD69^{+} CD4 T cell population in the presence of *Sles1*. The phenotypic regulatory CD4 T cell subset (CD25^{+}CD69^{-}) was comparable between all the

strains. These data demonstrate that *Sles1* suppresses the early onset lymphocyte activation normally observed in B6.*Sle1*|*yaa* mice.

Lack of Early and Accelerated B and T Cell Differentiation in B6.Sle1|Sles1|yaa Spleens

The early changes in lymphocyte activation phenotypes observed in B6.*Sle1*|*yaa* males suggest that the B and T cells consequently might be undergoing activation-induced differentiation, which we evaluated by examining for changes in plasma B and memory CD4 T cell populations.

As shown in Fig. 16A-B, there was a highly significant increase in the percentage of spleen cells having the $CD138^{+}CD19^{-}$ phenotype of plasma cells at 6-8 weeks of age in B6.*Sle1*|*yaa* mice compared to both B6 and B6.*yaa* ($p<0.001$; ANOVA), which was not observed in B6.*Sle1*|*Sles1*|*yaa* (Fig.16A-B). Notably, this accumulation was specific to the spleen, as the percentages of BM pre-plasma and plasma cells are comparable between all the groups (Table 8).

An early increase in the accrual of a highly differentiated population in B6.*Sle1*|*yaa* males was also seen within splenic CD4 T cells. As depicted in Table 8 and Fig.16C-D, there was a highly significant decrease in the percentage of naïve ($CD62L^{+}CD44^{lo}$) CD4 T cells with a corresponding increase in the phenotypic effector-memory ($CD62L^{-}CD44^{lo/hi}$) CD4 T cell population in B6.*Sle1*|*yaa* spleens. In the presence of *Sles1* these activation-induced differentiation phenotypes were absent, and naïve and memory CD4 T cell populations were scomparable to B6. This is consistent with the lack of activated lymphocyte phenotypes in

B6.*Sle1*|*Sles*|*yaa*, and demonstrates that *Sles1* suppresses the accelerated development of these populations.

Lack of an Early Increase in IFNγ Production in B6.Sle1|Sles1|yaa

As a preliminary examination of the cytokine profiles of the mice at this early age, splenic cells were cultured for 4 hours in the presence of PMA and ionomycin and the production of IFNγ by $CD4^+$ cells was measured using intracellular cytokine staining. Since the stimuli used bypassed proximal TCR-mediated signaling events, it allowed us to look at cells that were intrinsically capable of secreting IFNγ, and avoided the 'drift' effects seen when using longer culture periods. As shown in Fig.17A-B, about two times as many $CD4^+$ cells from B6.*Sle*|*yaa* mice produced IFNγ under these conditions compared to the other strains, indicating that the $CD4^+$ cells from these mice have a greater potential to produce IFNγ in response to stimulation. This increase in T cell effector-potential in B6.*Sle*|*yaa* mice provides support for the idea that early changes in the functional properties of the immune system preclude the development of autoimmunity. Notably, the response to stimulation is comparable to B6 in the presence of *Sles1*. Further investigation of T and B cell responses in terms of effector-function and proliferative potential, as well as a thorough cataloging of the production of different cytokines in response to different stimuli, including IL-4, IL-17, TNFα and IL-10, in these mice are underway.

Early Onset Autoantibody Production in B6.Sle1|yaa Abrogated by Sles1

The early increases in both B and T cell activation phenotypes and increased inherent capacity to produce IFNγ, as well as the accelerated accumulation of plasma cells in B6.*Sle1*|*yaa* spleens, suggested that autoAb production may be incipient at a very early age in this model. To investigate this possibility, we assayed for serum IgM and IgG anti-chromatin, anti-dsDNA and anti-GBM (glomerular basement membrane) autoAbs in the different mouse strains at 6-8 weeks.

As shown in Fig. 18A-F, the titres of serum IgM and IgG anti-chromatin, anti-dsDNA and anti-GBM autoantibodies were all significantly increased compared to the other genotypes in B6.*Sle1*|*yaa* mice at 6-8 weeks. The penetrance of B6.*Sle1*|*yaa* sero-positivity (average age and sex-matched B6 value + 4 standard deviations) against all three antigens for both isotypes at 6-8 weeks was greater than 70%. Though these increases are statistically significant, it is important to note that relative to the threshold value for being considered positive at older ages (as indicated by the dashed line in all six graphs), the titres at this timepoint were quite low, especially in the case of the IgG autoantibodies. The data does, however, demonstrate an early propensity towards humoral autoimmunity in B6.*Sle1*|*yaa* mice, which was not seen in the presence of *Sles1*.

Splenomegaly Not Observed in Older B6.Sle1*|*Sles1*|*yaa Mice

In order to determine whether the suppression mediated by *Sles1* on the phenotypes observed in B6.*Sle1*|*yaa* mice at 6-8 weeks is indicative of a delayed onset and change in the kinetics of autoimmunity development, or instead, a long-term continuous suppressive effect, we compared the different phenotypes in the different strains at 4-6 months of age.

As shown in Fig.19A, by 4-6 months of age, the mild but significant increase in the spleen sizes of B6.*Sle1*|*yaa* mice seen at 6-8 weeks, was dramatically amplified such that the average spleen weighed 641.8 ± 94.3 mg compared to the 86.7 ± 3.5 mg and 134.4 ± 6.7 mg seen in B6 and B6.*yaa* males respectively ($p < 0.001$; non-parametric ANOVA). *Sles1* continued to eliminate this phenotype, maintaining spleen weights at B6 levels (Table 9, Fig. 19A). This extreme reduction in the incidence and extent of splenomegaly due to *Sles1* was maintained to nine months, at which time the spleen weights averaged 112.9 ± 14.2 mg, which was similar in both distribution and average weight to that observed in B6 (114.1 ± 4.4 mg) (Fig. 19B). Spleens from the surviving male B6.*Sle1*|*yaa* mice were even larger than those observed at four to six months (958.7 ± 114.7 mg). Interestingly, B6.*yaa* males themselves had a small but significant increase in their spleen weights relative to B6 by nine months (194.7 ± 16.2 mg; $p < 0.05$; non-parametric ANOVA). In accordance with the recessive nature of *Sles1*, heterozygosity at this locus resulted in increased splenomegaly (Fig. 19B; $p < 0.001$; non-parametric ANOVA).

These data indicate that both *Sle1* and *yaa* make independent contributions to splenomegaly, and demonstrate that their epistatic interaction leads to the grossly abnormal spleen weights seen in B6.*Sle1*|*yaa* males, which is suppressed completely by *Sles1* homozygosity.

Normal Numbers and Percentages of Splenic Lineages in Aged B6.Sle1|Sles1|yaa Mice

To better characterize the changes contributing to the gross enlargement in spleen sizes seen in 4-6 month old B6.*Sle1*|*yaa* mice, flow-cytometric analyses of different BM and

splenic mononuclear populations was performed. As described in detail in Table 9, the changes in the spleen and BM populations were much greater than what was seen at 6-8 weeks.

As shown in Fig.20A, B6.*Sle1*|*yaa* mice had highly significant increases in overall numbers of both $B220^+$ and $CD3^+$ splenic lymphocytes, as might be expected from their abnormally large spleen sizes ($p<0.001$ *vs.* all groups; ANOVA). The percentages of these splenic populations however, were highly reduced due to the striking increase in both the overall number and percentage of $CD11b^+B220^-$ cells in the spleens of these mice (Fig.20A-C, Table 9). This monocytosis has also been reported in the parental BXSB.*yaa*, but is clearly not due to the effect of the *yaa* locus alone, as evidenced by the normal percentage of these cells in B6.*yaa* mice (Fig.20B-C) (320).

Consistent with their normal spleen sizes, these increases in overall cell numbers were absent in the presence of *Sles1* (Fig.20A). More importantly, as shown in Fig.20B-C, the proportions of the $B220^+$, $CD3^+$ and $CD11b^+$ populations were also maintained at levels comparable to B6 (Table 9), suggesting that the mechanisms underlying the expansion of the $CD11b^+$ population were associated with the overall increase in spleen size.

Decreased Bone Marrow B cells in B6.Sle1|yaa Mice

To investigate whether the decreased percentages of B cells in the spleens of B6.*Sle1*|*yaa* mice were reflected in late-onset perturbations in B cell development, we analyzed B cell developmental subsets in the BM and spleen.

A small increase was observed in the IgM^- population in the BM of B6.*Sle1*|*yaa* mice when compared to B6 (Table 9; $p<0.05$; ANOVA). Within this IgM^- population, there was a significant decrease in both the pro-B ($CD43^+B220^+$) and pre-B cell ($CD43^-B220^+$) subsets in B6.*Sle1*|*yaa* BM relative to B6 BM, but not when compared to the two other *yaa* containing groups (Table 9 and Fig. 21A; $p<0.01$ *vs.* B6; ANOVA). A similar decrease was also seen for the immature BM B cell population (IgM^+B220^{lo}), in which B6.*Sle1*|*yaa* differed from B6 but not when compared to B6.*yaa* or B6.*Sle1*|*Sles1yaa* (Fig. 21B; $p<0.01$; ANOVA). In contrast, the decrease in the mature, circulating BM B cell population (IgM^+B220^{hi}) in B6.*Sle1*|*yaa* was significant relative to all groups (Table 9 and Fig.21B). There was also a significant increase in the percentage of non-B cells in B6.*Sle1*|*yaa* BM ($IgM^-B220^-CD43^+$) compared to B6 (Fig. 21A; $p<0.001$; ANOVA).

The importance of these changes in BM B cell subsets in B6.*Sle1*|*yaa* mice is unclear, as many of them were seen only relative to B6, but not compared to the other *yaa* containing strains, which had values intermediate to B6 and B6.*Sle1*|*yaa*. The decrease in the mature, circulating BM B cells in B6.*Sle1*|*yaa*, which was significant compared to all the strains, may reflect a change in the homing capacity of splenic B cells in these mice, perhaps due to variations in homing receptor expression mediated by local changes in cytokines and chemokines in the spleen. These possibilities have yet to be investigated. It is important to note that no significant changes were seen in the presence of *Sles1* for all the subsets described above.

Maintenance of Sles1-Mediated Reconstitution of yaa-Associated Marginal Zone Defect.

As shown in Fig. 22A-B and Table 9, there was a significant increase at 4-6 months in cells with the surface phenotype of splenic T1 B cells in B6.*Sle1*|*yaa vs.* both B6.*yaa* and B6.*Sle1*|*Sles1*|*yaa*, but not B6 ($p<0.001$; ANOVA). This phenotype was not observed at 6-8 weeks. There continued to be a highly significant decrease in the percentage of the T2 B cell population in B6.*Sle1*|*yaa* mice compared to all groups (Fig.22A-B) ($p<0.001$; ANOVA), while B6.*yaa* was not significantly different from B6 at 4-6 months. As shown in the various panels of Fig.22 and Table 9, the significant reduction in the MZ population ($CD23^{-}$ $CD21^{+}IgM^{+}$) compared to B6 controls in both B6.*yaa* and B6.*Sle1*|*yaa* was maintained ($p<0.001$; ANOVA). Interestingly, at this older age there was also a decrease in the follicular B cell population in B6.*Sle1*|*yaa* mice relative to all groups, as shown in Fig.22A (lower) and 22B ($p<0.001$; ANOVA). Intriguingly, the MZ population continued to be maintained in B6.*Sle1*|*Sles1*|*yaa* spleens at levels comparable to B6, as shown in Fig.22A-C and Table 9 ($p>0.05$), but was significantly higher than both B6.*yaa* and B6.*Sle1*|*yaa* ($p<0.001$ *vs.* both; ANOVA). As mentioned earlier, the non-autoimmune *yaa* carrying strains (B6.*yaa*, BXSB.$H2^{d}$|*yaa* and BXSB.$E\alpha$|*yaa*) all showed a reduction in MZ B cells (315). This indicates that this phenotype is not dependent on the progression of autoimmunity or the expression of certain MHC molecules, such as Class II Eα, but instead may be contingent on the specificity and signaling strength associated with the BCR in these different model systems.

Age-Dependent Increases in Splenic B1 Populations Not Seen in B6.Sle1|Sles1|yaa Mice.

B1 cells represent a lineage of B cells contributing to innate responses and are found mainly in the peritoneum, but a small population is also present in the spleen. Based on their ability to produce 'natural' IgM antibodies that tend to be polyreactive with self-Ags, and the fact that in some lupus models their numbers are expanded, it has been postulated that they, like MZ B cells, might play a role in IgG autoantibody production in lupus (238, 288, 321, 322).

While there were no major changes at 6-8 weeks. there was a significant decrease in the percentage of conventional B2 cells ($CD5^-B220^+CD23^+$) in B6.*Sle1*|*yaa* spleens at 4-6 months compared to the other strains, similar to that seen for follicular B cell population (Fig.23 and Table 9). There was also a significant increase in the percentage of B1a B cells ($CD5^+B220^+CD23^-$) in B6.*Sle1*|*yaa* compared to B6.*yaa* and B6.*Sle1*|*Sles1*|*yaa*, but not to B6 ($p<0.01$ and $p<0.001$ respectively; ANOVA), and an increase compared to all groups in the population of B1b cells ($CD5^-B220^{lo}CD23^-$) in B6.*Sle1*|*yaa*. A significant decrease in the splenic B1a population was noted in B6.*Sle1*|*Sles1*|*yaa vs.* B6 at this age.

The importance of the splenic B1 population in autoimmune pathogenesis in this model remains unclear, and given that the changes occur at an older age may be reflective of the disease process. The increases observed in B6.*Sle1*|*yaa* at 4-6 months could be a consequence of local changes in the cytokine milieu, caused by the large increase in $CD11b^+$ cells in the spleen, which may promote the expansion of these cells and/or modify the cell-surface expression of the markers involved in defining these populations.

No Increase in the Percentages of Activated B and T Lymphocytes in B6.Sle1\|Sles1\|yaa Mice at 4-6 Months.

As the B6.*Sle1*|*yaa* aged, the early increase in activated B and T lymphocytes in spleens became amplified, such that ~20% of the B220 B cells expressed the early activation marker CD69, as shown in Fig.24A-B and Table 9 ($p<0.001$ *vs.* all groups; ANOVA). Interestingly, at this age B6.*yaa* also showed a significant increase in the percentages of these cells relative to B6 (Fig.24A-B, Table 9; $p<0.01$, ANOVA). A significant increase in the cell-surface density of CD69, as reflected by increased MFI, on B cells from B6.*Sle1*|*yaa* but not B6.*yaa* was seen as well (Fig.24C and Table 9). This increase in the activation status of the B cell compartment in B6.*Sle1*|*yaa* was further reflected in the increased cell surface density of the co-stimulatory molecule CD86 on follicular B cells as shown in Fig.24D and Table 9 ($p<0.001$; ANOVA). None of these changes indicative of an activated B cell compartment were observed in B6.*Sle1*|*Sles1*|*yaa* at 4-6 months, as shown by their percentages of $CD69^+$ B220, and their average cell-surface levels of both CD69 and CD86 (Table 9, Fig.24A-D).

The continued suppression of spontaneous lymphocyte activation mediated by *Sles1* extended to the T cell compartment as well. As shown in Fig.25A-B and Table 9, B6.*Sle1*|*yaa* mice had greatly increased percentages of activated CD3 T cells, such that ~50% were $CD69^+$, compared to the ~15% and ~22% seen in B6 and B6.*yaa*. Similar to the B cell population, there was also increased cell surface density of CD69 on CD3 T cells ($p < 0.001$, ANOVA; Fig.25C and Table 9). Further characterization of the CD4 population, revealed that at 4-6 months this increased $CD69^+$ T cell population was both $CD25^+$ and $CD25^-$, as

shown in Fig.25D-E (*p<0.001 vs.* B6 and B6.*yaa* for both; ANOVA). Interestingly, at 4-6 months the $CD69^+CD25^-$ CD4 T cell population in B6.*yaa* itself was increased relative to B6 (Fig.25D-E, Table 9; *p<0.001*; ANOVA). In sharp contrast, *Sles1* maintained the CD69 cell surface density and the percentage of $CD69^+$ CD3 T cells at levels comparable to B6 (Fig.25A-C). In agreement with these results, both the $CD69^+CD25^+$ and $CD69^+CD25^-$ CD4 populations were also normal in B6.*Sle1*|*Sles1*|*yaa* mice (Fig.25D-E and Table 9).

These data demonstrate that *yaa* by itself on the B6 background results in a later-onset mild lymphocyte activation, specific to increased $CD69^+$ percentages in both B and T cells; that these activation phenotypes manifest early and become highly amplified in the presence of *Sle1*, due to epistatic interactions between these loci; and that *Sles1* prevents the emergence of these activated lymphocytes at both ages examined.

Normal Percentages of Splenic Plasma B and Memory CD4 T Cells in Aged B6.Sle1|Sles1|yaa Mice.

The early increase in the kinetics of B and T lymphocyte differentiation into the plasma B and memory T cell subsets respectively, in B6.*Sle1*|*yaa*, was dramatically augmented at 4-6 months. As shown in Fig.26A-B and Table 9, ~5% of the B6.*Sle1*|*yaa* spleen had a plasma B cell phenotype (*p<0.001 vs.* all groups; ANOVA). Given the large increase in splenic cellularity in B6.*Sle1*|*yaa* mice, this increase in plasma cell percentages would translate into a very large increase in overall plasma cell numbers in these mice. Similar to the data at 6-8 weeks, this increase was specific to splenic, and not BM plasma cells (Table 9). In the presence of *Sles1* however, and in accordance with the lack of

activated B cell phenotypes, the splenic plasma cell percentages were maintained at B6 levels at this older age too (Fig.26A-B and Table 9).

As depicted in Fig.26C-D and Table 9, the proportion of splenic CD4 T cells that had differentiated to an effector-memory phenotype ($CD62L^{-}CD44^{hi}$) in B6.*Sle1*|*yaa* mice by 4-6 months was ~60%, compared to the ~20% seen in B6 ($p<0.01$; non-parametric ANOVA). A corresponding sharp decrease was seen in the percentage of naïve $CD4^{+}$ T cells. Consistent with their lack of activated lymphocyte populations at both ages investigated, this shift to a predominantly effector-memory CD4 population was not observed in the presence of *Sles1* (Fig.26C-D and Table 9).

These data demonstrate that with age, B6.*Sle1*|*yaa* mice accumulate increased percentages of effector phenotype B and CD4 T cells, similar to what has been reported in other models of spontaneous autoimmunity (189, 201, 240, 286). Analogous to the observations in in B6.*Sle1*|*Sles1* mice, the introduction of *Sles1* onto the B6.*Sle1*|*yaa* lupus model completely prevents the accrual of these plasma B and effector-memory CD4 T cells (227).

Normal Proliferative Responses and Cytokine Production in B6.Sle1|Sles1|yaa

It has been proposed that the accumulation of memory-phenotype cells in lupus-prone mice is a consequence of chronic activation leading to metabolically active cells that produce cytokines and autoAbs, but are in a state of replicative senescence (194). To examine whether cells from aged B6.*Sle1*|*yaa* mice displayed such characteristics, we performed an

initial characterization of *in vitro* stimulated splenic cells in terms of proliferative responses and cytokine production.

We used CFSE dilution assays to determine the proliferative responses of splenic B and T cells to α-IgM and α-CD3 stimulation respectively from the different mice at 4-6 months of age, as illustrated in Fig.27A. Lymphocytes from B6.*Sle1*|*yaa* mice divided less than the other strains, particularly the $CD4^+$ population, while those from B6.*Sle1*|*Sles1*|*yaa* proliferated comparably to B6 (Fig.27A-B).

As a preliminary investigation of intrinsic cytokine potential, similar to those performed on 6-8 week old mice, splenocytes were stimulated with PMA + ionomycin for four hours and IFNγ production examined. As shown in Fig.27C-D, in response to PMA + ionomycin stimulation, $CD4^+$ T cells from B6.*yaa,* B6.*Sle1* and B6.*Sle1*|*yaa* all showed increased IFNγ production. B6.*Sle1*|*yaa* had the greatest percentage of CD4 T cells producing IFNγ (~30%), about twice that seen in both B6.*yaa* and B6.*Sle1*. The increase observed in B6.*yaa* is somewhat surprising given that it has been reported that *yaa* acts in a B cell intrinsic fashion and has no effect on T cell phenotypes (195, 196, 198, 314). However, our cell-surface analyses did indicate increased activated T cells in B6.*yaa* mice as well, which may be reflected in the increased cytokine production.

In contrast, B6.*Sle1*|*Sles1*|*yaa* mice had levels of CD4 T cells producing IFNγ that were comparable to B6. While only 2 mice/genotype have been examined, it is interesting to note that both B6 and B6.*Sle1*|*Sles1*|*yaa* had roughly the same percentage of IFNγ producing CD4 T cells at 6-8 weeks and 4-6 months, even though both strains did show an increase in activated T cells over this time period. The significance of this is currently unclear, though it

does suggest that an increase in cell-surface activation phenotypes is not reflective of changes in effector functions, such as cytokine secretion. Current experiments are directed at replicating these results, further characterizing the cytokines produced under various stimulation conditions, and assessing how co-stimulation affects the replicative senescence phenotypes of B6.*Sle1*|*yaa*.

Repression of Autoantibody Production by Sles1

The data thus far demonstrates that profound changes in splenic populations and functions occur by the age of 4-6 months in B6.*Sle1*|*yaa* males, indicative of a chronically activated immune system. Similar to the analyses at 6-8 weeks, the degree of IgM and IgG autoAb production of different specificities at 4-6 months in the various strains was investigated, as well as in B6.*Sle1* and B6.*Sle1*|*Sles1*^{het}|*yaa*.

As shown in Fig.28A-B, B6.*yaa* itself had significantly increased titres of anti-chromatin autoAbs *vs.* B6, particularly of the IgM isotype ($p<0.01$ and $p<0.05$ for IgM and IgG respectively*;* non-parametric ANOVA). Interestingly, B6.*Sle1* mice at this age had a highly significant increase in their IgG anti-chromatin autoAbs relative to B6 ($p<0.001$; non-parametric ANOVA), and while IgM titres were increased as well, it was much less significant ($p<0.05$; non-parametric ANOVA). As might be expected from their chronic immune dysregulation and increase in plasma B cells, both serum IgM and IgG anti-chromatin autoAbs titres were extremely high in B6.*Sle1*|*yaa* at this time ($p<0.001$ for both; non-parametric ANOVA).

In the case of anti-dsDNA autoAbs, B6.*yaa* mice had increased IgM, but not IgG, titres relative to control B6 samples ($p<0.01$; non-parametric ANOVA). On the other hand, B6.*Sle1* showed a small increase in IgG, but not IgM, anti-dsDNA autoAbs at this age *vs.* B6 ($p<0.05$; non-parametric ANOVA). However, in B6.*Sle1*|*yaa* both IgM and IgG anti-dsDNA autoAbs were significantly increased relative to B6 (Fig.29A-B) ($p<0.001$ for both; non-parametric ANOVA).

As depicted in Fig.30A-B, at 4-6 months a significant increase was also seen in the titres of anti-GBM specific IgM autoAbs in B6.*yaa* mice relative to B6, with a slight increase in anti-GBM IgG as well ($p<0.001$ and $p<0.05$ respectively; non-parametric ANOVA). Surprisingly, despite the fact that B6.*Sle1* mice develop GN infrequently, there was a significant increase in IgG anti-GBM autoAbs in these mice at this relatively young age ($p<0.01$; non-parametric ANOVA) (225, 226). The increase in anti-GBM autoAbs in B6.*Sle1*|*yaa* mice however, was highly significant for both the IgM and IgG isotypes, exactly as observed for the anti-chromatin and anti-dsDNA autoAbs as well ($p<0.001$ for both; non-parametric ANOVA).

In stark contrast to the other strains, at 4-6 months no significant differences were seen in the levels of anti-chromatin, anti-dsDNA or anti-GBM autoantibodies of either IgM or IgG isotype in B6.*Sle1*|*Sles1*|*yaa* males (Fig.28-30). Interestingly however, heterozygosity at *Sles1* results in a small but significant increase in anti-chromatin IgG autoAbs at 4-6 months, which is consistent with the recessive nature of *Sles1*.

These data indicate that both *yaa* and *Sle1* make independent contributions to the development of autoantibodies, as evidenced by the increase in serum autoAbs in single congenic B6.*yaa* and B6.*Sle1* mice, which are both inhibited by *Sles1*.

Severe Mortality and Glomerulonephritis (GN) are Abrogated in the Presence of Sles1.

As shown in Fig.31A, at 4-6 months B6.*Sle1*|*yaa* mice showed clear evidence of kidney dysfunction, with 76.9% of the mice (10/13) having scores of 3 or 4, indicative of severe GN. In addition, 69% of the B6.*Sle1*|*yaa* kidneys analyzed showed mild to moderate lymphocyte infiltration. While none of the B6.*yaa* mice at this age had severe GN scores (median = 1.5), 82% of the kidneys analyzed also displayed mild to moderate lymphocyte infiltration, suggesting that this phenotype does not correlate with the development of severe GN. Consistent with their lack of autoAb production, the kidneys of 4-6 month old B6.*Sle1*|*Sles1*|*yaa* mice had low scores with a median GN value of 0.5 (n= 12), and none of the kidneys analyzed showed any evidence of lymphocytic infiltrates. The only significant difference in terms of GN scores between the four genotypes examined was that seen in male B6.*Sle1*|*yaa* ($p<0.01$ *vs.* all groups; non-parametric ANOVA).

The epistatic interaction between the *Sle1* and *yaa* loci on the B6 background has been shown to result in a dramatic increase in mortality, compared to either locus in isolation (201). Cohorts of B6.*yaa*, B6.*Sle1*|*yaa* and B6.*Sle1*|*Sles1*|*yaa* were aged to 9 months for the purpose of examining spontaneous mortality and the impact of *Sles1* on this phenotype. In our SPF colony, the mortality rates for male B6.*yaa* mice were 8.0% at both the four and nine-month timepoints. Consistent with previous data, B6.*Sle1*|*yaa* males had a cumulative

mortality of 9.0% at four months and 64.3% (9/14) by 9 months (Fig.31C). In stark contrast, all of the 23 male B6.*Sle1*|*Sles1*|*yaa* mice aged to nine months survived. Interestingly, heterozygosity at the *Sles1* locus (B6.*Sle1*|*Sles1*^{het}|*yaa*) resulted in a small increase in the nine-month mortality to 15.8% (3/19). These data are summarized in the survival curve shown in Fig.31C. Histological analyses of kidneys collected from the different mice at this endpoint revealed that none of the B6.*yaa* mice developed severe GN (median score = 1.75; Fig.31B). Of the five B6.*Sle1*|*yaa* mice that survived to nine months, for which histological analyses could be performed, all had GN scores of 4, indicative of hyalanized end-stage glomeruli. This contrasts sharply with the extent of GN seen in B6.*Sle1*|*Sles1*|*yaa* mice at 9 months in which only 2/19 samples had a severe GN score (3), with a median score of 1 (Fig.31B). Intriguingly, heterozygosity at *Sles1* resulted in an increased median GN score of 3 (n=10), which is interesting given that no major evidence for significant humoral autoimmunity was seen at 4-6 months.

Discussion

This study extends our previous work characterizing the suppression of autoimmunity mediated by *Sles1*, in which we introduce this *Sle1*-specific suppressive locus onto the B6.*Sle1*|*yaa* lupus prone mouse model. It has been previously shown that in this strain, the non-additive, epistatic interactions between the *Sle1* and *yaa* loci on the B6 background leads to highly penetrant systemic autoimmunity that culminates in fatal lupus nephritis (201). By comparing the development of a variety of pathological, immunological, functional and molecular phenotypes between the B6.*Sle1*|*yaa* and B6.*Sle1*|*Sles1*|*yaa* strains, we demonstrate that *Sles1* mediates a profound and complete suppression of systemic autoimmunity in this model.

The progression of systemic autoimmunity in B6.*Sle1*|*yaa* males was characterized by early indications of humoral autoimmunity, such that by 6-8 weeks of age there were significantly increased levels of autoAbs directed against chromatin, dsDNA and GBM, of both the IgM and IgG isotypes. With age, the mean titres of these autoAbs dramatically increased, correlating with the development of underlying pathogenic processes. The data demonstrate that the events leading to a breach in tolerance to self-antigens occur very early on in this model. Given that splenic seeding by BM-derived immature B cell precursors in the mouse is believed to be complete only after 4 weeks of age, and that subsequent peripheral selection events have been shown to be crucial in the purging of self-reactive B cells from the peripheral repertoire in both mice and humans, this suggests a dysregulation in peripheral selection events in this model that leads to the early emergence of functional, autoAb producing B cells (312, 323).

It would appear that *yaa* by itself specifically influences the development of IgM autoAbs, as at 4-6 months IgM titres of all three antigens tested were significantly higher than those found in age and gender-matched B6 controls. Given the fact that that BM chimera experiments have shown that *yaa* is a B cell intrinsic gene, while *Sle1* is functionally expressed in both B and T cells, and since *Sle1* by itself primarily mediates a loss in tolerance to chromatin, these data suggest that one contribution of *Sle1* to the humoral autoimmunity in this model could be the provision of appropriate T cell help to the polyclonal loss in tolerance promoted by *yaa* (196-198, 226, 228, 236, 315).

Intriguingly, despite the independent contributions to autoAb production by *yaa* and *Sle1*, the addition of *Sles1* to this genetic background completely shuts down the development of the humoral response to self-antigens. This supports the idea that *Sle1* and *yaa* impact a common pathway, hence allowing *Sles1* to modify both their contributions to autoimmunity.

Similar to the observations for humoral autoimmunity, a progression in the development of severe renal disease was seen in B6.*Sle1*|*yaa* males as the mice aged. By 4-6 months, 77% of the mice had severe GN scores, which coincided with a significant drop in survival at this time, and by 9 months, all of the surviving mice had the highest possible GN scores. Though B6.*yaa* males at both ages did not develop severe GN, both B6.*Sle1*|*yaa* and B6.*yaa* kidneys showed increased lymphocytic infiltrates. This suggests that *yaa* by itself may promote an increased lymphocyte infiltration of the kidneys, but alone is not sufficient for the development of renal damage and dysfunction. In conjunction with *Sle1* however, GN is elicited, due in part to the underlying humoral autoimmunity which promotes increased

formation and kidney deposition of IgG immune complexes. In addition, disease may be influenced by the kidney specific effects contributed by the *Sle1* locus, such as increased susceptibility to IC nephritis mediated by the *Sle1d* locus within *Sle1* ((153) and Tus *et al., unpublished observations*). The increased lymphocyte infiltration contributed by *yaa* may in turn allow for an accumulation of activated lymphocytes producing pro-inflammatory cytokines within the kidneys. Taken together, these data suggest complex interactions between the two loci leading to the renal pathology and consequent GN seen in B6.*Sle1*|*yaa*.

Despite these potent, systemic autoimmunity-inducing interactions between the *Sle1* and *yaa* loci, the introduction of *Sles1* completely abrogates the development of both humoral and pathogenic autoimmunity. At all ages examined, we found no significant differences in the titres of anti-chromatin, anti-dsDNA and anti-GBM autoAbs between B6 and B6.*Sle1*|*Sles1*|*yaa*. In fact, unlike B6.*yaa*, there was no increase seen in the IgM autoAb titres in the presence of *Sles1*. In accordance with the lack of autoAbs, GN scores were significantly reduced as well. Interestingly, there was little evidence for lymphocyte infiltration in B6.*Sle1*|*Sles1*|*yaa* kidneys.

We found that the epistatic interaction of *Sle1* and *yaa* on the B6 background led to an early and chronic dysregulation of various splenic immune cell populations, similar to what has been reported in other lupus models (162, 163, 189, 195). While there appeared to be no major changes in B and T cell development in the primary lymphoid organs, there were early indications of perturbations in the spleens of these animals, starting with a significant increase in spleen weights. Early characterization of splenic lineages revealed that an expansion of a single lineage did not account for the observed increase in spleen sizes. There

were however, significant increases in the percentages of activated B and T cells as well as plasma B cells, with a decrease in naïve CD4 T cells by 6-8 weeks of age. In addition, an increased percentage of CD4 T cells from these mice produced IFNγ in response to stimulation. These data correlate well with the increase in humoral autoimmunity evident by this age and are consistent with the idea that an early dysregulation of the functional properties of the immune system somehow permit the development of autoimmunity.

By 4-6 months of age, B6.*Sle1*|*yaa* mice had massive splenomegaly with a corresponding increase in total B and T lymphocyte numbers. The early shifts towards activated B and CD4 lymphocytes became highly augmented such that ~20% of the B cells and almost half the CD4 T cells displayed activated phenotypes in 4-6 month old B6.*Sle1*|*yaa* mice. The initial increases in lymphocyte differentiation phenotypes were also amplified, resulting in a significant accrual of splenic plasma and effector-memory CD4 cells in these animals. Given the overall massive increase in splenic cellularity, these percentages changes translated into tremendous increases in the number of activated and effector lymphocytes in B6.*Sle1*|*yaa* spleens. Functional evidence that these cells did indeed represent chronically stimulated lymphocytes was their lack of proliferative response and robust IFNγ production. We also found evidence for an increase in activated lymphocytes and IFNγ production in B6.*yaa*, without changes in plasma B or effector-memory CD4 T cells. In contrast, and consistent with their lack of autoimmunity, there was no evidence for an increase in activated or effector lymphocyte populations, decreased proliferative responses or augmented IFNγ production in B6.*Sle1*|*Sles1*|*yaa*.

While some of the changes in the spleens of B6.*Sle1*|*yaa* mice were observed at both ages examined, albeit at very different magnitudes, other splenic populations showed alterations only at an older age. Perhaps the most impressive difference was the increase in the $CD11b^+$ population in the spleens of B6.*Sle1*|*yaa* mice. While we are just beginning to further characterize this population, Croker *et al.* have shown that different myeloid populations all showed increased numbers in B6.*Sle1*|*yaa* spleens, and that the most striking difference was observed in the $CD11b^+CD11c^-CD19^-$ macrophage population (200). Monocytosis has also been reported in the BXSB.*yaa* model from which *yaa* is derived (320). Given that this large increase in the $CD11b^+$ population was not apparent at 6-8 weeks, it is tempting to speculate that the early and continued perturbations in lymphocyte development and differentiation could be facilitating the emergence of the expanded $CD11b^+$ population, perhaps due to changes in the local cytokine milieu. Clearly, *yaa* itself is not sufficient for the development of this population, as both B6.*yaa* and B6.*Sle1*|*Sles1*|*yaa* showed normal proportions of these cells at all ages examined.

In agreement with a recent report describing that the *yaa* locus was associated with a profound decrease in MZ B cells, we found a significant diminishment in this population in both B6.*yaa* and B6.*Sle1*|*yaa* (315). This decrease was evident early on and does not correlate with the development of autoimmunity, as it has been observed in the non-autoimmune B6.*yaa*, BXSB.$H2^d$|*yaa* and BXSB.*E*α|*yaa* strains, as well as the severely autoimmune BXSB.*yaa* and B6.*Sle1*|*yaa* mice (315). It was hence surprising to discover that the introduction of *Sles1* restored the MZ population to levels comparable to that seen in B6

at both ages examined. Reconstitution of MZ B cells was also observed when the SP6 anti-DNA/TNP transgene was introduced onto BXSB.*yaa* (315).

The functional significance and underlying mechanism for the MZ B cell decrease remains undetermined. It has been postulated that during the generation of peripheral, mature B-cell subsets, antigen *vs.* Toll-like receptor (TLR) signaling of transitional type 2 B cells can dictate whether follicular or MZ B cells are generated (324). In addition, genetic ablation and transgenic-overexpression of a variety of molecules involved in B cell signaling and homeostasis have been shown to impact the normal development of MZ *vs.* follicular B cell populations (reviewed in (325)). Key among the molecules implicated in dictating the outcomes of these developmental checkpoints are members of the Notch family of receptors and ligands (reviewed in (319)). The data suggest that the specificity of the BCR and/or the nature of the signals mediated by BCR *vs.* TLR signaling may be impacting the generation of this population. Given the ability of *Sles1* to restore the *yaa*-associated defect in the maintenance of the MZ population, and since differences in the strength of BCR signaling have been shown to influence whether B cells differentiate into MZ or follicular B cells, it suggests that *Sles1* could play a role in the modulation of BCR signal strength (reviewed in (318, 322, 324, 326)). Interestingly, a member of the Notch family, *Notch 4*, lies within the minimal *Sle1* interval (227).

We have demonstrated that a variety of changes in the immune system precede and accompany the onset of the systemic autoimmunity seen in the B6.*Sle1*|*yaa* lupus model, as depicted in Fig. 32. Both *Sle1* and *yaa* were found to make independent contributions to various phenotypes, but it is clear that their non-additive, epistatic interactions are required

for the development of the severe disease that culminates in renal dysfunction and mortality. Our data demonstrate that *Sles1* is able to suppress these phenotypes elicited by the epistatic interactions between *yaa* and *Sle1*, as well as certain *yaa* specific phenotypes. Since it was previously shown that *Sles1* acts in a *Sle1*-specific manner, having no effects on phenotypes caused by *Sle2* and *Sle3*, and also that the *yaa* locus does not epistatically interact with *Sle2* and *Sle3*, it suggests that *Sle1* and *yaa* impinge on the same pathway, thus allowing *Sles1* to modulate both their contributions to various phenotypes (201, 242). Further comparisons between and characterization of B6.*Sle1*|*yaa* and B6.*Sle1*|*Sles1*|*yaa* are clearly warranted and should provide insight into the modulation of pathways that potentiate and suppress the development of systemic autoimmunity.

Fig. 12

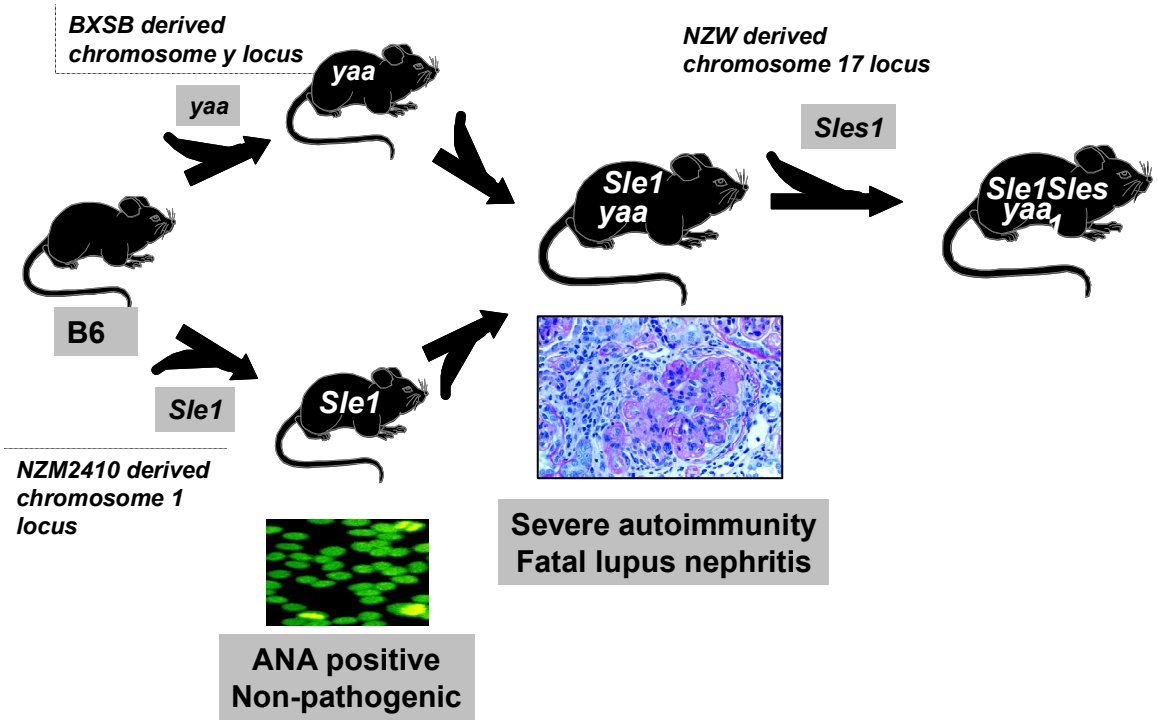

Figure 12. Schematic of Various Combinations of Loci Used in *yaa* Studies.

Table 8

	B6 (n=6)	B6.*yaa* (n=7)	B6.*Sle1*|*yaa* (n=8)	B6.*Sle1*|*Sles1*|*yaa* (n=8)
THYMUS[1]				
$CD4^-CD8^-$	4.0 ± 0.28	5.0 ± 0.58	4.8 ± 0.46	4.7 ± 0.21
$CD4^+CD8^+$	84.1 ± 1.23	82.0 ± 2.42	84.2 ± 0.49	80.4 ± 0.52
$CD4^+$	8.3 ± 0.64	8.7 ± 1.47	7.4 ± 0.19	10.4 ± 0.45
$CD8^+$	3.5 ± 0.38	4.2 ± 0.54	3.6 ± 0.16	4.5 ± 0.19
BONE MARROW[1]				
IgM^-	91.2 ± 0.83	92.4 ± 0.62	93.4 ± 0.65	92.6 ± 0.47
Pro B ($CD43^+B220^+$)	9.9 ± 0.92	9.4 ± 0.91	9.0 ± 0.8	10.0 ± 0.80
Pre B ($CD43^-B220^+$)	12.5 ± 0.82	11.0 ± 0.65	8.6 ± 0.44**	10.0 ± 0.65
Immature B (IgM^+B220^{lo})	5.4 ± 0.46	4.5 ± 0.32	4.2 ± 0.25	4.5 ± 0.21
Mature B (IgM^+B220^{hi})	4.2 ± 0.46	4.0 ± 0.42	2.7 ± 0.2*	3.4 ± 0.31
Pre-Plasma ($B220^{int}CD138^+$)	10.9 ± 2.26	10.1 ± 0.90	10.7 ± 1.4	11.2 ± 0.74
Plasma ($B220^-CD138^+$)	1.2 ± 0.15	1.2 ± 0.10	1.5 ± 0.22	1.2 ± 0.10
SPLEEN[1]				
Weight (mg)	76.7 ± 2.42	71.1 ± 3.36^{+++}	113.9 ± 6.11***	73.4 ± 2.75^{+++}
$B220^+$	56.6 ± 0.96	52.4 ± 1.73	49.7 ± 1.27	52.7 ± 1.01
%$CD69^+$	2.5 ± 0.26	3.1 ± 0.19^{+++}	5.3 ± 0.39***	2.5 ± 0.27^{+++}
CD69 MFI	42.4 ± 2.34	41.7 ± 2.26	48.5 ± 2.19	43.2 ± 1.70
$CD19^+$	57.9 ± 1.0	55.4 ± 1.10	54.4 ± 1.53	56.5 ± 0.92
T1 ($CD23^-CD21^-IgM^+$)	4.6 ± 0.37	4.0 ± 0.31	3.6 ± 0.25	3.5 ± 0.44
T2 ($CD23^+CD21^{hi}IgM^{hi}$)	2.6 ± 0.19	1.6 ± 0.20**	1.7 ± 0.2*	2.6 ± 0.19^{++}
Follicular ($CD23^+CD21^+IgM^{lo}$)	34.5 ± 1.0	37.0 ± 0.90	35.1 ± 1.0	34.4 ± 1.14
% $CD86^+$	0.27 ± 0.14	0.19 ± 0.06	0.35 ± 0.11	0.2 ± 0.05
MZ ($CD23^-CD21^-IgM^+$)	2.2 ± 0.40	1.1 ± 0.13**	1.3 ± 0.22*	1.8 ± 0.11^{++}
B1a ($CD5^+CD23^-B220^+$)	1.3 ± 0.05	1.3 ± 0.11	1.6 ± 0.17	1.0 ± 0.10^{+}
B1b ($CD5^-CD23^-B220^{lo}$)	4.8 ± 0.48	4.2 ± 0.41	4.9 ± 0.19	3.6 ± 0.24^{+}
B2 ($CD5^-CD23^+B220^+$)	45.3 ± 1.56	46.0 ± 1.09	42.4 ± 1.0	46.5 ± 0.64
$CD19^+CD11b^+$	1.4 ± 0.16	1.5 ± 0.14	2.0 ± 0.12	1.3 ± 0.12^{+}
Plasma ($CD19^-CD138^+$)	0.69 ± 0.07	0.88 ± 0.04^{+++}	1.4 ± 0.12***	0.71 ± 0.05^{+++}
$CD3^+$	28.5 ± 0.94	32.1 ± 0.48	31.1 ± 0.79	31.7 ± 0.87
%$CD69^+$	6.6 ± 0.48	8.3 ± 0.37^{+}	10.9 ± 1.07***	5.9 ± 0.43^{+++}
CD69 MFI	39.3 ± 2.33	41.5 ± 2.21	42.7 ± 2.60	38.0 ± 1.77
$CD4^+$	19.2 ± 0.49	20.8 ± 0.83	18.4 ± 1.15	19.5 ± 0.81
%$CD25^+CD69^-$	10.5 ± 0.75	9.5 ± 0.54	8.5 ± 0.34	8.3 ± 0.64
%$CD25^+CD69^+$	3.9 ± 0.75	3.9 ± 1.00	6.9 ± 0.89	3.5 ± 0.39^{+}
%$CD69^+CD25^-$	5.7 ± 0.95	6.1 ± 1.55^{++}	11.7 ± 0.92**	6.2 ± 0.65^{++}
%$CD62L^+CD44^{lo}$	73.5 ± 0.82	73.1 ± 1.2^{+++}	62.6 ± 2.48***	77.7 ± 0.79^{+++}
%$CD62L^-CD44^{lo}$	7.6 ± 0.46	7.8 ± 0.66^{++}	12.2 ± 1.45**	6.9 ± 0.33^{++}
%$CD62L^-CD44^{hi}$	10.8 ± 1.00	11.8 ± 0.92	15.3 ± 1.31*	8.3 ± 0.64^{+++}
%$CD62L^+CD44^{hi}$	8.3 ± 0.90	7.6 ± 1.07	10.4 ± 0.80	7.0 ± 0.53^{+}
$CD8^+$	11.5 ± 0.26	12.6 ± 0.55	11.9 ± 0.62	12.7 ± 0.5
$CD11b^+$	3.8 ± 0.21	3.7 ± 0.40	4.8 ± 0.33	3.9 ± 0.25
$NK1.1^+$	2.0 ± 0.20	1.4 ± 0.19	1.7 ± 0.27	1.5 ± 0.10
$CD3^+NK1.1^+$	1.7 ± 0.19	1.7 ± 0.22	2.5 ± 0.54	1.8 ± 0.22

Table 8. Cellular Compositions of B6, B6.*yaa*, B6.*Sle1*|*yaa* and B6.*Sle1*|*Sles1*|*yaa* Thymus, BM and Spleens at 6-8 weeks.

[1] Thymic, BM and splenic cells from 6-8 week old male B6, B6.*yaa*, B6.*Sle1*|*yaa* and B6.*Sle1*|*Sles1*|*yaa* mice were subjected to 4-color flow-cytometric analyses as described in Chapter II. Six to eight male mice from each strain were analyzed and shown values represent mean ± SEM. Indented subsets indicate that the listed percentages are representative of the non-indented parent population listed above. All remaining values are percentages of live cells as determined by forward and side scatter profiles. All statistical analyses were conducted using parametric and non-parametric ANOVAs between all three groups, as determined by InStat3. Only significant differences *vs.* B6 or B6.*Sle1*|*yaa* are shown. $^{*}p<0.05$, $^{**}p<0.01$, $^{***}p<0.001$ *vs.* B6; $^{+}p<0.05$, $^{++}p<0.01$, $^{+++}p<0.001$ *vs.* B6.*Sle1*|*yaa* (ANOVA).

Fig. 13A

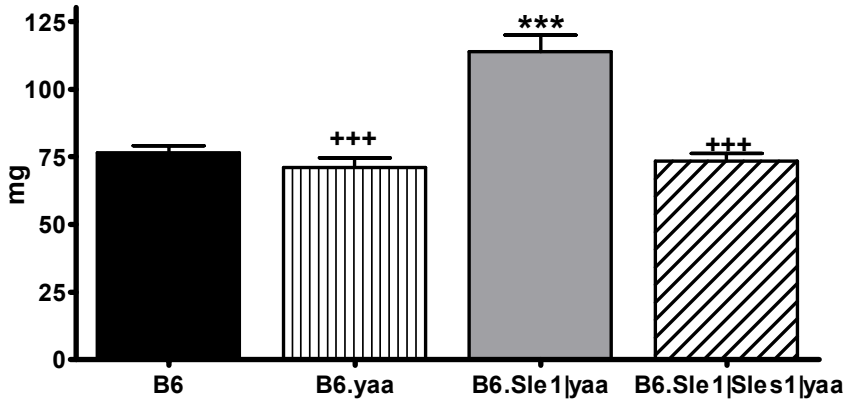

Fig. 13B

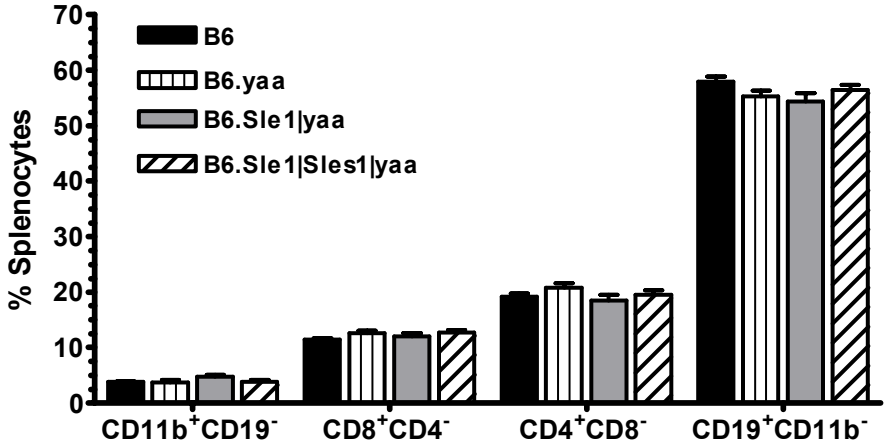

Figure 13. *Sles1* Suppresses the Early-onset Splenomegaly Seen in Young B6.*Sle1*|*yaa* Males. Spleens were collected from 6-8 week-old mice at time of sacrifice and weighed. Flow-cytometric analyses of splenocytes were performed to assay for changes in the major splenic lineages. A. Comparison of spleen weights at 6-8 weeks of age. B6.*Sle1*|*yaa* spleens were significantly larger than those from age and gender-matched B6, B6.*yaa* and B6.*Sle1*|*Sles1*|*yaa*. No other differences were observed between the genotypes. $^{***}p<0.001$ *vs.* B6; $^{+++}p<0.001$ *vs.* B6.*Sle1*|*yaa* (ANOVA). B. Comparable percentages of $CD4^+$, $CD8^+$, $CD19^+$ and $CD11b^+$ splenocytes. Spleen cells were stained with 4-color combinations of antibodies against CD4, CD8, CD19 and CD11b. No statistically significant differences in percentages were observed between the different genotypes (ANOVA). Mean ± SEM.

Fig. 14A

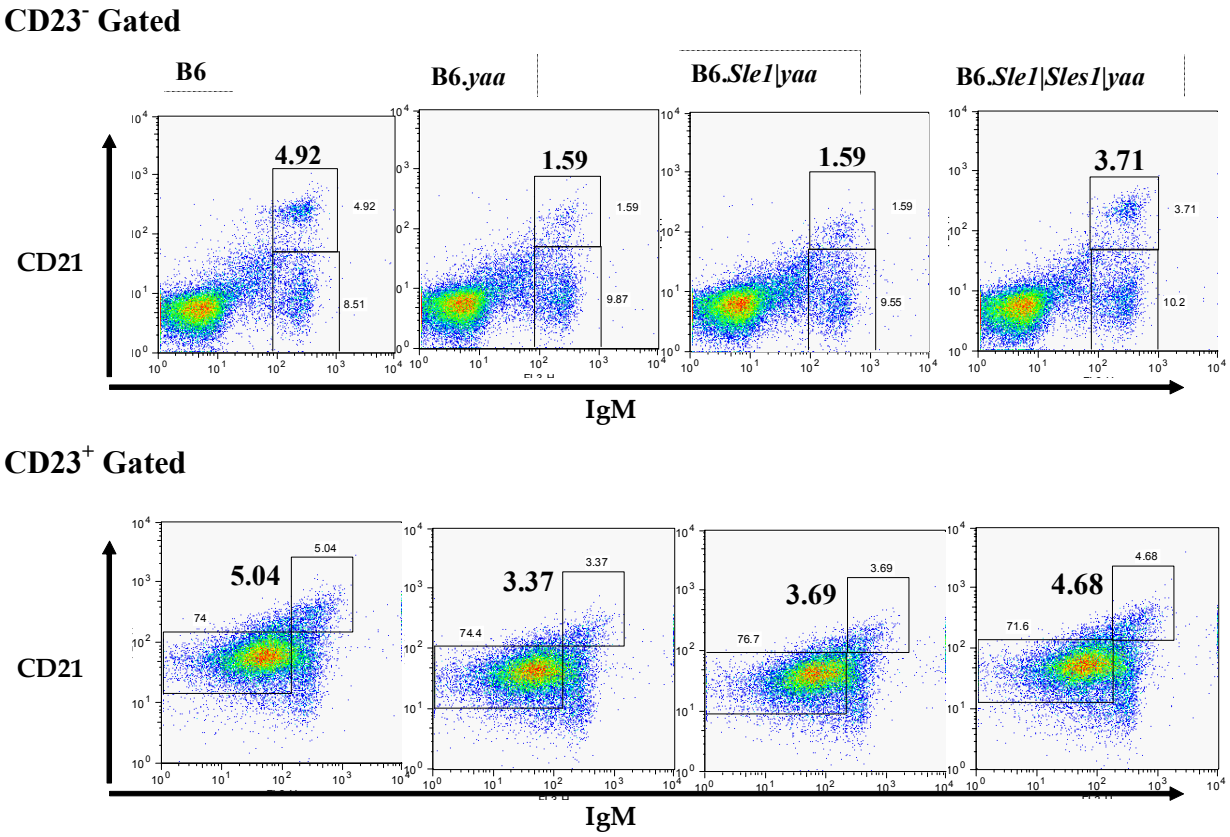

Fig. 14B

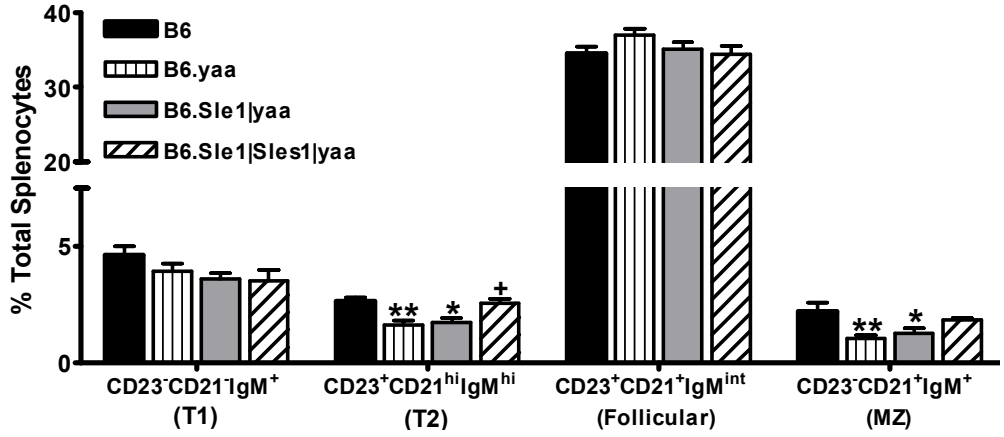

Figure 14. *yaa*-Associated Defect in Splenic T2 and MZ B cells Restored in the Presence of *Sles1*. Flow-cytometric analyses of splenocytes were performed to assay for changes in the development of splenic T1 ($CD23^{-}CD21^{-}IgM^{+}$), T2 ($CD23^{+}CD21^{hi}IgM^{hi}$), follicular

($CD23^{+}CD21^{+}IgM^{int}$) and MZ ($CD23^{-}CD21^{+}IgM^{+}$) B cells. A. Representative dot-plots of live cells from the different strains pre-gated on $CD23^{-}$ (upper) and $CD23^{+}$ (lower) and examined for CD21 *vs.* IgM expression to delineate the various populations described above. B6.*Sle1*|*Sles1*|*yaa* mice showed comparable MZ and T2 populations relative to B6, while both B6.*yaa* and B6.*Sle1*|*yaa* demonstrated a decreased percentage of both these populations. Bold numbers represent percentages of $CD21^{+}IgM^{+}$ (upper) and $CD21^{hi}IgM^{hi}$ (lower) cells as a percentage of $CD23^{-}$ and $CD23^{+}$ cells respectively. B. Cumulative data demonstrating the decrease in T2 and MZ B cells in B6.*yaa* and B6.*Sle1*|*yaa*, which was restored in the presence of *Sles1*. Percentages indicate percent of lymphocytes for each population. Mean ± SEM. $^{*}p<0.05$, $^{**}p<0.01$ *vs.* B6; $^{+}p<0.05$ *vs.* B6.*Sle1*|*yaa* (ANOVA).

Fig. 15A

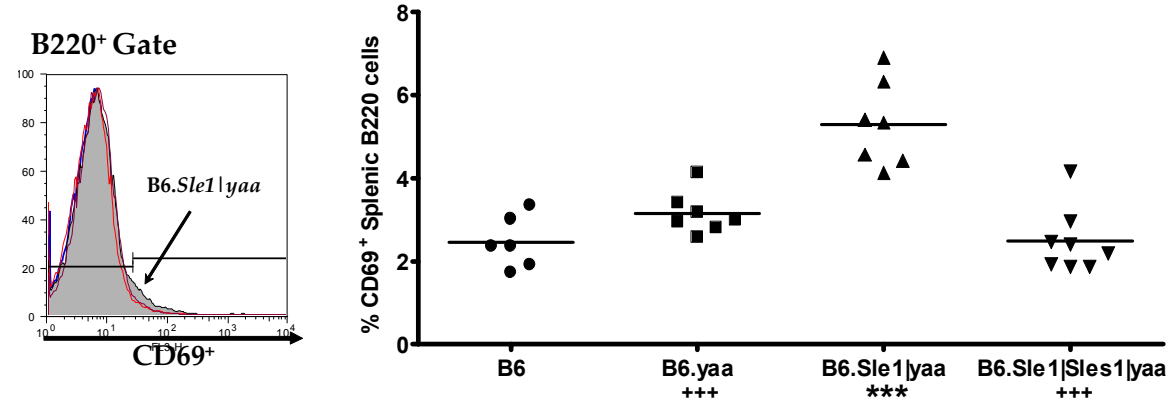

Fig. 15B

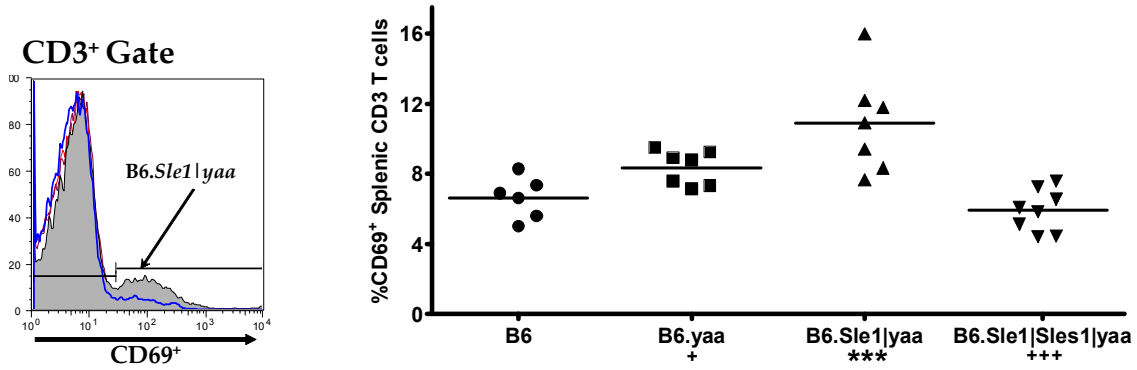

Fig. 15C

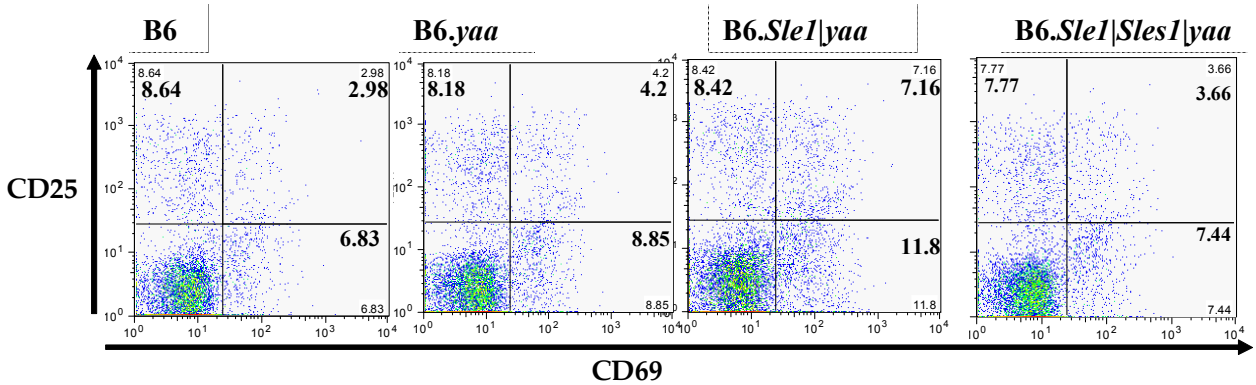

Fig. 15D

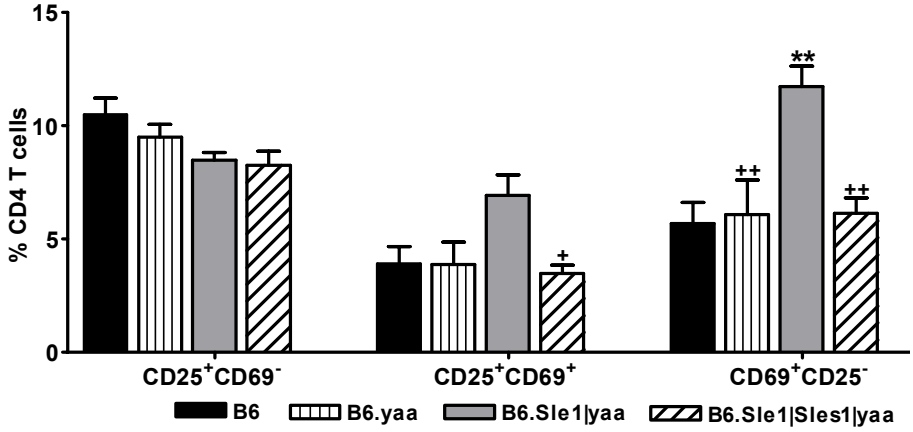

Figure 15. Early Indications of Activated B and T cells in B6.*Sle1*|*yaa* are Absent in the Presence of *Sles1*. Flow-cytometric analyses of splenocytes were performed to assay for changes in activation marker expression on B and T cells in 6-8 week old mice of the different strains. A-B. Representative histograms and cumulative data demonstrating the increased percentage of $CD69^+$ $B220^+$ B (A.) and $CD69^+$ $CD3^+$ T cells (B.) in B6.*Sle1*|*yaa* spleens, which was not seen in the presence of *Sles1*. Shaded histograms- B6.*Sle1*|*yaa*; bold histogram- B6.*Sle1*|*Sles1*|*yaa*. C-D. Representative dot-plots and cumulative data demonstrating the increased percentage of $CD69^+CD25^-$ CD4 T cells observed in B6.*Sle1*|*yaa* spleens, which was absent in the presence of *Sles1*. Values in the quadrants in (C.) represent the percentage of that population within total CD4 T cells. Symbols represent individual mice. Mean ± SEM. $^{**}p<0.01$, $^{***}p<0.001$ *vs.* B6; $^{+}p<0.05$, $^{++}p<0.01$, $^{+++}p<0.001$ *vs.* B6.*Sle1*|*yaa* (ANOVA).

Fig. 16A

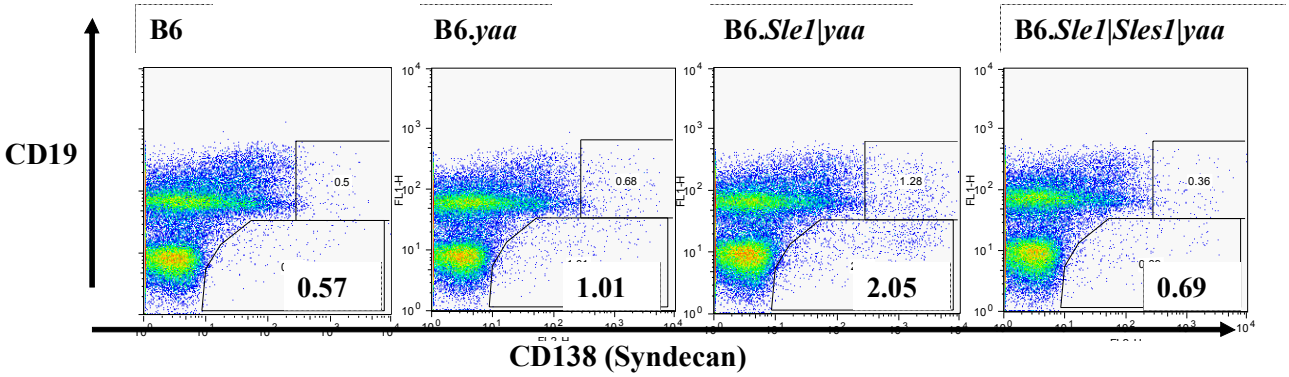

Fig. 16B

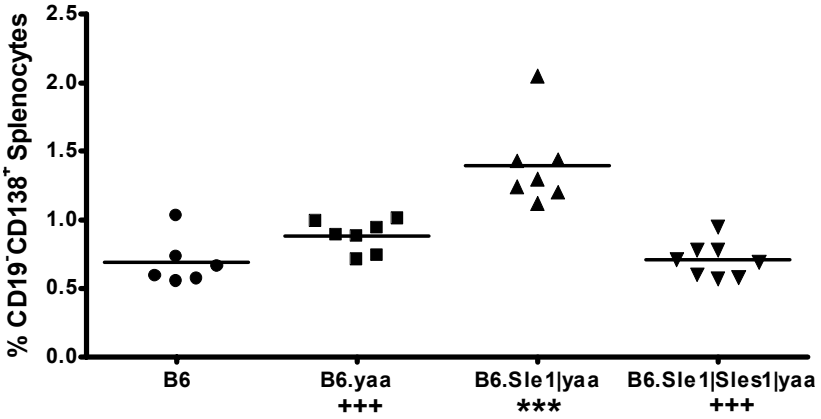

Fig. 16C

$CD4^+$ Gated

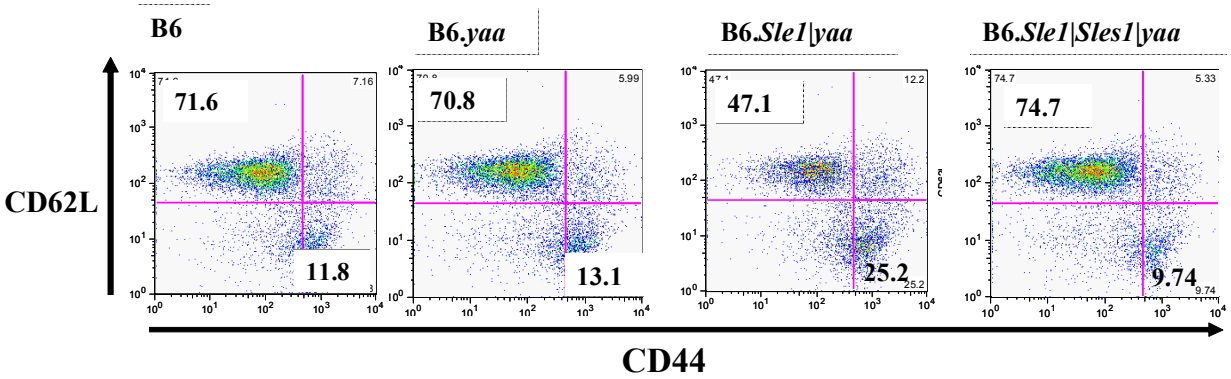

Fig. 16D

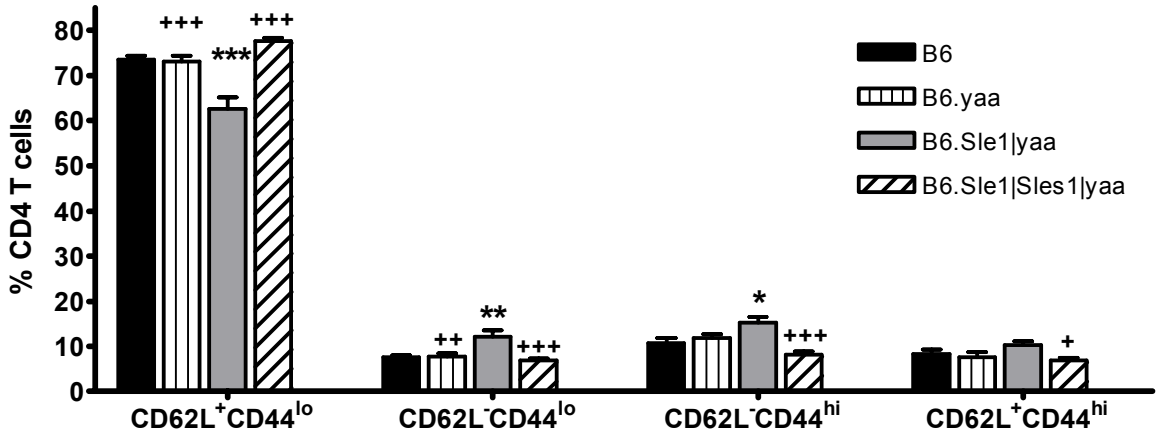

Figure 16. Accelerated B and T cell Differentiation Phenotypes Abrogated by *Sles1*. Flow-cytometric analyses of splenocytes were performed to assay for changes in differentiation marker expression on B and T cells in 6-8 week old mice of the different strains. A-B. Representative dot-plots and cumulative data showing the increased accumulation of $CD19^{-}CD138^{+}$ plasma cells in B6.*Sle1*|*yaa* spleens, which was not seen in the presence of *Sles1*. Numbers in gates represent percentage of live cells. C-D. Representative dot-plots and cumulative data demonstrating the increased percentage of $CD62L^{-}CD44^{lo}$ and $CD62L^{-}CD44^{hi}$ CD4 T cells observed in B6.*Sle1*|*yaa* spleens. These increases were not observed in B6.*Sle1*|*Sles1*|*yaa*. Values in the quadrants in (C.) represent the percentage of that population within total CD4 T cells. Symbols represent individual mice. Mean ± SEM. $^{*}p<0.05$, $^{**}p<0.01$, $^{***}p<0.001$ *vs.* B6; $^{+}p<0.05$, $^{++}p<0.01$, $^{+++}p<0.001$ *vs.* B6.*Sle1*|*yaa* (ANOVA).

Fig. 17A

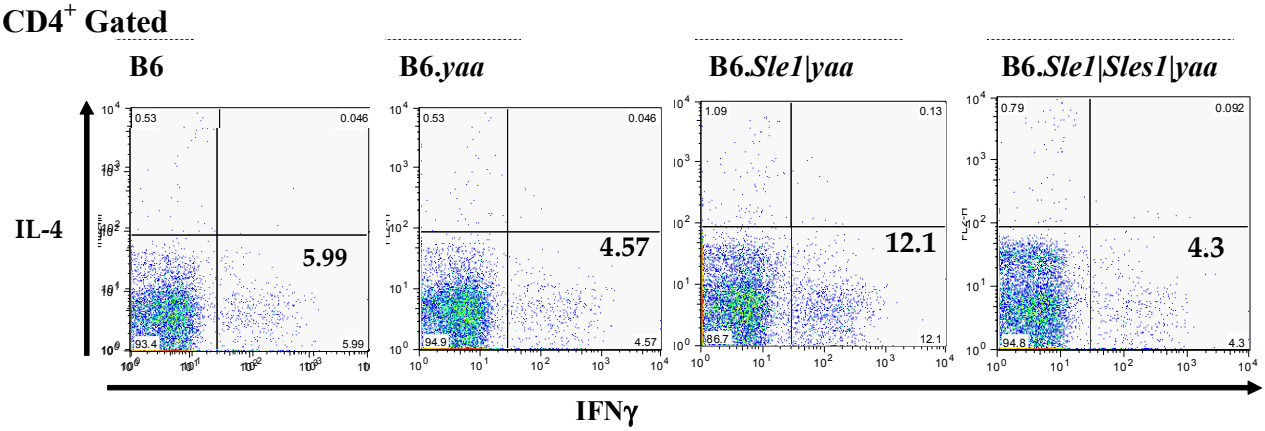

Fig. 17B

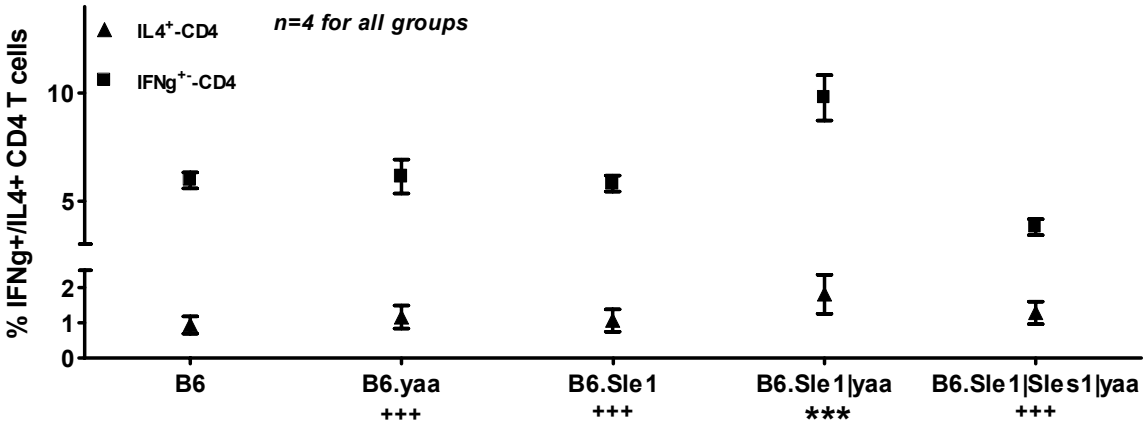

Figure 17. Increased *ex vivo* IFNγ Production Not Observed in B6.*Sle1*|*Sles1*|*yaa*. Splenocytes, prestained with CD4, were stimulated for 4 hours with PMA and ionomycin in the presence of BD Golgi Stop. Cells were surface-stained, fixed, permeabilized and then stained with antibodies against IL-4 and IFNγ. B6.*Sle1*|*Sles1*|*yaa* cells do not show the ~2-fold increase in *ex vivo* IFNγ producing CD4$^+$ cells seen in B6.*Sle1*|*yaa*. A. Representative dot-plots. B. Cumulative data for 4 mice/genotype. Values in the quadrants represent the percentage of that population within total CD4 T cells. $^{***}p<0.001$ *vs.* B6; $^{+++}p<0.001$ *vs.* B6.*Sle1*|*yaa* (ANOVA).

Fig. 18A

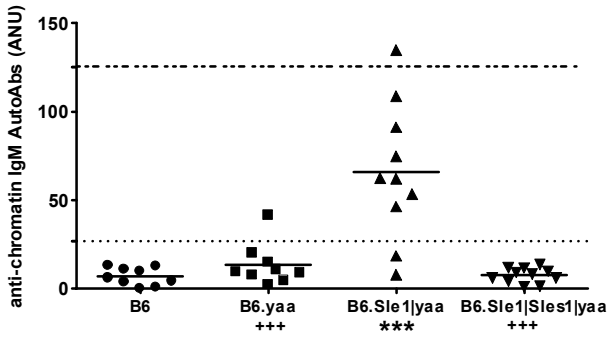

Fig. 18B

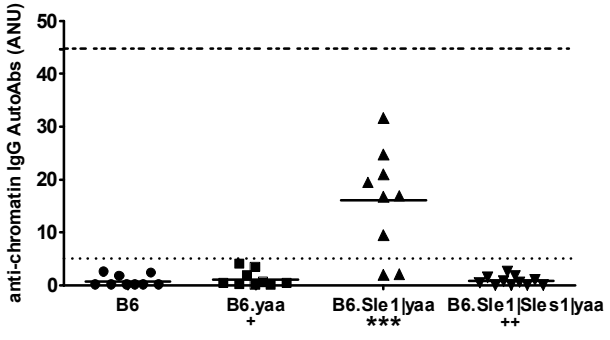

Fig. 18C

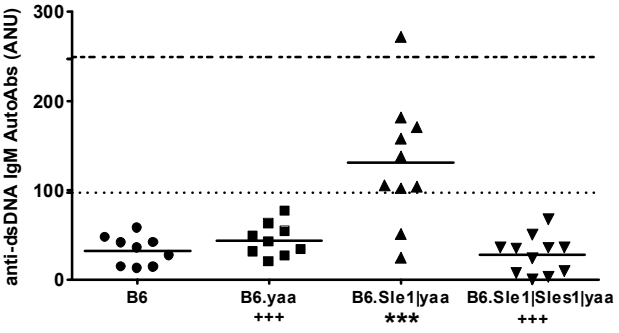

Fig. 18D

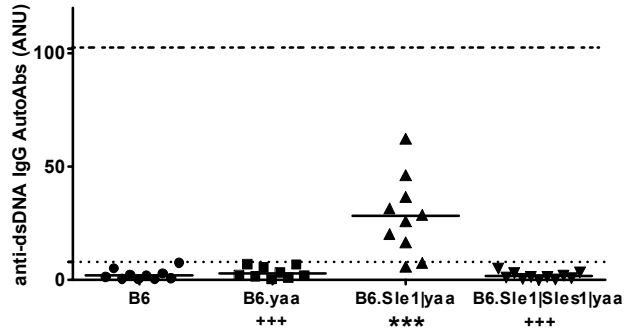

Fig. 18E

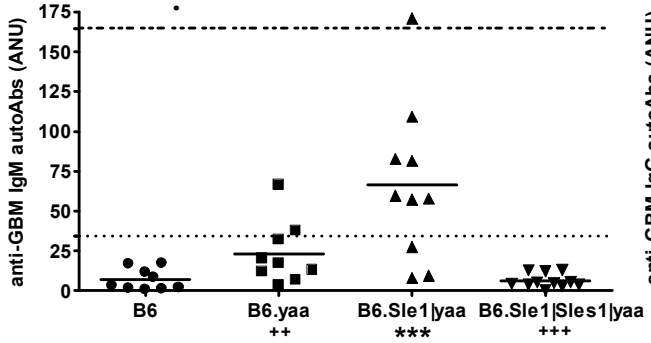

Fig. 18F

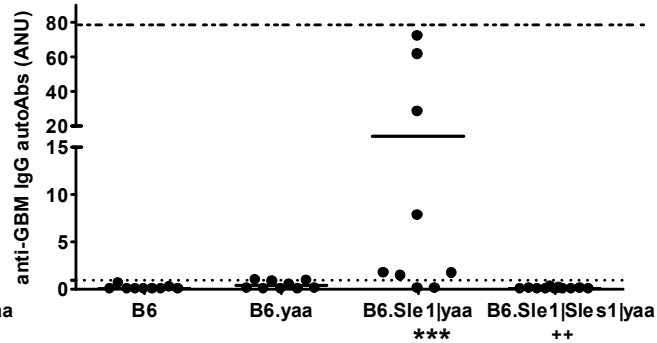

Figure 18. Lack of Early Humoral Autoimmunity in B6.*Sle1*|*Sles1*|*yaa*. Serum levels of IgM and IgG anti-chromatin, anti-dsDNA and anti-GBM autoAbs were determined by ELISA for samples obtained at 6-8 weeks of age. Duplicate samples were assayed simultaneously, in duplicate, on plates coated in parallel to allow for interplate comparisons of mean titres. Samples were deemed positive if they exceeded the mean B6 value + 4SD for a given antigen. Dotted and dashed lines indicate the thresholds for being considered positive at 6-8 weeks and 4-6 months respectively. A-B. Anti-chromatin IgM and IgG respectively. C-D. Anti-dsDNA IgM and IgG respectively. E-F. Anti-GBM IgM and IgG respectively. $^{***}p<0.001$ *vs.* B6; $^{+}p<0.05$, $^{++}p<0.01$, $^{+++}p<0.001$ *vs.* B6.*Sle1*|*yaa* (ANOVA).

Fig. 19A

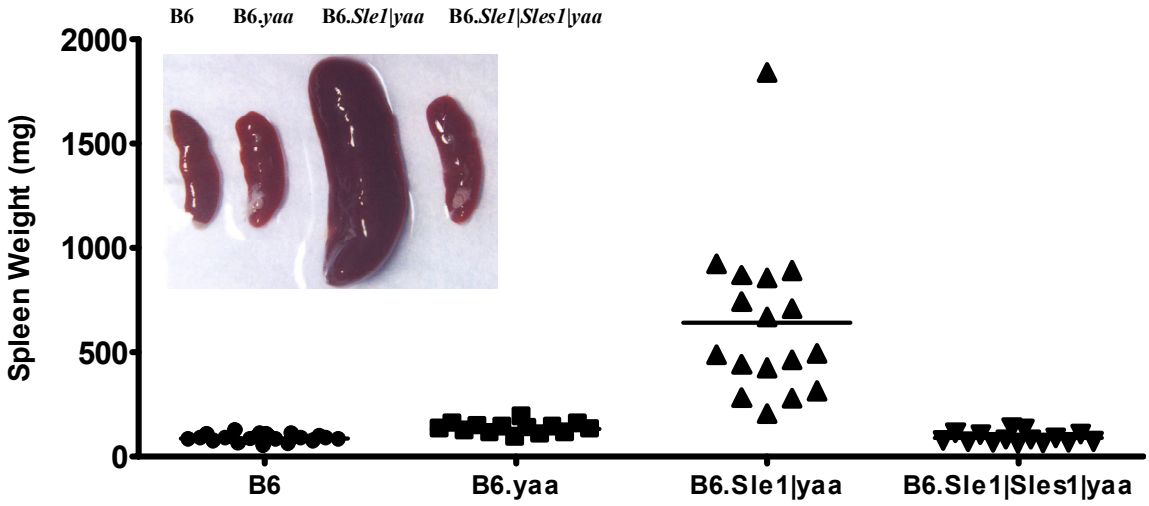

Fig. 19B

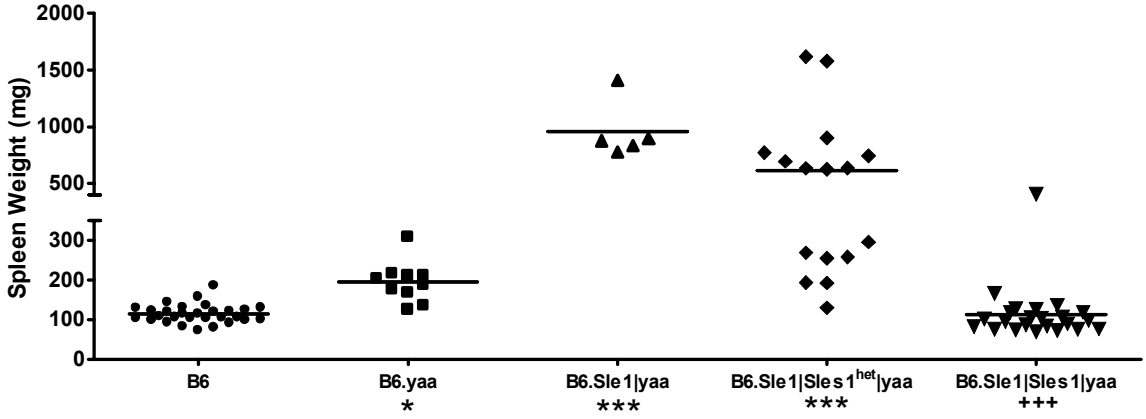

Figure 19. Lack of Splenomegaly in B6.*Sle1*|*Sles1*|*yaa* Mice Maintained to 9 months. Spleens were collected from 4-6 month and 9 month old mice at the time of sacrifice and weighed. A. Spleen weights at 4-6 months. Inset shows photograph of representative spleens. There is no evidence of increased spleen weights in B6.*Sle1*|*Sles1*|*yaa*. B. Spleen weights at 9 months. Splenomegaly remains absent in B6.*Sle1*|*Sles1*|*yaa* but is present in B6.*Sle1*|*Sles1*^{het}|*yaa*. Symbols represent individual mice. Mean ± SEM. $^{*}p<0.05$, $^{***}p<0.001$ *vs.* B6; $^{+++}p<0.001$ *vs.* B6.*Sle1*|*yaa* (ANOVA).

Table 9.

	B6 (n=7)	B6.*yaa* (n=9)	B6.*Sle1*|*yaa* (n=10)	B6.*Sle1*|*Sles1*|*yaa* (n=10)
SPLEEN				
Weights (mg)	86.4 ± 3.54	134.4 ± 6.67^{+++}	641.8 ± 94.3***	89.5 ± 6.34^{+++}
# B220^{+} (X 10^{6})	55.4 ± 5.78	63.3 ± 4.41^{+++}	119.4 ± 11.7***	42.5 ± 2.59***
% B220^{+}	56.6 ± 0.96	54.2 ± 2.0^{+++}	32.7 ± 4.61***	52.6 ± 2.0^{+++}
%CD69^{+}	2.4 ± 0.3	6.8 ± 0.86$^{+++, **}$	18.3 ± 1.27***	2.3 ± 0.12^{+++}
CD69 MFI	40.7 ± 1.51	45.3 ± 1.32^{+++}	56.6 ± 1.88***	41.8 ± 1.37^{+++}
T1 (CD23^{-}CD21^{-}IgM^{+})	3.8 ± 0.35	3.2 ± 0.2^{+++}	4.9 ± 0.40	2.3 ± 0.18$^{+++, **}$
T2 (CD23^{+}CD21^{hi}IgM^{hi})	2.1 ± 0.19	1.8 ± 0.22^{+++}	0.61 ± 0.1***	2.7 ± 0.18^{+++}
Follicular (CD23^{+}CD21^{+}IgM^{lo})	34.2 ± 0.8	36.1 ± 1.27^{+++}	18.4 ± 3.91***	34.1 ± 1.6^{+++}
CD86 MFI	64.3 ± 8.81	71.3 ± 7.75^{+++}	87.0 ± 7.3***	59.2 ± 9.1^{+++}
MZ (CD23^{-}CD21^{-}IgM^{+})	3.39 ± 0.28	1.2 ± 0.12***	0.48 ± 0.11***	2.9 ± 0.3^{+++}
B1a (CD5^{+}CD23^{-}B220^{+})	1.1 ± 0.1	0.8 ± 0.06^{++}	1.3 ± 0.14	0.62 ± 0.03$^{+++, **}$
B1b (CD5^{-}CD23^{-}B220^{lo})	2.7 ± 0.24	3.5 ± 0.22^{+++}	7.7 ± 0.54***	2.9 ± 0.21^{+++}
B2 (CD5^{-}CD23^{+}B220^{+})	41.0 ± 2.32	43.1 ± 2.3^{+++}	20.5 ± 4.47**	39.3 ± 2.4^{+++}
B220^{+}CD11b^{+}	1.2 ± 0.33	2.2 ± 0.3^{+++}	4.5 ± 0.48***	1.2 ± 0.22^{+++}
Plasma (CD19^{-}CD138^{+})	1.1 ± 0.24	1.8 ± 0.23^{+++}	5.0 ± 0.57***	0.8 ± 0.09^{+++}
# CD3^{+} (X 10^{6})	27.7 ± 4.0	30.8 ± 2.91^{+++}	58.6 ± 6.40***	21.5 ± 1.80^{+++}
CD3^{+}	27.3 ± 2.34	26.3 ± 2.0^{+++}	15.1 ± 1.22***	26.0 ± 1.57^{+++}
%CD69^{+}	14.6 ± 0.74	21.5 ± 1.37^{+++}	46.6 ± 2.9***	14.9 ± 0.65^{+++}
CD69 MFI	36.8 ± 0.93	44.6 ± 1.38^{+++}	74.1 ± 5.35***	35.8 ± 0.69^{+++}
CD4^{+}	20.0 ± 1.59	19.3 ± 1.14^{+++}	13.3 ± 1.08***	18.5 ± 0.80^{+++}
%CD25^{+}CD69^{-}	10.6 ± 0.25	8.7 ± 0.39	9.0 ± 0.47	9.8 ± 0.26
%CD25^{+}CD69^{+}	7.8 ± 0.73	9.6 ± 0.38^{+++}	21.0 ± 1.62***	7.0 ± 0.57^{+++}
%CD69^{+}CD25^{-}	6.2 ± 0.62	13.1 ± 0.89$^{+++, ***}$	20.1 ± 0.84***	5.1 ± 0.3^{+++}
%CD62L^{+}CD44^{lo}	58.8 ± 3.62	49.6 ± 2.51^{+++}	10.1 ± 3.84***	63.1 ± 3.14^{+++}
%CD62L^{-} CD44^{lo}	10.1 ± 0.85	13.5 ± 1.21^{+}	17.9 ± 1.18***	9.7 ± 1.03^{+++}
%CD62L^{-} CD44^{hi}	18.4 ± 1.58	25.0 ± 2.4^{+++}	60.6 ± 4.22***	13.8 ± 0.9^{+++}
%CD62L^{+}CD44^{hi}	12.7 ± 2.7	12.0 ± 2.19	11.5 ± 0.89	13.4 ± 2.28
CD11b^{+}	5.1 ± 0.44	4.9 ± 0.38^{+++}	13.6 ± 1.9***	4.7 ± 0.23^{+++}
NK1.1^{+}	2.0 ± 0.26	2.4 ± 0.28	2.2 ± 0.22	2.1 ± 0.3
CD3^{+}NK1.1^{+}	2.1 ± 0.29	2.3 ± 0.35	3.4 ± 0.42	2.6 ± 0.37
BONE MARROW				
IgM^{-}	93.6 ± 0.45	94.5 ± 0.56	96.1 ± 0.63*	95.3 ± 0.31
Pro B (CD43^{+}B220^{+})	5.8 ± 0.52	4.6 ± 0.4	3.6 ± 0.58**	4.4 ± 0.2
Pre B (CD43^{-}B220^{+})	7.4 ± 1.0	5.3 ± 0.57	2.7 ± 0.91**	4.8 ± 0.64
Non-B (CD43^{+}B220^{-})	61.8 ± 3.4	69.5 ± 1.76	78.8 ± 2.52***	69.3 ± 0.95
Immature B (IgM^{+}B220^{lo})	3.1 ± 0.26	2.3 ± 0.16	1.4 ± 0.35**	1.9 ± 0.12
Mature B (IgM^{+}B220^{hi})	3.9 ± 0.54	3.2 ± 0.53^{+}	0.8 ± 0.26***	3.0 ± 0.38^{++}
Pre-Plasma (B220^{int}CD138^{+})	4.7 ± 0.92	3.0 ± 0.39	2.0 ± 0.75	2.8 ± 0.3
Plasma (B220^{-}CD138^{+})	1.5 ± 0.22	1.7 ± 0.16	2.3 ± 0.58	1.6 ± 0.15

Table 9. Cellular Compositions of B6, B6.*yaa*, B6.*Sle1*|*yaa* and B6.*Sle1*|*Sles1*|*yaa* BM and Spleens at 4-6 months. BM and splenic cells from 4-6 month old male B6, B6.*yaa*,

B6.*Sle1*|*yaa* and B6.*Sle1*|*Sles1*|*yaa* mice were subjected to 4-color flow-cytometric analyses as described in Chapter II. Seven to ten male mice from each strain were analyzed and shown values represent mean ± SEM. Indented subsets indicate that the listed percentages are representative of the non-indented parent population listed above. All remaining values are percentages of live cells as determined by forward and side scatter profiles. All statistical analyses were conducted using parametric and non-parametric ANOVAs between all three groups, as determined by InStat3. Only significant differences *vs.* B6 or B6.*Sle1*|*yaa* are shown. $^{*}p<0.05$, $^{**}p<0.01$, $^{***}p<0.001$ *vs.* B6; $^{+}p<0.05$, $^{++}p<0.01$, $^{+++}p<0.001$ *vs.* B6.*Sle1*|*yaa* (ANOVA).

Fig. 20A

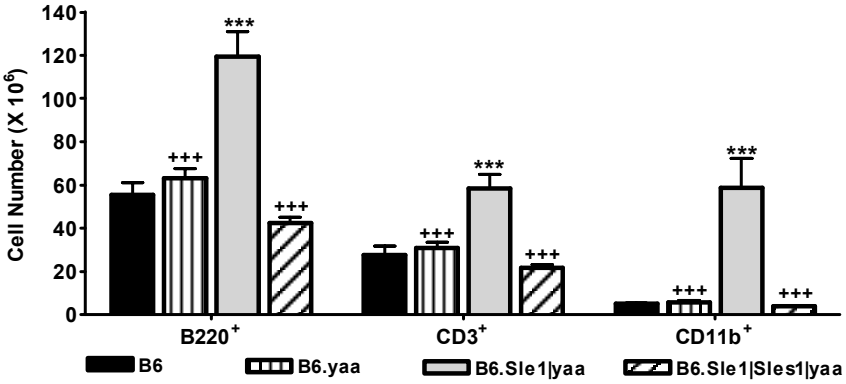

Fig. 20B

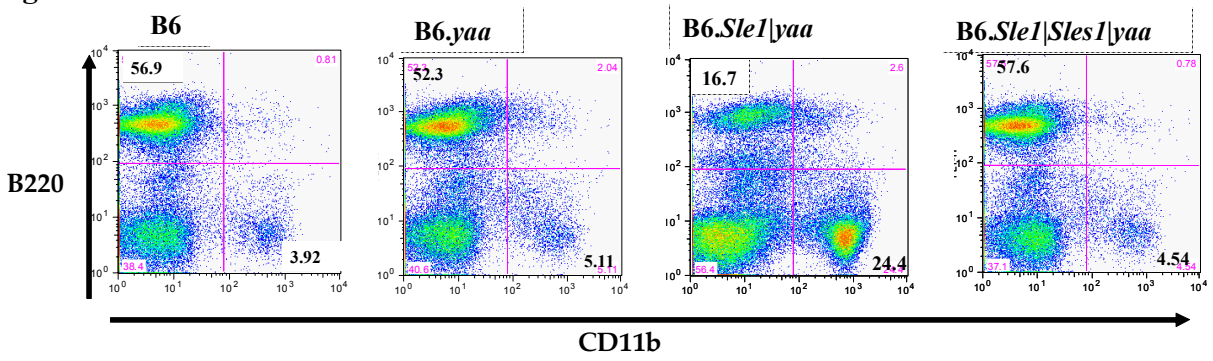

Fig. 20C

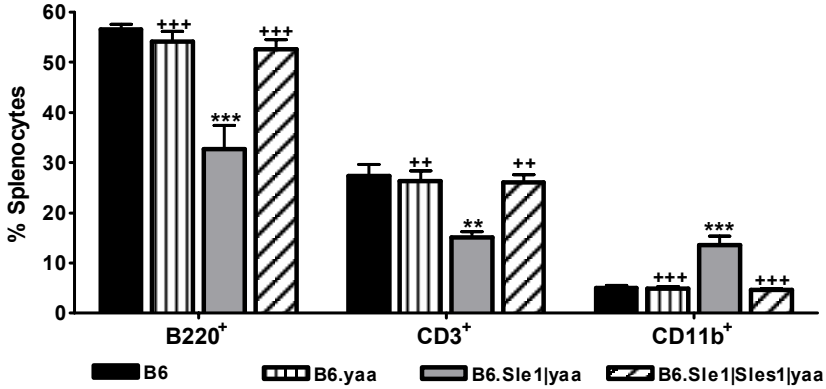

Figure 20. Normal Numbers and Percentages of Splenic Lineages in Aged B6.*Sle1*|*Sles1*|*yaa* Mice. Flow-cytometric analyses of splenocytes stained with combinations of antibodies against CD3, B220 and CD11b were performed to assay for changes in the major lineages at 4-6 months in the different strains. A. Numbers of $CD3^+$, $B220^+$ and $CD11b^+$ cells. B-C. Representative dot-plots and cumulative data of the percentage of different splenic populations. Values in the quadrants in (B.) represent the percentage of that population within live cells. Mean ± SEM. $^{**}p<0.01$, $^{***}p<0.001$ *vs.* B6; $^{++}p<0.01$, $^{+++}p<0.001$ *vs.* B6.*Sle1*|*yaa* (ANOVA).

Fig. 21A

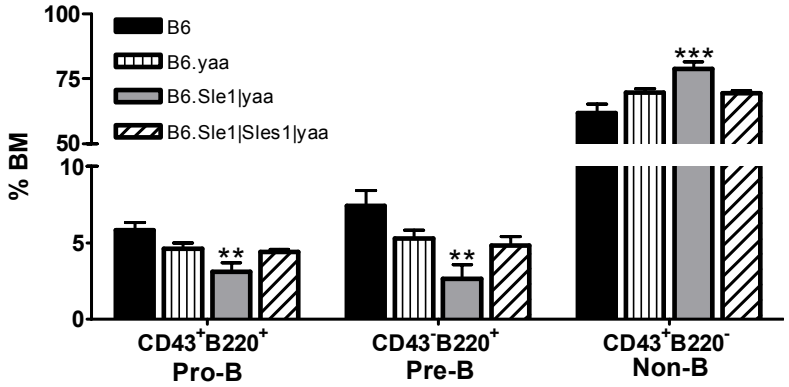

Fig. 21B

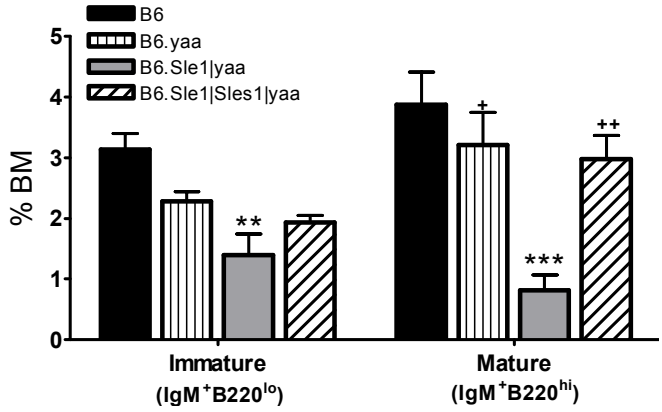

Figure 21. Decreased BM B cells in B6.*Sle1*|*yaa* Relative to B6. BM cells were prepared as described in Chapter II and flow-cytometric analyses performed to assay for changes in various BM subsets. A. Decreased pro- and pre-B but increased non-B cells in B6.*Sle1*|*yaa* compared to B6. Live BM cells were pre-gated on IgM^- and examined for CD43 *vs.* B220 expression to delineate the pro-B ($IgM^-CD43^+B220^+$), pre-B ($IgM^-CD43^-B220^+$) and non-B ($IgM^-CD43^+B220^-$) BM populations. Values represent percentages of total BM cells. B. Decreased immature and mature B cells in B6.*Sle1*|*yaa*. Live BM cells were stained for IgM and B220 to look at immature (IgM^+B220^{lo}) and mature (IgM^+B220^{hi}) B cells. B6.*Sle1*|*yaa* had less immature B cells relative to B6 and decreased mature B cells compared to all groups. Mean ± SEM. $^{*}p<0.05$, $^{**}p<0.01$, $^{***}p<0.001$ *vs.* B6; $^{+}p<0.05$, $^{++}p<0.01$ *vs.* B6.*Sle1*|*yaa* (ANOVA).

Fig. 22A

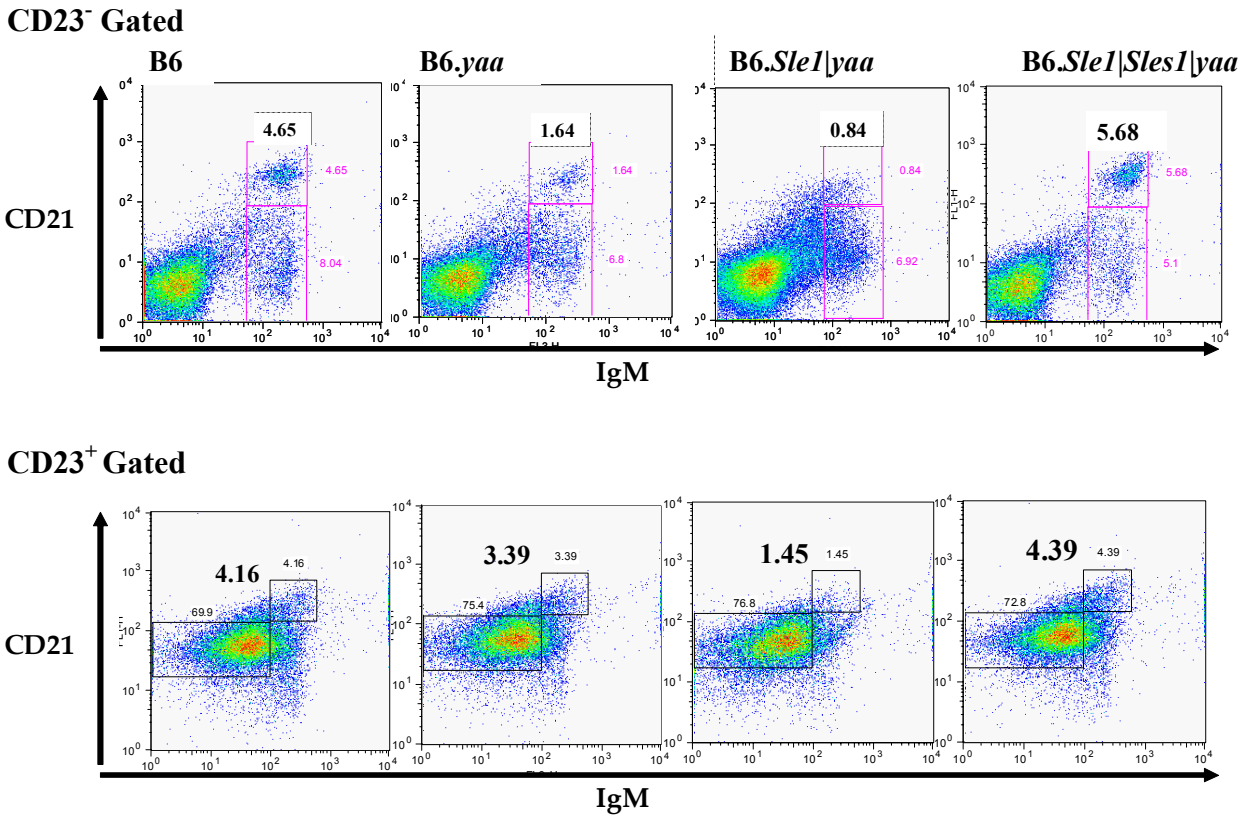

Fig. 22B

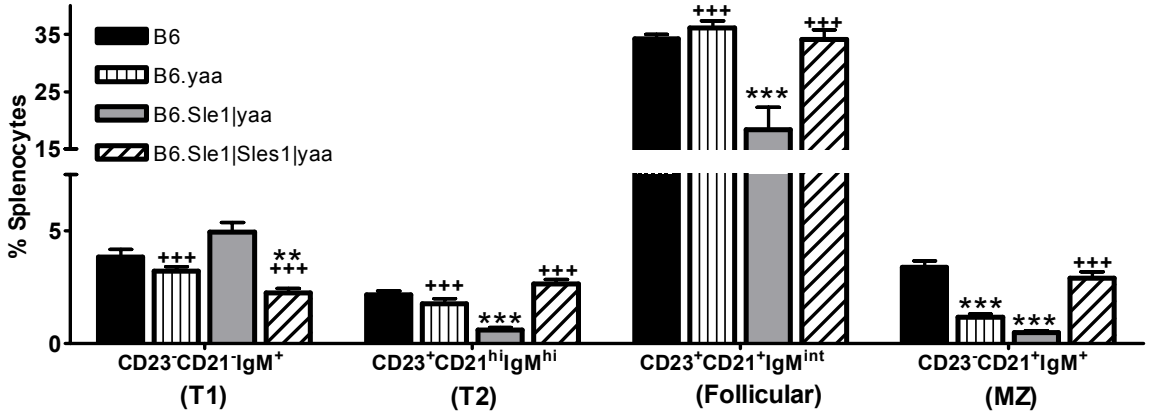

Fig. 22C

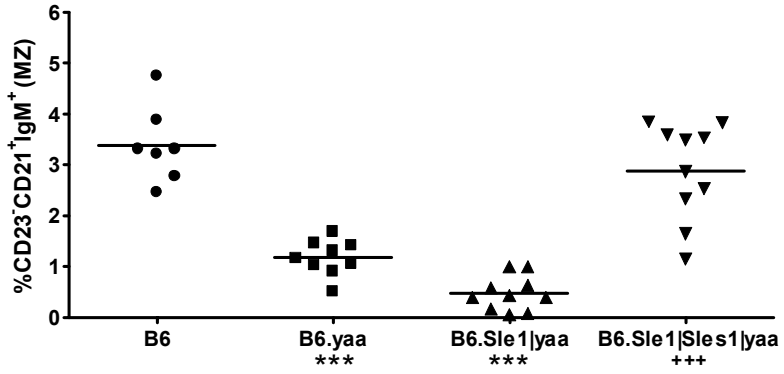

Figure 22. *Sles1* Reconstitution of *yaa*-Associated Defect in Splenic T2 and MZ B cells Maintained at Older Ages. Flow-cytometric analyses of splenocyte suspensions from 4-6 month old mice were performed to assay for changes in the development of splenic T1 ($CD23^{-}CD21^{-}IgM^{+}$), T2 ($CD23^{+}CD21^{hi}IgM^{hi}$), follicular ($CD23^{+}CD21^{+}IgM^{int}$) and MZ ($CD23^{-}CD21^{+}IgM^{+}$) B cells. A. Representative dot-plots of live cells from the different strains pre-gated on $CD23^{-}$ (upper) and $CD23^{+}$ (lower) and examined for CD21 *vs.* IgM expression to delineate the various populations described above. B6.*Sle1*|*Sles1*|*yaa* mice showed comparable MZ and T2 populations relative to B6, while B6.*Sle1*|*yaa* demonstrated a decreased percentage of both these populations. B6.*yaa* only showed a decreased MZ population relative to B6. Bold numbers represent percentages of $CD21^{+}IgM^{+}$ (upper) and $CD21^{hi}IgM^{hi}$ (lower) cells as a percentage of $CD23^{-}$ and $CD23^{+}$ cells respectively. B. Cumulative data demonstrating the decrease in T2 and MZ B cells in B6.*Sle1*|*yaa* that was restored in the presence of *Sles1*. Percentages indicate percent of live splenocytes for each population. C. Data from individual mice to show the decreased frequency of MZ B cells in B6.*yaa* and B6.*Sle1*|*yaa*. Mean ± SEM. $^{**}p<0.01$, $^{***}p<0.001$ *vs.* B6; $^{+++}p<0.001$ *vs.* B6.*Sle1*|*yaa* (ANOVA).

Fig. 23A

CD5⁻ Gated

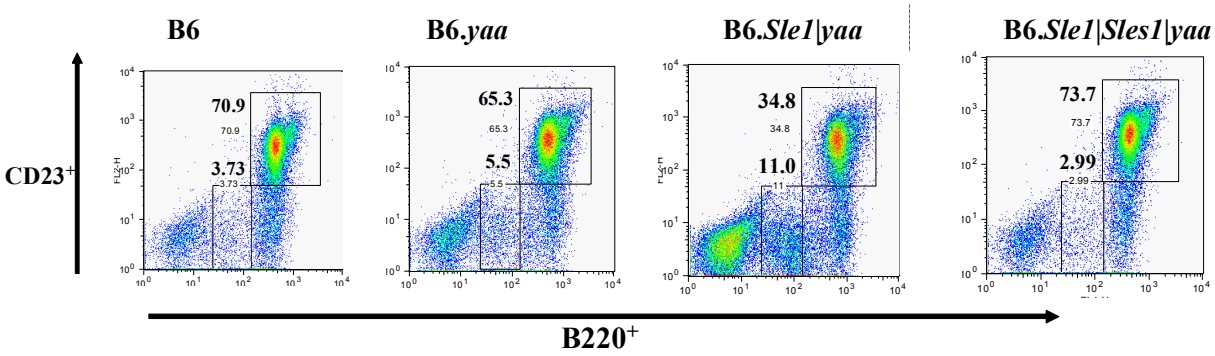

Fig. 23B

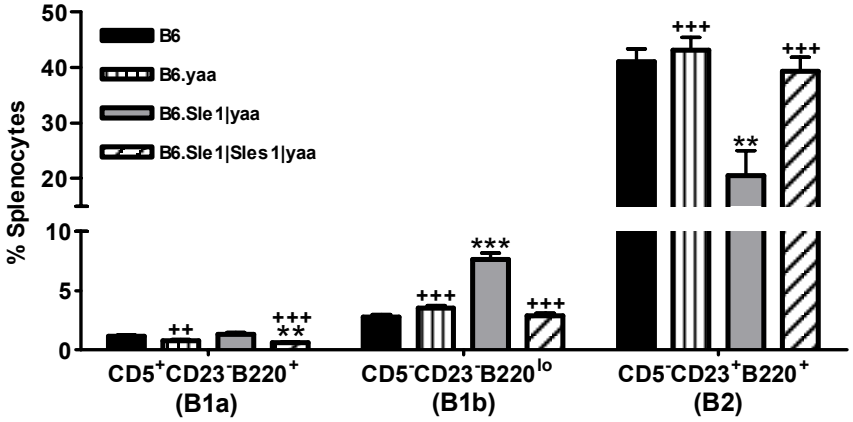

Figure 23. No Increase in Splenic B1 Cells Seen in Aged B6.*Sle1|Sles1|yaa*. Flow-cytometric analyses of splenocytes from 4-6 month old mice were performed to assay for changes in the development of splenic B1a ($CD5^+CD23^-B220^+$), B1b ($CD5^-CD23^-B220^{lo}$) and B2 ($CD5^-CD23^+B220^+$) B cells. A. Representative dot-plots of cells from the different strains pre-gated pre-gated on $CD5^-$ and examined for CD23 *vs.* B220 expression to delineate the various populations described above. Bold numbers represent percentages of $CD23^-B220^{lo}$ and $CD23^+B220^+$ cells as a percentage of $CD5^-$. B. Cumulative data on the B1a, B1b and B2 B cell populations. B6.*Sle1|Sles1|yaa* mice showed comparable B1b and B2, but decreased populations relative to B6, while B6.*Sle1|yaa* demonstrated an increased and decreased percentage of B1b and B2 cells respectively relative to all the strains. An increase in the B1a population in B6.*Sle1|yaa* was only seen *vs.* B6 and B6.*Sle1|Sles1|yaa*. Mean ± SEM. $^{**}p<0.01$, $^{***}p<0.001$ *vs.* B6; $^{++}p<0.01$, $^{+++}p<0.001$ *vs.* B6.*Sle1|yaa* (ANOVA).

Fig. 24A

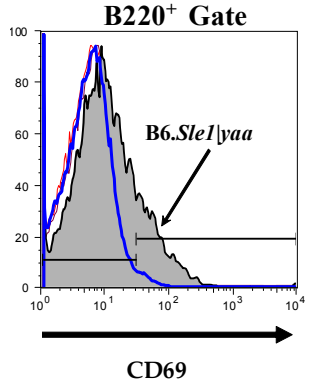

Fig. 24B

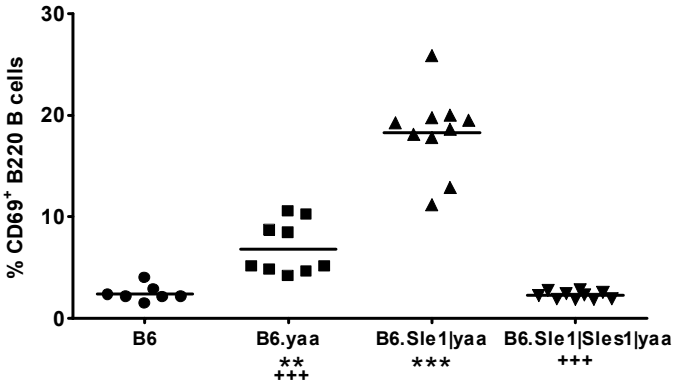

Fig. 24C

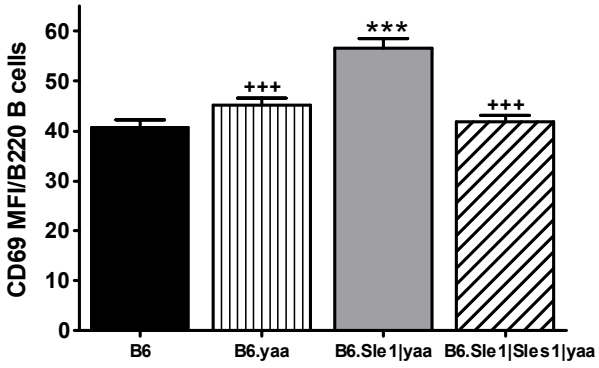

Fig. 24D

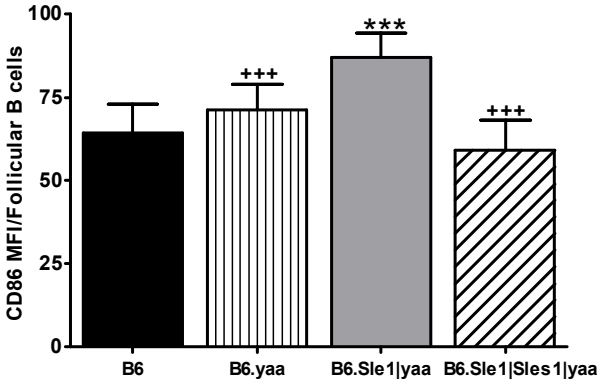

Figure 24. No Increase in Activated B Cells at 4-6 months in B6.*Sle1*|*Sles1*|*yaa*. Flow-cytometric analyses of splenocytes were performed to assay for changes in activation marker expression on B cells from 4-6 month old mice of the different strains. A-B. Representative histograms and cumulative data demonstrating the increased percentage of $CD69^+$ B220 B cells in B6.*Sle1*|*yaa* spleens, which was not observed in the presence of *Sles1*. Increased $CD69^+$ B cell percentages were also seen in B6.*yaa*. Shaded histograms- B6.*Sle1*|*yaa*; bold histogram- B6.*Sle1*|*Sles1*|*yaa*. C-D. Cumulative data demonstrating the lack of increased cell-surface expression (MFI) of CD69 (C.) and CD86 (D.) on $B220^+$ (C.) and follicular (D.) B cells from B6.*Sle1*|*Sles1*|*yaa* spleens. Symbols represent individual mice. Mean ± SEM. $^{**}p<0.01$, $^{***}p<0.001$ *vs.* B6; $^{+++}p<0.001$ *vs.* B6.*Sle1*|*yaa* (ANOVA).

Fig. 25A

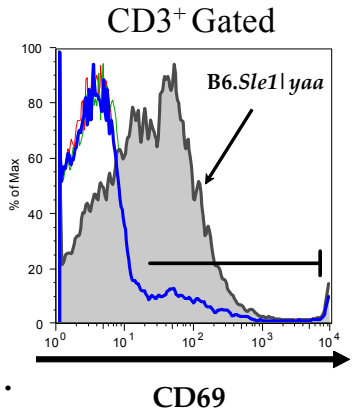

Fig. 25B

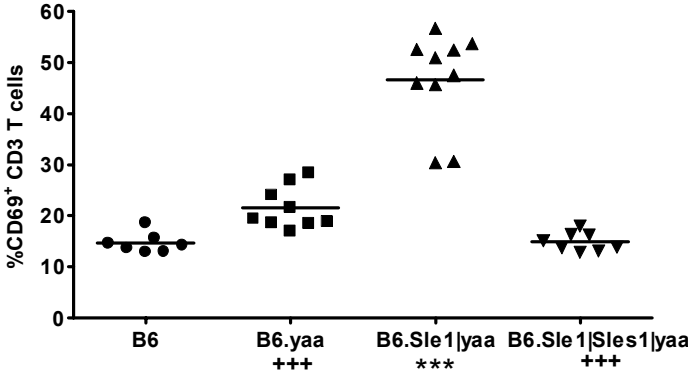

Fig. 25C

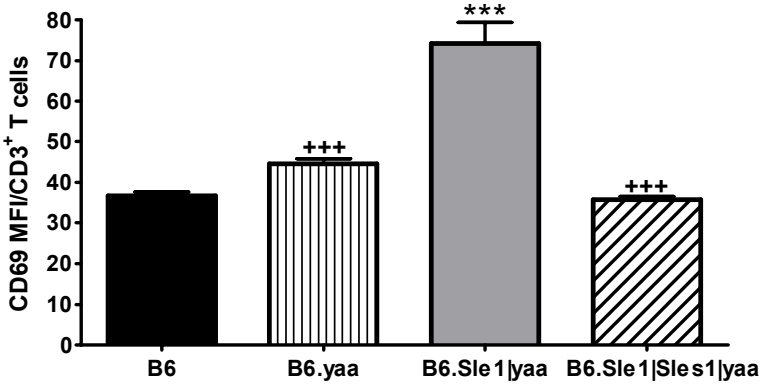

Fig. 25D

CD4+ Gated

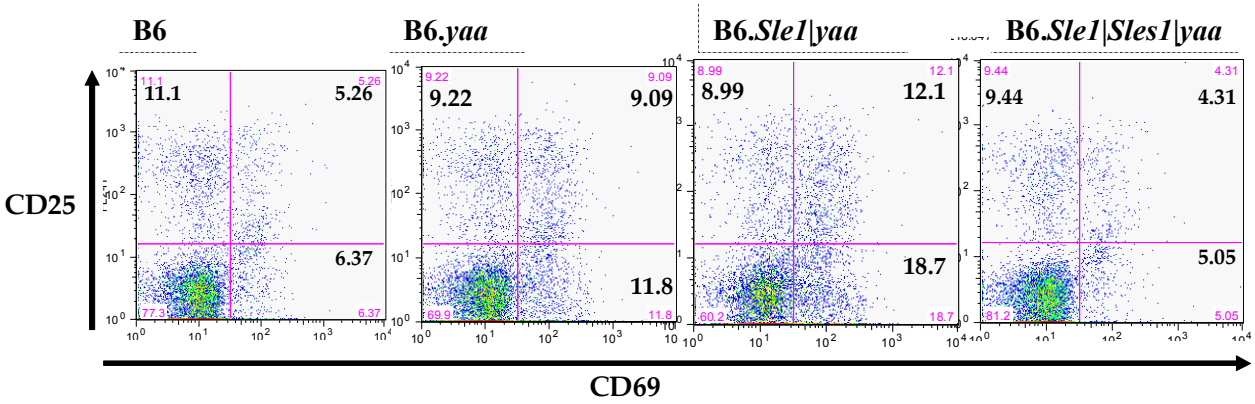

Fig. 25E

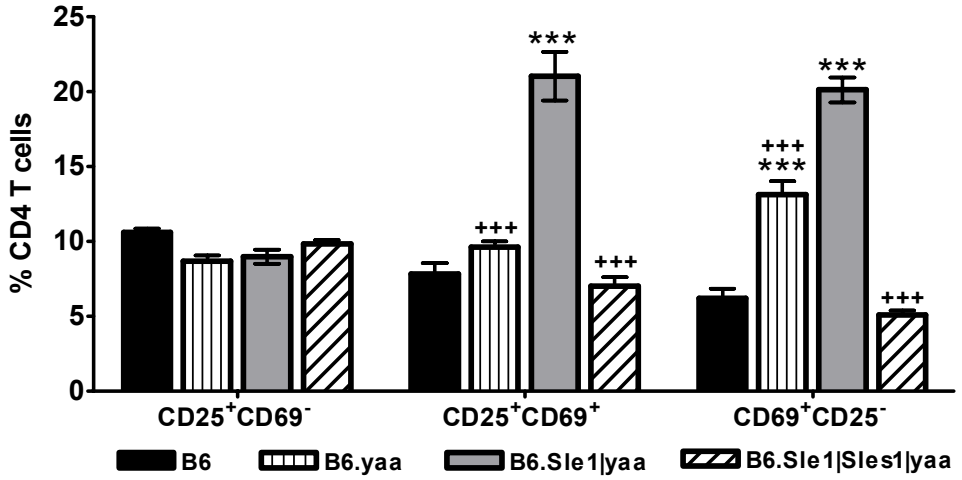

Figure 25. No Accumulation of Activated T Cells in 4-6 month old B6.*Sle1*|*Sles1*|*yaa* Spleens. Flow-cytometric analyses of splenocytes were performed to assay for changes in activation marker expression on T cells from 4-6 month old mice of the different strains. A-B. Representative histograms and cumulative data demonstrating the increased percentage of $CD69^+$ CD3 T cells in B6.*Sle1*|*yaa* spleens, which was not seen in B6.*Sle1*|*Sles1*|*yaa*. Shaded histograms- B6.*Sle1*|*yaa*; bold histogram- B6.*Sle1*|*Sles1*|*yaa*. C. Cumulative data demonstrating the lack of increased cell-surface expression (MFI) of CD69 on $CD3^+$ T cells from B6.*Sle1*|*Sles1*|*yaa* spleens. D-E. Representative dot-plots and cumulative data demonstrating the increased percentage of $CD69^+CD25^+$ and $CD69^+CD25^-$ CD4 T cells observed in B6.*Sle1*|*yaa* spleens, which was not observed in the presence of *Sles1*. An increased percentage of $CD69^+CD25^-$ CD4 T cells was seen in B6.yaa as well. Values in the quadrants in (C.) represent the percentage of that population within total CD4 T cells. Symbols represent individual mice. Mean ± SEM. $^{***}p<0.001$ *vs.* B6; $^{+++}p<0.001$ *vs.* B6.*Sle1*|*yaa* (ANOVA).

Fig. 26A

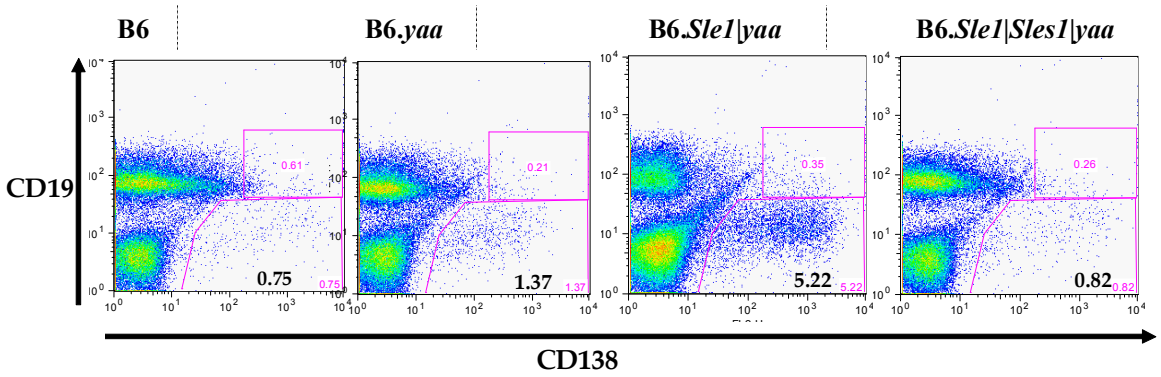

Fig. 26B

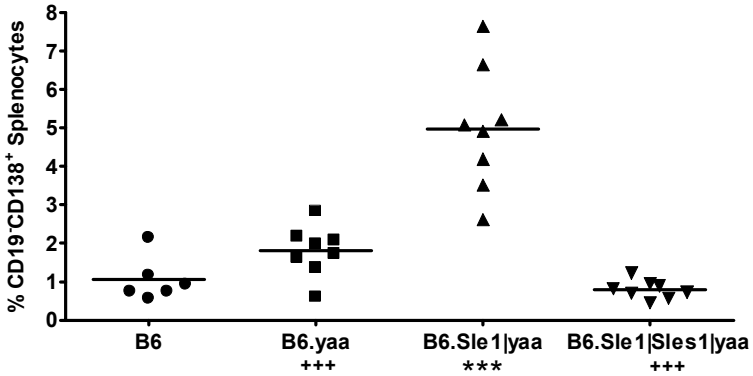

Fig. 26C

$CD4^+$ Gated

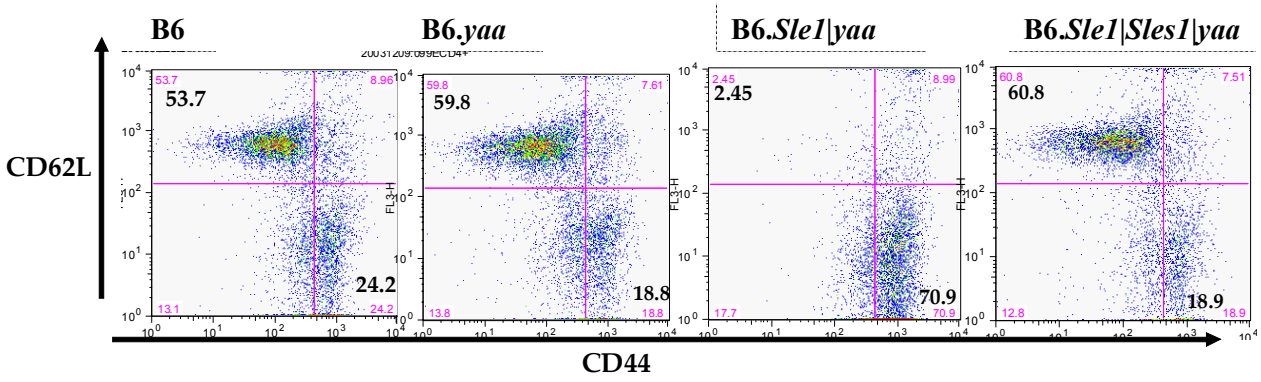

Fig. 26D

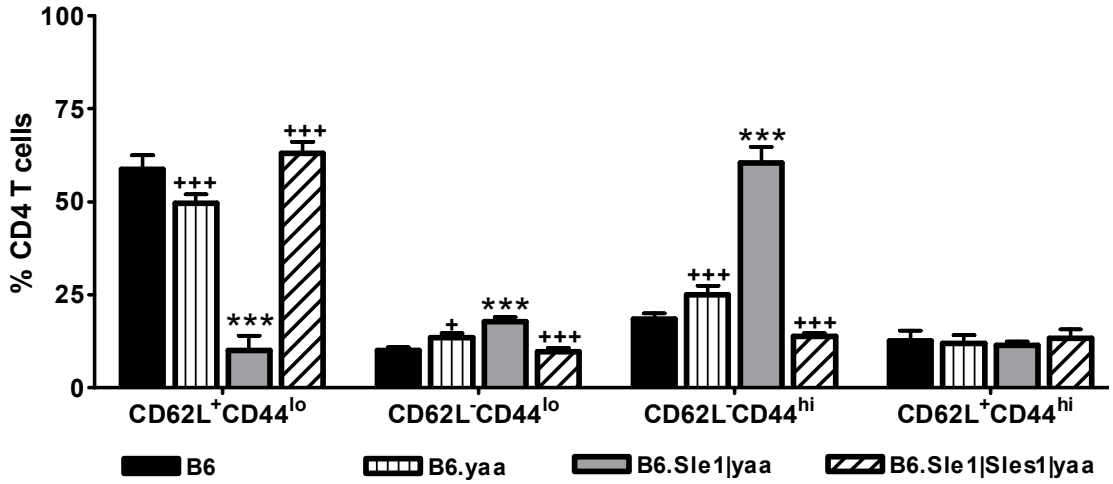

Figure 26. Accelerated B and T cell Differentiation Phenotypes Not Observed in B6.*Sle*|*Sles1*|*yaa* Spleens. Flow-cytometric analyses of splenocytes were performed to assay for changes in differentiation marker expression on B and T cells in 4-6 month old mice of the different strains. A-B. Representative dot-plots and cumulative data showing the increased accumulation of $CD19^{-}CD138^{+}$ plasma cells in B6.*Sle1*|*yaa* spleens, which was not observed in the presence of *Sles1*. Numbers in gates represent percentage of live cells. C-D. Representative dot-plots and cumulative data demonstrating that percentages of $CD62L^{+}CD44^{lo}$, $CD62L^{-}CD44^{lo}$ and $CD62L^{-}CD44^{hi}$ CD4 T cells are comparable to B6 in B6.*Sle1*|*Sles1*|*yaa* spleens. Values in the quadrants in (C.) represent the percentage of that population within total CD4 T cells. Symbols represent individual mice. Mean ± SEM. $^{***}p<0.001$ *vs.* B6; $^{+}p<0.05$, $^{+++}p<0.001$ *vs.* B6.*Sle1*|*yaa* (ANOVA).

Fig. 27A

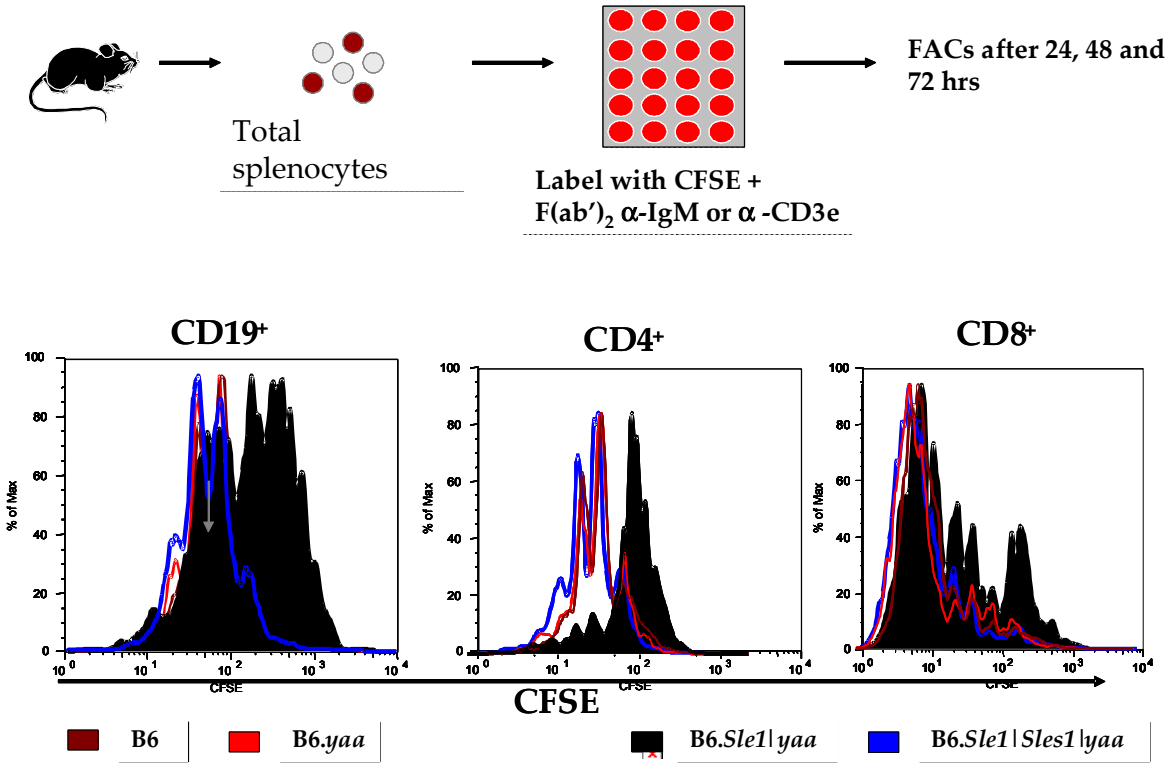

Fig.27B

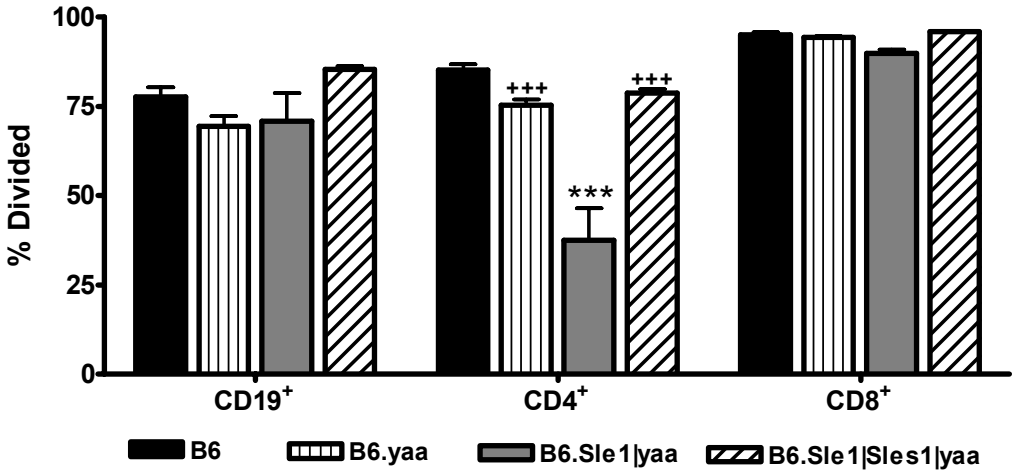

Fig. 27C

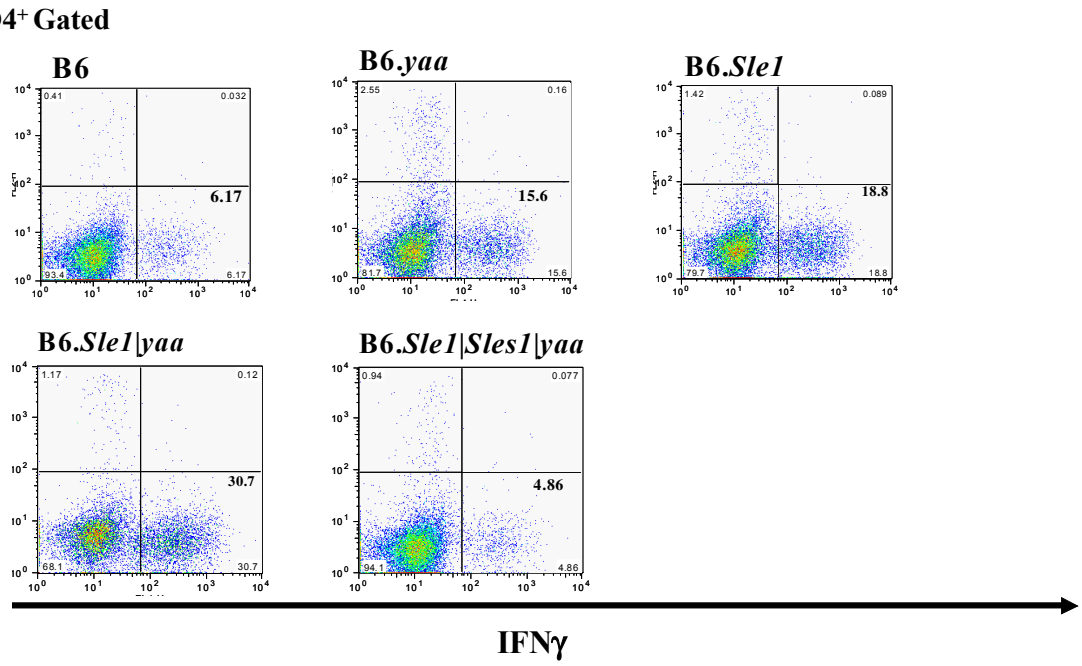

Fig. 27D

Figure 27. Normal Proliferative Response and IFNγ Production in B6.*Sle1*|*Sles1*|*yaa*. A-B. Splenocytes were labeled with CFSE and subjected to culture in the presence of αCD3 or αIgM. Harvested cells were stained with antibodies to CD19, CD4 and CD8 and analyzed by flow cytometry. C-D. Splenocytes, prestained with CD4, were stimulated for 4 hours with PMA and ionomycin in the presence of BD Golgi Stop. Cells were surface-stained, fixed, permeabilized and then stained with antibodies against IL-4 and IFNγ. B6.*Sle1*|*Sles1*|*yaa* cells did not show the increase in *ex vivo* IFNγ producing $CD4^+$ cells seen in B6.*yaa*, B6.*Sle1* and B6.*Sle1*|*yaa*. C. Representaive dot-plots. D. Cumulative data for 2 mice/genotype.

Values in the quadrants represent the percentage of that population within total CD4 T cells. $^{***}p<0.001$ *vs.* B6; $^{+++}p<0.001$ *vs.* B6.*Sle1*|*yaa* (ANOVA).

Fig. 28A

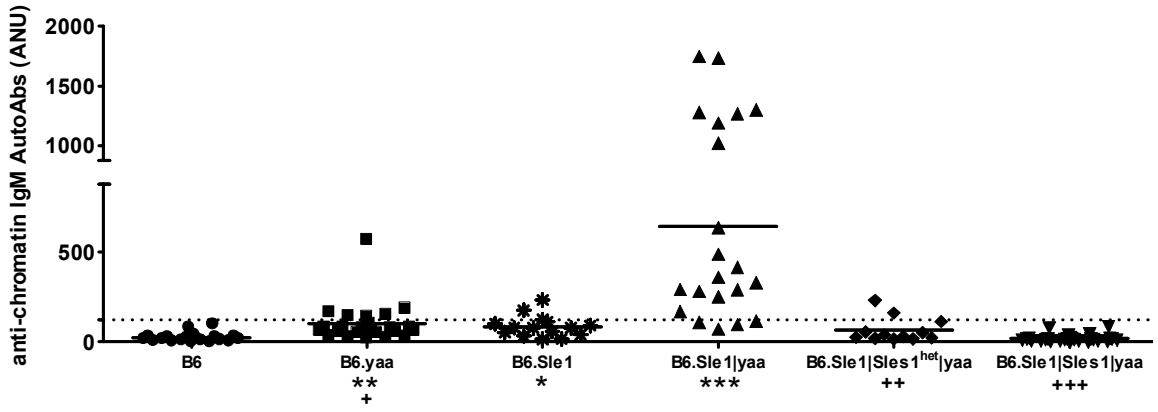

Fig. 28B

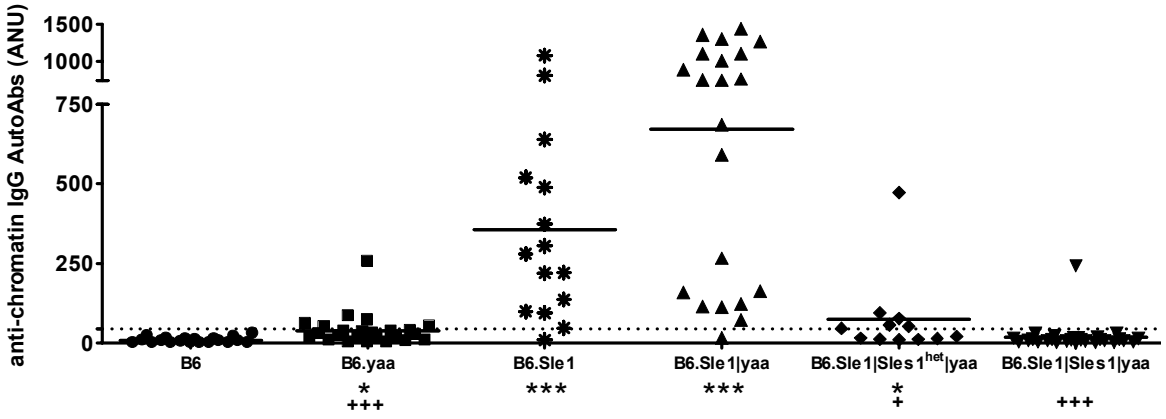

Figure 28. Long-term suppression of anti-chromatin autoAbs by *Sles1*. Serum levels of IgM and IgG anti-chromatin autoAbs were determined by ELISA for samples obtained at 4-6 months of age. Samples were assayed simultaneously, in duplicate, on plates coated in parallel to allow for interplate comparisons of mean titres. Samples were deemed positive if they exceeded the mean B6 value + 4SD. Dotted lines indicate the thresholds for being considered positive. A-B. Anti-chromatin IgM and IgG respectively. For both isotypes, B6.*Sle1|Sles1|yaa* was comparable to B6, while a highly significant increase relative to B6 controls was seen in B6.*Sle1|yaa* samples. B6.*yaa* and B6.*Sle1* showed increased titres as well. $^{*}p<0.05$, $^{**}p<0.01$, $^{***}p<0.001$ *vs.* B6; $^{+}p<0.05$, $^{++}p<0.01$, $^{+++}p<0.001$ *vs.* B6.*Sle1|yaa* (ANOVA).

Fig. 29A

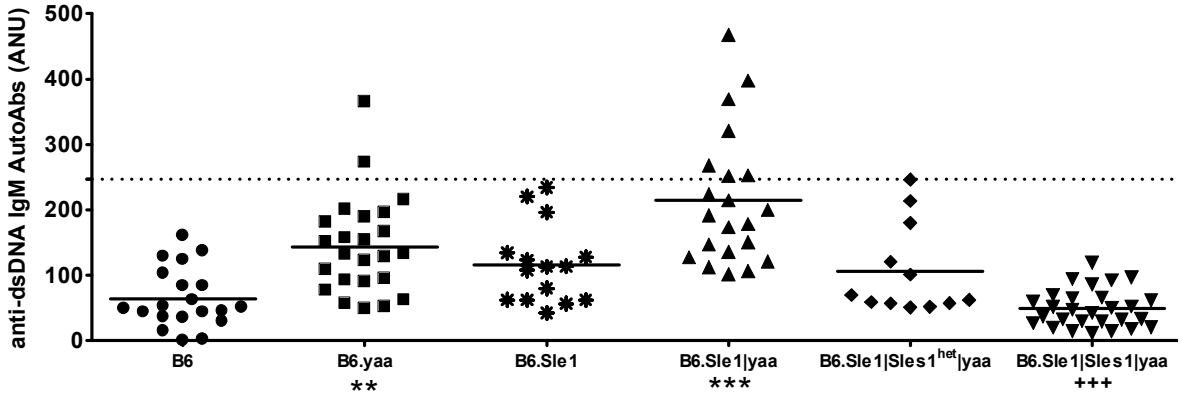

Fig. 29B

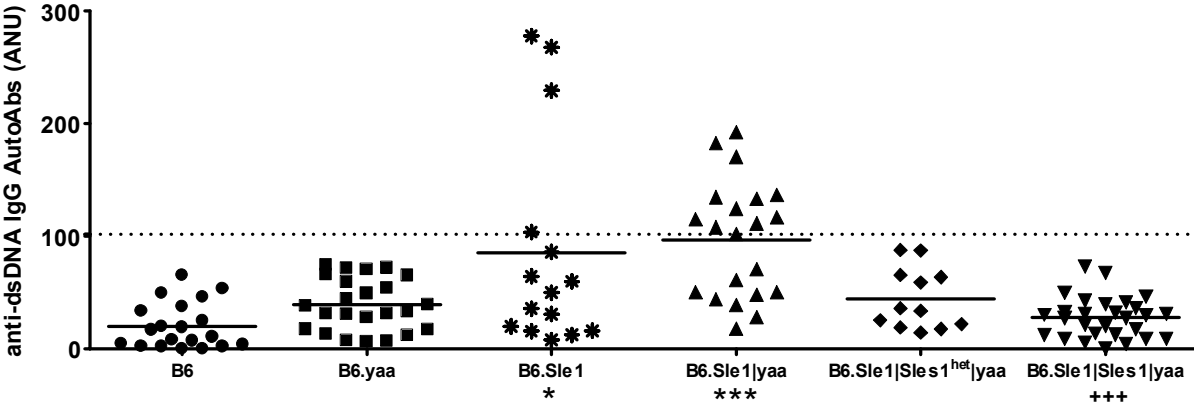

Figure 29. Suppression of anti-dsDNA autoAbs by *Sles1*. Serum levels of IgM and IgG anti-dsDNA autoAbs were determined by ELISA for samples obtained at 4-6 months of age. Samples were assayed simultaneously, in duplicate, on plates coated in parallel to allow for interplate comparisons of mean titres. Samples were deemed positive if they exceeded the mean B6 value + 4SD. Dotted lines indicate the thresholds for being considered positive. A-B. Anti-dsDNA IgM and IgG respectively. For both isotypes, while B6.*Sle1|Sles1|yaa* was comparable to B6, a highly significant increase relative to B6 controls was observed in B6.*Sle1|yaa* samples. B6.*yaa* and B6.*Sle1* showed increased titres of IgM and IgG respectively. $^{*}p<0.05$, $^{**}p<0.01$, $^{***}p<0.001$ *vs.* B6; $^{+++}p<0.001$ *vs.* B6.*Sle1|yaa* (ANOVA).

Fig. 30A

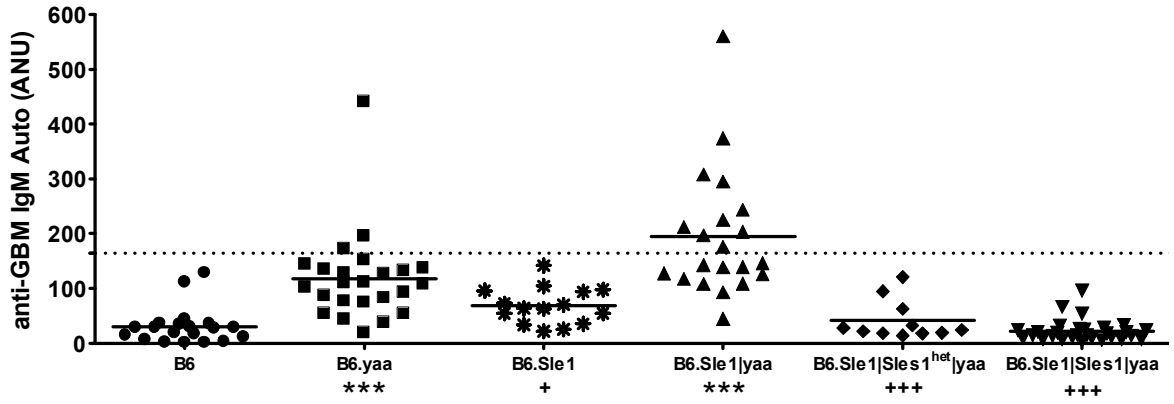

Fig. 30B

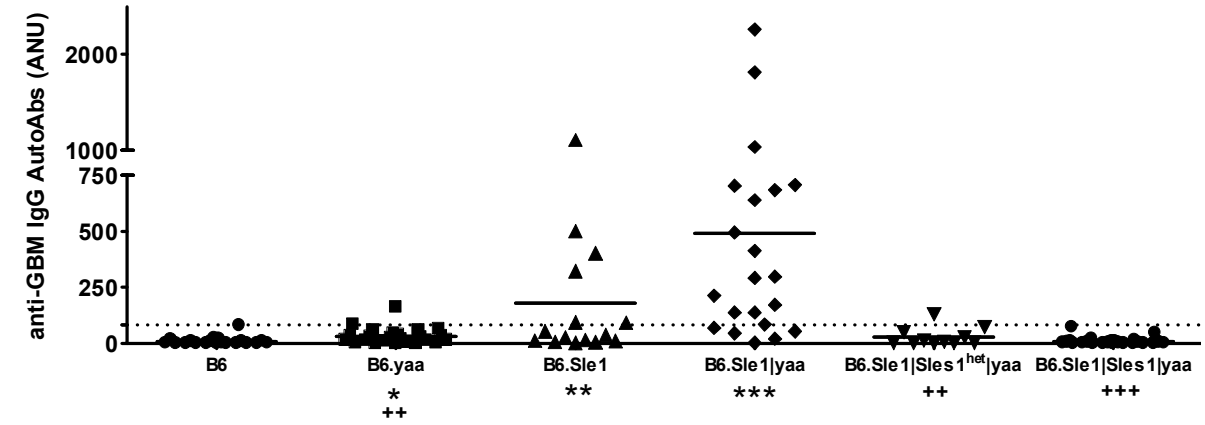

Figure 30. Suppression of anti-GBM autoAbs by *Sles1*. Serum levels of IgM and IgG anti-GBM autoAbs were determined by ELISA for samples obtained at 4-6 months of age. Samples were assayed simultaneously, in duplicate, on plates coated in parallel to allow for interplate comparisons of mean titres. Samples were deemed positive if they exceeded the mean B6 value + 4SD. Dotted lines indicate the thresholds for being considered positive. A-B. Anti-GBM IgM and IgG respectively. For both isotypes, B6.*Sle1|Sles1|yaa* was comparable to B6, while a highly significant increase relative to B6 controls was seen in B6.*Sle1|yaa* samples. B6.*yaa* and B6.*Sle1* showed increased titres as well. $^{*}p<0.05$, $^{**}p<0.01$, $^{***}p<0.001$ *vs.* B6; $^{+}p<0.05$, $^{++}p<0.01$, $^{+++}p<0.001$ *vs.* B6.*Sle1|yaa* (ANOVA).

Fig. 31A

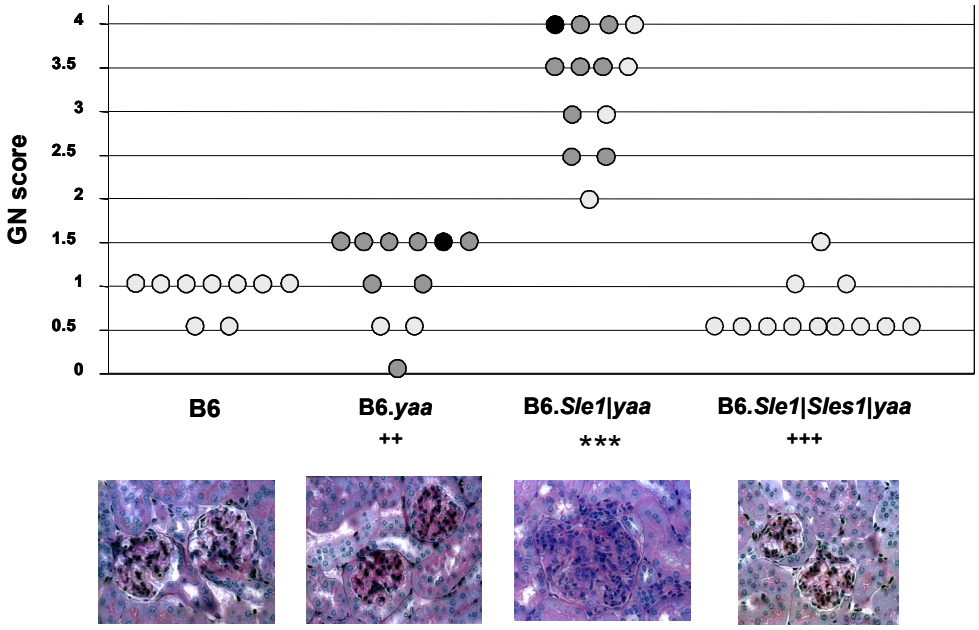

Fig. 31B

Fig. 31C

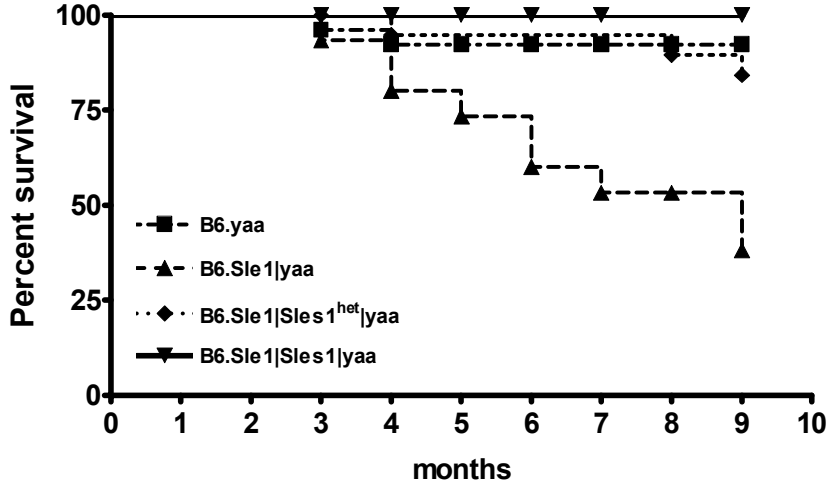

Figure 31. Mortality and Severe GN are Abrogated by *Sles1.* A-B. Kidneys were collected from the different mice at the time of sacrifice and fixed sections were examined for evidence of pathologic changes in the glomeruli, tubules or interstitial areas and glomerular lymphocyte infiltration, as detailed in Chapter II. A. Kidney sections from 4-6 month old mice. Neither GN nor lymphocyte infiltration was observed at this age in B6.*Sle1*|*Sles1*|*yaa*. Representative slides from each strain are shown below. B. Kidney sections from 9 month old mice. B6.*Sle1*|*Sles1*|*yaa* kidneys had significantly lower GN scores than B6.*Sle1*|*yaa*, with a very low incidence of lymphocyte infiltration. Scores: 0: normal 1: mild increase in mesangial cellularity, matrix 2: moderate increase in mesangial cellularity & matrix; thickening of GBM 3: focal endocapillary hypercellularity with substantial thickening &/ irregularity of GBM 4: Diffuse endocapillary hypercellularity, segmental necrosis, hyalinized end-stage glomeruli; Light gray: No lymphocyte infiltration, Dark gray: Mild lymphocyte infiltration Black: Moderate lymphocyte infiltration. C. 9-Month Survival Curves. In contrast to the 64% mortality seen in B6.*Sle1*|*yaa*, all 23 B6.*Sle1*|*Sles1*|*yaa* survived to 9 months. $^{***}p<0.001$ *vs.* B6; $^{++}p<0.01$, $^{+++}p<0.001$ *vs.* B6.*Sle1*|*yaa* (ANOVA).

Fig. 32

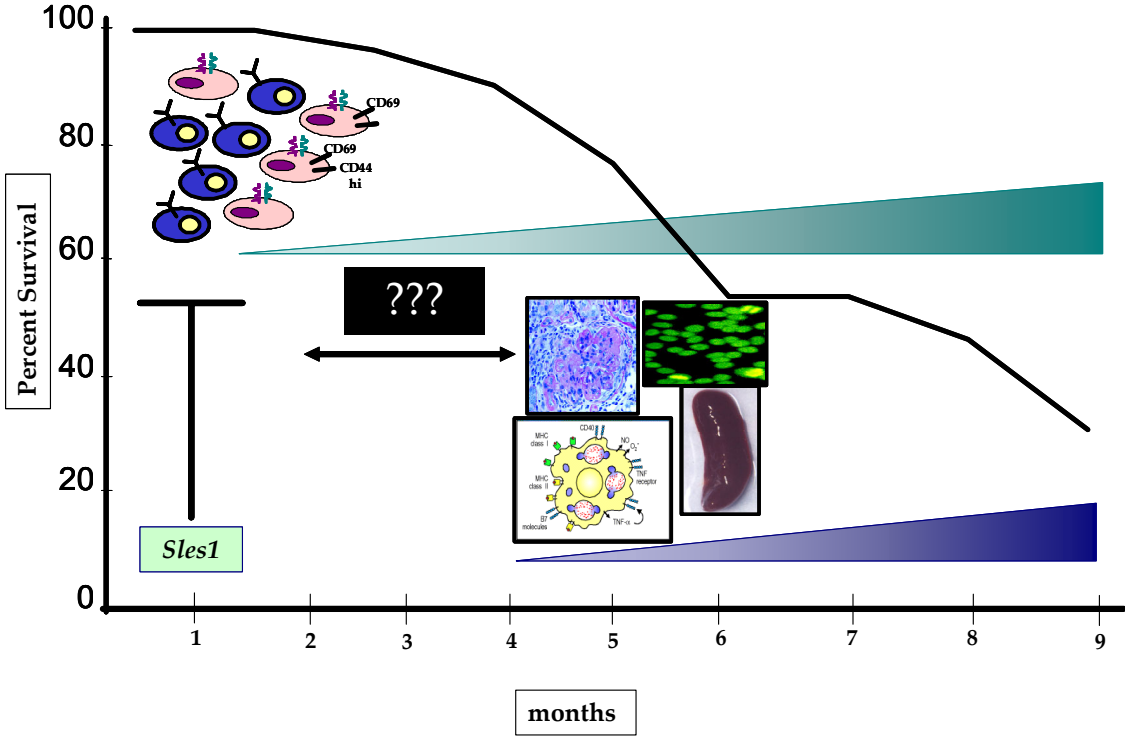

Figure 32. Schematic depicting the timecourse of autoimmunity in B6.*Sle1*\|*yaa* and the suppression mediated by *Sles1*.

Chapter V. Epistatic Suppression of SLE:

Partial Protective Effects Mediated by *Sles1*, *Sles2* and *Sles3*

Introduction

Genetic interactions, classically termed epistasis, have been shown to play a major role in the development and modulation of the systemic autoimmune disorder SLE. It has been postulated that autoimmune susceptibility may be a consequence of specific combinations of common alleles that dysregulate normal immune functions and responses (reviewed in (18)). Understanding how such susceptibility loci interact has been a major focus of research in multiple laboratories studying different animal models of lupus, and in addition, recent human genetic studies have begun to explore the combined impact of predisposing alleles in lupus patients (56, 59, 67, 83, 148, 157, 185, 186, 199, 200, 231, 240, 242, 252, 286).

Linkage analyses of the NZM2410 lupus-prone strain initially revealed the presence of three NZW-derived susceptibility intervals, *Sle1*, *Sle2* and *Sle3/5*, on chromosomes 1, 4 and 7 respectively, which were necessary and sufficient to reconstitute fatal lupus nephritis on the C57Bl/6 (B6) background (146, 201). Given the lack of fatal autoimmunity seen in the parental NZW strain, it was postulated that this could be due to the presence of epistatic modifiers in the NZW genome, which cumulatively suppress the development of lupus nephritis. Analyses of [B6.*Sle1* X NZW]F_1 X NZW backcross progeny, for linkage to GN and anti-dsDNA autoAbs, confirmed this hypothesis and revealed the existence of four such

suppressive modifiers termed the *Sles1-4* (*SLE suppressor*) loci on chromosomes 17, 4, 3 and 9 respectively (242).

These linkage studies indicated that: *Sles1* was strongly associated with suppression of both GN (LOD 10.9) and humoral autoimmunity (LOD 8.54); *Sles2* and *Sles3* had greater effects on humoral autoimmunity (LOD 3.07 and LOD 2.9 respectively) and *Sles4* had a male-specific effect on GN (LOD 2.14). In the backcross progeny, it was also shown that the number of active (NZW homozygous) *Sles* loci negatively correlated with the penetrance of GN and humoral autoimmunity. Furthermore, it was demonstrated by introgressing *Sles1* onto B6.*Sle1*, B6.*Sle2* and B6.*Sle3/5* that the suppression mediated by *Sles1* is specific for *Sle1* and has no effect on the phenotypes of *Sle2* and *Sle3/5* (242).

We have recently shown that *Sles1* maps to a ~956 KB region and, using genetic complementation tests, that the 129/SvJ strain appears to harbor a complementary suppressive allele (227). Furthermore, we have demonstrated that the introduction of *Sles1* onto the B6.*Sle1*|*yaa* lupus model completely abrogates the male-specific development of severe, highly penetrant systemic autoimmunity and related immunological abnormalities associated with this strain (Chapter IV). These data indicate that, in the right genomic context, *Sles1* can mediate a profound and complete suppression of systemic autoimmunity.

In this study, similar to the original studies with *Sles1*, we introduced the *Sles2* and *Sles3* loci onto the B6.*Sle1* model and compared the degree of humoral autoimmunity and related phenotypes elicited in these two bicongenic strains. We find that both *Sles2* and *Sles3* modulate the titres and penetrance of autoAb production normally observed in the B6.*Sle1* model, such that a partial suppressive effect is observed, and, consistent with the lower LOD

scores of the initial linkage study, these effects are much less than that observed previously for *Sles1* (227, 242).

In addition, we present evidence suggesting that the ability of *Sles1* to suppress autoimmunity is highly dependent on the nature of the additional loci interacting with its target locus, *Sle1*. We introgressed *Sles1* onto the B6.*Sle1*|*Sle2*|*Sle3/5* (B6.*TC*) lupus model and tested its ability to suppress the systemic autoimmunity observed in this strain. We find that, in contrast to the B6.*Sle1*|*yaa* lupus model, the introduction of *Sles1* does not prevent the development of autoimmunity, but instead appears to delay the kinetics and degree of disease. These data are consistent with the development of autoimmunity observed in the NZM2410 strain, which harbors the NZW *Sles1* allele, and indicate that *Sles1* is not a global suppressor of autoimmunity *per se*. These studies provide insights into the complex genetic interactions that mediate and modulate the development of systemic autoimmunity.

Results

Sles2 and Sles3 Impact the Kinetics and Degree of Humoral Autoimmunity Mediated by Sle1

Bicongenic strains bearing the suppressive modifier loci *Sles2* (~39.4 Mb) and *Sles3* (~33 Mb) on the B6.*Sle1* background were generated by marker assisted selection as described previously, using the markers described in Table 5 and illustrated in Fig.33 (327). Cohorts of female B6, B6.*Sle1*, B6.*Sle1*|*Sles2* and B6.*Sle1*|*Sles3* mice were aged and assayed for anti-chromatin IgG autoAbs at 4, 7 and 9-12 months of age by ELISA.

Fig.34A presents the mean (± SEM) titres from the various groups at the three different timepoints. In the case of the B6.*Sle1* mice, the anti-chromatin IgG autoAb titres differed significantly from B6 at all ages examined ($p < 0.01$; ANOVA), and in addition, demonstrated an age-dependent increase in the mean titres. Interestingly, the introduction of *Sles2* and *Sles3* resulted in decreased mean titres relative to B6.*Sle1* at all timepoints examined (Fig.34A). At 4 and 7 months, the mean anti-chromatin IgG titres in B6.*Sle1*|*Sles2* and B6.*Sle1*|*Sles3* mice differed significantly from B6.*Sle1*, but not from B6. By 12 months of age, however, the average titres for these two strains were intermediate between and significantly different from both B6 and B6.*Sle1*, as shown in Fig.34A (ANOVA). On the other hand, the mean titres of B6.*Sle1*|*Sles2* and B6.*Sle1*|*Sles3* were not statistically different from each other.

This same data is presented in Fig.34B, as a function of penetrance at each age. This is defined as the percent of mice having titres that exceeded the mean + 4SD of the age and gender-matched B6 controls assayed in these experiments. This method of analysis also

provides clear evidence of the suppression mediated by *Sles2* and *Sles3*. Somewhat surprisingly, the penetrance of the B6.*Sle1* positive controls were higher than what has been previously reported at these ages (153, 226). However, these results have been replicated in independent repeats of the same sample sets and this increase may hence be specific to the cohort of animals used in these studies.

These data demonstrate that both *Sles2* and *Sles3* significantly impact the humoral autoimmunity elicited by the *Sle1* locus on the B6 background at all ages examined. In contrast to *Sles1*, and consistent with their lower LOD scores, the suppression mediated by these loci is incomplete, but does appear to be maintained in ~25% of the animals until 12 months of age.

Sles2 and Sles3 Suppress Splenomegaly and Impact Cell-Surface Phenotypes

At the 12-month terminal sacrifice, spleens were weighed to assess for suppression of the mild splenomegaly observed in aged B6.*Sle1* mice. As shown in Fig.35A, in accordance with previous reports, the average spleen from a 9-12 month old B6.*Sle1* mouse weighed approximately twice as much as that of age and gender-matched B6 controls (235.4 ± 16.8 mg *vs.* 113.2 ± 4.14 mg; $p<0.001$, ANOVA) (153, 226). In contrast, B6.*Sle1*|*Sles2* and B6.*Sle1*|*Sles3* mice had intermediate spleen weights (149.4 ± 13.92 mg and 158.9 ± 27.59 mg, respectively), which differed significantly from B6.*Sle1* ($p<0.001$ and $p<0.05$ respectively; ANOVA) but not from B6 or each other.

We have previously shown that the humoral autoimmunity mediated by the *Sle1* locus on the B6 background is accompanied by an age-associated increase in cell-surface

activation markers on splenic B and T lymphocytes, indicative of a chronically activated immune system. In order to determine whether these phenotypes are impacted by the presence of the suppressive modifiers *Sles2* and *Sles3*, we performed preliminary flow cytometric analyses of splenocytes from 12-month old mice.

An increase in the percentage of splenic B and CD4 T cells expressing the early-activation marker CD69 is a consistent and relatively robust phenotype observed in aged B6.*Sle1* mice. As shown in Fig.35B-C, both B220 B and CD3 T cells from B6.*Sle1*|*Sles2* mice showed an increase in the percentage of cells expressing CD69, relative to control B6 samples ($p<0.05$ and $p<0.01$ respectively; ANOVA). While these p values are less significant that what was observed for B6.*Sle1* mice, in particular for the B cells, it does suggest that a portion of the lymphocytes remain activated in these mice. Further investigation of the CD4 T cell population for distribution of the activation markers CD25 and CD69 (Fig.35D), revealed no significant differences in the activation status of the CD4 T cells in B6.*Sle1*|*Sles2 vs.* B6.*Sle1*. Statistical results are not indicated for the B6.*Sle1*|*Sles3* mice, as only three mice have been analyzed, which is insufficient for ANOVA testing. The preliminary data from these three mice does however suggest increased lymphocyte activation *vs.* B6 and a reduction *vs.* B6.*Sle1*, particularly in the CD4 population. Further mice will have to be analyzed for both genotypes in order to make any definitive conclusions.

These data demonstrate that *Sles2* and *Sles3* mediate a partial suppression of the humoral autoimmunity and splenomegaly elicited by *Sle1*, such that both these phenotypes are intermediate between what is normally observed in B6 and B6.*Sle1* mice at this age (153, 226). While the flow-cytometric analyses of spleens from these mice remain incomplete, the

data generated thus far suggest that, consistent with the partial suppression seen for humoral autoimmunity and splenomegaly, the various lymphocyte activation phenotypes are also partially modulated in the presence of *Sles2* and *Sles3*.

Sles1 Mediates a Reduction in the Degree and Penetrance of Humoral Autoimmunity in the B6.TC Lupus-Prone Mouse

It has been previously shown that *Sle1* is necessary for the reconstitution of severe lupus nephritis observed in the B6.*Sle1*|*Sle2*|*Sle3/5* (triple congenic; B6.*TC*) lupus model, perhaps due to the fact that *Sle1* interacts epistatically with both *Sle2* and *Sle3/5*, while in contrast, the interaction between *Sle2* and *Sle3/5* appears non-epistatic (201, 240). Also, as described earlier, it has been demonstrated that *Sles1* specifically suppresses the humoral autoimmunity elicited by the *Sle1* locus on the B6 background, but has no effects on the phenotypes mediated by the *Sle2* and *Sle3/5* loci (242). Given these different potentiating and suppressive epistatic interactions seen between the different *Sle* and *Sles* loci on the B6 background, we wished to test whether the introduction of *Sles1* has any effect on the systemic autoimmunity seen in the TC lupus model. We hence introduced *Sles1* onto the TC lupus-model using marker-assisted selection, as described in Chapter II.

Cohorts of female B6.*Sle1*|*Sle2*|*Sle3/5* (B6.*TC*) and B6.*Sle1*|*Sle2*|*Sle3/5*|*Sles1* (quadruple congenic; B6.*QC*) mice were aged to 12 months and assayed for anti-chromatin and anti-dsDNA IgG autoAbs at 4, 7 and 9-12 months of age by ELISA. B6 and B6.*Sle1* age and gender-matched serum samples were used as negative and positive controls respectively. As shown in Fig.36A, both B6.*Sle1* and B6.*TC* had higher mean titres of anti-chromatin IgG

autoAbs *vs.* B6 at all timepoints tested ($p<0.001$ for both at all ages; ANOVA). Interestingly, starting at 7 months, B6.*TC* samples had significantly higher mean titres relative even to B6.*Sle1* ($p<0.01$ at 7 and $p<0.001$ at 9-12 months; ANOVA). In contrast, B6.*QC* samples had mean titres intermediate between B6 and B6.*Sle1* at both 4 and 7 months and were not significantly different from either group (ANOVA). By 12 months, the overall mean titre increased in the B6.*QC* samples such that they did not differ signficantly from B6.*Sle1*, but were significantly more and less than B6 and B6.*QC* samples respectively ($p<0.001$ for both; ANOVA).

This same data is presented in Fig.36B as a function of penetrance. In accordance with the reduced mean titres at the different ages, the percentage of positive samples of the B6.*QC* genotype was less than that seen in both B6.*Sle1* and B6.*TC* at 4, 7 and 9-12 months. These data demonstrate that the introduction of *Sles1* significantly affects both the mean titre and penetrance of anti-chromatin IgG autoAbs at all ages tested.

We also compared the levels of anti-dsDNA IgG autoAbs between the various genotypes at different ages, as shown in Fig.37A. At 4 months of age, B6.*TC* samples had significantly higher mean titres of these autoAbs than B6, B6.*Sle1* and B6.*QC* ($p<0.001$, $p<0.05$ and $p<0.05$ respectively, ANOVA). At 7 months of age, while both B6.*TC* and B6.*Sle1* had increased mean titres relative to B6 ($p<0.001$; ANOVA), B6.*QC* did not differ significantly from any group. In contrast, at 9-12 months of age both B6.*TC* and B6.*QC* had significantly increased titres of anti-dsDNA IgG autoAbs relative to B6. These data were not as consistent between the different genotypes at the various ages as was observed with the titres of anti-chromatin IgG autoAbs. The most uniform differences seen here were for the

B6.*TC* samples, which had an increased mean anti-dsDNA titre relative to all the groups at all ages, though this value only reached significance *vs.* B6 consistently. Importantly, B6.*QC* did not appear to follow the same pattern of increased titres with age as B6.*TC*, and did not differ significantly from B6 until 12 months of age (Fig.37A).

Differences are also seen in the penetrance of anti-dsDNA IgG autoAbs when B6.*QC* is compared to B6.*TC*, as shown in Fig.37B. B6.*Sle1* had a low penetrance of anti-dsDNA autoAb positive mice, which reached roughly 12% by 9-12 months of age. Consistent with previous reports and the increased severity of systemic disease, B6.*TC* had a high penetrance of positive mice, which was evident as early as 4 months of age and reached ~67% by 9-12 months (201). In contrast, the onset and development of highly penetrant anti-dsDNA autoAbs appears delayed in B6.*QC*, as evidenced by the fact that only at 9-12 months did the penetrance increase in the B6.*QC* strain, and even then was lower than that observed in B6.*TC* at 4 months of age (Fig.37B).

These data demonstrate that the introduction of *Sles1* appears to delay the kinetics and decrease the severity of autoAb production normally observed in the B6.*TC* strain, without completely abrogating these phenotypes altogether. This is in contrast to what we have observed in the B6.*Sle1*|*Sles1*|*yaa* model (Chapter IV) and suggests that the ability of *Sles1* to suppress humoral autoimmunity is highly dependent on the additional loci interacting with its target locus *Sle1*.

Sles1 Does Not Suppress Splenomegaly But Impacts Cell-Surface Phenotypes

Measurement of spleen weights from the different mice post-sacrifice at 9-12 months of age revealed that while B6.*Sle1*, B6.*TC* and B6.*QC* all had increased spleen sizes relative to B6 ($p<0.001$; non-parametric ANOVA), these three genotypes did not differ significantly from each other (Fig.38A). This indicates that the introduction of *Sles1* does not significantly impact the splenomegaly normally elicited in the B6.*TC* mice (201). However, it is possible that examination of the spleen weights at earlier ages may have revealed differing kinetics, similar to what was observed for autoAb production in the B6.*QC* mice.

Flow-cytometric analyses of splenocytes and BM cells were performed in order to determine whether changes in different immune cell populations, normally observed in aged B6.*TC* mice, are modified by the introduction of *Sles1*. Analyses of BM B cell precursor populations revealed comparable percentages between B6, B6.*TC* and B6.*QC*. In the spleen, comparable splenic B cell development was observed for both B6.*TC* and B6.*QC* mice, as well as normal percentages of $CD19^+$, $CD4^+$, $CD8^+$ and $CD11b^+$ cells. The major changes observed between the B6.*TC* and B6.*QC* groups were in various activation phenotypes and in splenic plasma B cell differentiation, as described below.

As shown in Fig.38B, both B6.*Sle1* and B6.*TC* mice displayed an increased percentage of $CD3^+$ T cells expressing the early activation marker CD69 *vs.* B6 ($p<0.001$ for both; ANOVA). In addition, both groups had greater cell-surface expression of CD69 on $CD3^+$ T cells, as evidenced by increased MFIs relative to B6 (Fig.38C) ($p<0.001$ for both; ANOVA). In contrast, B6.*QC* mice had reduced percentages of $CD69^+$ CD3 T cells compared to both B6.*Sle1* and B6.*TC* ($p<0.001$ for both; ANOVA) (Fig.38B). A small increase in CD69 cell-surface expression on $CD3^+$ T cells was observed in B6.*QC* mice

relative to B6 ($p<0.05$; ANOVA), but compared to B6.*TC* samples, there was a significant decrease ($p<0.01$; ANOVA) (Fig.38C). Similar to what was observed in the analyses of $CD3^+$ T cells, there was an increased percentage of activated CD4 T cells ($CD69^+CD25^+/CD69^+CD25^-$) in B6.*Sle1* and B6.*TC*, as depicted in Fig.38D ($p<0.01$; ANOVA). While there was no change in the percentage of $CD69^+CD25^+$ CD4 T cells between B6.*QC* and the other groups, an increase relative to B6 but a decrease compared to B6.*TC* was observed for the $CD69^+CD25^-$ CD4 population ($p<0.01$ for both; ANOVA). Interestingly, an increased proportion of $CD25^+CD69^-$ CD4 T cells in B6.*QC* mice were seen relative to B6.*TC* ($p<0.01$; ANOVA), with no differences in this population occurring between the other groups (Fig.38D).

Like the T cell compartment, the percentage of $CD69^+$ B220 B cells was increased in both B6.*Sle1* and B6.*TC* relative to B6 at 9-12 months of age ($p<0.001$ and $p<0.01$ respectively; ANOVA) (Fig.38E). This phenotype was not observed in the presence of *Sles1*, such that the percentage of activated B cells in the B6.*QC* group was significantly less than that in both B6.*Sle1* and B6.*TC* ($p<0.001$ *vs.* both), but comparable to that seen in B6, as shown in Fig.38E. Somewhat surprisingly, given the humoral autoimmunity seen in the B6.*QC* strain with age, there are less splenic plasma cells ($CD19^-CD138^+$) relative to both B6.*Sle1* and B6.*TC*, as shown in Fig.38F (ANOVA). Both B6.*Sle1* and B6.*TC* showed a mild increase relative to B6 in this population ($p<0.05$; ANOVA).

These data illustrate that even though introduction of *Sles1* onto the B6.*TC* model does not completely prevent the development of humoral autoimmunity, it does however, significantly impact the degree of activated lymphocytes normally observed in this lupus-

prone strain. This is in contrast to what has been observed in other spontaneous lupus-prone models where the phenotypes of lymphocyte activation and humoral autoimmunity are closely correlated, especially as the mice are aged. This suggests that the B6.*QC* model could provide insight into dysregulated pathways leading to autoimmunity in the absence of a chronically activated lymphocyte population.

Increased Survival but Comparable GN in the Presence of Sles1

As shown in Fig.39A, introduction of *Sles1* increased the 9-month survival observed in the B6.*TC* animals used in this study from 55.6% to 95% ($p=0.0064$; log-rank test). Given this increased survival, it is interesting to note that the average GN scores between B6.*TC* and B6.*QC* are comparable, with mean scores of 2.5 (Fig.39B). The similar degree of GN between these two groups is hence perhaps more reflective of the similar degree of anti-dsDNA IgG autoAbs seen at this age. These data may also be skewed due to the increased mortality seen in the B6.*TC* mice, wherein the mice having severe GN (score ≥ 3) would have been the ones that died, thus enriching for mice with less severe GN.

Discussion

The results of these studies illustrate the different effects modifier loci can have on the phenotypic expression of potent susceptibility loci. In addition, we demonstrate that the degree of suppression can be highly dependent on the specific combination of susceptibility loci present, similar to the background genome effect on phenotypes seen in many gene-targeted lupus models.

Sles1, *Sles2* and *Sles3* were originally identified in a linkage-analysis designed to identify loci that prevented the development of lupus nephritis in the NZW mouse strain. While the LOD scores for the *Sles2* and *Sles3* loci were relatively weak, especially when compared to *Sles1*, multivariate analyses of disease penetrance did suggest a significant role for these latter two loci as well in the lack of humoral autoimmunity in the NZW mouse. Those initial studies also revealed, using different bi-congenic systems, that *Sles1* specifically suppresses the effects mediated by the *Sle1* locus on the B6 background, and does not appear to impact the phenotypes seen in B6.*Sle2* and B6.*Sle3/5* mice (242). The impact of *Sles2* and *Sles3* on component phenotypes in isolated bi-congenic models was not addressed in these original analyses.

Hence, in order to characterize the consequences of *Sles2* and *Sles3* on the phenotypes mediated by the *Sle1* locus on the B6 background, bi-congenic mice were generated and characterized for suppression of these different *Sle1* phenotypes. To test for effects on humoral autoimmunity, cohorts of B6, B6.*Sle1*, B6.*Sle1*|*Sles2* and B6.*Sle1*|*Sles3* female mice were aged and bled at 4, 7 and 9-12 months of age and the sera analyzed by ELISA for anti-chromatin IgG autoAbs. In terms of penetrance and mean titres, clear effects

were seen in the presence of *Sles2* and *Sles3.* In both bi-congenic strains, a significant reduction was observed in mean titres at all ages tested, relative to B6.*Sle1*. Similar results were also noted for the overall penetrance of autoAb production. Significantly, the effects of *Sles2* and *Sles3* were greatest at the younger timepoints, suggesting that stochastic events impact the likelihood of autoAb production in these mice as they age. In addition, the mean spleen weights from the two bi-congenic strains were intermediate between B6 and B6.*Sle1*, but differed significantly only from B6.*Sle1*. We can hence conclude that *Sles2* and *Sles3* can alter the kinetics and degree of humoral autoimmunity and mediate a reduction in the average spleen weight when combined with *Sle1* on the B6 background.

The data regarding modulation of lymphocyte activation remains much more inconclusive, especially given the fact that only three B6.*Sle1*|*Sles3* mice have so far been analyzed. The existing data does however suggest that *Sles2* has a greater effect on reducing the percentage of activated B cells than it does on T cells (Fig.35B-D). Even though a relatively large sample size of B6.*Sle1*|*Sles2* animals have been examined (n=9), larger numbers may still be required in order to draw meaningful conclusions.

In these studies, we also examined the effects of the introduction of *Sles1* onto the lupus-prone B6.*TC* strain. This model (B6.*QC*) combines the most potent susceptibility loci identified in NZM2410 (*Sle1*, *Sle2* and *Sle3/5*) with the most potent suppressive modifier locus found in NZW, *Sles1* (146, 242). ELISA analyses for anti-chromatin and anti-dsDNA IgG autoAbs was conducted on serum samples from mice of 4, 7 and 9-12 months of age, Comparison of the two strains, B6.*TC* and B6.*QC*, revealed decreased titres and penetrance of both these IgG autoAbs in the presence of *Sles1* at all ages examined. Similar to what was

observed in the B6.*Sle1*|*Sles2* and B6.*Sle1*|*Sles3* studies, the suppressive effect of *Sles1* appeared greatest at the younger ages, again implicating stochastic factors in the development of humoral autoimmunity.

No difference was observed in the degree of splenomegaly seen between the B6.*TC* and B6.*QC* animals, but similar to what was observed for humoral autoimmunity, a comparison of younger mice may have revealed greater variation between the two groups. Despite no significant differences in the severity of GN between these two groups, B6.*QC* animals had significantly increased survival. As mentioned earlier, this may be a consequence of enrichment for lower GN scores in the B6.*TC* group, due to their greater mortality.

Flow-cytometric analyses of different cell populations revealed that there was significant reduction in the percentage of activated B and T lymphocytes and splenic plasma cells in B6.*QC* mice relative to B6.*TC*. Interestingly, there was an increase only compared to B6.*TC* in the $CD25^{+}CD69^{-}$ CD4 population in B6.*QC* mice. The significance of this reduced population in B6.*TC* mice, which has the cell-surface characteristics of the regulatory CD4 T cell population, remains unclear. While a large number of B6.*QC* mice (n=19) were analyzed, due to the increased mortality in the B6.*TC* strain, only five animals from this group were left for analysis. In order to get a better idea of the differences in different splenic populations between these two strains, it may be instead necessary to perform these analyses on mice of a slightly younger age (7-8 months) with more equivalent sample sizes. Nonetheless, these data do demonstrate that *Sles1* has a partial suppressive effect on the different autoimmune phenotypes assayed in these studies. The fact that the effect is incomplete is consistent with

the fact that, as has been shown previously, *Sles1* has no effect on the phenotypes of *Sle2* and *Sle3/5* (242). Hence, it may be that while *Sles1* is able to impinge upon some of the pathways *Sle1* modulates, it cannot influence those pathways that are affected by the epistatic interactions of *Sle1* with *Sle2* and *Sle3/5*, thus resulting in the partial reduction in the different autoimmune phenotypes.

These studies also illustrate that there are some important factors to consider when studying such partially suppressed phenotypes. Since, for any given phenotype, the ranges of the experimental values are increased, due to the partial modulatory effect, the standard deviations are much larger than what is observed in the positive and negative control strains. This reduces the power of statistical comparisons and greatly increases the number of samples that must be analyzed in order to make meaningful comparisons. This also makes the effects of experiment-to-experiment variation highly magnified. In the case of analyzing autoAb titres by ELISA, systematic experimental variation can be overcome by the fact that sera collected on different days can be stored and assayed simultaneously, as done in these studies. Since spleen weights are an absolute measurement, this phenotype is also less affected by such experimental variations.

However, flow-cytometric analyses appear particularly sensitive to small differences between experiments, since the phenotypes being measured are themselves only slightly modulated by the suppressive loci. Such difficulties were also noted in studies using B6 BAC (Bacterial Artificial Chromosome) transgenic animals to look for suppression of the phenotypes mediated by the endogenous *Sle1b* locus (N. Limaye *et al.*, *unpublished results*). Furthermore, it can be difficult to get appropriate numbers of age and gender-matched

animals from multiple strains. Hence, the flow-cytometric assays are performed with different sub-groups of strains on different days. Even in the presence of appropriate negative, non-autoimmune controls, these experimental differences combined with the inherent biological variation can make it difficult to make any definitive conclusions. Also, due to the fact that these phenotypes may differ significantly at various ages, the range of time within which these assays can be performed and compared becomes limiting as well. These are important caveats to consider when studying the effects of partial immunomodulatory loci.

These studies demonstrate that *Sles2* and *Sles3* can modulate various phenotypes associated with *Sle1*, but most importantly the potent humoral autoimmunity elicited by this locus. The next challenge will be to fine-map these two loci, which should prove quite complicated and will require large numbers of progeny based on their partial suppressive effects. While such efforts may prove quite complicated and cumbersome, they could provide insight into alleles having potent and specific immunomodulatory functions. It would also be interesting to determine whether a greater, longer-lasting effect on suppression of autoAb production would be obtained if these two loci were combined together on the B6.*Sle1* background. Furthermore, we show that the ability of *Sles1* to suppress systemic autoimmunity is highly dependent on the nature of the additional susceptibility loci interacting with *Sle1*, as evidenced by the complete suppression seen in the B6.*Sle1*|*Sles1*|*yaa* model (Chapter IV) *vs.* the partial suppression seen in the B6.*QC* system, described here. These data provide insight into the complex genetic interactions that influence the development of systemic autoimmunity.

Fig. 33

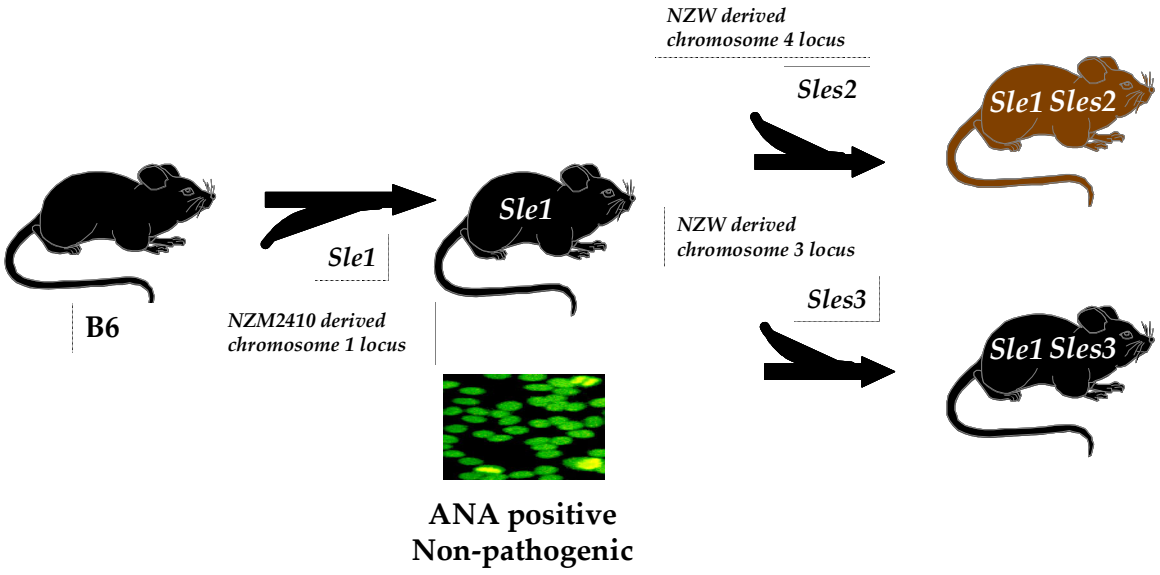

Figure 33. Schematic Depicting the Generation of B6.*Sle1*|*Sles2* and B6.*Sle1*|*Sles3* Mice.

Fig. 34A

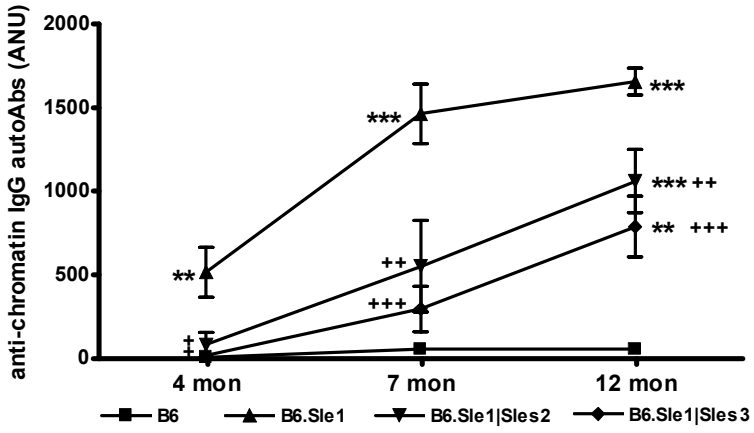

Fig. 34B

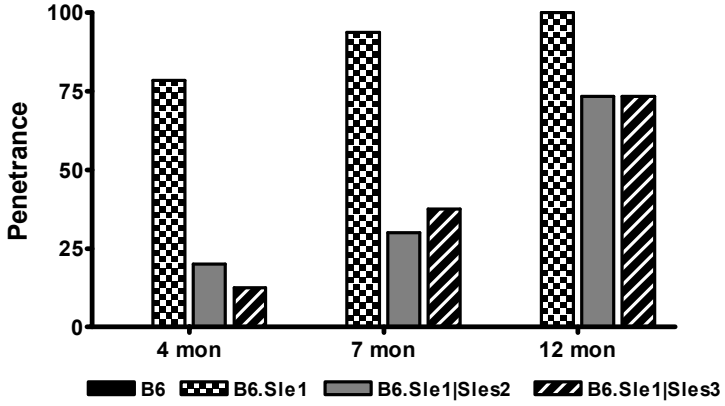

Figure 34. Reduced Mean Titres and Penetrance of anti-chromatin IgG autoAbs in the Presence of *Sles2* and *Sles3* at All Ages. Serum levels of IgG anti-chromatin autoAbs were determined by ELISA for samples obtained at 4, 7 and 9-12 months of age. Samples were assayed simultaneously, in duplicate, on plates coated in parallel to allow for interplate comparisons of mean titres. Samples were deemed positive if they exceeded the mean B6 value + 4SD. A. Comparison of mean titres and B. Comparison of penetrance of autoAb production between the different strains at 4, 7 and 9-12 months of age. ** *p<0.01,* ****p<0.001 vs.* B6; $^{+}$*p<0.05*, $^{++}$ *p<0.01,* $^{+++}$*p<0.001 vs.* B6.*Sle1* (ANOVA). n = 8-25 /genotype/timepoint.

Fig. 35A

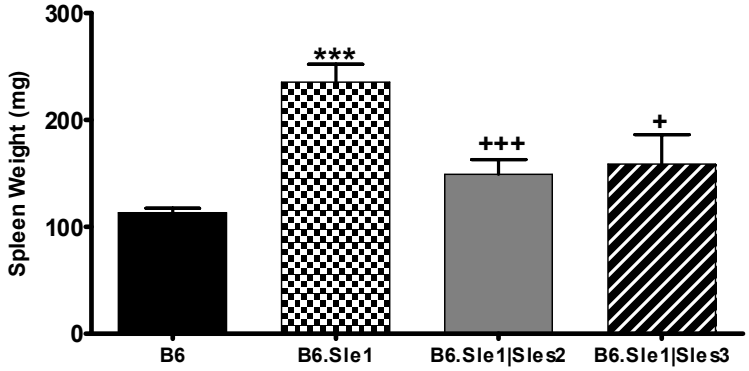

Fig. 35B

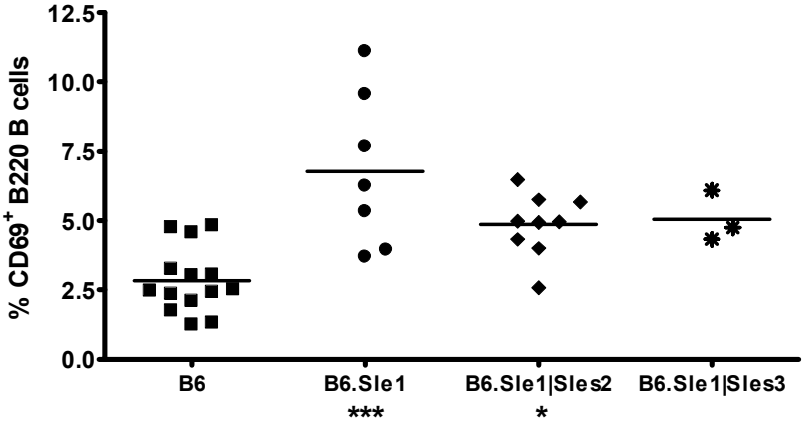

Fig. 35C

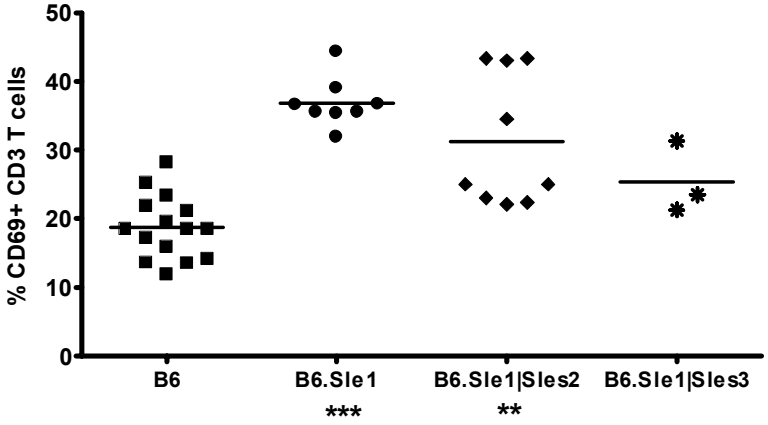

Fig. 35D

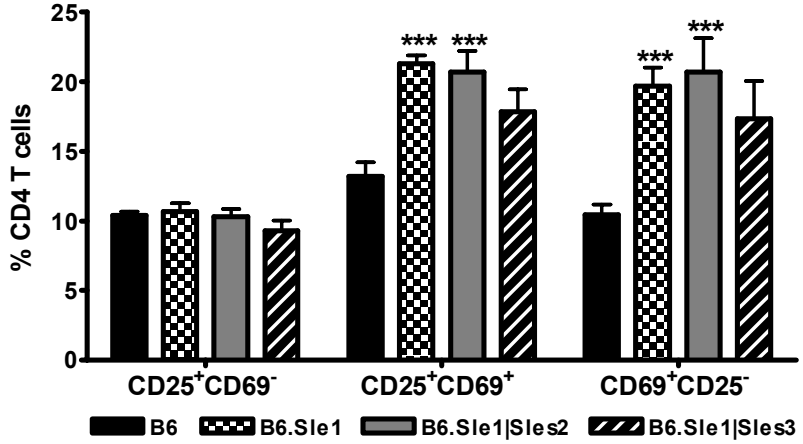

Figure 35. *Sles2* and *Sles3* Mediate Suppression of Splenomegaly but Do Not Impact Cell-Surface Activation Phenotypes. Spleens were collected from the mice at time of sacrifice (9-12 months) and weighed. Flow-cytometric analyses of splenocyte suspensions were performed to assay for suppression of *Sle1*-mediated activation phenotypes (153, 226). B6.*Sle1*|*Sles2* and B6.*Sle1*|*Sles3* were compared by ANOVA to B6, B6.*Sle1* and each other for the different phenotypes. A. Comparison of spleen weights at 9-12 months of age. Both B6.*Sle1*|*Sles2* and B6.*Sle1*|*Sles3* differed significantly from age and gender-matched B6.*Sle1* spleens, but not B6 (n= 7-31). $^{***}p<0.001$ *vs.* B6; $^{+}p<0.05$, $^{+++}p<0.001$ *vs.* B6.*Sle1* (ANOVA). B-C. Percentage of $B220^{+}$ B (B.) and $CD3^{+}$ T (C.) cells expressing the early activation marker CD69. D. Percentage of $CD4^{+}$ T cells expressing combinations of the activation markers CD25 and CD69. B6.*Sle1*|*Sles2* had significantly more positive cells than B6 in both B and T cells, and do not differ significantly from B6.*Sle1*. Statistical values for the flow-cytometric analyses are not indicated for B6.*Sle1*|*Sles3* mice, as only three mice have thus far been analyzed. $^{*}p<0.05$, $^{**}p<0.01$, $^{***}p<0.001$ *vs.* B6 (ANOVA).

Fig. 36A

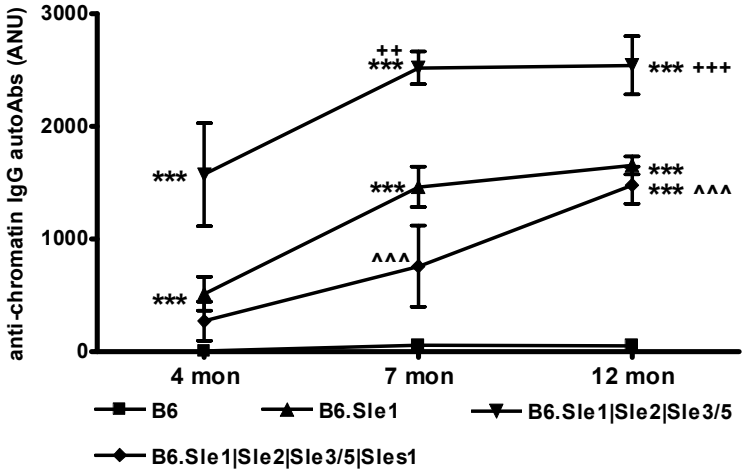

Fig. 36B

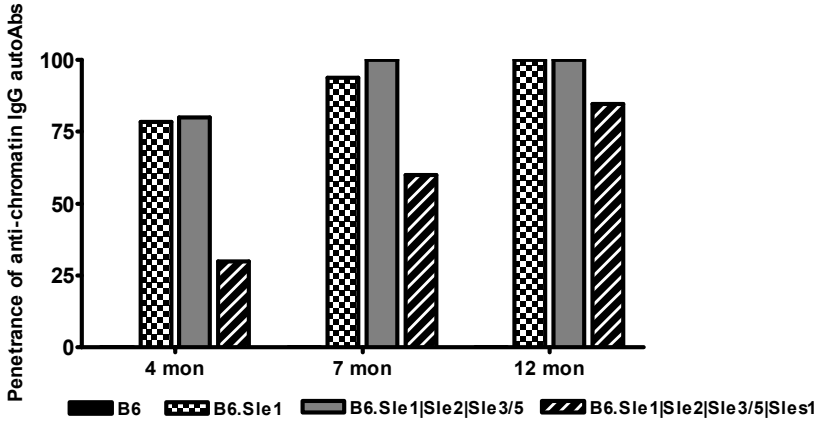

Figure 36. **Reduced Mean Titres and Penetrance of anti-chromatin IgG autoAbs in B6.*QC* at All Ages.** Serum levels of IgG anti-chromatin autoAbs were determined by ELISA for samples obtained at 4, 7 and 9-12 months of age. Samples were assayed simultaneously, in duplicate, on plates coated in parallel to allow for interplate comparisons of mean titres. Samples were deemed positive if they exceeded the mean B6 value + 4SD. A. Comparison of mean titres and B. Comparison of penetrance of autoAb production between the different strains at 4, 7 and 9-12 months of age. $^{***}p<0.001$ *vs.* B6; $^{++}p<0.01$, $^{+++}p<0.001$ *vs.* B6.*Sle1* and $^{\wedge\wedge\wedge}p<0.001$ *vs.* B6.*TC* (ANOVA). n = 5-25 /genotype/timepoint.

Fig. 37A

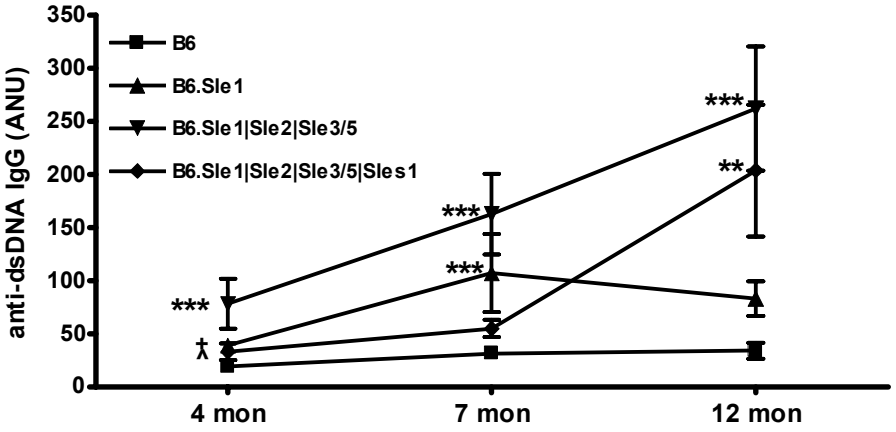

Fig. 37B

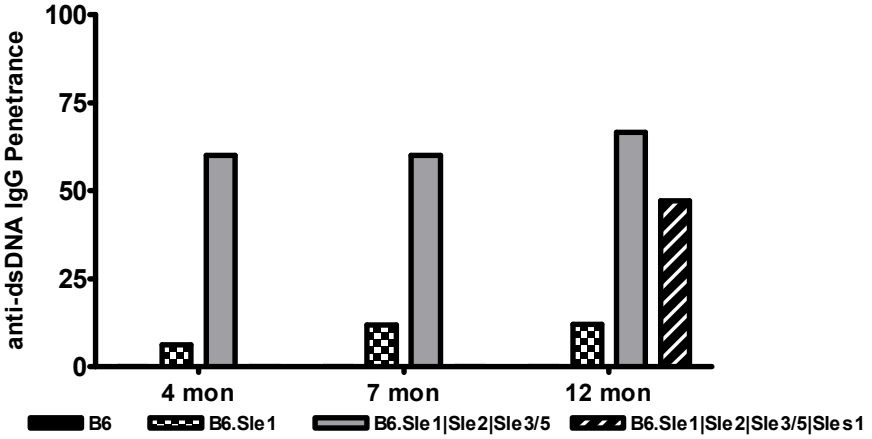

Figure 37. **Decreased Mean Titres and Penetrance of anti-dsDNA IgG autoAbs in B6.*QC* at All Ages.** Serum levels of anti-dsDNA autoAbs were determined by ELISA for samples obtained at 4, 7 and 9-12 months of age. Samples were assayed simultaneously, in duplicate, on plates coated in parallel to allow for interplate comparisons of mean titres. Samples were deemed positive if they exceeded the mean B6 value + 4SD. A. Comparison of mean titres and B. Comparison of penetrance of autoAb production between the different strains at 4, 7 and 9-12 months of age. $^{**}p<0.01$, $^{***}p<0.001$ *vs.* B6; $^{+}p<0.05$, *vs.* B6.*Sle1* and $^{\wedge}p<0.05$ *vs.* B6.*TC* (ANOVA). n = 5-25 /genotype/timepoint.

Fig. 38A

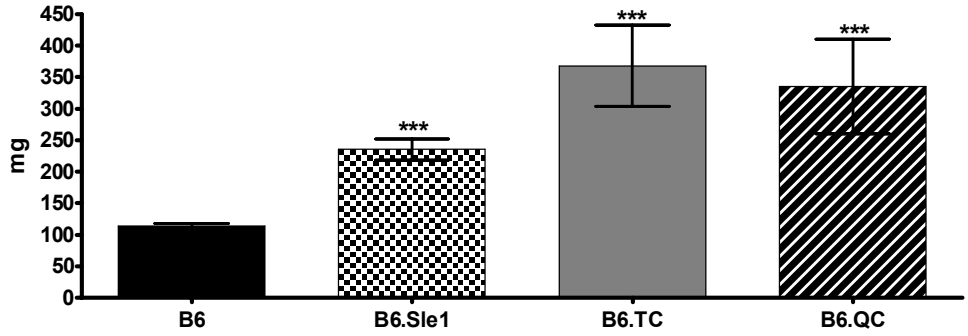

Fig. 38B

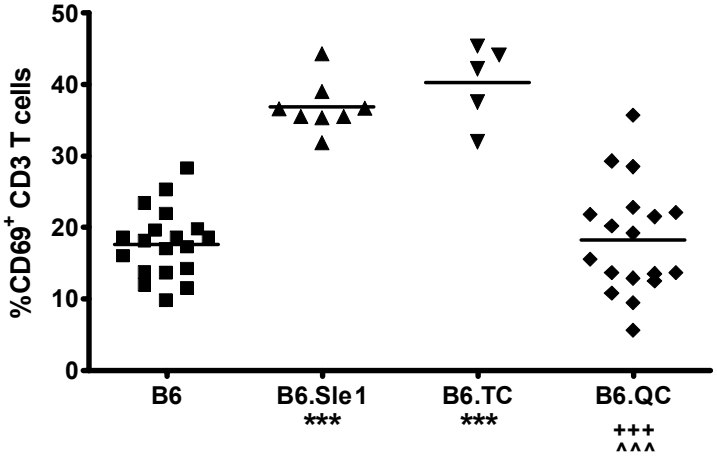

Fig. 38C

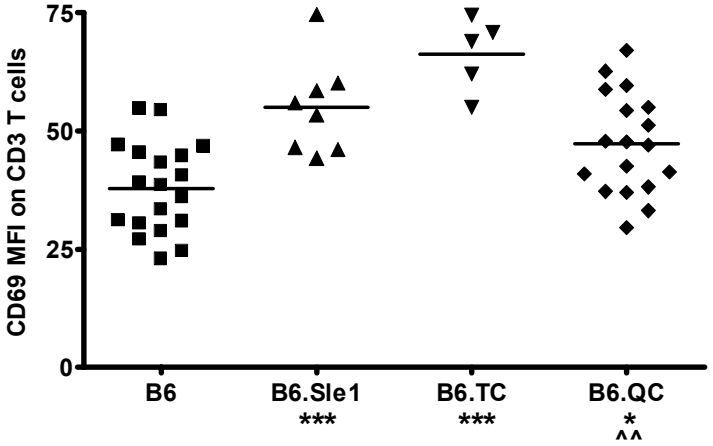

Fig. 38D

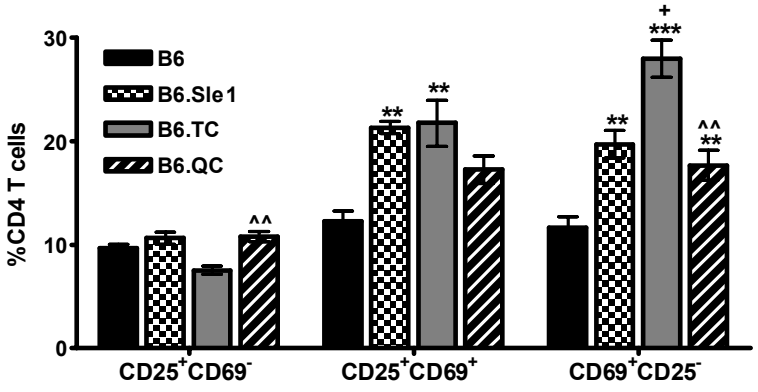

Fig. 38E

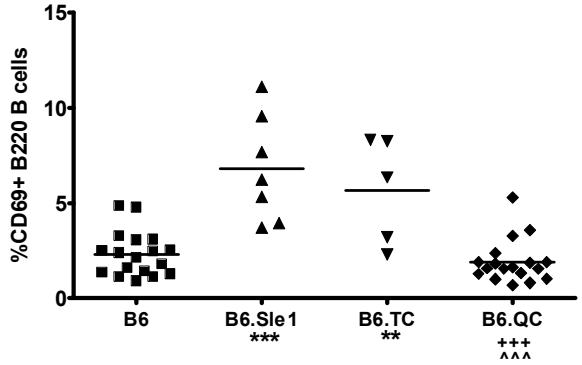

Fig. 38F

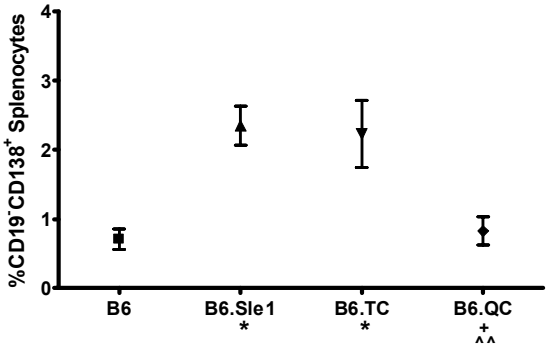

Figure 38. *Sles1* Does Not Affect Splenomegaly but Impacts Cell-Surface Activation Phenotypes. Spleens were collected from the mice at time of sacrifice (9-12 months) and weighed. Flow-cytometric analyses of splenocyte suspensions were performed to assay for suppression of activation phenotypes. B6.*TC* and B6.*QC* were compared by ANOVA to both B6, B6.*Sle1* and each other. A. Comparison of spleen weights at 9-12 months of age. B6.*Sle1*, B6.*TC* and B6.*QC* differed significantly from age and gender-matched B6 but not each other (n= 5-25). B-C. Percentage and MFI of $CD3^+$ T cells expressing the early activation marker CD69. B6.*Sle1* and B6.*TC* had significantly increased values relative to B6 for all parameters. In contrast, B6.*QC* had decreased levels relative to B6.*TC* for the different phenotypes. D. Percentage of CD4 cells expressing combinations of the activation markers CD25 and CD69. B6.*QC* had decreased values relative to B6.*TC*, but increased $CD69^+CD25^-$ CD4 T cells compared to B6. E-F. Percentage of B220 B cells expressing the activation markers CD69 (E.) and $CD19^-CD138^+$ plasma B cells (F.) B6.*QC* had decreased percentages relative to B6.*Sle1* and B6.*TC* for these different phenotypes, but was not significantly different from B6. $^*p<0.05$, $^{**}p<0.01$, $^{***}p<0.001$ *vs.* B6; $^+p<0.05$, $^{+++}p<0.001$ *vs.* B6.*Sle1*; $^{++}p<0.01$, $^{+++}p<0.001$ *vs.* B6.*TC* (ANOVA)

Fig. 39A

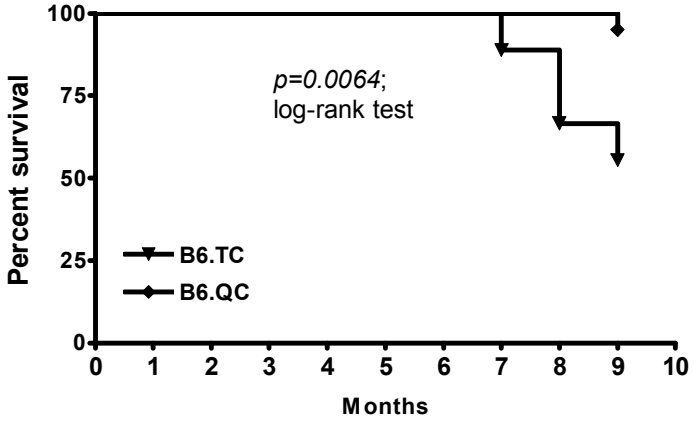

Fig. 39B

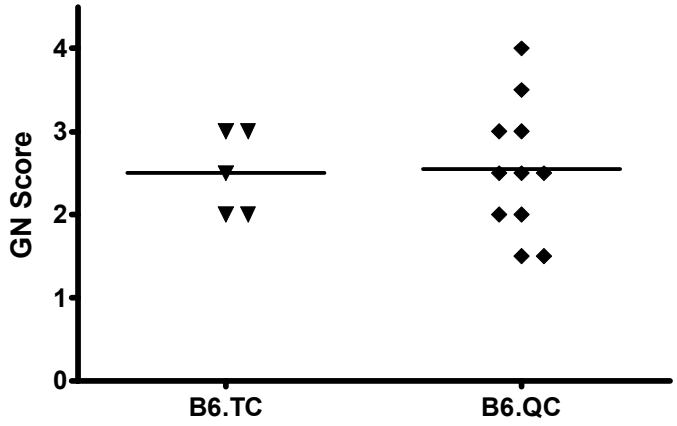

Figure 39. *Sles1* Increased Survival but Did Not Affect GN. A. Comparison of nine-months survival curves between B6.*TC* and B6.*QC*. The introduction of *Sles1* increased survival from 55.6% to 95% (*p=0.0064*; log-rank test). B. GN scores from 9-12 month old B6.*TC* and B6.*QC* mice. Despite the decreased mortality in B6.*QC*, no significant differences are seen in the GN scores between B6.*TC* and B6.*QC*.

Chapter VI: Discussion

There is growing evidence and appreciation for the fact that autoimmunity may arise as a consequence of 'unfortunate' combinations of common, non-deleterious allelic variants at multiple, immunoregulatory loci (reviewed in (17, 18)). It has been hypothesized that these autoimmune predisposing genes, some of which have been shown to be highly diversified and polymorphic, are being selected for and maintained in response to pathogen-driven selection mechanisms. Historically, HLA polymorphisms that have been associated with predisposition to autoimmunity are the best example of this type of genetic element. How then do these common variants elicit systemic autoimmunity? We, and others, have proposed that epistatic interactions between different combinations of polymorphic genes lead to subtle alterations in the regulation and functional responsiveness of the immune system that can ultimately lead to the development and progression of autoimmunity (18). The challenge ahead lies in trying to decipher the underlying mechanisms by which these allelic polymorphisms confer susceptibility to autoimmune disorders like SLE.

Furthermore, in addition to the inherent genetic risk conferred by these common allelic variants, both environmental factors and stochastic events influence the likelihood of disease development and progression. This results in a probabilistic relationship between the genetic variants and autoimmunity, in contrast to the deterministic association between genotype and the disease state seen in simple Mendelian disorders, as depicted in Fig. 40 (reviewed in (17)).

We have previously shown that *Sle1*, *Sle2* and *Sle3/5*, on chromosomes 1, 4 and 7 respectively, are the major loci contributing to lupus predisposition in the NZM2410 mouse strain (146). By creating congenic strains of these loci on the B6 background, it has been shown that each locus mediates unique phenotypes, in terms of both autoimmune pathology and intrinsic immune responsiveness and functions (225, 226, 235, 238, 279). Subsequent genetic reconstitution experiments of these three intervals demonstrated that: (i) these loci are sufficient to cause systemic autoimmunity on the B6 background and (ii) *Sle1* is required for the epistatic interactions needed to generate autoimmunity when these loci are combined (201, 240).

The fact that all three *Sle* loci originate from the non-autoimmune NZW parent of NZM2410, yet are sufficient to mediate systemic autoimmunity when combined on the B6 background, led to the hypothesis that suppressive modifier loci in the NZW genome prevent the development of autoimmunity in this strain. Linkage analyses confirmed the presence of four such modifers, termed the *Sles1-4* loci, and bi-congenic analyses demonstrated that *Sles1* specifically suppressed the phenotypes of *Sle1*, but had no effect on those of *Sle2* and *Sle3* (242).

In order to study the role of epistatic interactions in the suppression of autoimmunity, we introduced the *Sles1-3* loci onto our different autoimmune-prone congenic models to assay their effects on the modulation of both humoral and systemic autoimmunity. This allowed us to further characterize our existing autoimmune models and study how the introduction of a single locus, originally identified as a suppressive modifier, affected the development of autoimmunity. Our data demonstrate that such an approach can indeed reveal

subtle changes in the degree of different autoimmune phenotypes, as illustrated by our findings that while the mice remain clearly seropositive, the introduction of *Sles2* and *Sles3* cause a drop in the mean anti-chromatin autoAb titres normally observed in B6.*Sle1*.

Characterization of suppression mediated by *Sles1* revealed that the ability of this locus to epistatically modulate the autoimmune cascade elicited by *Sle1* is highly dependent on the nature of the additional interacting susceptibility loci. Hence, while *Sles1* completely abrogates the autoimmune phenotypes, systemic and humoral, seen in B6.*Sle1*|*yaa*, its effects on the B6.*TC* model are much less impressive and bear further careful investigation. Using a recombinant fine-mapping strategy, we have found that *Sles1* maps to a ~956 Kb interval that is highly gene-dense and polymorphic. Interestingly and of much practical relevance, our data indicates that the non-autoimmune 129 strains harbors a 'complementary' *Sles1*-allele (227). The quest ahead lies in determining how the epistatic relationships between the causal genes within the various loci translate to modulations in immune cell interactions and function.

Polymorphisms, Dysregulation of Immune Tolerance and the Development of Lupus

A consistent observation in a variety of natural and genetically engineered lupus models is the spontaneous development of populations of activated and effector-phenotype B and T lymphocytes. It has been posited that these cells arise and accumulate due to failures in peripheral tolerance and regulation mechanisms (189, 194, 195, 213, 226, 235, 236, 238). Both knock-out and transgenic lupus models have provided insight on how aberrant signaling, proliferation and antigen clearance can contribute to the dysregulation of the immune

response and consequent disease development, as detailed in Chapter I. This begets the question: in the case of spontaneous models how do the underlying common polymorphisms in susceptibility genes lead to failures in tolerance mechanisms and the emergence of autoreactive B and T cells? While we do not yet have clear mechanistic explanations, emerging data from our group and others suggest that the underlying polymorphisms could affect multiple aspects of peripheral tolerance, which cumulatively engender autoimmunity.

Defects in Central Tolerance and the Development of Autoimmunity

T cells undergo a highly regulated series of positive and negative selection events in the thymus in order to form peripheral repertoires capable of recognizing foreign peptides in the context of presentation by self-MHC. TCRs that weakly bind self-peptide MHC complexes undergo positive selection events in the thymic cortical epithelium. At this stage, some cells expressing highly self-reactive TCRs undergo editing of the TCRα chain. Medullary thymic epithelial and interdigitating DCs are the agents of negative selection and test TCRs for reactivity to self-peptide-MHC complexes. TCRs that bind self too strongly undergo clonal deletion via TCR signaling induced activation of the Fas and BIM pro-apoptotic pathways (2). It is believed that failure to appropriately present peripheral self-peptides at this stage of selection allows for the emergence of autoreactive cells, particularly in organ-specific autoimmune diseases (1). Evidence for this comes from the fact that defects in the AIRE transcription factor, in both humans and mice, has been shown to lead to failures in ectopic thymic presentation of peripheral antigens, and polyglandular autoimmune syndromes. This has been postulated as being due the ability of AIRE to transcriptionally

regulate the expression of tissue-specific antigens, as well as genes involved in MHC presentation and thymic migration (328, 329). Interestingly, AIRE has a C4HC3 zinc-finger-like motif, PHD, reminiscent of, but distinct from the C3HC4 type RING finger domain found in *Ring1* and *Rnf5* in the *Sles1* interval, as well as in the novel autoimmunity-promoting *roquin* gene and the E3 ubiquitin ligase *c-cbl* ((227, 330) and reviewed in (331)). Similarly, a point mutation in the ZAP-70 protein, signaling through which is essential for thymocyte deletion, has been found to lead to the escape of autoreactive T cells and the development of a murine disorder closely resembling rheumatoid arthritis (332). While no gross differences in thymic selection events, based on thymocyte staining for CD3, CD4, CD8 and CD5, have been observed in B6.*Sle1*, B6.*Sle1*|*yaa*, B6.*Sle1*|*Sles1*|*yaa* mice, it is possible that using a system that can reveal qualitative and quantitative changes in positive and negative selection events, such as the HY-TCR Tg model, may reveal subtle differences.

Recent studies have demonstrated that in both mice and humans, due to the random receptor rearrangements involved in generating the BCR in the BM, an impressive percentage of immature B cells have autoreactive specificities. Most of these are removed from the naïve repertoire due to central tolerance mechanisms in the BM, in which further maturation of autoreactive B lymphocytes is prevented when the strength of receptor signaling during selection events exceeds specific thresholds (323, 333). If a B cell clone undergoes successful receptor editing, it survives, but failure to rescue the autoreactive B cell leads to clonal deletion, due in part to lack of BAFF-mediated survival signals and expression of pro-apoptotic molecules such as BIM (1). Clear evidence regarding how defects in B cell central tolerance mechanisms in the BM leads to lupus-like phenotypes have

not yet been demonstrated, and we have not seen any significant changes in BM subsets in any of the strains we have examined. However, using the α-HEL BCR-mHEL double Tg model of central tolerance, it has been shown that *Sle1* does not impact effective central tolerance mechanisms (K. Raman *et al.*, *unpublished observations*).

Defects in Peripheral Tolerance: Multiple Mechanisms Can Lead to Autoimmunity

Despite these mechanisms of clonal deletion and editing of autoreactive B and T cells in the BM and thymus, a subset of the immature B cells and naïve T cells that emerge into the periphery have autoreactive receptors. This can be due to the fact that their self-specificity was not of high enough avidity to trigger clonal deletion, or because of the self-antigen was not 'seen' in the primary lymphoid organ during selection. Peripheral tolerance mechanisms depend on the interactions between lymphocytes, as well as APCs and stromal cells, and different peripheral checkpoints occur within specialized microenvironments in the spleen and LN (1).

We, and others, have shown that the emergence of humoral and systemic autoimmunity in a variety of different lupus models is preceded and accompanied by age-associated changes in the activation status and functional responses of both B and T lymphocytes, albeit with differing kinetics (189, 194, 195, 213, 226, 235, 236, 238). We found that differences in the activation status of splenic B and T cells can be observed as early as 6-8 weeks in the B6.*Sle1*|*yaa* lupus model. Furthermore, early differentiation of B and T lymphocytes into phenotypic 'effector' plasma and effector-memory populations respectively was observed. Consistent with these observations, we saw increased levels of

both IgM and IgG self-specific autoAbs, relative to normal, age-matched controls. The underlying mechanisms mediated by the epistatic interactions between *Sle1* and *yaa* that lead to these early-onset phenotypes, and what is the role of *Sles1* in preventing them, remains to be determined, but some possibilities are discussed below.

Given that we have not observed significant changes in B and T cell development phenotypes in the BM or thymus in our different models, yet have seen significant and early changes in B and T cell accumulation, development and differentiation in the spleen, we postulate that the underlying allelic variants modulate the ability to effectively regulate peripheral tolerance, quite possibly at multiple levels. Evidence for the fact that *Sle1* can impact these mechanisms comes from studies of the α-HEL BCR-sHEL double Tg model of peripheral tolerance, where it has been shown that *Sle1* causes α-HEL BCR B cells, normally rendered anergic by the presence of soluble HEL, to remain functionally responsive and undergo less receptor editing (K. Raman *et al.*, *unpublished observations*).

Maintenance of peripheral B cell tolerance is believed to be a consequence of decreased display of self-reactive BCRs, molecular feedback mechanisms that change thresholds for BCR signaling, competition for survival signals with less autoreactive cells, and regulation of co-stimulatory molecules and immunogenic stimuli. While the precise molecular mechanisms guiding these processes have yet to be determined, it is believed that events during peripheral selection in the spleen play an important role. It is important to note, however, that the ability of the BCR to undergo somatic hypermutation in the GCs can increase the self-specificity of the BCR (1).

It has been shown that in the non-autoimmune B6.*yaa* strain, B cell responsiveness to a variety of stimuli, including PMA/Ionomycin, LPS, anti-IgM and anti-CD40, are significantly heightened (195). This may indicate that the variation in the gene encoded by *yaa* somehow modifies the regulatory and molecular feedback mechanisms that adjust thresholds for BCR signaling. In addition, we, and others, have observed increases in overall IgM levels, with elevated self-reactive IgM autoAbs in non-autoimmune B6.*yaa* mice, which may be a consequence of this intrinsic hyper-responsiveness of the B cell compartment (334). This would suggest that the triggering of self-reactive BCRs in these mice activates sufficient signaling pathways, such as NFκB1, to allow for the survival of these autoreactive B cells, due to this inherent hyper-reactivity. The failure of B6.*yaa* mice to progress to the development of high-titred IgG autoAbs has been postulated as being due to lack of T cell help, as *yaa* has been shown to act in a B cell intrinsic manner (196). However, recent experiments, which have shown that WT CD4 T cells can interact with *yaa* B cells to promote severe autoimmunity, suggest this explanation is insufficient to explain the lack of autoimmune progression (194).

To date, despite the fact that aged B6.*Sle1* mice have much stronger humoral autoimmunity and activated B cell phenotypes than B6.*yaa*, we have not observed any robust changes in B cell responsiveness to external stimuli at young ages, in terms of CFSE proliferation in response to IgM stimulus (data not shown). These experiments bear repeating with doses of different stimuli including α-IgM, α-CD40, LPS, CpG and PMA/ionomycin and simultaneous comparison of responses between young 6-8 week old female B6, B6.*Sle1* and B6.*Sle1*|*Sles1* and male B6, B6.*yaa*, B6.*Sle1*, B6.*Sle1*|*yaa* and B6.*Sle1*|*Sles1*|*yaa*.

In addition, the *yaa* gene has been shown to result in a significant reduction in the development of splenic MZ B cells. This population of mature B cells plays an important role in the early T-independent defense against blood-borne pathogens due to their specialized anatomical location at the border of the splenic white and red pulp and limited repertoire. MZ B cells have been shown to be enriched for self-specificities, and it has been suggested that both TLR9 and BCR signaling dictates their peripheral selection. Studies of mice deficient in a variety signaling molecules, such as CD19, CD21, Btk, Aiolos and CD22, have demonstrated differential requirements of these proteins for the development of the MZ, follicular and B1 mature B cell subsets (319, 325). Furthermore, deficiencies in different members of the Notch family of receptors and ligands, which are involved in cell-fate and differentiation determination, have been shown to have specific effects on the development of this B cell population (306, 310).

The role of the MZ population and the development of lupus has been a subject of much interest and debate. Like B1 B cells, because of their ability to secrete self-reactive 'natural' autoAbs, it has been postulated that failure to regulate MZ B cells may play a role in the development of autoreactive B cells (217, 318, 319). In addition, an early expansion of this population has been shown in the lupus-prone BWF_1 mouse strain, as well as in mice over-expressing the B cell survival factor BAFF, which also develop a lupus-like disease (217). However, the *yaa*-associated deficiency in MZ B cells argues against a major role for these cells in the autoAb production seen in this model. Instead, the *yaa*-associated MZ B cell deficiency may be a consequence of alterations in antigen-receptor derived signal thresholds, as various analyses indicate that weak antigen receptor-derived signals favors MZ

B-cell generation, while relatively strong signals favor the development of mature follicular B cells and even stronger signals derived from the antigen receptor are believed to favor the generation of B1 B cells (322). The ability of *Sles1* to reconstitute this population suggests an effect of the gene contained within this locus on 'resetting' signaling thresholds, though conclusive proof of this remains to be shown. It is important to note that neither endogenous nor Tg Class II IE-α expression was able to restore this population, eliminating this gene as a possible candidate in the *Sles1*-mediated rescue of MZ B cells in this model (315).

Similar to the various mechanisms regulating the development and specificity of the mature B cell subsets (follicular, MZ and B1), the events leading to terminal B cell differentiation into plasma cells (PCs) are also highly regulated. PCs can be formed from either MZ or follicular B cell precursors. Following activation by antigen, naive B cells in both the MZ and follicles rapidly can rapidly develop into short-lived plasma cells. In addition, follicular B cells can undergo a germinal-center (GC) reaction, and following repeated rounds of proliferation, affinity maturation and class-switch recombination, both memory B cells and plasma cells can be generated. The mechanisms and factors guiding the commitment of B cells to the memory B cell or PC fate is a subject of intense research and has been shown to involve various transcription factors (BLIMP1, BCL6, Pax5) and cytokines (IL-4, IL-21) (335).

An increase in cells with a PC phenotype ($CD19^{+}CD138^{-}$) was observed in older female B6.*Sle1* mice, and in both young and older B6.*Sle1*|*yaa* males, while no differences were observed in this population in female B6.*Sle1*|*Sles1* and male B6.*yaa* or B6.*Sle1*|*Sles1*|*yaa*. Interestingly, no increase was observed in the proportion of BM PCs in

either B6.*Sle1* or B6.*Sle1*|*yaa*. Recent work on the AM14 Ig-Tg, which is specific for IgG2a^a, and is used as a model for the anti-rheumatoid factor response, has described that, despite the lack of a GC response, there is extensive Ab-forming cell (AFC) generation in the spleen, accompanying somatic hypermutation but, like both B6.*Sle1* and B6.*Sle1*|*yaa*, no accumulation of PCs in the BM. The immune response was also shown to correlate with the levels of IgG2a-chromatin ICs but not total IgG2a, implicating an important role for immune complexes in the activation of these B cells (336). These events were found to occur outside the follicles and instead at the splenic T-B border, and the AFCs were found to have rapid turnover and phenotypic characteristics of plasmablasts, rather than true plasma cells (337). In contrast, it has been shown, using the anti-dsDNA specific 3H9 Ig-Tg system, that on the MRL.*lpr* background Tg-B cells accumulate within the B cell follicle, and this localization is dependent on *lpr* (338). Whether anti-self specific B cells in B6.*Sle1* and B6.*Sle1*|*yaa* mice show preferential splenic accumulation has yet to be determined, and further characterization, both by flow-cytometry for changes in chemokine receptor expression and markers of GC B cells, as well as histological analyses of spleens, are clearly warranted.

Dysregulation of T cells and Peripheral Tolerance

Unlike B cells, T cells that emerge into the periphery are developmentally mature and do not undergo peripheral selection. However, by the very nature of their selection on self-MHC, the TCR has inherent self-specificity, and in fact, ‘tonic’ interactions between the T cell and self-peptide MHC complexes, as well as various survival cytokines (IL-7) are required for the maintenance of peripheral T cells. Furthermore, recent work has

demonstrated that the $CD25^{+}Foxp3^{+}$ CD4 T_{reg} population has a higher degree of self-reactivity than their non-regulatory counterparts. T cell tolerance is maintained in peripheral lymphoid tissues through a variety of mechanisms that include increased expression of the inhibitory receptor CD5, the negative co-stimulatory receptors CTLA-4 and PD-1 (on naïve and activated T cells respectively), as well as various ubiquitin ligases (CBL-B, GRAIL and ITCH), in addition to competition for growth factors (IL-7) and T_{reg} function (1, 339).

We have found that development of humoral autoimmunity in B6.*Sle1* and systemic autoimmunity in B6.*Sle1*|*yaa* is accompanied by the development of activated and effector-memory CD4 T cells. In the latter model, changes in the peripheral splenic CD4 population are detectable as early as 6-8 weeks, and are associated with a roughly two-fold increase in the percentage of cells with the ability to secrete IFNγ in response to PMA/ionomycin stimulation at this young age.

The ability of a naïve T cell to discriminate between interactions that lead to survival, immunity or tolerance is believed to be due to differences in inherent TCR-mediated signaling thresholds, determined during positive selection, as well as the degree of co-stimulation received from mature DCs. It is well known that failure to receive appropriate co-stimulation leads to tolerance induction, but it has been recently suggested that aberrations in homeostatic proliferation can to lead to disruptions in normal tolerogenic mechanisms. According to this hypothesis, inherent changes in 'survival' *vs.* 'tolerogenic' thresholds lead to the maintenance of functional autoreactive T cells (1, 89, 340). We can hence postulate that altered signaling thresholds in B6.*Sle1*|*yaa* T cells leads to an accumulation of 'effector-memory' phenotype CD4 T cells. The SLAM/CD2 haplotype provided by *Sle1* may

influence the avidity of the TCR 'tickling' interactions with APC presented self-peptide-MHC complexes and thus facilitate the survival of these autoreactive cells, by reducing the requirements for CD28 mediated signaling. For example, it has been posited that modulation of the PI3K-PKB/Akt pathway can circumvent the requirements for CD28 mediated co-stimulation (340). Lending support for this hypothesis, is the fact that the SLAM/CD2 family is known to signal via the PI3K-PKB (Akt) axis, and that B6.*Sle1b* and B6.*Sle1b.lpr* mice show alterations in this pathway (C. Xie *et al.*, *unpublished observations*) (234). In addition, the temporal differences in the emergence of these CD4 T cells between B6.*Sle1* and B6.*Sle1*|*yaa* mice may reflect the increased B cell interactions with CD4 T cells provided when both *Sle1* and *yaa* are epistatically interacting, given that both these loci impact the B cell compartment.

With age, we find that both B6.*Sle1* and B6.*Sle1*|*yaa* mice accumulate greater percentages of these 'effector-memory' phenotype CD4 T cells and became unresponsive to anti-CD3 induced stimulation. These data suggest that the CD4 T cells from these lupus prone mice, which are continually self-antigen stimulated and/or inherently hyper-responsive, undergo cell-cycle arrest leading to apoptosis and replication resistant phenotypes. It is believed that continual activation of MAPK signaling, in contrast to transient activation, leads to cell-cycle arrest. It may be that such chronic activation, presumably through self-antigen, leads to the accumulation of memory-phenotype CD4s that are metabolically active and make pro-inflammatory cytokines, such as IFN-γ (194). Interestingly, $pep^{-/-}$ mice, which lack the inhibitory phosphatase Pep/PTPN22, a protein implicated in human autoimmune susceptibility, demonstrate a similar accumulation of 'effector-memory' T cells, which show

enhanced TCR-mediated functions, as well as increased GC formation and splenomegaly, yet fail to elicit systemic autoimmunity (341). Such data indicate that enhanced B or CD4 T cell responsiveness alone is not a predictor of the ability to lose peripheral tolerance.

Lymphocyte Interactions in Autoimmunity: Emerging Evidence for Follicular T_H cells

The numerous cell types and factors implicated in lupus susceptibility have made a cohesive, encompassing picture of the various interactions key to generating systemic autoimmunity tremendously difficult to ascertain. For a variety of reasons, most studies focus on *ex vivo* cell-surface phenotypes and *in vitro* responses, which, while contributing valuable information, cannot give an *in vivo* 'picture' of the actual cell interactions occurring in the peripheral lymphoid organs. It has been hypothesized that the specialized anatomical localization of various immune cells, such as B and T lymphocytes, can serve as a method of extrinsic regulation of peripheral tolerance, by preventing interactions between autoreactive lymphocytes, as well an intrinsically hyper-responsive APCs, such as those found in B6.*Sle3/5* (1, 237).

While there has been no unequivocal demonstration of 'follicular exclusion' as a method for regulating tolerance, recent work concerning the newly described follicular CD4 T cell (T_{FH}) population sheds insight on the significance of this population in autoimmunity and has potentially important implications for our different NZM2410-derived lupus models. A genetic defect in the Roquin RING-finger protein that leads to defective regulation of CD4 T_{FH} cells has been proposed as the causal mechanism leading to the systemic autoimmunity

seen in *sanroque* mice (330). T_{FH} cells are found in the GCs and have been recently shown to have a transcriptional program of differentiation unique from extrafollicular cells (342).

Importantly, and of high relevance to the humoral autoimmunity mediated by *Sle1b*, members of the SLAM/CD2 family, including CD84, CD229, and their downstream adaptor SAP (SLAM-Associated Protein) are differentially upregulated in T_{FH}, relative to other CD4 cells, in both mouse and human. It is tempting to speculate that the lack of ability to maintain long-term humoral immunity in *Sap*$^{-/-}$ mice may be a consequence of impaired functionality of these cells (343). In addition, these T_{FH} cells have been shown to display increased levels of CXCR5, CD200, ICOS and IL-21 message and protein (330, 342).

Given their unique localization within the B cell follicle and GC, and their B cell maturation promoting transcription profile, it has been suggested that T_{FH} cells may serve as additional regulators of antigen-dependent B cell humoral responses, via their unique cytokine and chemokine profiles, separate from the classical IL-4 secreting T_H2 CD4 cell. For example, *in vitro* B cell stimulation with α-IgM and IL-21 has been shown to significantly promote PC differentiation *in vitro*, which was not observed when α-IgM and IL-4 were used. Furthermore, in complete contrast to the inhibitory effect of IL-4 on IFNγ production, a key component of the T_H1/T_H2 paradigm, IL-21 has been shown to promote IFN-γ production by T cells. Interestingly, serum IL-21 levels have been shown to be elevated in the BXSB.*yaa* strain, while TCR-engagement induced IL-4 production has been found to be impaired in the B6.*Sle1b* strain, as well as in *Slam*$^{-/-}$ and *Ly108*$^{-/-}$ mice ((233, 344, 345) and C. Nguyen *et al.*, *unpublished observations*). Defects in the regulation of the T_{FH}

population may also explain the Fas dependent accumulation within the B cell follicle of both anti-dsDNA specific Tg-B cells and CD4 cells in the MRL.*lpr* 3H9 Tg (338).

It is tempting to speculate that the polymorphisms in the *Sle1b* SLAM/CD2 haplotype, which cause structural changes in the extracellular-binding domains and differential isoform expression of family members, could be influencing the outcomes of antigen-receptor mediated signaling in follicular B and T_{FH} cells, leading to increased interactions and differentiation, as well as modulation of the local cytokine milieu, such as elevated IL-21 and IFNγ, but decreased IL-4 production. This may promote the emergence of IgG switched anti-chromatin specific B cells, the maintenance of which was originally facilitated by changes in mechanisms of homeostatic maintenance by the SLAM/CD2 family polymorphisms during peripheral selection events. The addition of *yaa* to this scenario transitions these humoral aberrations to systemic autoimmunity, via its epistatic interaction with *Sle1b/Sle1*, possibly by impinging on similar downstream pathways and by influencing kidney susceptibility to lymphocyte infiltration.

Adding a further layer of complexity to the possible scenarios and mechanisms described is the ability of *Sles1* to prevent *Sle1*-mediated autoimmunity. Our genetic fine-mapping analysis excluded many MHC genes, including *TNF-α*, a lupus susceptibility candidate gene implicated in both human and murine studies, but still left 69 genes as possible *Sles1* candidates (55, 291-293).

As detailed earlier, the association of Class II genes in mediating susceptibility to lupus has proven quite complicated and dependent on epistatic interactions, resulting in a variety of hypotheses such as mixed haplotype/isotype Class II molecules, suppression

mediated by increased Class II I-E expression and peptide competition leading to decreased self-peptide presentation during thymic development, as mechanisms by which polymorphisms in these genes can lead to autoimmunity (146, 148, 210, 211, 216). While our genetic fine-mapping analyses have not yet positionally eliminated Class II genes as candidates for *Sles1*, our genetic complementation experiments with 129 strongly argue against these molecules as being causal. Our contention that the 129 *Sles1* interval harbors a suppressive modifier is supported by evidence from a recent [B6 X 129]F_2 intercross study, which showed that the chromosome 17 interval from B6 is permissive for the autoimmunity elicited by a 129-derived chromosome 1 interval, while that from 129 is suppressive (252). These studies indicate that 129 and B6, despite sharing the $H2^b$ Class II haplotype, are not completely identical at this region (289).

In addition to the Class II genes, the *Sles1* interval harbors a plethora of candidate genes with known immunological function and relevance, including *C4*, *Daxx*, *Hspa1* and *Notch4*. These genes and/or their family members have all been shown to play roles in regulation of lymphocyte function and/or development (25, 41, 301, 308). While many of these studies have used knockouts or transgenic approaches to interrogate the roles of these genes in immune function, it is quite likely that polymorphisms in these genes can impact many of the phenotypes they have been shown to mediate when completely absent or over-expressed. For example, *Daxx* plays a role as a transcriptional repressor in IFN-αβ-mediated suppression of B cell development and induction of apoptosis (25). Aberrant activation of this pathway, as a result of the underlying polymorphisms in the genes within the *Sle1* locus, could lead to defective regulation of B cell development only in the context of the B6 *Daxx*

allele. While completely conjectural, this provides an example of how these complex genetic interactions could lead to different outcomes, one permissive for autoimmunity and the other suppressive.

It is important to note that despite being one of the most characterized regions of the genome, there are many genes within the MHC region that are novel and poorly characterized. Key examples of such genes are the *Ring*-family members, *Ring1* and *Rnf5*, and the *butyrophilin-like* genes *O70355* (*Btnl2*), *O35441* and *O70358*, within the minimal *Sles1* interval, as shown in Fig.11.

Ring1 and *Rnf5* both contain the RING-finger protein-interaction domain, a specialized C3HC4-type Zn-finger of 40 to 60 residues that binds two atoms of zinc and has been implicated in a diverse range of biological processes. *Ring1* is a ubiquitously-expressed member of the polycomb group (PcG) of transcriptional repressors and is a member of an E3 ubiquitin-ligase complex. Interestingly, the T-cell anergy factors, CBL-B, C-CBL and GRAIL all contain a RING domain. These molecules are believed to interfere with and downregulate TCR-mediated signaling via tagging TCR-CD28 and/or cytokine receptor molecules with ubiquitin, and thus promote endocytosis and proteolytic degradation of these signaling moieties (reviewed in (331, 346, 347)). Whether *Ring1* (or *Rnf5*) function similarly is currently unknown, but RING1 expression has been shown to correlate with different B cell differentiation stages in humans (348). Recently, the RING domain containing ubiquitin ligase *Roquin* has been shown to be essential for repressing ICOS expression and regulation of T_{FH} cells, and failure in these mechanisms, due to a mutation in Roquin, has been postulated to account for the lupus phenotype seen in *san roque* mice (330). This makes

Ring1 and *Rnf5* particular intriguing, given the association of the SLAM/CD2 family with T_{FH} cells.

The butyrophilin proteins, *O70355* (*Btnl2*), *O35441* and *O70358*, are also emerging as exciting, novel candidate genes for *Sles1*. These genes are cell-surface proteins and members of the Ig superfamily and have been shown to have homology to the B7 family of co-stimulatory molecules (reviewed in (32)). The B7 family and their ligands have been shown to have tremendous impact on immune regulation and function, as has been extensively reviewed. Recently, a truncating splice site mutation in *BTNL2* was found to be associated with the polygenic immune disorder sarcoidosis (349). *BTNL2* is expressed in a variety of tissues, including leukocytes and thymus, and expression can be upregulated by pro-inflammatory cytokines such as TNF-α and IL1-β. Interestingly, treatment with BTN induced tolerance in a murine EAE model and *BTNL2* has been shown to be a target gene of the transcription factor E2A, known to have critical roles in regulating B and T cell development (350, 351). Given these roles for BTNL2, polymorphisms in this gene and/or its family members could quite potentially mediate the suppressive role of *Sles1* by impacting tolerance mechanisms and providing enhanced inhibitory signals.

Conclusions and Future Directions

The studies we have presented herein illustrate the importance of epistatic interactions in both the potentiation and suppression of autoimmunity. Our results suggest that various combinations of immunoregulatory genes lead to alternate versions of a 'normal' immune system, as illustrated in the transcription profiles of B6 and B6.*Sles*|*Sles1* in splenic

B and CD4 T cells in Fig.41. Both of these strains are non-autoimmune, yet have very different patterns of gene-regulation, indicating that there are many pathways leading to 'normal'. We postulate that the suppression mediated by *Sles1* is a dynamic one, and that the balance between autoimmunity and tolerance achieved by *Sles1* is a fine one. Consistent with this, we find intrinsic B cell ERK hyperphosphorylation in B6.*Sles*|*Sles1*, and despite the potent suppression of humoral and systemic autoimmunity in both the B6.*Sle1* and B6.*Sle1*|*yaa* models by *Sles1*, we find the occasional *Sles1*-bearing mouse that is seropositive or has kidney disease respectively.

Identifying *Sles1* is a top priority and elucidating the mechanisms by which it suppresses *Sle1*-mediated autoimmunity will provide enormous insight into the dysregulated pathways leading to autoimmunity. The interval contains both well-studied and novel genes that can be postulated as having roles in ensuring immune regulation. The fact that the 129 strain bears a suppressive allele will allow us to utilize 129-derived ES cells and BACs libraries to perform *in vivo* identification of *Sles1*, as well as identify which cell-lineage *Sles1* is expressed in. Importantly, identification of the causal mutation will be simplified, as the degree of variability between the B6 and 129 intervals is much less, and allow us to focus on the polymorphisms shared between 129 and NZW that are divergent from B6. Emerging technologies in genomics and genetics, such as recombineered BAC knock-in strategies and lineage specific deletion strategies, will help to interrogate the role of individual SNPs in candidate *Sles* genes and facilitate causal gene identification and function. Further characterization of cytokines, chemokines and immunoregulatory cell-surface receptors, as well as elucidation of variations in downstream signaling molecules, using transcription

arrays, flow-cytometry and Western blot strategies will enhance our understanding of changes in different biological pathways elicited by *Sles1* suppression.

The schematics in Fig.42 and Fig.43 provide models to illustrate the complex genetic and cellular mechanisms that underlie the balance between a normal and autoimmune state. There are numerous paths leading to immune dysregulation, a result of the inherent conflict between sustaining responsiveness to rapidly evolving pathogens and preserving tolerance to self, and variations in genes like *Sles1* help to maintain this exquisitely fine balance.

Fig. 40

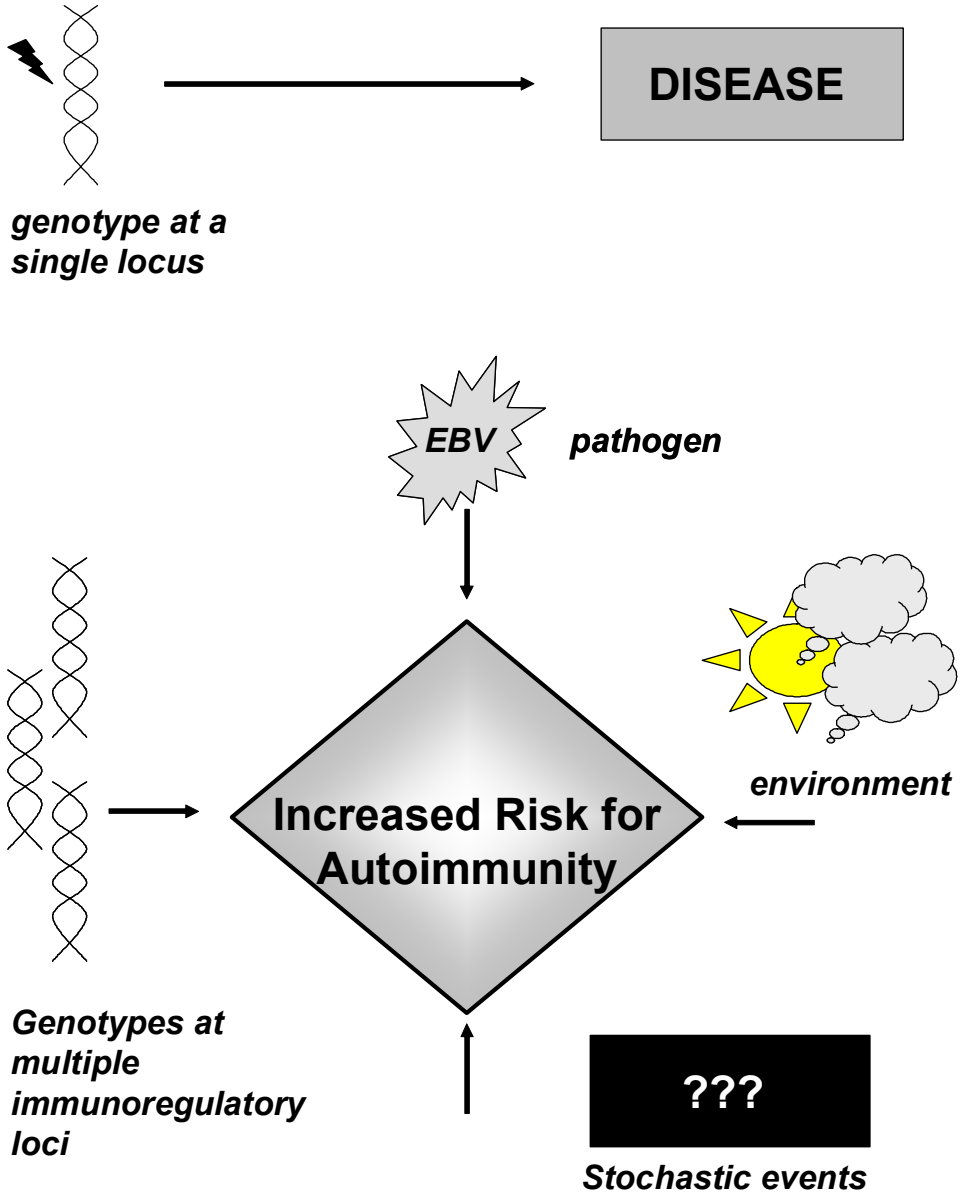

Figure 40. Model Comparing the Development of Mendelian Disorders with Complex Traits, such as Autoimmunity.

Fig. 41

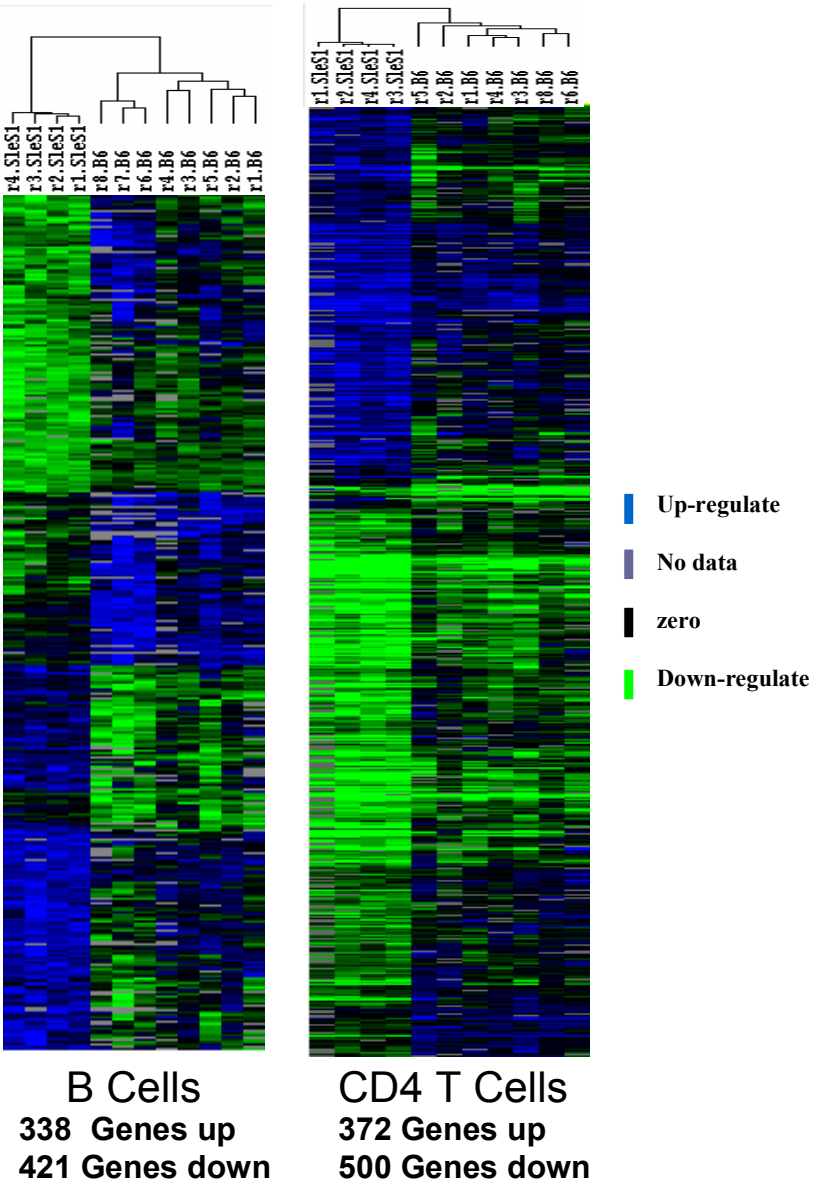

Figure 41. Differential Gene Expression Between B6 and B6.*Sle1*|*Sles1* Illustrate Two Versions of 'Normal'. Splenic CD4 T and B220 B cells from 9-12 month old mice were purified using the MoFlo high-speed cell sorter. RNA was extracted and hybridizations performed on a mouse 22K oligo chip generated in the Microarray Core at UT Southwestern. Comparisons represent 8 B6 and 4 B6.*Sle1*|*Sles1* mice and demonstrate that the transcriptional profiles of both T and B cells differ significantly between these two non-autoimmune strains, suggesting that there is no 'normal' profile of the immune system.

Fig. 42

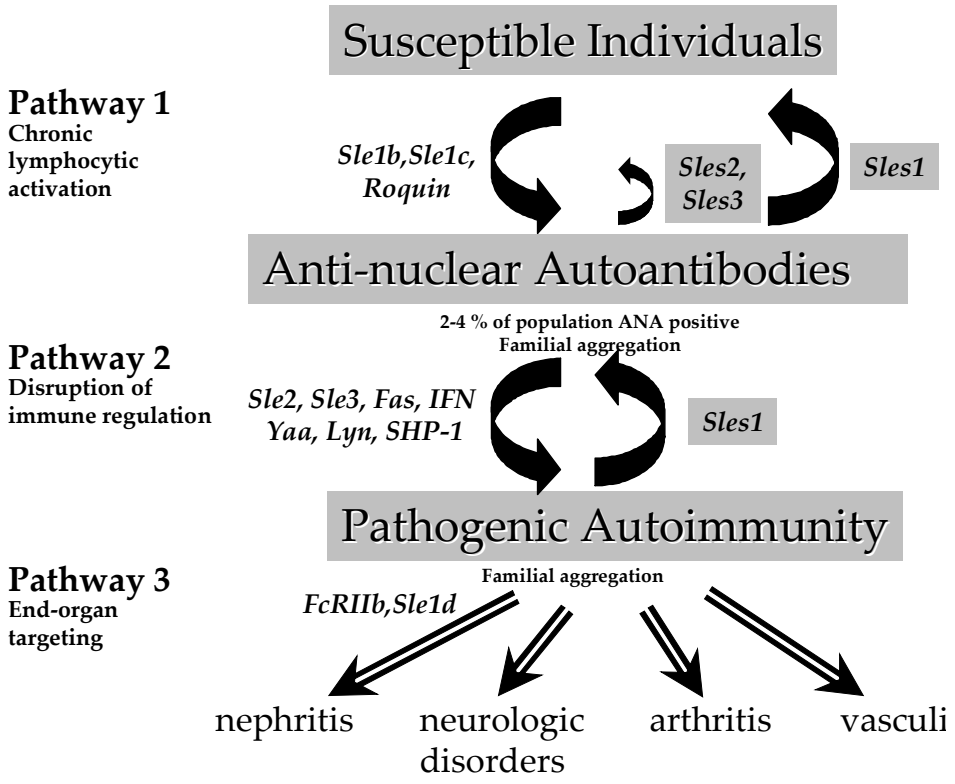

Figure 42. Revised Model of Epistatic Interactions Involved in SLE Susceptibility Incorporating both Potentiating and Suppressive Loci.

Fig. 43

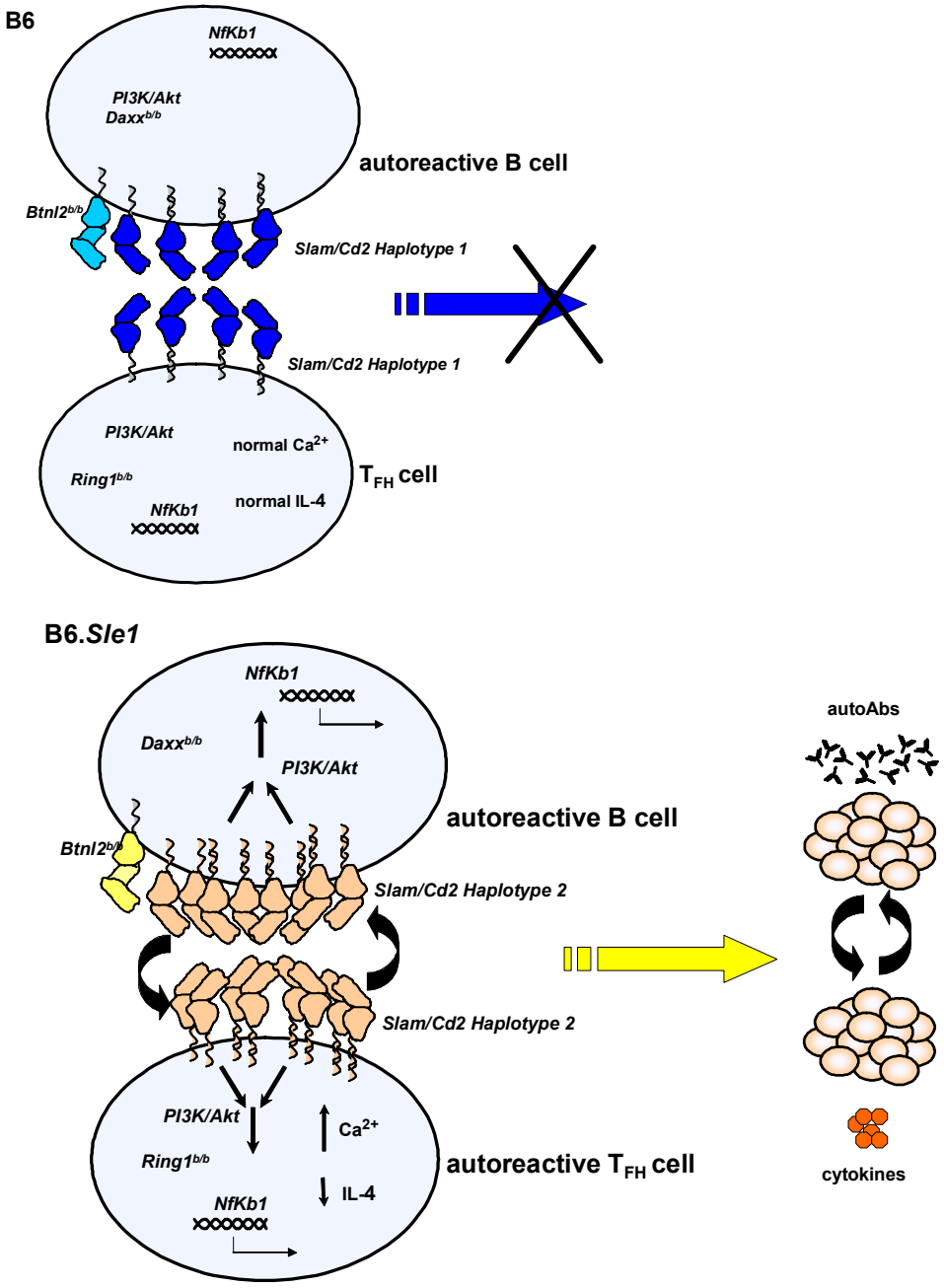
B6
NfKb1
PI3K/Akt
Daxx b/b
autoreactive B cell
Btnl2 b/b
Slam/Cd2 Haplotype 1
Slam/Cd2 Haplotype 1
PI3K/Akt
normal Ca2+
Ring1 b/b
TFH cell
NfKb1
normal IL-4
B6.Sle1
NfKb1
Daxx b/b
PI3K/Akt
autoreactive B cell
Btnl2 b/b
Slam/Cd2 Haplotype 2
Slam/Cd2 Haplotype 2
PI3K/Akt
Ca2+
Ring1 b/b
autoreactive TFH cell
NfKb1
IL-4
autoAbs
cytokines

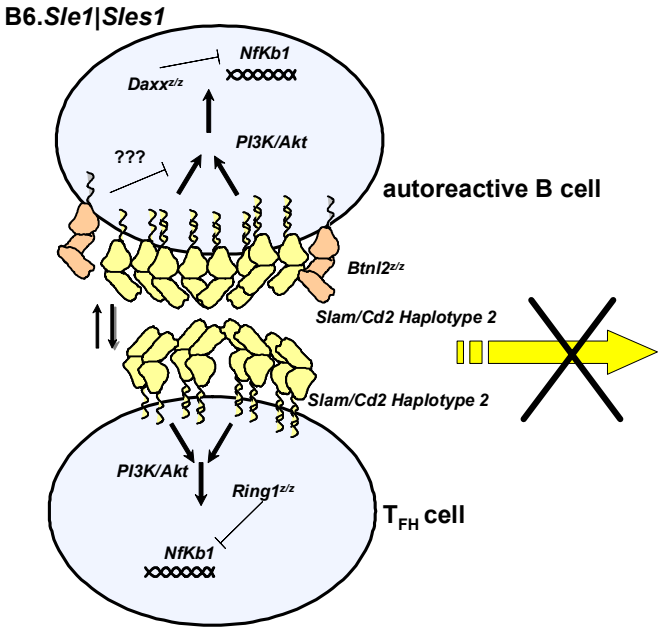

Figure 43. Hypothetical Model Illustrating Interactions Leading to Autoimmunity. On the B6 background, *Slam/Cd2* haplotype 1 interactions are minimal and do not lead to autoimmunity. *Slam/Cd2* haplotype 2 results in increased basal and activation-inducaed expression, increased interactions and is permissive for autoimmunity in the context of the B6 *Sles1* allele, hypothetically shown as *Ring1*, *Daxx* and *Btnl2* ((231)and C. Nguyen *et al*., *unpublished observations*). While the basal expression patterns of the *Slam/Cd2* haplotype 2 family members are similar in B6.*Sle1*|*Sles1* (data not shown), in the context of the NZW *Sles1* allele, these interactions are not permissive for autoimmunity. This could be due to transcriptional repression mediated by a gene like *Ring1* or *Daxx*, or due to inhibition of signaling by the B7 homolog *Btnl2*.

Bibliography

1. Goodnow, C. C., J. Sprent, B. F. de St Groth, and C. G. Vinuesa. 2005. Cellular and genetic mechanisms of self tolerance and autoimmunity. *Nature* 435:590-597.
2. Nemazee, D. 2000. Receptor selection in B and T lymphocytes. *Annu Rev Immunol* 18:19-51.
3. Wakeland, E. K., K. Liu, R. R. Graham, and T. W. Behrens. 2001. Delineating the genetic basis of systemic lupus erythematosus. *Immunity* 15:397-408.
4. Hochberg, M. C. 1997. Updating the American College of Rheumatology revised criteria for the classification of systemic lupus erythematosus. *Arthritis Rheum* 40:1725.
5. Deapen, D., A. Escalante, L. Weinrib, D. Horwitz, B. Bachman, P. Roy-Burman, A. Walker, and T. M. Mack. 1992. A revised estimate of twin concordance in systemic lupus erythematosus. *Arthritis Rheum* 35:311-318.
6. Block, S. R., J. B. Winfield, M. D. Lockshin, W. A. D'Angelo, and C. L. Christian. 1975. Studies of twins with systemic lupus erythematosus. A review of the literature and presentation of 12 additional sets. *Am J Med* 59:533-552.
7. Wandstrat, A., and E. Wakeland. 2001. The genetics of complex autoimmune diseases: non-MHC susceptibility genes. *Nat Immunol* 2:802-809.
8. Venter, J. C., M. D. Adams, E. W. Myers, P. W. Li, R. J. Mural, G. G. Sutton, H. O. Smith, M. Yandell, C. A. Evans, R. A. Holt, J. D. Gocayne, P. Amanatides, R. M. Ballew, D. H. Huson, J. R. Wortman, Q. Zhang, C. D. Kodira, X. H. Zheng, L. Chen, M. Skupski, G. Subramanian, P. D. Thomas, J. Zhang, G. L. Gabor Miklos, C. Nelson,

S. Broder, A. G. Clark, J. Nadeau, V. A. McKusick, N. Zinder, A. J. Levine, R. J. Roberts, M. Simon, C. Slayman, M. Hunkapiller, R. Bolanos, A. Delcher, I. Dew, D. Fasulo, M. Flanigan, L. Florea, A. Halpern, S. Hannenhalli, S. Kravitz, S. Levy, C. Mobarry, K. Reinert, K. Remington, J. Abu-Threideh, E. Beasley, K. Biddick, V. Bonazzi, R. Brandon, M. Cargill, I. Chandramouliswaran, R. Charlab, K. Chaturvedi, Z. Deng, V. Di Francesco, P. Dunn, K. Eilbeck, C. Evangelista, A. E. Gabrielian, W. Gan, W. Ge, F. Gong, Z. Gu, P. Guan, T. J. Heiman, M. E. Higgins, R. R. Ji, Z. Ke, K. A. Ketchum, Z. Lai, Y. Lei, Z. Li, J. Li, Y. Liang, X. Lin, F. Lu, G. V. Merkulov, N. Milshina, H. M. Moore, A. K. Naik, V. A. Narayan, B. Neelam, D. Nusskern, D. B. Rusch, S. Salzberg, W. Shao, B. Shue, J. Sun, Z. Wang, A. Wang, X. Wang, J. Wang, M. Wei, R. Wides, C. Xiao, C. Yan, A. Yao, J. Ye, M. Zhan, W. Zhang, H. Zhang, Q. Zhao, L. Zheng, F. Zhong, W. Zhong, S. Zhu, S. Zhao, D. Gilbert, S. Baumhueter, G. Spier, C. Carter, A. Cravchik, T. Woodage, F. Ali, H. An, A. Awe, D. Baldwin, H. Baden, M. Barnstead, I. Barrow, K. Beeson, D. Busam, A. Carver, A. Center, M. L. Cheng, L. Curry, S. Danaher, L. Davenport, R. Desilets, S. Dietz, K. Dodson, L. Doup, S. Ferriera, N. Garg, A. Gluecksmann, B. Hart, J. Haynes, C. Haynes, C. Heiner, S. Hladun, D. Hostin, J. Houck, T. Howland, C. Ibegwam, J. Johnson, F. Kalush, L. Kline, S. Koduru, A. Love, F. Mann, D. May, S. McCawley, T. McIntosh, I. McMullen, M. Moy, L. Moy, B. Murphy, K. Nelson, C. Pfannkoch, E. Pratts, V. Puri, H. Qureshi, M. Reardon, R. Rodriguez, Y. H. Rogers, D. Romblad, B. Ruhfel, R. Scott, C. Sitter, M. Smallwood, E. Stewart, R. Strong, E. Suh, R. Thomas, N. N. Tint, S. Tse, C. Vech, G. Wang, J. Wetter, S. Williams, M. Williams, S. Windsor, E. Winn-

Deen, K. Wolfe, J. Zaveri, K. Zaveri, J. F. Abril, R. Guigo, M. J. Campbell, K. V. Sjolander, B. Karlak, A. Kejariwal, H. Mi, B. Lazareva, T. Hatton, A. Narechania, K. Diemer, A. Muruganujan, N. Guo, S. Sato, V. Bafna, S. Istrail, R. Lippert, R. Schwartz, B. Walenz, S. Yooseph, D. Allen, A. Basu, J. Baxendale, L. Blick, M. Caminha, J. Carnes-Stine, P. Caulk, Y. H. Chiang, M. Coyne, C. Dahlke, A. Mays, M. Dombroski, M. Donnelly, D. Ely, S. Esparham, C. Fosler, H. Gire, S. Glanowski, K. Glasser, A. Glodek, M. Gorokhov, K. Graham, B. Gropman, M. Harris, J. Heil, S. Henderson, J. Hoover, D. Jennings, C. Jordan, J. Jordan, J. Kasha, L. Kagan, C. Kraft, A. Levitsky, M. Lewis, X. Liu, J. Lopez, D. Ma, W. Majoros, J. McDaniel, S. Murphy, M. Newman, T. Nguyen, N. Nguyen, M. Nodell, S. Pan, J. Peck, M. Peterson, W. Rowe, R. Sanders, J. Scott, M. Simpson, T. Smith, A. Sprague, T. Stockwell, R. Turner, E. Venter, M. Wang, M. Wen, D. Wu, M. Wu, A. Xia, A. Zandieh, and X. Zhu. 2001. The sequence of the human genome. *Science* 291:1304-1351.

9. Cargill, M., D. Altshuler, J. Ireland, P. Sklar, K. Ardlie, N. Patil, N. Shaw, C. R. Lane, E. P. Lim, N. Kalyanaraman, J. Nemesh, L. Ziaugra, L. Friedland, A. Rolfe, J. Warrington, R. Lipshutz, G. Q. Daley, and E. S. Lander. 1999. Characterization of single-nucleotide polymorphisms in coding regions of human genes. *Nat Genet* 22:231-238.

10. Vyse, T. J., and B. L. Kotzin. 1998. Genetic susceptibility to systemic lupus erythematosus. *Annu Rev Immunol* 16:261-292.

11. Kelly, J. A., K. Thompson, J. Kilpatrick, T. Lam, S. K. Nath, C. Gray-McGuire, J. Reid, B. Namjou, C. E. Aston, G. R. Bruner, R. H. Scofield, and J. B. Harley. 2002. Evidence for a susceptibility gene (SLEH1) on chromosome 11q14 for systemic lupus erythematosus (SLE) families with hemolytic anemia. *Proc Natl Acad Sci U S A* 99:11766-11771.

12. Namjou, B., S. K. Nath, J. Kilpatrick, J. A. Kelly, J. Reid, J. A. James, and J. B. Harley. 2002. Stratification of pedigrees multiplex for systemic lupus erythematosus and for self-reported rheumatoid arthritis detects a systemic lupus erythematosus susceptibility gene (SLER1) at 5p15.3. *Arthritis Rheum* 46:2937-2945.

13. Namjou, B., S. K. Nath, J. Kilpatrick, J. A. Kelly, J. Reid, M. Reichlin, J. A. James, and J. B. Harley. 2002. Genome scan stratified by the presence of anti-double-stranded DNA (dsDNA) autoantibody in pedigrees multiplex for systemic lupus erythematosus (SLE) establishes linkages at 19p13.2 (SLED1) and 18q21.1 (SLED2). *Genes Immun* 3 Suppl 1:S35-41.

14. Quintero-Del-Rio, A. I., J. A. Kelly, J. Kilpatrick, J. A. James, and J. B. Harley. 2002. The genetics of systemic lupus erythematosus stratified by renal disease: linkage at 10q22.3 (SLEN1), 2q34-35 (SLEN2), and 11p15.6 (SLEN3). *Genes Immun* 3 Suppl 1:S57-62.

15. Sawalha, A. H., B. Namjou, S. K. Nath, J. Kilpatrick, A. Germundson, J. A. Kelly, D. Hutchings, J. James, and J. Harley. 2002. Genetic linkage of systemic lupus erythematosus with chromosome 11q14 (SLEH1) in African-American families stratified by a nucleolar antinuclear antibody pattern. *Genes Immun* 3 Suppl 1:S31-34.

16. Scofield, R. H., G. R. Bruner, J. A. Kelly, J. Kilpatrick, D. Bacino, S. K. Nath, and J. B. Harley. 2003. Thrombocytopenia identifies a severe familial phenotype of systemic lupus erythematosus and reveals genetic linkages at 1q22 and 11p13. *Blood* 101:992-997.

17. Rioux, J. D., and A. K. Abbas. 2005. Paths to understanding the genetic basis of autoimmune disease. *Nature* 435:584-589.

18. Subramanian, S., and E. K. Wakeland. 2005. The importance of epistatic interactions in the development of autoimmunity. In *The gentics of autoimmunity*. Wiley, Chichester. 76-93.

19. Lipsky, P. E. 2001. Systemic lupus erythematosus: an autoimmune disease of B cell hyperactivity. *Nat Immunol* 2:764-766.

20. Hoffman, R. W. 2004. T cells in the pathogenesis of systemic lupus erythematosus. *Clin Immunol* 113:4-13.

21. Banchereau, J., V. Pascual, and A. K. Palucka. 2004. Autoimmunity through cytokine-induced dendritic cell activation. *Immunity* 20:539-550.

22. Carroll, M. C. 1998. The role of complement and complement receptors in induction and regulation of immunity. *Annu Rev Immunol* 16:545-568.

23. Gao, N., T. Dang, W. A. Dunnick, J. T. Collins, B. R. Blazar, and D. Yuan. 2005. Receptors and counterreceptors involved in NK-B cell interactions. *J Immunol* 174:4113-4119.

24. Martin, F., and A. C. Chan. 2004. Pathogenic roles of B cells in human autoimmunity; insights from the clinic. *Immunity* 20:517-527.

25. Gongora, R., R. P. Stephan, Z. Zhang, and M. D. Cooper. 2001. An essential role for Daxx in the inhibition of B lymphopoiesis by type I interferons. *Immunity* 14:727-737.

26. Blanco, P., A. K. Palucka, M. Gill, V. Pascual, and J. Banchereau. 2001. Induction of dendritic cell differentiation by IFN-alpha in systemic lupus erythematosus. *Science* 294:1540-1543.

27. Ronnblom, L., and G. V. Alm. 2002. The natural interferon-alpha producing cells in systemic lupus erythematosus. *Hum Immunol* 63:1181-1193.

28. Baechler, E. C., F. M. Batliwalla, G. Karypis, P. M. Gaffney, W. A. Ortmann, K. J. Espe, K. B. Shark, W. J. Grande, K. M. Hughes, V. Kapur, P. K. Gregersen, and T. W. Behrens. 2003. Interferon-inducible gene expression signature in peripheral blood cells of patients with severe lupus. *Proc Natl Acad Sci U S A* 100:2610-2615.

29. Bennett, L., A. K. Palucka, E. Arce, V. Cantrell, J. Borvak, J. Banchereau, and V. Pascual. 2003. Interferon and granulopoiesis signatures in systemic lupus erythematosus blood. *J Exp Med* 197:711-723.

30. Jorgensen, T. N., M. R. Gubbels, and B. L. Kotzin. 2004. New insights into disease pathogenesis from mouse lupus genetics. *Curr Opin Immunol* 16:787-793.

31. Xie, T., L. Rowen, B. Aguado, M. E. Ahearn, A. Madan, S. Qin, R. D. Campbell, and L. Hood. 2003. Analysis of the gene-dense major histocompatibility complex class III region and its comparison to mouse. *Genome Res* 13:2621-2636.

32. Kumanovics, A., T. Takada, and K. F. Lindahl. 2003. Genomic organization of the mammalian MHC. *Annu Rev Immunol* 21:629-657.

33. Pickering, M. C., M. Botto, P. R. Taylor, P. J. Lachmann, and M. J. Walport. 2000. Systemic lupus erythematosus, complement deficiency, and apoptosis. *Adv Immunol* 76:227-324.

34. Blanchong, C. A., E. K. Chung, K. L. Rupert, Y. Yang, Z. Yang, B. Zhou, J. M. Moulds, and C. Y. Yu. 2001. Genetic, structural and functional diversities of human complement components C4A and C4B and their mouse homologues, Slp and C4. *Int Immunopharmacol* 1:365-392.

35. Yang, Y., E. K. Chung, B. Zhou, K. Lhotta, L. A. Hebert, D. J. Birmingham, B. H. Rovin, and C. Y. Yu. 2004. The intricate role of complement component C4 in human systemic lupus erythematosus. *Curr Dir Autoimmun* 7:98-132.

36. Trendelenburg, M., A. P. Manderson, L. Fossati-Jimack, M. J. Walport, and M. Botto. 2004. Monocytosis and accelerated activation of lymphocytes in C1q-deficient autoimmune-prone mice. *Immunology* 113:80-88.

37. Paul, E., O. O. Pozdnyakova, E. Mitchell, and M. C. Carroll. 2002. Anti-DNA autoreactivity in C4-deficient mice. *Eur J Immunol* 32:2672-2679.

38. Mitchell, D. A., M. C. Pickering, J. Warren, L. Fossati-Jimack, J. Cortes-Hernandez, H. T. Cook, M. Botto, and M. J. Walport. 2002. C1q deficiency and autoimmunity: the effects of genetic background on disease expression. *J Immunol* 168:2538-2543.

39. Chen, Z., S. B. Koralov, and G. Kelsoe. 2000. Complement C4 inhibits systemic autoimmunity through a mechanism independent of complement receptors CR1 and CR2. *J Exp Med* 192:1339-1352.

40. Walport, M. J. 2002. Complement and systemic lupus erythematosus. *Arthritis Res* 4 Suppl 3:S279-293.

41. Manderson, A. P., M. Botto, and M. J. Walport. 2004. The role of complement in the development of systemic lupus erythematosus. *Annu Rev Immunol* 22:431-456.

42. Gibofsky, A., R. J. Winchester, M. Patarroyo, M. Fotino, and H. G. Kunkel. 1978. Disease associations of the Ia-like human alloantigens. Contrasting patterns in rheumatoid arthritis and systemic lupus erythematosus. *J Exp Med* 148:1728-1732.

43. Reinertsen, J. L., J. H. Klippel, A. H. Johnson, A. D. Steinberg, J. L. Decker, and D. L. Mann. 1978. B-lymphocyte alloantigens associated with systemic lupus erythematosus. *N Engl J Med* 299:515-518.

44. Larsen, C. E., and C. A. Alper. 2004. The genetics of HLA-associated disease. *Curr Opin Immunol* 16:660-667.

45. Zanelli, E., F. C. Breedveld, and R. R. de Vries. 2000. HLA class II association with rheumatoid arthritis: facts and interpretations. *Hum Immunol* 61:1254-1261.

46. Liblau, R., and A. M. Gautam. 2000. HLA, molecular mimicry and multiple sclerosis. *Rev Immunogenet* 2:95-104.

47. Tan, F. K., and F. C. Arnett. 1998. The genetics of lupus. *Curr Opin Rheumatol* 10:399-408.

48. Harley, J. B., K. L. Moser, P. M. Gaffney, and T. W. Behrens. 1998. The genetics of human systemic lupus erythematosus. *Curr Opin Immunol* 10:690-696.

49. Lee, H. S., Y. H. Chung, T. G. Kim, T. H. Kim, J. B. Jun, S. Jung, S. C. Bae, and D. H. Yoo. 2003. Independent association of HLA-DR and FCgamma receptor

polymorphisms in Korean patients with systemic lupus erythematosus. *Rheumatology (Oxford)* 42:1501-1507.

50. Graham, R. R., C. D. Langefeld, P. M. Gaffney, W. A. Ortmann, S. A. Selby, E. C. Baechler, K. B. Shark, T. C. Ockenden, K. E. Rohlf, K. L. Moser, W. M. Brown, S. E. Gabriel, R. P. Messner, R. A. King, P. Horak, J. T. Elder, P. E. Stuart, S. S. Rich, and T. W. Behrens. 2001. Genetic linkage and transmission disequilibrium of marker haplotypes at chromosome 1q41 in human systemic lupus erythematosus. *Arthritis Res* 3:299-305.

51. Studnicka-Benke, A., G. Steiner, P. Petera, and J. S. Smolen. 1996. Tumour necrosis factor alpha and its soluble receptors parallel clinical disease and autoimmune activity in systemic lupus erythematosus. *Br J Rheumatol* 35:1067-1074.

52. Gomez, D., P. A. Correa, L. M. Gomez, J. Cadena, J. F. Molina, and J. M. Anaya. 2004. Th1/Th2 cytokines in patients with systemic lupus erythematosus: is tumor necrosis factor alpha protective? *Semin Arthritis Rheum* 33:404-413.

53. Abraham, L. J., and K. M. Kroeger. 1999. Impact of the -308 TNF promoter polymorphism on the transcriptional regulation of the TNF gene: relevance to disease. *J Leukoc Biol* 66:562-566.

54. Bayley, J. P., H. de Rooij, P. J. van den Elsen, T. W. Huizinga, and C. L. Verweij. 2001. Functional analysis of linker-scan mutants spanning the -376, -308, -244, and -238 polymorphic sites of the TNF-alpha promoter. *Cytokine* 14:316-323.

55. Wilson, A. G., C. Gordon, F. S. di Giovine, N. de Vries, L. B. van de Putte, P. Emery, and G. W. Duff. 1994. A genetic association between systemic lupus erythematosus and tumor necrosis factor alpha. *Eur J Immunol* 24:191-195.

56. Rudwaleit, M., M. Tikly, M. Khamashta, K. Gibson, J. Klinke, G. Hughes, and P. Wordsworth. 1996. Interethnic differences in the association of tumor necrosis factor promoter polymorphisms with systemic lupus erythematosus. *J Rheumatol* 23:1725-1728.

57. Chen, C. J., J. H. Yen, W. C. Tsai, C. S. Wu, W. Chiang, J. J. Tsai, and H. W. Liu. 1997. The TNF2 allele does not contribute towards susceptibility to systemic lupus erythematosus. *Immunol Lett* 55:1-3.

58. Sullivan, K. E., C. Wooten, B. J. Schmeckpeper, D. Goldman, and M. A. Petri. 1997. A promoter polymorphism of tumor necrosis factor alpha associated with systemic lupus erythematosus in African-Americans. *Arthritis Rheum* 40:2207-2211.

59. Rood, M. J., M. V. van Krugten, E. Zanelli, M. W. van der Linden, V. Keijsers, G. M. Schreuder, W. Verduyn, R. G. Westendorp, R. R. de Vries, F. C. Breedveld, C. L. Verweij, and T. W. Huizinga. 2000. TNF-308A and HLA-DR3 alleles contribute independently to susceptibility to systemic lupus erythematosus. *Arthritis Rheum* 43:129-134.

60. van der Linden, M. W., A. R. van der Slik, E. Zanelli, M. J. Giphart, E. Pieterman, G. M. Schreuder, R. G. Westendorp, and T. W. Huizinga. 2001. Six microsatellite markers on the short arm of chromosome 6 in relation to HLA-DR3 and TNF-308A in systemic lupus erythematosus. *Genes Immun* 2:373-380.

61. Tsuchiya, N., A. Kawasaki, B. P. Tsao, T. Komata, J. M. Grossman, and K. Tokunaga. 2001. Analysis of the association of HLA-DRB1, TNFalpha promoter and TNFR2 (TNFRSF1B) polymorphisms with SLE using transmission disequilibrium test. *Genes Immun* 2:317-322.

62. Parks, C. G., J. P. Pandey, M. A. Dooley, E. L. Treadwell, E. W. St Clair, G. S. Gilkeson, C. A. Feghali-Bostwick, and G. S. Cooper. 2004. Genetic polymorphisms in tumor necrosis factor (TNF)-alpha and TNF-beta in a population-based study of systemic lupus erythematosus: associations and interaction with the interleukin-1alpha-889 C/T polymorphism. *Hum Immunol* 65:622-631.

63. Cheng, J., K. Turksen, Q. C. Yu, H. Schreiber, M. Teng, and E. Fuchs. 1992. Cachexia and graft-vs.-host-disease-type skin changes in keratin promoter-driven TNF alpha transgenic mice. *Genes Dev* 6:1444-1456.

64. Grewal, I. S., K. D. Grewal, F. S. Wong, D. E. Picarella, C. A. Janeway, Jr., and R. A. Flavell. 1996. Local expression of transgene encoded TNF alpha in islets prevents autoimmune diabetes in nonobese diabetic (NOD) mice by preventing the development of auto-reactive islet-specific T cells. *J Exp Med* 184:1963-1974.

65. Alexopoulou, L., M. Pasparakis, and G. Kollias. 1997. A murine transmembrane tumor necrosis factor (TNF) transgene induces arthritis by cooperative p55/p75 TNF receptor signaling. *Eur J Immunol* 27:2588-2592.

66. Ravetch, J. V., and S. Bolland. 2001. IgG Fc receptors. *Annu Rev Immunol* 19:275-290.

67. Bolland, S., and J. V. Ravetch. 2000. Spontaneous autoimmune disease in Fc(gamma)RIIB-deficient mice results from strain-specific epistasis. *Immunity* 13:277-285.

68. Kimberly, R. P., J. Wu, A. W. Gibson, K. Su, H. Qin, X. Li, and J. C. Edberg. 2002. Diversity and duplicity: human FCgamma receptors in host defense and autoimmunity. *Immunol Res* 26:177-189.

69. Pearse, R. N., T. Kawabe, S. Bolland, R. Guinamard, T. Kurosaki, and J. V. Ravetch. 1999. SHIP recruitment attenuates Fc gamma RIIB-induced B cell apoptosis. *Immunity* 10:753-760.

70. Bolland, S., and J. V. Ravetch. 1999. Inhibitory pathways triggered by ITIM-containing receptors. *Adv Immunol* 72:149-177.

71. Manger, K., R. Repp, B. M. Spriewald, A. Rascu, A. Geiger, R. Wassmuth, N. A. Westerdaal, B. Wentz, B. Manger, J. R. Kalden, and J. G. van de Winkel. 1998. Fcgamma receptor IIa polymorphism in Caucasian patients with systemic lupus erythematosus: association with clinical symptoms. *Arthritis Rheum* 41:1181-1189.

72. Norsworthy, P., E. Theodoridis, M. Botto, P. Athanassiou, H. Beynon, C. Gordon, D. Isenberg, M. J. Walport, and K. A. Davies. 1999. Overrepresentation of the Fcgamma receptor type IIA R131/R131 genotype in caucasoid systemic lupus erythematosus patients with autoantibodies to C1q and glomerulonephritis. *Arthritis Rheum* 42:1828-1832.

73. Dijstelbloem, H. M., M. Bijl, R. Fijnheer, R. H. Scheepers, W. W. Oost, M. D. Jansen, W. J. Sluiter, P. C. Limburg, R. H. Derksen, J. G. van de Winkel, and C. G.

Kallenberg. 2000. Fcgamma receptor polymorphisms in systemic lupus erythematosus: association with disease and in vivo clearance of immune complexes. *Arthritis Rheum* 43:2793-2800.

74. Zuniga, R., S. Ng, M. G. Peterson, J. D. Reveille, B. A. Baethge, G. S. Alarcon, and J. E. Salmon. 2001. Low-binding alleles of Fcgamma receptor types IIA and IIIA are inherited independently and are associated with systemic lupus erythematosus in Hispanic patients. *Arthritis Rheum* 44:361-367.

75. Edberg, J. C., C. D. Langefeld, J. Wu, K. L. Moser, K. M. Kaufman, J. Kelly, V. Bansal, W. M. Brown, J. E. Salmon, S. S. Rich, J. B. Harley, and R. P. Kimberly. 2002. Genetic linkage and association of Fcgamma receptor IIIA (CD16A) on chromosome 1q23 with human systemic lupus erythematosus. *Arthritis Rheum* 46:2132-2140.

76. Karassa, F. B., T. A. Trikalinos, and J. P. Ioannidis. 2002. Role of the Fcgamma receptor IIa polymorphism in susceptibility to systemic lupus erythematosus and lupus nephritis: a meta-analysis. *Arthritis Rheum* 46:1563-1571.

77. Manger, K., R. Repp, M. Jansen, M. Geisselbrecht, R. Wassmuth, N. A. Westerdaal, A. Pfahlberg, B. Manger, J. R. Kalden, and J. G. van de Winkel. 2002. Fcgamma receptor IIa, IIIa, and IIIb polymorphisms in German patients with systemic lupus erythematosus: association with clinical symptoms. *Ann Rheum Dis* 61:786-792.

78. Chen, J. Y., C. M. Wang, K. C. Tsao, Y. H. Chow, J. M. Wu, C. L. Li, H. H. Ho, Y. J. Wu, and S. F. Luo. 2004. Fcgamma receptor IIa, IIIa, and IIIb polymorphisms of systemic lupus erythematosus in Taiwan. *Ann Rheum Dis* 63:877-880.

79. Jonsen, A., A. A. Bengtsson, G. Sturfelt, and L. Truedsson. 2004. Analysis of HLA DR, HLA DQ, C4A, FcgammaRIIa, FcgammaRIIIa, MBL, and IL-1Ra allelic variants in Caucasian systemic lupus erythematosus patients suggests an effect of the combined FcgammaRIIa R/R and IL-1Ra 2/2 genotypes on disease susceptibility. *Arthritis Res Ther* 6:R557-562.

80. Magnusson, V., B. Johanneson, G. Lima, J. Odeberg, D. Alarcon-Segovia, and M. E. Alarcon-Riquelme. 2004. Both risk alleles for FcgammaRIIA and FcgammaRIIIA are susceptibility factors for SLE: a unifying hypothesis. *Genes Immun* 5:130-137.

81. Seligman, V. A., C. Suarez, R. Lum, S. E. Inda, D. Lin, H. Li, J. L. Olson, M. F. Seldin, and L. A. Criswell. 2001. The Fcgamma receptor IIIA-158F allele is a major risk factor for the development of lupus nephritis among Caucasians but not non-Caucasians. *Arthritis Rheum* 44:618-625.

82. Lee, E. B., Y. J. Lee, H. J. Baek, S. W. Kang, E. S. Chung, C. H. Shin, K. M. Hong, B. P. Tsao, B. H. Hahn, and Y. W. Song. 2002. Fcgamma receptor IIIA polymorphism in Korean patients with systemic lupus erythematosus. *Rheumatol Int* 21:222-226.

83. Bolland, S., Y. S. Yim, K. Tus, E. K. Wakeland, and J. V. Ravetch. 2002. Genetic modifiers of systemic lupus erythematosus in FcgammaRIIB(-/-) mice. *J Exp Med* 195:1167-1174.

84. Kyogoku, C., H. M. Dijstelbloem, N. Tsuchiya, Y. Hatta, H. Kato, A. Yamaguchi, T. Fukazawa, M. D. Jansen, H. Hashimoto, J. G. van de Winkel, C. G. Kallenberg, and K. Tokunaga. 2002. Fcgamma receptor gene polymorphisms in Japanese patients

with systemic lupus erythematosus: contribution of FCGR2B to genetic susceptibility. *Arthritis Rheum* 46:1242-1254.

85. Siriboonrit, U., N. Tsuchiya, M. Sirikong, C. Kyogoku, S. Bejrachandra, P. Suthipinittharm, K. Luangtrakool, D. Srinak, R. Thongpradit, K. Fujiwara, D. Chandanayingyong, and K. Tokunaga. 2003. Association of Fcgamma receptor IIb and IIIb polymorphisms with susceptibility to systemic lupus erythematosus in Thais. *Tissue Antigens* 61:374-383.

86. Chu, Z. T., N. Tsuchiya, C. Kyogoku, J. Ohashi, Y. P. Qian, S. B. Xu, C. Z. Mao, J. Y. Chu, and K. Tokunaga. 2004. Association of Fcgamma receptor IIb polymorphism with susceptibility to systemic lupus erythematosus in Chinese: a common susceptibility gene in the Asian populations. *Tissue Antigens* 63:21-27.

87. Okazaki, T., Y. Iwai, and T. Honjo. 2002. New regulatory co-receptors: inducible co-stimulator and PD-1. *Curr Opin Immunol* 14:779-782.

88. Kristiansen, O. P., Z. M. Larsen, and F. Pociot. 2000. CTLA-4 in autoimmune diseases--a general susceptibility gene to autoimmunity? *Genes Immun* 1:170-184.

89. Chen, L. 2004. Co-inhibitory molecules of the B7-CD28 family in the control of T-cell immunity. *Nat Rev Immunol* 4:336-347.

90. Heward, J., C. Gordon, A. Allahabadia, A. H. Barnett, J. A. Franklyn, and S. C. Gough. 1999. The A-G polymorphism in exon 1 of the CTLA-4 gene is not associated with systemic lupus erythematosus. *Ann Rheum Dis* 58:193-195.

91. Pullmann, R., Jr., J. Lukac, M. Skerenova, J. Rovensky, J. Hybenova, V. Melus, S. Celec, R. Pullmann, and R. Hyrdel. 1999. Cytotoxic T lymphocyte antigen 4 (CTLA-

4) dimorphism in patients with systemic lupus erythematosus. *Clin Exp Rheumatol* 17:725-729.

92. D'Alfonso, S., M. Rampi, D. Bocchio, G. Colombo, R. Scorza-Smeraldi, and P. Momigliano-Richardi. 2000. Systemic lupus erythematosus candidate genes in the Italian population: evidence for a significant association with interleukin-10. *Arthritis Rheum* 43:120-128.

93. Matsushita, M., N. Tsuchiya, M. Shiota, T. Komata, K. Matsuta, K. Zama, T. Oka, T. Juji, A. Yamane, and K. Tokunaga. 1999. Lack of a strong association of CTLA-4 exon 1 polymorphism with the susceptibility to rheumatoid arthritis and systemic lupus erythematosus in Japanese: an association study using a novel variation screening method. *Tissue Antigens* 54:578-584.

94. Ahmed, S., K. Ihara, S. Kanemitsu, H. Nakashima, T. Otsuka, K. Tsuzaka, T. Takeuchi, and T. Hara. 2001. Association of CTLA-4 but not CD28 gene polymorphisms with systemic lupus erythematosus in the Japanese population. *Rheumatology (Oxford)* 40:662-667.

95. Barreto, M., E. Santos, R. Ferreira, C. Fesel, M. F. Fontes, C. Pereira, B. Martins, R. Andreia, J. F. Viana, F. Crespo, C. Vasconcelos, C. Ferreira, and A. M. Vicente. 2004. Evidence for CTLA4 as a susceptibility gene for systemic lupus erythematosus. *Eur J Hum Genet* 12:620-626.

96. Torres, B., F. Aguilar, E. Franco, E. Sanchez, J. Sanchez-Roman, J. Jimenez Alonso, A. Nunez-Roldan, J. Martin, and M. F. Gonzalez-Escribano. 2004. Association of the

CT60 marker of the CTLA4 gene with systemic lupus erythematosus. *Arthritis Rheum* 50:2211-2215.

97. Parks, C. G., L. L. Hudson, G. S. Cooper, M. A. Dooley, E. L. Treadwell, E. W. St Clair, G. S. Gilkeson, and J. P. Pandey. 2004. CTLA-4 gene polymorphisms and systemic lupus erythematosus in a population-based study of whites and African-Americans in the southeastern United States. *Lupus* 13:784-791.

98. Liu, M. F., H. S. Liu, C. R. Wang, and H. Y. Lei. 1998. Expression of CTLA-4 molecule in peripheral blood T lymphocytes from patients with systemic lupus erythematosus. *J Clin Immunol* 18:392-398.

99. Liu, M. F., C. R. Wang, P. C. Chen, and L. L. Fung. 2003. Increased expression of soluble cytotoxic T-lymphocyte-associated antigen-4 molecule in patients with systemic lupus erythematosus. *Scand J Immunol* 57:568-572.

100. Hirashima, M., T. Fukazawa, K. Abe, Y. Morita, M. Kusaoi, and H. Hashimoto. 2004. Expression and activity analyses of CTLA4 in peripheral blood lymphocytes in systemic lupus erythematosus patients. *Lupus* 13:24-31.

101. Lindqvist, A. K., K. Steinsson, B. Johanneson, H. Kristjansdottir, A. Arnasson, G. Grondal, I. Jonasson, V. Magnusson, G. Sturfelt, L. Truedsson, E. Svenungsson, I. Lundberg, J. D. Terwilliger, U. B. Gyllensten, and M. E. Alarcon-Riquelme. 2000. A susceptibility locus for human systemic lupus erythematosus (hSLE1) on chromosome 2q. *J Autoimmun* 14:169-178.

102. Nishimura, H., M. Nose, H. Hiai, N. Minato, and T. Honjo. 1999. Development of lupus-like autoimmune diseases by disruption of the PD-1 gene encoding an ITIM motif-carrying immunoreceptor. *Immunity* 11:141-151.

103. Nishimura, H., T. Okazaki, Y. Tanaka, K. Nakatani, M. Hara, A. Matsumori, S. Sasayama, A. Mizoguchi, H. Hiai, N. Minato, and T. Honjo. 2001. Autoimmune dilated cardiomyopathy in PD-1 receptor-deficient mice. *Science* 291:319-322.

104. Prokunina, L., C. Castillejo-Lopez, F. Oberg, I. Gunnarsson, L. Berg, V. Magnusson, A. J. Brookes, D. Tentler, H. Kristjansdottir, G. Grondal, A. I. Bolstad, E. Svenungsson, I. Lundberg, G. Sturfelt, A. Jonssen, L. Truedsson, G. Lima, J. Alcocer-Varela, R. Jonsson, U. B. Gyllensten, J. B. Harley, D. Alarcon-Segovia, K. Steinsson, and M. E. Alarcon-Riquelme. 2002. A regulatory polymorphism in PDCD1 is associated with susceptibility to systemic lupus erythematosus in humans. *Nat Genet* 32:666-669.

105. Prokunina, L., I. Gunnarsson, G. Sturfelt, L. Truedsson, V. A. Seligman, J. L. Olson, M. F. Seldin, L. A. Criswell, and M. E. Alarcon-Riquelme. 2004. The systemic lupus erythematosus-associated PDCD1 polymorphism PD1.3A in lupus nephritis. *Arthritis Rheum* 50:327-328.

106. Ferreiros-Vidal, I., J. J. Gomez-Reino, F. Barros, A. Carracedo, P. Carreira, F. Gonzalez-Escribano, M. Liz, J. Martin, J. Ordi, J. L. Vicario, and A. Gonzalez. 2004. Association of PDCD1 with susceptibility to systemic lupus erythematosus: evidence of population-specific effects. *Arthritis Rheum* 50:2590-2597.

107. Nielsen, C., H. Laustrup, A. Voss, P. Junker, S. Husby, and S. T. Lillevang. 2004. A putative regulatory polymorphism in PD-1 is associated with nephropathy in a population-based cohort of systemic lupus erythematosus patients. *Lupus* 13:510-516.

108. Cote, J. F., P. L. Chung, J. F. Theberge, M. Halle, S. Spencer, L. A. Lasky, and M. L. Tremblay. 2002. PSTPIP is a substrate of PTP-PEST and serves as a scaffold guiding PTP-PEST toward a specific dephosphorylation of WASP. *J Biol Chem* 277:2973-2986.

109. Davidson, D., and A. Veillette. 2001. PTP-PEST, a scaffold protein tyrosine phosphatase, negatively regulates lymphocyte activation by targeting a unique set of substrates. *Embo J* 20:3414-3426.

110. Bottini, N., L. Musumeci, A. Alonso, S. Rahmouni, K. Nika, M. Rostamkhani, J. MacMurray, G. F. Meloni, P. Lucarelli, M. Pellecchia, G. S. Eisenbarth, D. Comings, and T. Mustelin. 2004. A functional variant of lymphoid tyrosine phosphatase is associated with type I diabetes. *Nat Genet* 36:337-338.

111. Gregersen, P. K. 2005. Pathways to gene identification in rheumatoid arthritis: PTPN22 and beyond. *Immunol Rev* 204:74-86.

112. Viken, M. K., S. S. Amundsen, T. K. Kvien, K. M. Boberg, I. M. Gilboe, V. Lilleby, L. M. Sollid, O. T. Forre, E. Thorsby, A. Smerdel, and B. A. Lie. 2005. Association analysis of the 1858C>T polymorphism in the PTPN22 gene in juvenile idiopathic arthritis and other autoimmune diseases. *Genes Immun* 6:271-273.

113. Lee, A. T., W. Li, A. Liew, C. Bombardier, M. Weisman, E. M. Massarotti, J. Kent, F. Wolfe, A. B. Begovich, and P. K. Gregersen. 2005. The PTPN22 R620W

polymorphism associates with RF positive rheumatoid arthritis in a dose-dependent manner but not with HLA-SE status. *Genes Immun* 6:129-133.

114. Orozco, G., E. Sanchez, M. A. Gonzalez-Gay, M. A. Lopez-Nevot, B. Torres, R. Caliz, N. Ortego-Centeno, J. Jimenez-Alonso, D. Pascual-Salcedo, A. Balsa, R. de Pablo, A. Nunez-Roldan, M. F. Gonzalez-Escribano, and J. Martin. 2005. Association of a functional single-nucleotide polymorphism of PTPN22, encoding lymphoid protein phosphatase, with rheumatoid arthritis and systemic lupus erythematosus. *Arthritis Rheum* 52:219-224.

115. Begovich, A. B., V. E. Carlton, L. A. Honigberg, S. J. Schrodi, A. P. Chokkalingam, H. C. Alexander, K. G. Ardlie, Q. Huang, A. M. Smith, J. M. Spoerke, M. T. Conn, M. Chang, S. Y. Chang, R. K. Saiki, J. J. Catanese, D. U. Leong, V. E. Garcia, L. B. McAllister, D. A. Jeffery, A. T. Lee, F. Batliwalla, E. Remmers, L. A. Criswell, M. F. Seldin, D. L. Kastner, C. I. Amos, J. J. Sninsky, and P. K. Gregersen. 2004. A missense single-nucleotide polymorphism in a gene encoding a protein tyrosine phosphatase (PTPN22) is associated with rheumatoid arthritis. *Am J Hum Genet* 75:330-337.

116. Qu, H., M. C. Tessier, T. J. Hudson, and C. Polychronakos. 2005. Confirmation of the association of the R620W polymorphism in the protein tyrosine phosphatase PTPN22 with type 1 diabetes in a family based study. *J Med Genet* 42:266-270.

117. Zheng, W., and J. X. She. 2005. Genetic association between a lymphoid tyrosine phosphatase (PTPN22) and type 1 diabetes. *Diabetes* 54:906-908.

118. Ladner, M. B., N. Bottini, A. M. Valdes, and J. A. Noble. 2005. Association of the single nucleotide polymorphism C1858T of the PTPN22 gene with type 1 diabetes. *Hum Immunol* 66:60-64.

119. Onengut-Gumuscu, S., K. G. Ewens, R. S. Spielman, and P. Concannon. 2004. A functional polymorphism (1858C/T) in the PTPN22 gene is linked and associated with type I diabetes in multiplex families. *Genes Immun* 5:678-680.

120. Smyth, D., J. D. Cooper, J. E. Collins, J. M. Heward, J. A. Franklyn, J. M. Howson, A. Vella, S. Nutland, H. E. Rance, L. Maier, B. J. Barratt, C. Guja, C. Ionescu-Tirgoviste, D. A. Savage, D. B. Dunger, B. Widmer, D. P. Strachan, S. M. Ring, N. Walker, D. G. Clayton, R. C. Twells, S. C. Gough, and J. A. Todd. 2004. Replication of an association between the lymphoid tyrosine phosphatase locus (LYP/PTPN22) with type 1 diabetes, and evidence for its role as a general autoimmunity locus. *Diabetes* 53:3020-3023.

121. Kyogoku, C., C. D. Langefeld, W. A. Ortmann, A. Lee, S. Selby, V. E. Carlton, M. Chang, P. Ramos, E. C. Baechler, F. M. Batliwalla, J. Novitzke, A. H. Williams, C. Gillett, P. Rodine, R. R. Graham, K. G. Ardlie, P. M. Gaffney, K. L. Moser, M. Petri, A. B. Begovich, P. K. Gregersen, and T. W. Behrens. 2004. Genetic association of the R620W polymorphism of protein tyrosine phosphatase PTPN22 with human SLE. *Am J Hum Genet* 75:504-507.

122. Mori, M., R. Yamada, K. Kobayashi, R. Kawaida, and K. Yamamoto. 2005. Ethnic differences in allele frequency of autoimmune-disease-associated SNPs. *J Hum Genet*.

123. Hill, N., and N. Sarvetnick. 2002. Cytokines: promoters and dampeners of autoimmunity. *Curr Opin Immunol* 14:791-797.

124. Moore, K. W., R. de Waal Malefyt, R. L. Coffman, and A. O'Garra. 2001. Interleukin-10 and the interleukin-10 receptor. *Annu Rev Immunol* 19:683-765.

125. Houssiau, F. A., C. Lefebvre, M. Vanden Berghe, M. Lambert, J. P. Devogelaer, and J. C. Renauld. 1995. Serum interleukin 10 titers in systemic lupus erythematosus reflect disease activity. *Lupus* 4:393-395.

126. Llorente, L., Y. Richaud-Patin, J. Couderc, D. Alarcon-Segovia, R. Ruiz-Soto, N. Alcocer-Castillejos, J. Alcocer-Varela, J. Granados, S. Bahena, P. Galanaud, and D. Emilie. 1997. Dysregulation of interleukin-10 production in relatives of patients with systemic lupus erythematosus. *Arthritis Rheum* 40:1429-1435.

127. Capper, E. R., J. K. Maskill, C. Gordon, and A. I. Blakemore. 2004. Interleukin (IL)-10, IL-1ra and IL-12 profiles in active and quiescent systemic lupus erythematosus: could longitudinal studies reveal patient subgroups of differing pathology? *Clin Exp Immunol* 138:348-356.

128. Lauwerys, B. R., N. Garot, J. C. Renauld, and F. A. Houssiau. 2000. Interleukin-10 blockade corrects impaired in vitro cellular immune responses of systemic lupus erythematosus patients. *Arthritis Rheum* 43:1976-1981.

129. Llorente, L., Y. Richaud-Patin, C. Garcia-Padilla, E. Claret, J. Jakez-Ocampo, M. H. Cardiel, J. Alcocer-Varela, L. Grangeot-Keros, D. Alarcon-Segovia, J. Wijdenes, P. Galanaud, and D. Emilie. 2000. Clinical and biologic effects of anti-interleukin-10

monoclonal antibody administration in systemic lupus erythematosus. *Arthritis Rheum* 43:1790-1800.

130. Mok, C. C., J. S. Lanchbury, D. W. Chan, and C. S. Lau. 1998. Interleukin-10 promoter polymorphisms in Southern Chinese patients with systemic lupus erythematosus. *Arthritis Rheum* 41:1090-1095.

131. Lazarus, M., A. H. Hajeer, D. Turner, P. Sinnott, J. Worthington, W. E. Ollier, and I. V. Hutchinson. 1997. Genetic variation in the interleukin 10 gene promoter and systemic lupus erythematosus. *J Rheumatol* 24:2314-2317.

132. Schotte, H., M. Gaubitz, P. Willeke, N. Tidow, G. Assmann, W. Domschke, and B. Schluter. 2004. Interleukin-10 promoter microsatellite polymorphisms in systemic lupus erythematosus: association with the anti-Sm immune response. *Rheumatology (Oxford)* 43:1357-1363.

133. Khoa, P. D., T. Sugiyama, and T. Yokochi. 2005. Polymorphism of interleukin-10 promoter and tumor necrosis factor receptor II in Vietnamese patients with systemic lupus erythematosus. *Clin Rheumatol* 24:11-13.

134. Alarcon-Riquelme, M. E., A. K. Lindqvist, I. Jonasson, B. Johanneson, S. Sandino, J. Alcocer-Varela, J. Granados, H. Kristjansdottir, G. Grondal, E. Svenungsson, I. Lundberg, K. Steinsson, L. Klareskog, G. Sturfelt, L. Truedsson, D. Alarcon-Segovia, and U. B. Gyllensten. 1999. Genetic analysis of the contribution of IL10 to systemic lupus erythematosus. *J Rheumatol* 26:2148-2152.

135. D' Alfonso, S., M. Giordano, M. Mellai, M. Lanceni, N. Barizzone, M. Marchini, R. Scorza, M. G. Danieli, M. Cappelli, P. Rovere, M. G. Sabbadini, and P. Momigliano-

Richiardi. 2002. Association tests with systemic lupus erythematosus (SLE) of IL10 markers indicate a direct involvement of a CA repeat in the 5' regulatory region. *Genes Immun* 3:454-463.

136. Gibson, A. W., J. C. Edberg, J. Wu, R. G. Westendorp, T. W. Huizinga, and R. P. Kimberly. 2001. Novel single nucleotide polymorphisms in the distal IL-10 promoter affect IL-10 production and enhance the risk of systemic lupus erythematosus. *J Immunol* 166:3915-3922.

137. Chong, W. P., W. K. Ip, W. H. Wong, C. S. Lau, T. M. Chan, and Y. L. Lau. 2004. Association of interleukin-10 promoter polymorphisms with systemic lupus erythematosus. *Genes Immun* 5:484-492.

138. Wakeland, E. K., and A. E. Wandstrat. 2002. Analyzing genomes: current realities and future possibilities. *Curr Opin Immunol* 14:622-626.

139. Nath, S. K., J. Kilpatrick, and J. B. Harley. 2004. Genetics of human systemic lupus erythematosus: the emerging picture. *Curr Opin Immunol* 16:794-800.

140. Johansson, C. M., R. Zunec, M. A. Garcia, H. R. Scherbarth, G. A. Tate, S. Paira, S. M. Navarro, C. E. Perandones, S. Gamron, A. Alvarellos, C. E. Graf, J. Manni, G. A. Berbotto, S. A. Palatnik, L. J. Catoggio, C. G. Battagliotti, G. D. Sebastiani, S. Migliaresi, M. Galeazzi, B. A. Pons-Estel, and M. E. Alarcon-Riquelme. 2004. Chromosome 17p12-q11 harbors susceptibility loci for systemic lupus erythematosus. *Hum Genet* 115:230-238.

141. Lander, E., and L. Kruglyak. 1995. Genetic dissection of complex traits: guidelines for interpreting and reporting linkage results. *Nat Genet* 11:241-247.

142. Nath, S. K., B. Namjou, D. Hutchings, C. P. Garriott, C. Pongratz, J. Guthridge, and J. A. James. 2004. Systemic lupus erythematosus (SLE) and chromosome 16: confirmation of linkage to 16q12-13 and evidence for genetic heterogeneity. *Eur J Hum Genet* 12:668-672.

143. Nath, S. K., B. Namjou, C. P. Garriott, S. Frank, P. A. Joslin, J. Kilpatrick, J. A. Kelly, and J. B. Harley. 2004. Linkage analysis of SLE susceptibility: confirmation of SLER1 at 5p15.3. *Genes Immun* 5:209-214.

144. Moser, K. L., C. Gray-McGuire, J. Kelly, N. Asundi, H. Yu, G. R. Bruner, M. Mange, R. Hogue, B. R. Neas, and J. B. Harley. 1999. Confirmation of genetic linkage between human systemic lupus erythematosus and chromosome 1q41. *Arthritis Rheum* 42:1902-1907.

145. Nath, S. K., A. I. Quintero-Del-Rio, J. Kilpatrick, L. Feo, M. Ballesteros, and J. B. Harley. 2004. Linkage at 12q24 with systemic lupus erythematosus (SLE) is established and confirmed in Hispanic and European American families. *Am J Hum Genet* 74:73-82.

146. Morel, L., U. H. Rudofsky, J. A. Longmate, J. Schiffenbauer, and E. K. Wakeland. 1994. Polygenic control of susceptibility to murine systemic lupus erythematosus. *Immunity* 1:219-229.

147. Drake, C. G., S. J. Rozzo, T. J. Vyse, E. Palmer, and B. L. Kotzin. 1995. Genetic contributions to lupus-like disease in (NZB x NZW)F1 mice. *Immunol Rev* 144:51-74.

148. Rozzo, S. J., T. J. Vyse, C. G. Drake, and B. L. Kotzin. 1996. Effect of genetic background on the contribution of New Zealand black loci to autoimmune lupus nephritis. *Proc Natl Acad Sci U S A* 93:15164-15168.

149. Vyse, T. J., S. J. Rozzo, C. G. Drake, S. Izui, and B. L. Kotzin. 1997. Control of multiple autoantibodies linked with a lupus nephritis susceptibility locus in New Zealand black mice. *J Immunol* 158:5566-5574.

150. Wither, J. E., A. D. Paterson, and B. Vukusic. 2000. Genetic dissection of B cell traits in New Zealand black mice. The expanded population of B cells expressing up-regulated costimulatory molecules shows linkage to Nba2. *Eur J Immunol* 30:356-365.

151. Gaffney, P. M., W. A. Ortmann, S. A. Selby, K. B. Shark, T. C. Ockenden, K. E. Rohlf, N. L. Walgrave, W. P. Boyum, M. L. Malmgren, M. E. Miller, G. M. Kearns, R. P. Messner, R. A. King, S. S. Rich, and T. W. Behrens. 2000. Genome screening in human systemic lupus erythematosus: results from a second Minnesota cohort and combined analyses of 187 sib-pair families. *Am J Hum Genet* 66:547-556.

152. Gaffney, P. M., G. M. Kearns, K. B. Shark, W. A. Ortmann, S. A. Selby, M. L. Malmgren, K. E. Rohlf, T. C. Ockenden, R. P. Messner, R. A. King, S. S. Rich, and T. W. Behrens. 1998. A genome-wide search for susceptibility genes in human systemic lupus erythematosus sib-pair families. *Proc Natl Acad Sci U S A* 95:14875-14879.

153. Morel, L., K. R. Blenman, B. P. Croker, and E. K. Wakeland. 2001. The major murine systemic lupus erythematosus susceptibility locus, Sle1, is a cluster of functionally related genes. *Proc Natl Acad Sci U S A* 98:1787-1792.

154. Cantor, R. M., J. Yuan, S. Napier, N. Kono, J. M. Grossman, B. H. Hahn, and B. P. Tsao. 2004. Systemic lupus erythematosus genome scan: support for linkage at 1q23, 2q33, 16q12-13, and 17q21-23 and novel evidence at 3p24, 10q23-24, 13q32, and 18q22-23. *Arthritis Rheum* 50:3203-3210.

155. Nguyen, C., N. Limaye, and E. K. Wakeland. 2002. Susceptibility genes in the pathogenesis of murine lupus. *Arthritis Res* 4 Suppl 3:S255-263.

156. Moser, K. L., B. R. Neas, J. E. Salmon, H. Yu, C. Gray-McGuire, N. Asundi, G. R. Bruner, J. Fox, J. Kelly, S. Henshall, D. Bacino, M. Dietz, R. Hogue, G. Koelsch, L. Nightingale, T. Shaver, N. I. Abdou, D. A. Albert, C. Carson, M. Petri, E. L. Treadwell, J. A. James, and J. B. Harley. 1998. Genome scan of human systemic lupus erythematosus: evidence for linkage on chromosome 1q in African-American pedigrees. *Proc Natl Acad Sci U S A* 95:14869-14874.

157. Gray-McGuire, C., K. L. Moser, P. M. Gaffney, J. Kelly, H. Yu, J. M. Olson, C. M. Jedrey, K. B. Jacobs, R. P. Kimberly, B. R. Neas, S. S. Rich, T. W. Behrens, and J. B. Harley. 2000. Genome scan of human systemic lupus erythematosus by regression modeling: evidence of linkage and epistasis at 4p16-15.2. *Am J Hum Genet* 67:1460-1469.

158. Nath, S. K., J. A. Kelly, J. Reid, T. Lam, C. Gray-McGuire, B. Namjou, C. E. Aston, and J. B. Harley. 2002. SLEB3 in systemic lupus erythematosus (SLE) is strongly related to SLE families ascertained through neuropsychiatric manifestations. *Hum Genet* 111:54-58.

159. Shai, R., F. P. Quismorio, Jr., L. Li, O. J. Kwon, J. Morrison, D. J. Wallace, C. M. Neuwelt, C. Brautbar, W. J. Gauderman, and C. O. Jacob. 1999. Genome-wide screen for systemic lupus erythematosus susceptibility genes in multiplex families. *Hum Mol Genet* 8:639-644.

160. Watanabe-Fukunaga, R., C. I. Brannan, N. G. Copeland, N. A. Jenkins, and S. Nagata. 1992. Lymphoproliferation disorder in mice explained by defects in Fas antigen that mediates apoptosis. *Nature* 356:314-317.

161. Watson, M. L., J. K. Rao, G. S. Gilkeson, P. Ruiz, E. M. Eicher, D. S. Pisetsky, A. Matsuzawa, J. M. Rochelle, and M. F. Seldin. 1992. Genetic analysis of MRL-lpr mice: relationship of the Fas apoptosis gene to disease manifestations and renal disease-modifying loci. *J Exp Med* 176:1645-1656.

162. Vratsanos, G. S., S. Jung, Y. M. Park, and J. Craft. 2001. CD4(+) T cells from lupus-prone mice are hyperresponsive to T cell receptor engagement with low and high affinity peptide antigens: a model to explain spontaneous T cell activation in lupus. *J Exp Med* 193:329-337.

163. Zielinski, C. E., S. N. Jacob, F. Bouzahzah, B. E. Ehrlich, and J. Craft. 2005. Naive CD4+ T cells from lupus-prone Fas-intact MRL mice display TCR-mediated hyperproliferation due to intrinsic threshold defects in activation. *J Immunol* 174:5100-5109.

164. Hron, J. D., and S. L. Peng. 2004. Type I IFN protects against murine lupus. *J Immunol* 173:2134-2142.

165. Miwa, T., M. A. Maldonado, L. Zhou, X. Sun, H. Y. Luo, D. Cai, V. P. Werth, M. P. Madaio, R. A. Eisenberg, and W. C. Song. 2002. Deletion of decay-accelerating factor (CD55) exacerbates autoimmune disease development in MRL/lpr mice. *Am J Pathol* 161:1077-1086.

166. Yin, Z., G. Bahtiyar, N. Zhang, L. Liu, P. Zhu, M. E. Robert, J. McNiff, M. P. Madaio, and J. Craft. 2002. IL-10 regulates murine lupus. *J Immunol* 169:2148-2155.

167. Liang, B., R. J. Gee, M. J. Kashgarian, A. H. Sharpe, and M. J. Mamula. 1999. B7 costimulation in the development of lupus: autoimmunity arises either in the absence of B7.1/B7.2 or in the presence of anti-b7.1/B7.2 blocking antibodies. *J Immunol* 163:2322-2329.

168. Lenda, D. M., E. R. Stanley, and V. R. Kelley. 2004. Negative role of colony-stimulating factor-1 in macrophage, T cell, and B cell mediated autoimmune disease in MRL-Fas(lpr) mice. *J Immunol* 173:4744-4754.

169. Kevil, C. G., M. J. Hicks, X. He, J. Zhang, C. M. Ballantyne, C. Raman, T. R. Schoeb, and D. C. Bullard. 2004. Loss of LFA-1, but not Mac-1, protects MRL/MpJ-Fas(lpr) mice from autoimmune disease. *Am J Pathol* 165:609-616.

170. Morito, N., K. Yoh, A. Hirayama, K. Itoh, M. Nose, A. Koyama, M. Yamamoto, and S. Takahashi. 2004. Nrf2 deficiency improves autoimmune nephritis caused by the fas mutation lpr. *Kidney Int* 65:1703-1713.

171. Robey, I. F., M. Peterson, M. S. Horwitz, D. H. Kono, T. Stratmann, A. N. Theofilopoulos, N. Sarvetnick, L. Teyton, and A. J. Feeney. 2004. Terminal deoxynucleotidyltransferase deficiency decreases autoimmune disease in diabetes-

prone nonobese diabetic mice and lupus-prone MRL-Fas(lpr) mice. *J Immunol* 172:4624-4629.

172. Xiao, S., S. S. Sung, S. M. Fu, and S. T. Ju. 2003. Combining Fas mutation with interleukin-2 deficiency prevents Colitis and Lupus: implicating interleukin-2 for auto-reactive T cell expansion and Fas ligand for colon epithelial cell death. *J Biol Chem* 278:52730-52738.

173. Kikawada, E., D. M. Lenda, and V. R. Kelley. 2003. IL-12 deficiency in MRL-Fas(lpr) mice delays nephritis and intrarenal IFN-gamma expression, and diminishes systemic pathology. *J Immunol* 170:3915-3925.

174. Watanabe, H., G. Garnier, A. Circolo, R. A. Wetsel, P. Ruiz, V. M. Holers, S. A. Boackle, H. R. Colten, and G. S. Gilkeson. 2000. Modulation of renal disease in MRL/lpr mice genetically deficient in the alternative complement pathway factor B. *J Immunol* 164:786-794.

175. Tada, Y., K. Nagasawa, A. Ho, F. Morito, S. Koarada, O. Ushiyama, N. Suzuki, A. Ohta, and T. W. Mak. 1999. Role of the costimulatory molecule CD28 in the development of lupus in MRL/lpr mice. *J Immunol* 163:3153-3159.

176. Schwarting, A., T. Wada, K. Kinoshita, G. Tesch, and V. R. Kelley. 1998. IFN-gamma receptor signaling is essential for the initiation, acceleration, and destruction of autoimmune kidney disease in MRL-Fas(lpr) mice. *J Immunol* 161:494-503.

177. Lin, L., and S. L. Peng. 2005. Interleukin-18 receptor signaling is not required for autoantibody production and end-organ disease in murine lupus. *Arthritis Rheum* 52:984-986.

178. Matsumoto, K., N. Watanabe, B. Akikusa, K. Kurasawa, R. Matsumura, Y. Saito, I. Iwamoto, and T. Saito. 2003. Fc receptor-independent development of autoimmune glomerulonephritis in lupus-prone MRL/lpr mice. *Arthritis Rheum* 48:486-494.

179. Vidal, S., D. H. Kono, and A. N. Theofilopoulos. 1998. Loci predisposing to autoimmunity in MRL-Fas lpr and C57BL/6-Faslpr mice. *J Clin Invest* 101:696-702.

180. Gu, L., A. Weinreb, X. P. Wang, D. J. Zack, J. H. Qiao, R. Weisbart, and A. J. Lusis. 1998. Genetic determinants of autoimmune disease and coronary vasculitis in the MRL-lpr/lpr mouse model of systemic lupus erythematosus. *J Immunol* 161:6999-7006.

181. Kamogawa, J., M. Terada, M. Nishihara, S. Mizuki, S. Mori, S. Nakatsuru, Y. Nakamura, and M. Nose. 1999. [Susceptibility loci to autoimmune arthritis in MRL/lpr mice]. *Nihon Rinsho Meneki Gakkai Kaishi* 22:487-490.

182. Nishihara, M., M. Terada, J. Kamogawa, Y. Ohashi, S. Mori, S. Nakatsuru, Y. Nakamura, and M. Nose. 1999. Genetic basis of autoimmune sialadenitis in MRL/lpr lupus-prone mice: additive and hierarchical properties of polygenic inheritance. *Arthritis Rheum* 42:2616-2623.

183. Nakatsuru, S., M. Terada, M. Nishihara, J. Kamogawa, T. Miyazaki, W. M. Qu, K. Morimoto, C. Yazawa, H. Ogasawara, Y. Abe, K. Fukui, G. Ichien, M. R. Ito, S. Mori, Y. Nakamura, and M. Nose. 1999. Genetic dissection of the complex pathological manifestations of collagen disease in MRL/lpr mice. *Pathol Int* 49:974-982.

184. Kamogawa, J., M. Terada, S. Mizuki, M. Nishihara, H. Yamamoto, S. Mori, Y. Abe, K. Morimoto, S. Nakatsuru, Y. Nakamura, and M. Nose. 2002. Arthritis in MRL/lpr

mice is under the control of multiple gene loci with an allelic combination derived from the original inbred strains. *Arthritis Rheum* 46:1067-1074.

185. Hudgins, C. C., R. T. Steinberg, D. M. Klinman, M. J. Reeves, and A. D. Steinberg. 1985. Studies of consomic mice bearing the Y chromosome of the BXSB mouse. *J Immunol* 134:3849-3854.

186. Kikuchi, S., L. Fossati-Jimack, T. Moll, H. Amano, E. Amano, A. Ida, N. Ibnou-Zekri, C. Laporte, M. L. Santiago-Raber, S. J. Rozzo, B. L. Kotzin, and S. Izui. 2005. Differential role of three major New Zealand Black-derived loci linked with Yaa-induced murine lupus nephritis. *J Immunol* 174:1111-1117.

187. Santiago, M. L., C. Mary, D. Parzy, C. Jacquet, X. Montagutelli, R. M. Parkhouse, R. Lemoine, S. Izui, and L. Reininger. 1998. Linkage of a major quantitative trait locus to Yaa gene-induced lupus-like nephritis in (NZW x C57BL/6)F1 mice. *Eur J Immunol* 28:4257-4267.

188. Merino, R., M. Iwamoto, M. E. Gershwin, and S. Izui. 1994. The Yaa gene abrogates the major histocompatibility complex association of murine lupus in (NZB x BXSB)F1 hybrid mice. *J Clin Invest* 94:521-525.

189. Chu, E. B., D. N. Ernst, M. V. Hobbs, and W. O. Weigle. 1994. Maturational changes in CD4+ cell subsets and lymphokine production in BXSB mice. *J Immunol* 152:4129-4138.

190. Crispin, J. C., and J. Alcocer-Varela. 1998. Interleukin-2 and systemic lupus erythematosus--fifteen years later. *Lupus* 7:214-222.

191. Juang, Y. T., Y. Wang, E. E. Solomou, Y. Li, C. Mawrin, K. Tenbrock, V. C. Kyttaris, and G. C. Tsokos. 2005. Systemic lupus erythematosus serum IgG increases CREM binding to the IL-2 promoter and suppresses IL-2 production through CaMKIV. *J Clin Invest* 115:996-1005.

192. Chowdhury, B., C. G. Tsokos, S. Krishnan, J. Robertson, C. U. Fisher, R. G. Warke, V. G. Warke, M. P. Nambiar, and G. C. Tsokos. 2005. Decreased Stability and Translation of T Cell Receptor {zeta} mRNA with an Alternatively Spliced 3'-Untranslated Region Contribute to {zeta} Chain Down-regulation in Patients with Systemic Lupus Erythematosus. *J Biol Chem* 280:18959-18966.

193. Chu, E. B., M. V. Hobbs, C. B. Wilson, C. G. Romball, P. S. Linsley, and W. O. Weigle. 1996. Intervention of CD4+ cell subset shifts and autoimmunity in the BXSB mouse by murine CTLA4Ig. *J Immunol* 156:1262-1268.

194. Lawson, B. R., R. Baccala, J. Song, M. Croft, D. H. Kono, and A. N. Theofilopoulos. 2004. Deficiency of the cyclin kinase inhibitor p21(WAF-1/CIP-1) promotes apoptosis of activated/memory T cells and inhibits spontaneous systemic autoimmunity. *J Exp Med* 199:547-557.

195. DesJardin, L. E., E. J. Butfiloski, E. S. Sobel, and J. Schiffenbauer. 1996. Hyperproliferation of BXSB B cells is linked to the Yaa allele. *Clin Immunol Immunopathol* 81:145-152.

196. Merino, R., L. Fossati, M. Lacour, and S. Izui. 1991. Selective autoantibody production by Yaa+ B cells in autoimmune Yaa(+)-Yaa- bone marrow chimeric mice. *J Exp Med* 174:1023-1029.

197. Lawson, B. R., S. I. Koundouris, M. Barnhouse, W. Dummer, R. Baccala, D. H. Kono, and A. N. Theofilopoulos. 2001. The role of alpha beta+ T cells and homeostatic T cell proliferation in Y-chromosome-associated murine lupus. *J Immunol* 167:2354-2360.

198. Fossati, L., E. S. Sobel, M. Iwamoto, P. L. Cohen, R. A. Eisenberg, and S. Izui. 1995. The Yaa gene-mediated acceleration of murine lupus: Yaa- T cells from non-autoimmune mice collaborate with Yaa+ B cells to produce lupus autoantibodies in vivo. *Eur J Immunol* 25:3412-3417.

199. Haywood, M. E., N. J. Rogers, S. J. Rose, J. Boyle, A. McDermott, J. M. Rankin, V. Thiruudaian, M. R. Lewis, L. Fossati-Jimack, S. Izui, M. J. Walport, and B. J. Morley. 2004. Dissection of BXSB lupus phenotype using mice congenic for chromosome 1 demonstrates that separate intervals direct different aspects of disease. *J Immunol* 173:4277-4285.

200. Croker, B. P., G. Gilkeson, and L. Morel. 2003. Genetic interactions between susceptibility loci reveal epistatic pathogenic networks in murine lupus. *Genes Immun* 4:575-585.

201. Morel, L., B. P. Croker, K. R. Blenman, C. Mohan, G. Huang, G. Gilkeson, and E. K. Wakeland. 2000. Genetic reconstitution of systemic lupus erythematosus immunopathology with polycongenic murine strains. *Proc Natl Acad Sci U S A* 97:6670-6675.

202. Morel, L., and E. K. Wakeland. 1998. Susceptibility to lupus nephritis in the NZB/W model system. *Curr Opin Immunol* 10:718-725.

203. Wither, J. E., V. Roy, and L. A. Brennan. 2000. Activated B cells express increased levels of costimulatory molecules in young autoimmune NZB and (NZB x NZW)F(1) mice. *Clin Immunol* 94:51-63.

204. Wellmann, U., M. Letz, A. Schneider, K. Amann, and T. H. Winkler. 2001. An Ig mu-heavy chain transgene inhibits systemic lupus erythematosus immunopathology in autoimmune (NZB x NZW)F1 mice. *Int Immunol* 13:1461-1469.

205. Wellmann, U., A. Werner, and T. H. Winkler. 2001. Altered selection processes of B lymphocytes in autoimmune NZB/W mice, despite intact central tolerance against DNA. *Eur J Immunol* 31:2800-2810.

206. Sato, T., S. Ishikawa, K. Akadegawa, T. Ito, H. Yurino, M. Kitabatake, H. Yoneyama, and K. Matsushima. 2004. Aberrant B1 cell migration into the thymus results in activation of CD4 T cells through its potent antigen-presenting activity in the development of murine lupus. *Eur J Immunol* 34:3346-3358.

207. Ito, T., S. Ishikawa, T. Sato, K. Akadegawa, H. Yurino, M. Kitabatake, S. Hontsu, T. Ezaki, H. Kimura, and K. Matsushima. 2004. Defective B1 cell homing to the peritoneal cavity and preferential recruitment of B1 cells in the target organs in a murine model for systemic lupus erythematosus. *J Immunol* 172:3628-3634.

208. Ishikawa, S., T. Sato, M. Abe, S. Nagai, N. Onai, H. Yoneyama, Y. Zhang, T. Suzuki, S. Hashimoto, T. Shirai, M. Lipp, and K. Matsushima. 2001. Aberrant high expression of B lymphocyte chemokine (BLC/CXCL13) by C11b+CD11c+ dendritic cells in murine lupus and preferential chemotaxis of B1 cells towards BLC. *J Exp Med* 193:1393-1402.

209. Mihara, M., I. Tan, Y. Chuzhin, B. Reddy, L. Budhai, A. Holzer, Y. Gu, and A. Davidson. 2000. CTLA4Ig inhibits T cell-dependent B-cell maturation in murine systemic lupus erythematosus. *J Clin Invest* 106:91-101.

210. Drake, C. G., S. K. Babcock, E. Palmer, and B. L. Kotzin. 1994. Genetic analysis of the NZB contribution to lupus-like autoimmune disease in (NZB x NZW)F1 mice. *Proc Natl Acad Sci U S A* 91:4062-4066.

211. Vyse, T. J., C. G. Drake, S. J. Rozzo, E. Roper, S. Izui, and B. L. Kotzin. 1996. Genetic linkage of IgG autoantibody production in relation to lupus nephritis in New Zealand hybrid mice. *J Clin Invest* 98:1762-1772.

212. Hirose, S., H. Tsurui, H. Nishimura, Y. Jiang, and T. Shirai. 1994. Mapping of a gene for hypergammaglobulinemia to the distal region on chromosome 4 in NZB mice and its contribution to systemic lupus erythematosus in (NZB x NZW)F1 mice. *Int Immunol* 6:1857-1864.

213. Xie, S., S. Chang, P. Yang, C. Jacob, A. Kaliyaperumal, S. K. Datta, and C. Mohan. 2001. Genetic contributions of nonautoimmune SWR mice toward lupus nephritis. *J Immunol* 167:7141-7149.

214. Tucker, R. M., T. J. Vyse, S. Rozzo, C. L. Roark, S. Izui, and B. L. Kotzin. 2000. Genetic control of glycoprotein 70 autoantigen production and its influence on immune complex levels and nephritis in murine lupus. *J Immunol* 165:1665-1672.

215. Kono, D. H., R. W. Burlingame, D. G. Owens, A. Kuramochi, R. S. Balderas, D. Balomenos, and A. N. Theofilopoulos. 1994. Lupus susceptibility loci in New Zealand mice. *Proc Natl Acad Sci U S A* 91:10168-10172.

216. Vyse, T. J., L. Morel, F. J. Tanner, E. K. Wakeland, and B. L. Kotzin. 1996. Backcross analysis of genes linked to autoantibody production in New Zealand White mice. *J Immunol* 157:2719-2727.

217. Atencio, S., H. Amano, S. Izui, and B. L. Kotzin. 2004. Separation of the New Zealand Black genetic contribution to lupus from New Zealand Black determined expansions of marginal zone B and B1a cells. *J Immunol* 172:4159-4166.

218. Rozzo, S. J., J. D. Allard, D. Choubey, T. J. Vyse, S. Izui, G. Peltz, and B. L. Kotzin. 2001. Evidence for an interferon-inducible gene, Ifi202, in the susceptibility to systemic lupus. *Immunity* 15:435-443.

219. Vyse, T. J., R. K. Halterman, S. J. Rozzo, S. Izui, and B. L. Kotzin. 1999. Control of separate pathogenic autoantibody responses marks MHC gene contributions to murine lupus. *Proc Natl Acad Sci U S A* 96:8098-8103.

220. Drake, C. G., S. J. Rozzo, H. F. Hirschfeld, N. P. Smarnworawong, E. Palmer, and B. L. Kotzin. 1995. Analysis of the New Zealand Black contribution to lupus-like renal disease. Multiple genes that operate in a threshold manner. *J Immunol* 154:2441-2447.

221. Vyse, T. J., S. J. Rozzo, C. G. Drake, V. B. Appel, M. Lemeur, S. Izui, E. Palmer, and B. L. Kotzin. 1998. Contributions of Ea(z) and Eb(z) MHC genes to lupus susceptibility in New Zealand mice. *J Immunol* 160:2757-2766.

222. Rozzo, S. J., T. J. Vyse, C. S. David, E. Palmer, S. Izui, and B. L. Kotzin. 1999. Analysis of MHC class II genes in the susceptibility to lupus in New Zealand mice. *J Immunol* 162:2623-2630.

223. Morel, L., and E. K. Wakeland. 2000. Lessons from the NZM2410 model and related strains. *Int Rev Immunol* 19:423-446.

224. Morel, L., C. Mohan, Y. Yu, J. Schiffenbauer, U. H. Rudofsky, N. Tian, J. A. Longmate, and E. K. Wakeland. 1999. Multiplex inheritance of component phenotypes in a murine model of lupus. *Mamm Genome* 10:176-181.

225. Morel, L., C. Mohan, Y. Yu, B. P. Croker, N. Tian, A. Deng, and E. K. Wakeland. 1997. Functional dissection of systemic lupus erythematosus using congenic mouse strains. *J Immunol* 158:6019-6028.

226. Mohan, C., E. Alas, L. Morel, P. Yang, and E. K. Wakeland. 1998. Genetic dissection of SLE pathogenesis. Sle1 on murine chromosome 1 leads to a selective loss of tolerance to H2A/H2B/DNA subnucleosomes. *J Clin Invest* 101:1362-1372.

227. Subramanian, S., Y. S. Yim, K. Liu, K. Tus, X. J. Zhou, and E. K. Wakeland. 2005. Epistatic Suppression of Systemic Lupus Erythematosus: Fine-mapping of Sles1 to Less Than 1 Mb. *Journal of Immunology* 175.

228. Sobel, E. S., C. Mohan, L. Morel, J. Schiffenbauer, and E. K. Wakeland. 1999. Genetic dissection of SLE pathogenesis: adoptive transfer of Sle1 mediates the loss of tolerance by bone marrow-derived B cells. *J Immunol* 162:2415-2421.

229. Sobel, E. S., M. Satoh, Y. Chen, E. K. Wakeland, and L. Morel. 2002. The major murine systemic lupus erythematosus susceptibility locus Sle1 results in abnormal functions of both B and T cells. *J Immunol* 169:2694-2700.

230. Boackle, S. A., V. M. Holers, X. Chen, G. Szakonyi, D. R. Karp, E. K. Wakeland, and L. Morel. 2001. Cr2, a candidate gene in the murine Sle1c lupus susceptibility locus, encodes a dysfunctional protein. *Immunity* 15:775-785.

231. Wandstrat, A. E., C. Nguyen, N. Limaye, A. Y. Chan, S. Subramanian, X. H. Tian, Y. S. Yim, A. Pertsemlidis, H. R. Garner, Jr., L. Morel, and E. K. Wakeland. 2004. Association of extensive polymorphisms in the SLAM/CD2 gene cluster with murine lupus. *Immunity* 21:769-780.

232. Mooney, J. M., J. Klem, C. Wulfing, L. A. Mijares, P. L. Schwartzberg, M. Bennett, and J. D. Schatzle. 2004. The murine NK receptor 2B4 (CD244) exhibits inhibitory function independent of signaling lymphocytic activation molecule-associated protein expression. *J Immunol* 173:3953-3961.

233. Wang, N., A. Satoskar, W. Faubion, D. Howie, S. Okamoto, S. Feske, C. Gullo, K. Clarke, M. R. Sosa, A. H. Sharpe, and C. Terhorst. 2004. The cell surface receptor SLAM controls T cell and macrophage functions. *J Exp Med* 199:1255-1264.

234. Veillette, A., and S. Latour. 2003. The SLAM family of immune-cell receptors. *Curr Opin Immunol* 15:277-285.

235. Mohan, C., Y. Yu, L. Morel, P. Yang, and E. K. Wakeland. 1999. Genetic dissection of Sle pathogenesis: Sle3 on murine chromosome 7 impacts T cell activation, differentiation, and cell death. *J Immunol* 162:6492-6502.

236. Sobel, E. S., L. Morel, R. Baert, C. Mohan, J. Schiffenbauer, and E. K. Wakeland. 2002. Genetic dissection of systemic lupus erythematosus pathogenesis: evidence for functional expression of Sle3/5 by non-T cells. *J Immunol* 169:4025-4032.

237. Zhu, J., X. Liu, C. Xie, M. Yan, Y. Yu, E. S. Sobel, E. K. Wakeland, and C. Mohan. 2005. T cell hyperactivity in lupus as a consequence of hyperstimulatory antigen-presenting cells. *J Clin Invest*.

238. Mohan, C., L. Morel, P. Yang, and E. K. Wakeland. 1997. Genetic dissection of systemic lupus erythematosus pathogenesis: Sle2 on murine chromosome 4 leads to B cell hyperactivity. *J Immunol* 159:454-465.

239. Xu, Z., E. J. Butfiloski, E. S. Sobel, and L. Morel. 2004. Mechanisms of peritoneal B-1a cells accumulation induced by murine lupus susceptibility locus Sle2. *J Immunol* 173:6050-6058.

240. Mohan, C., L. Morel, P. Yang, H. Watanabe, B. Croker, G. Gilkeson, and E. K. Wakeland. 1999. Genetic dissection of lupus pathogenesis: a recipe for nephrophilic autoantibodies. *J Clin Invest* 103:1685-1695.

241. Erickson, L. D., L. L. Lin, B. Duan, L. Morel, and R. J. Noelle. 2003. A genetic lesion that arrests plasma cell homing to the bone marrow. *Proc Natl Acad Sci U S A* 100:12905-12910.

242. Morel, L., X. H. Tian, B. P. Croker, and E. K. Wakeland. 1999. Epistatic modifiers of autoimmunity in a murine model of lupus nephritis. *Immunity* 11:131-139.

243. Morel, L. 2004. Mouse models of human autoimmune diseases: essential tools that require the proper controls. *PLoS Biol* 2:E241.

244. Botto, M., C. Dell'Agnola, A. E. Bygrave, E. M. Thompson, H. T. Cook, F. Petry, M. Loos, P. P. Pandolfi, and M. J. Walport. 1998. Homozygous C1q deficiency causes glomerulonephritis associated with multiple apoptotic bodies. *Nat Genet* 19:56-59.

245. Nauta, A. J., L. A. Trouw, M. R. Daha, O. Tijsma, R. Nieuwland, W. J. Schwaeble, A. R. Gingras, A. Mantovani, E. C. Hack, and A. Roos. 2002. Direct binding of C1q to apoptotic cells and cell blebs induces complement activation. *Eur J Immunol* 32:1726-1736.

246. Korb, L. C., and J. M. Ahearn. 1997. C1q binds directly and specifically to surface blebs of apoptotic human keratinocytes: complement deficiency and systemic lupus erythematosus revisited. *J Immunol* 158:4525-4528.

247. Casciola-Rosen, L., A. Rosen, M. Petri, and M. Schlissel. 1996. Surface blebs on apoptotic cells are sites of enhanced procoagulant activity: implications for coagulation events and antigenic spread in systemic lupus erythematosus. *Proc Natl Acad Sci U S A* 93:1624-1629.

248. Navratil, J. S., S. C. Watkins, J. J. Wisnieski, and J. M. Ahearn. 2001. The globular heads of C1q specifically recognize surface blebs of apoptotic vascular endothelial cells. *J Immunol* 166:3231-3239.

249. Cocca, B. A., A. M. Cline, and M. Z. Radic. 2002. Blebs and apoptotic bodies are B cell autoantigens. *J Immunol* 169:159-166.

250. Bickerstaff, M. C., M. Botto, W. L. Hutchinson, J. Herbert, G. A. Tennent, A. Bybee, D. A. Mitchell, H. T. Cook, P. J. Butler, M. J. Walport, and M. B. Pepys. 1999. Serum amyloid P component controls chromatin degradation and prevents antinuclear autoimmunity. *Nat Med* 5:694-697.

251. Gillmore, J. D., W. L. Hutchinson, J. Herbert, A. Bybee, D. A. Mitchell, R. P. Hasserjian, K. Yamamura, M. Suzuki, C. A. Sabin, and M. B. Pepys. 2004.

Autoimmunity and glomerulonephritis in mice with targeted deletion of the serum amyloid P component gene: SAP deficiency or strain combination? *Immunology* 112:255-264.

252. Bygrave, A. E., K. L. Rose, J. Cortes-Hernandez, J. Warren, R. J. Rigby, H. T. Cook, M. J. Walport, T. J. Vyse, and M. Botto. 2004. Spontaneous autoimmunity in 129 and C57BL/6 mice-implications for autoimmunity described in gene-targeted mice. *PLoS Biol* 2:E243.

253. Napirei, M., H. Karsunky, B. Zevnik, H. Stephan, H. G. Mannherz, and T. Moroy. 2000. Features of systemic lupus erythematosus in Dnase1-deficient mice. *Nat Genet* 25:177-181.

254. Cohen, P. L., R. Caricchio, V. Abraham, T. D. Camenisch, J. C. Jennette, R. A. Roubey, H. S. Earp, G. Matsushima, and E. A. Reap. 2002. Delayed apoptotic cell clearance and lupus-like autoimmunity in mice lacking the c-mer membrane tyrosine kinase. *J Exp Med* 196:135-140.

255. Salvador, J. M., M. C. Hollander, A. T. Nguyen, J. B. Kopp, L. Barisoni, J. K. Moore, J. D. Ashwell, and A. J. Fornace, Jr. 2002. Mice lacking the p53-effector gene Gadd45a develop a lupus-like syndrome. *Immunity* 16:499-508.

256. Salvador, J. M., P. R. Mittelstadt, G. I. Belova, A. J. Fornace, Jr., and J. D. Ashwell. 2005. The autoimmune suppressor Gadd45alpha inhibits the T cell alternative p38 activation pathway. *Nat Immunol* 6:396-402.

257. Balomenos, D., J. Martin-Caballero, M. I. Garcia, I. Prieto, J. M. Flores, M. Serrano, and A. C. Martinez. 2000. The cell cycle inhibitor p21 controls T-cell proliferation and sex-linked lupus development. *Nat Med* 6:171-176.

258. Di Cristofano, A., P. Kotsi, Y. F. Peng, C. Cordon-Cardo, K. B. Elkon, and P. P. Pandolfi. 1999. Impaired Fas response and autoimmunity in Pten+/- mice. *Science* 285:2122-2125.

259. Suzuki, A., M. T. Yamaguchi, T. Ohteki, T. Sasaki, T. Kaisho, Y. Kimura, R. Yoshida, A. Wakeham, T. Higuchi, M. Fukumoto, T. Tsubata, P. S. Ohashi, S. Koyasu, J. M. Penninger, T. Nakano, and T. W. Mak. 2001. T cell-specific loss of Pten leads to defects in central and peripheral tolerance. *Immunity* 14:523-534.

260. Suzuki, A., T. Kaisho, M. Ohishi, M. Tsukio-Yamaguchi, T. Tsubata, P. A. Koni, T. Sasaki, T. W. Mak, and T. Nakano. 2003. Critical roles of Pten in B cell homeostasis and immunoglobulin class switch recombination. *J Exp Med* 197:657-667.

261. Borlado, L. R., C. Redondo, B. Alvarez, C. Jimenez, L. M. Criado, J. Flores, M. A. Marcos, A. C. Martinez, D. Balomenos, and A. C. Carrera. 2000. Increased phosphoinositide 3-kinase activity induces a lymphoproliferative disorder and contributes to tumor generation in vivo. *Faseb J* 14:895-903.

262. Miyamoto, A., K. Nakayama, H. Imaki, S. Hirose, Y. Jiang, M. Abe, T. Tsukiyama, H. Nagahama, S. Ohno, S. Hatakeyama, and K. I. Nakayama. 2002. Increased proliferation of B cells and auto-immunity in mice lacking protein kinase Cdelta. *Nature* 416:865-869.

263. Murga, M., O. Fernandez-Capetillo, S. J. Field, B. Moreno, L. R. Borlado, Y. Fujiwara, D. Balomenos, A. Vicario, A. C. Carrera, S. H. Orkin, M. E. Greenberg, and A. M. Zubiaga. 2001. Mutation of E2F2 in mice causes enhanced T lymphocyte proliferation, leading to the development of autoimmunity. *Immunity* 15:959-970.

264. Strasser, A., S. Whittingham, D. L. Vaux, M. L. Bath, J. M. Adams, S. Cory, and A. W. Harris. 1991. Enforced BCL2 expression in B-lymphoid cells prolongs antibody responses and elicits autoimmune disease. *Proc Natl Acad Sci U S A* 88:8661-8665.

265. Bouillet, P., D. Metcalf, D. C. Huang, D. M. Tarlinton, T. W. Kay, F. Kontgen, J. M. Adams, and A. Strasser. 1999. Proapoptotic Bcl-2 relative Bim required for certain apoptotic responses, leukocyte homeostasis, and to preclude autoimmunity. *Science* 286:1735-1738.

266. Nishizumi, H., I. Taniuchi, Y. Yamanashi, D. Kitamura, D. Ilic, S. Mori, T. Watanabe, and T. Yamamoto. 1995. Impaired proliferation of peripheral B cells and indication of autoimmune disease in lyn-deficient mice. *Immunity* 3:549-560.

267. Hibbs, M. L., D. M. Tarlinton, J. Armes, D. Grail, G. Hodgson, R. Maglitto, S. A. Stacker, and A. R. Dunn. 1995. Multiple defects in the immune system of Lyn-deficient mice, culminating in autoimmune disease. *Cell* 83:301-311.

268. Yu, C. C., T. S. Yen, C. A. Lowell, and A. L. DeFranco. 2001. Lupus-like kidney disease in mice deficient in the Src family tyrosine kinases Lyn and Fyn. *Curr Biol* 11:34-38.

269. Majeti, R., Z. Xu, T. G. Parslow, J. L. Olson, D. I. Daikh, N. Killeen, and A. Weiss. 2000. An inactivating point mutation in the inhibitory wedge of CD45 causes lymphoproliferation and autoimmunity. *Cell* 103:1059-1070.

270. Sun, H., B. Lu, R. Q. Li, R. A. Flavell, and R. Taneja. 2001. Defective T cell activation and autoimmune disorder in Stra13-deficient mice. *Nat Immunol* 2:1040-1047.

271. Drappa, J., L. A. Kamen, E. Chan, M. Georgiev, D. Ashany, F. Marti, and P. D. King. 2003. Impaired T cell death and lupus-like autoimmunity in T cell-specific adapter protein-deficient mice. *J Exp Med* 198:809-821.

272. Layer, K., G. Lin, A. Nencioni, W. Hu, A. Schmucker, A. N. Antov, X. Li, S. Takamatsu, T. Chevassut, N. A. Dower, S. L. Stang, D. Beier, J. Buhlmann, R. T. Bronson, K. B. Elkon, J. C. Stone, L. Van Parijs, and B. Lim. 2003. Autoimmunity as the consequence of a spontaneous mutation in Rasgrp1. *Immunity* 19:243-255.

273. Sommers, C. L., C. S. Park, J. Lee, C. Feng, C. L. Fuller, A. Grinberg, J. A. Hildebrand, E. Lacana, R. K. Menon, E. W. Shores, L. E. Samelson, and P. E. Love. 2002. A LAT mutation that inhibits T cell development yet induces lymphoproliferation. *Science* 296:2040-2043.

274. Aguado, E., S. Richelme, S. Nunez-Cruz, A. Miazek, A. M. Mura, M. Richelme, X. J. Guo, D. Sainty, H. T. He, B. Malissen, and M. Malissen. 2002. Induction of T helper type 2 immunity by a point mutation in the LAT adaptor. *Science* 296:2036-2040.

275. Khare, S. D., I. Sarosi, X. Z. Xia, S. McCabe, K. Miner, I. Solovyev, N. Hawkins, M. Kelley, D. Chang, G. Van, L. Ross, J. Delaney, L. Wang, D. Lacey, W. J. Boyle, and

H. Hsu. 2000. Severe B cell hyperplasia and autoimmune disease in TALL-1 transgenic mice. *Proc Natl Acad Sci U S A* 97:3370-3375.

276. Gross, J. A., J. Johnston, S. Mudri, R. Enselman, S. R. Dillon, K. Madden, W. Xu, J. Parrish-Novak, D. Foster, C. Lofton-Day, M. Moore, A. Littau, A. Grossman, H. Haugen, K. Foley, H. Blumberg, K. Harrison, W. Kindsvogel, and C. H. Clegg. 2000. TACI and BCMA are receptors for a TNF homologue implicated in B-cell autoimmune disease. *Nature* 404:995-999.

277. Seshasayee, D., P. Valdez, M. Yan, V. M. Dixit, D. Tumas, and I. S. Grewal. 2003. Loss of TACI causes fatal lymphoproliferation and autoimmunity, establishing TACI as an inhibitory BLyS receptor. *Immunity* 18:279-288.

278. Sato, S., M. Hasegawa, M. Fujimoto, T. F. Tedder, and K. Takehara. 2000. Quantitative genetic variation in CD19 expression correlates with autoimmunity. *J Immunol* 165:6635-6643.

279. Morel, L., Y. Yu, K. R. Blenman, R. A. Caldwell, and E. K. Wakeland. 1996. Production of congenic mouse strains carrying genomic intervals containing SLE-susceptibility genes derived from the SLE-prone NZM2410 strain. *Mamm Genome* 7:335-339.

280. Zhou, X. J., Z. Laszik, X. Q. Wang, F. G. Silva, and N. D. Vaziri. 2000. Association of renal injury with increased oxygen free radical activity and altered nitric oxide metabolism in chronic experimental hemosiderosis. *Lab Invest* 80:1905-1914.

281. Liang, Z., C. Xie, C. Chen, D. Kreska, K. Hsu, L. Li, X. J. Zhou, and C. Mohan. 2004. Pathogenic profiles and molecular signatures of antinuclear autoantibodies rescued from NZM2410 lupus mice. *J Exp Med* 199:381-398.

282. Raman, K., and C. Mohan. 2003. Genetic underpinnings of autoimmunity--lessons from studies in arthritis, diabetes, lupus and multiple sclerosis. *Curr Opin Immunol* 15:651-659.

283. Santiago-Raber, M. L., B. R. Lawson, W. Dummer, M. Barnhouse, S. Koundouris, C. B. Wilson, D. H. Kono, and A. N. Theofilopoulos. 2001. Role of cyclin kinase inhibitor p21 in systemic autoimmunity. *J Immunol* 167:4067-4074.

284. Wakui, M., J. Kim, E. J. Butfiloski, L. Morel, and E. S. Sobel. 2004. Genetic dissection of lupus pathogenesis: Sle3/5 impacts IgH CDR3 sequences, somatic mutations, and receptor editing. *J Immunol* 173:7368-7376.

285. Liu, K., C. Liang, Z. Liang, K. Tus, and E. K. Wakeland. 2005. Sle1ab Mediates the Aberrant Activation of STAT3 and Ras-ERK Signaling Pathways in B Lymphocytes. *J Immunol* 174:1630-1637.

286. Shi, X., C. Xie, D. Kreska, J. A. Richardson, and C. Mohan. 2002. Genetic dissection of SLE: SLE1 and FAS impact alternate pathways leading to lymphoproliferative autoimmunity. *J Exp Med* 196:281-292.

287. Chen, Y., C. Cuda, and L. Morel. 2005. Genetic determination of T cell help in loss of tolerance to nuclear antigens. *J Immunol* 174:7692-7702.

288. Mohan, C., L. Morel, P. Yang, and E. K. Wakeland. 1998. Accumulation of splenic B1a cells with potent antigen-presenting capability in NZM2410 lupus-prone mice. *Arthritis Rheum* 41:1652-1662.

289. Klein, J., F. Figueroa, and C. S. David. 1983. H-2 haplotypes, genes and antigens: second listing. II. The H-2 complex. *Immunogenetics* 17:553-596.

290. Horton, R., L. Wilming, V. Rand, R. C. Lovering, E. A. Bruford, V. K. Khodiyar, M. J. Lush, S. Povey, C. C. Talbot, Jr., M. W. Wright, H. M. Wain, J. Trowsdale, A. Ziegler, and S. Beck. 2004. Gene map of the extended human MHC. *Nat Rev Genet* 5:889-899.

291. Jacob, C. O., and H. O. McDevitt. 1988. Tumour necrosis factor-alpha in murine autoimmune 'lupus' nephritis. *Nature* 331:356-358.

292. Brennan, D. C., M. A. Yui, R. P. Wuthrich, and V. E. Kelley. 1989. Tumor necrosis factor and IL-1 in New Zealand Black/White mice. Enhanced gene expression and acceleration of renal injury. *J Immunol* 143:3470-3475.

293. Blenman, K. R., F. R. Bahjat, L. L. Moldawer, and L. Morel. 2004. Aberrant signaling in the TNFalpha/TNF receptor 1 pathway of the NZM2410 lupus-prone mouse. *Clin Immunol* 110:124-133.

294. Podolin, P. L., P. Denny, N. Armitage, C. J. Lord, N. J. Hill, E. R. Levy, L. B. Peterson, J. A. Todd, L. S. Wicker, and P. A. Lyons. 1998. Localization of two insulin-dependent diabetes (Idd) genes to the Idd10 region on mouse chromosome 3. *Mamm Genome* 9:283-286.

295. Hattori, M., E. Yamato, N. Itoh, H. Senpuku, T. Fujisawa, M. Yoshino, M. Fukuda, E. Matsumoto, T. Toyonaga, I. Nakagawa, M. Petruzzelli, A. McMurray, H. Weiner, T. Sagai, K. Moriwaki, T. Shiroishi, R. Maron, and T. Lund. 1999. Cutting edge: homologous recombination of the MHC class I K region defines new MHC-linked diabetogenic susceptibility gene(s) in nonobese diabetic mice. *J Immunol* 163:1721-1724.

296. Babcock, S. K., V. B. Appel, M. Schiff, E. Palmer, and B. L. Kotzin. 1989. Genetic analysis of the imperfect association of H-2 haplotype with lupus-like autoimmune disease. *Proc Natl Acad Sci U S A* 86:7552-7555.

297. Zhang, D., K. Fujio, Y. Jiang, J. Zhao, N. Tada, K. Sudo, H. Tsurui, K. Nakamura, K. Yamamoto, H. Nishimura, T. Shira, and S. Hirose. 2004. Dissection of the role of MHC class II A and E genes in autoimmune susceptibility in murine lupus models with intragenic recombination. *Proc Natl Acad Sci U S A* 101:13838-13843.

298. Prodeus, A. P., S. Goerg, L. M. Shen, O. O. Pozdnyakova, L. Chu, E. M. Alicot, C. C. Goodnow, and M. C. Carroll. 1998. A critical role for complement in maintenance of self-tolerance. *Immunity* 9:721-731.

299. Santiago-Raber, M. L., R. Baccala, K. M. Haraldsson, D. Choubey, T. A. Stewart, D. H. Kono, and A. N. Theofilopoulos. 2003. Type-I interferon receptor deficiency reduces lupus-like disease in NZB mice. *J Exp Med* 197:777-788.

300. Asea, A., S. K. Kraeft, E. A. Kurt-Jones, M. A. Stevenson, L. B. Chen, R. W. Finberg, G. C. Koo, and S. K. Calderwood. 2000. HSP70 stimulates cytokine production

through a CD14-dependant pathway, demonstrating its dual role as a chaperone and cytokine. *Nat Med* 6:435-442.

301. Ohashi, P. S. 2003. Negative selection and autoimmunity. *Curr Opin Immunol* 15:668-676.

302. McCright, B. 2003. Notch signaling in kidney development. *Curr Opin Nephrol Hypertens* 12:5-10.

303. Hozumi, K., N. Abe, S. Chiba, H. Hirai, and S. Habu. 2003. Active form of Notch members can enforce T lymphopoiesis on lymphoid progenitors in the monolayer culture specific for B cell development. *J Immunol* 170:4973-4979.

304. Saito, T., S. Chiba, M. Ichikawa, A. Kunisato, T. Asai, K. Shimizu, T. Yamaguchi, G. Yamamoto, S. Seo, K. Kumano, E. Nakagami-Yamaguchi, Y. Hamada, S. Aizawa, and H. Hirai. 2003. Notch2 is preferentially expressed in mature B cells and indispensable for marginal zone B lineage development. *Immunity* 18:675-685.

305. Kumano, K., S. Chiba, A. Kunisato, M. Sata, T. Saito, E. Nakagami-Yamaguchi, T. Yamaguchi, S. Masuda, K. Shimizu, T. Takahashi, S. Ogawa, Y. Hamada, and H. Hirai. 2003. Notch1 but not Notch2 is essential for generating hematopoietic stem cells from endothelial cells. *Immunity* 18:699-711.

306. Witt, C. M., W. J. Won, V. Hurez, and C. A. Klug. 2003. Notch2 haploinsufficiency results in diminished B1 B cells and a severe reduction in marginal zone B cells. *J Immunol* 171:2783-2788.

307. Witt, C. M., V. Hurez, C. S. Swindle, Y. Hamada, and C. A. Klug. 2003. Activated Notch2 potentiates CD8 lineage maturation and promotes the selective development of B1 B cells. *Mol Cell Biol* 23:8637-8650.

308. Vercauteren, S. M., and H. J. Sutherland. 2004. Constitutively active Notch4 promotes early human hematopoietic progenitor cell maintenance while inhibiting differentiation and causes lymphoid abnormalities in vivo. *Blood* 104:2315-2322.

309. Tacchini-Cottier, F., C. Allenbach, L. A. Otten, and F. Radtke. 2004. Notch1 expression on T cells is not required for CD4+ T helper differentiation. *Eur J Immunol* 34:1588-1596.

310. Hozumi, K., N. Negishi, D. Suzuki, N. Abe, Y. Sotomaru, N. Tamaoki, C. Mailhos, D. Ish-Horowicz, S. Habu, and M. J. Owen. 2004. Delta-like 1 is necessary for the generation of marginal zone B cells but not T cells in vivo. *Nat Immunol* 5:638-644.

311. Radtke, F., A. Wilson, and H. R. MacDonald. 2004. Notch signaling in T- and B-cell development. *Curr Opin Immunol* 16:174-179.

312. Loder, F., B. Mutschler, R. J. Ray, C. J. Paige, P. Sideras, R. Torres, M. C. Lamers, and R. Carsetti. 1999. B cell development in the spleen takes place in discrete steps and is determined by the quality of B cell receptor-derived signals. *J Exp Med* 190:75-89.

313. Myrick, C., R. DiGuisto, J. DeWolfe, E. Bowen, J. Kappler, P. Marrack, and E. K. Wakeland. 2002. Linkage analysis of variations in CD4:CD8 T cell subsets between C57BL/6 and DBA/2. *Genes Immun* 3:144-150.

314. Izui, S. 1990. Autoimmune accelerating genes, lpr and Yaa, in murine systemic lupus erythematosus. *Autoimmunity* 6:113-129.

315. Amano, H., E. Amano, T. Moll, D. Marinkovic, N. Ibnou-Zekri, E. Martinez-Soria, I. Semac, T. Wirth, L. Nitschke, and S. Izui. 2003. The Yaa mutation promoting murine lupus causes defective development of marginal zone B cells. *J Immunol* 170:2293-2301.

316. Izui, S., M. Higaki, D. Morrow, and R. Merino. 1988. The Y chromosome from autoimmune BXSB/MpJ mice induces a lupus-like syndrome in (NZW x C57BL/6)F1 male mice, but not in C57BL/6 male mice. *Eur J Immunol* 18:911-915.

317. Chung, J. B., M. Silverman, and J. G. Monroe. 2003. Transitional B cells: step by step towards immune competence. *Trends Immunol* 24:343-349.

318. Allman, D., B. Srivastava, and R. C. Lindsley. 2004. Alternative routes to maturity: branch points and pathways for generating follicular and marginal zone B cells. *Immunol Rev* 197:147-160.

319. Lopes-Carvalho, T., J. Foote, and J. F. Kearney. 2005. Marginal zone B cells in lymphocyte activation and regulation. *Curr Opin Immunol* 17:244-250.

320. Wofsy, D., C. E. Kerger, and W. E. Seaman. 1984. Monocytosis in the BXSB model for systemic lupus erythematosus. *J Exp Med* 159:629-634.

321. Martin, F., and J. F. Kearney. 2001. B1 cells: similarities and differences with other B cell subsets. *Curr Opin Immunol* 13:195-201.

322. Pillai, S., A. Cariappa, and S. T. Moran. 2004. Positive selection and lineage commitment during peripheral B-lymphocyte development. *Immunol Rev* 197:206-218.

323. Yurasov, S., H. Wardemann, J. Hammersen, M. Tsuiji, E. Meffre, V. Pascual, and M. C. Nussenzweig. 2005. Defective B cell tolerance checkpoints in systemic lupus erythematosus. *J Exp Med* 201:703-711.

324. Su, T. T., B. Guo, B. Wei, J. Braun, and D. J. Rawlings. 2004. Signaling in transitional type 2 B cells is critical for peripheral B-cell development. *Immunol Rev* 197:161-178.

325. Cariappa, A., M. Tang, C. Parng, E. Nebelitskiy, M. Carroll, K. Georgopoulos, and S. Pillai. 2001. The follicular versus marginal zone B lymphocyte cell fate decision is regulated by Aiolos, Btk, and CD21. *Immunity* 14:603-615.

326. Srivastava, B., R. C. Lindsley, N. Nikbakht, and D. Allman. 2005. Models for peripheral B cell development and homeostasis. *Semin Immunol* 17:175-182.

327. Wakeland, E., L. Morel, K. Achey, M. Yui, and J. Longmate. 1997. Speed congenics: a classic technique in the fast lane (relatively speaking). *Immunol Today* 18:472-477.

328. Johnnidis, J. B., E. S. Venanzi, D. J. Taxman, J. P. Ting, C. O. Benoist, and D. J. Mathis. 2005. Chromosomal clustering of genes controlled by the aire transcription factor. *Proc Natl Acad Sci U S A* 102:7233-7238.

329. Kuroda, N., T. Mitani, N. Takeda, N. Ishimaru, R. Arakaki, Y. Hayashi, Y. Bando, K. Izumi, T. Takahashi, T. Nomura, S. Sakaguchi, T. Ueno, Y. Takahama, D. Uchida, S. Sun, F. Kajiura, Y. Mouri, H. Han, A. Matsushima, G. Yamada, and M. Matsumoto.

2005. Development of autoimmunity against transcriptionally unrepressed target antigen in the thymus of Aire-deficient mice. *J Immunol* 174:1862-1870.

330. Vinuesa, C. G., M. C. Cook, C. Angelucci, V. Athanasopoulos, L. Rui, K. M. Hill, D. Yu, H. Domaschenz, B. Whittle, T. Lambe, I. S. Roberts, R. R. Copley, J. I. Bell, R. J. Cornall, and C. C. Goodnow. 2005. A RING-type ubiquitin ligase family member required to repress follicular helper T cells and autoimmunity. *Nature* 435:452-458.

331. Mueller, D. L. 2004. E3 ubiquitin ligases as T cell anergy factors. *Nat Immunol* 5:883-890.

332. Sakaguchi, N., T. Takahashi, H. Hata, T. Nomura, T. Tagami, S. Yamazaki, T. Sakihama, T. Matsutani, I. Negishi, S. Nakatsuru, and S. Sakaguchi. 2003. Altered thymic T-cell selection due to a mutation of the ZAP-70 gene causes autoimmune arthritis in mice. *Nature* 426:454-460.

333. Wardemann, H., S. Yurasov, A. Schaefer, J. W. Young, E. Meffre, and M. C. Nussenzweig. 2003. Predominant autoantibody production by early human B cell precursors. *Science* 301:1374-1377.

334. Moll, T., E. Martinez-Soria, M. L. Santiago-Raber, H. Amano, M. Pihlgren-Bosch, D. Marinkovic, and S. Izui. 2005. Differential activation of anti-erythrocyte and anti-DNA autoreactive B lymphocytes by the Yaa mutation. *J Immunol* 174:702-709.

335. Calame, K. L., K. I. Lin, and C. Tunyaplin. 2003. Regulatory mechanisms that determine the development and function of plasma cells. *Annu Rev Immunol* 21:205-230.

336. William, J., C. Euler, E. Leadbetter, A. Marshak-Rothstein, and M. J. Shlomchik. 2005. Visualizing the onset and evolution of an autoantibody response in systemic autoimmunity. *J Immunol* 174:6872-6878.

337. William, J., C. Euler, and M. J. Shlomchik. 2005. Short-lived plasmablasts dominate the early spontaneous rheumatoid factor response: differentiation pathways, hypermutating cell types, and affinity maturation outside the germinal center. *J Immunol* 174:6879-6887.

338. Mandik-Nayak, L., S. J. Seo, C. Sokol, K. M. Potts, A. Bui, and J. Erikson. 1999. MRL-lpr/lpr mice exhibit a defect in maintaining developmental arrest and follicular exclusion of anti-double-stranded DNA B cells. *J Exp Med* 189:1799-1814.

339. Kronenberg, M., and A. Rudensky. 2005. Regulation of immunity by self-reactive T cells. *Nature* 435:598-604.

340. Ohashi, P. S. 2002. T-cell signalling and autoimmunity: molecular mechanisms of disease. *Nat Rev Immunol* 2:427-438.

341. Hasegawa, K., F. Martin, G. Huang, D. Tumas, L. Diehl, and A. C. Chan. 2004. PEST domain-enriched tyrosine phosphatase (PEP) regulation of effector/memory T cells. *Science* 303:685-689.

342. Chtanova, T., S. G. Tangye, R. Newton, N. Frank, M. R. Hodge, M. S. Rolph, and C. R. Mackay. 2004. T follicular helper cells express a distinctive transcriptional profile, reflecting their role as non-Th1/Th2 effector cells that provide help for B cells. *J Immunol* 173:68-78.

343. Crotty, S., E. N. Kersh, J. Cannons, P. L. Schwartzberg, and R. Ahmed. 2003. SAP is required for generating long-term humoral immunity. *Nature* 421:282-287.

344. Ozaki, K., R. Spolski, R. Ettinger, H. P. Kim, G. Wang, C. F. Qi, P. Hwu, D. J. Shaffer, S. Akilesh, D. C. Roopenian, H. C. Morse, 3rd, P. E. Lipsky, and W. J. Leonard. 2004. Regulation of B cell differentiation and plasma cell generation by IL-21, a novel inducer of Blimp-1 and Bcl-6. *J Immunol* 173:5361-5371.

345. Howie, D., F. S. Laroux, M. Morra, A. R. Satoskar, L. E. Rosas, W. A. Faubion, A. Julien, S. Rietdijk, A. J. Coyle, C. Fraser, and C. Terhorst. 2005. Cutting edge: the SLAM family receptor Ly108 controls T cell and neutrophil functions. *J Immunol* 174:5931-5935.

346. Duan, L., A. L. Reddi, A. Ghosh, M. Dimri, and H. Band. 2004. The Cbl family and other ubiquitin ligases: destructive forces in control of antigen receptor signaling. *Immunity* 21:7-17.

347. Liu, Y. C. 2004. Ubiquitin ligases and the immune response. *Annu Rev Immunol* 22:81-127.

348. Raaphorst, F. M., F. J. van Kemenade, E. Fieret, K. M. Hamer, D. P. Satijn, A. P. Otte, and C. J. Meijer. 2000. Cutting edge: polycomb gene expression patterns reflect distinct B cell differentiation stages in human germinal centers. *J Immunol* 164:1-4.

349. Valentonyte, R., J. Hampe, K. Huse, P. Rosenstiel, M. Albrecht, A. Stenzel, M. Nagy, K. I. Gaede, A. Franke, R. Haesler, A. Koch, T. Lengauer, D. Seegert, N. Reiling, S. Ehlers, E. Schwinger, M. Platzer, M. Krawczak, J. Muller-Quernheim, M. Schurmann,

and S. Schreiber. 2005. Sarcoidosis is associated with a truncating splice site mutation in BTNL2. *Nat Genet* 37:357-364.

350. Greenbaum, S., and Y. Zhuang. 2002. Identification of E2A target genes in B lymphocyte development by using a gene tagging-based chromatin immunoprecipitation system. *Proc Natl Acad Sci U S A* 99:15030-15035.

351. Mana, P., M. Goodyear, C. Bernard, R. Tomioka, M. Freire-Garabal, and D. Linares. 2004. Tolerance induction by molecular mimicry: prevention and suppression of experimental autoimmune encephalomyelitis with the milk protein butyrophilin. *Int Immunol* 16:489-499.

VITAE

Srividya Subramanian was born in Madras, India on March 3, 1977, the daughter of Meena Subramanian and Ananth 'Andy' Subramanian. She completed her Cambridge O Levels at Marymount Convent School in Singapore in 1993, and finished her high school education and the Indian School Certificate examinations at Sishya, in Chennai, Madras in 1995. She entered the Birla Institute of Technology and Science (BITS) in Pilani, Rajasthan (India) in 1995 and received a Masters of Science (Hons.) in Biological Sciences in 1999. She moved to Dallas and entered the Graduate School of Biomedical Sciences at the University of Texas Southwestern Medical Center in August, 1999. She completed her studies in July, 2005, and was awarded the degree of Doctor of Philosophy, with an emphasis in immunology, in August of 2005.

Permanent Address: 11609 Larch Valley Drive

Austin, Texas 78754